Neural basis of self-representation in the non-human primate thanks to functional magnetic resonance imaging (fMRT)

Olivier Guipponi

Année 2013

THESE DE L'UNIVERSITE DE LYON

Délivrée par

L'UNIVERSITE CLAUDE BERNARD LYON 1

ECOLE DOCTORALE de NEUROSCIENCES ET COGNITION

DIPLOME DE DOCTORAT

(arrêté du 7 août 2006)

soutenue publiquement le Mercredi 30 Octobre 2013 par

Olivier GUIPPONI

BASES NEURALES DE LA REPRESENTATION DE SOI CHEZ LE PRIMATE NON-HUMAIN GRACE A L'IMAGERIE PAR RESONANCE MAGNETIQUE FONCTIONNELLE (IRMF)

Directrices de thèse :	Dr. Suliann BEN HAMED	
	Dr. Claire WARDAK (membre invité)	
JURY :	Dr. Pascal BARONE	Rapporteur
	Dr. Suliann BEN HAMED	Directrice de thèse
	Dr. Frank BREMMER	Rapporteur
	Pr. Rémi GERVAIS	Président du jury

REMERCIEMENTS

Je remercie tout d'abord :

- Pascal Barone et Frank Bremmer d'avoir accepté d'être rapporteurs de cette thèse. Vos domaines d'expertise respectifs constituent la garantie de commentaires pertinents sur les travaux réalisés au cours de cette thèse.
- Rémi Gervais d'avoir accepté d'être Président du jury.

Jean-René, merci d'avoir pris le temps de me présenter le laboratoire, ses équipes et de m'avoir dérigé vers Suliann et Claire quand je recherchais un stage de Master : je n'avais à l'époque l'intention de ne faire que les stages de recherche prévus dans ma scolarité. Finalement, l'émulation scientifique et l'ambiance du laboratoire m'ont convaincu de poursuivre l'aventure !

Claire, merci de m'avoir initié à l'entrainement des animaux et à l'analyse des données d'imagerie. La route est encore longue mais j'espère que tous les travaux réalisés ensemble vont porter leur fruit dans un avenir proche !

Suliann, ces dernières années sont passées à une vitesse incroyable. J'ai l'impression que notre première conversation dans ton bureau date d'hier. Merci pour tout, en particulier pour l'accompagnement quotidien, la confiance que tu m'as accordée et les discussions que nous avons pues avoir. Je ne retire que des points positifs de cette expérience et suis certain que nous trouverons encore des projets communs, aussi bien scientifiques que pédagogiques.

Serge, merci de ta disponibilité et de ton aide dans l'élaboration des scripts mais aussi dans la construction des dispositifs expérimentaux divers et variés que nous avons dû effectuer.

Philippe, merci de m'avoir confié l'élaboration de TD ainsi que la correction des épreuves de contrôle continu : cela a été pour moi l'occasion d'interagir avec les élèves de Licence et de sortir peu à peu de l'environnement scolaire que j'avais connu jusqu'alors. Cette expérience devrait m'être bien utile pour la suite !

Sylvia, merci pour tes conseils distillés au cours des repas et de tes relectures pour la publication du premier article. Les conversations que nous avons pu avoir au sujet de l'enseignement ont également été très instructives et me permettront de mieux appréhender le regard des parents sur l'évaluation et le suivi de leurs enfants.

Un merci tout particulier à Nathalie et Elise pour leurs conseils avisés concernant le traitement des données d'imagerie. Votre aide m'a permis de gagner un temps non négligeable et de mieux apprécier les contraintes et limites de l'IRM.

Je tiens également à remercier Jean-Luc et Fabrice sans qui le quotidien à l'animalerie serait bien différent ! Merci aux étudiants, post-doctorants et ingénieurs avec qui les repas quotidiens me manqueront : Aurélie, Elodie, Romain, Eric, Raphaëlle, Flavia, Nazied, Justine, Augustin, Marion(s). Merci aux étudiants que j'ai l'occasion d'encadrer et de suivre au cours de leur stage : Kévin, Stephen et Justine. Justine, ton aide de ces derniers mois m'a réellement soulagé. Merci ! Ton dynamisme et ta persévérance vont, je n'en doute pas, te permettre de t'épanouir en thèse. Je tâcherai de t'accompagner à distance, il me reste encore sûrement quelques petites choses à t'apprendre !

Un grand merci à Elaine, dont la compagnie et le soutien au cours de ces trois années ont été précieux. J'espère que notre amitié perdurera même si nous nous engageons dans des voies différentes. Bon courage pour la dernière ligne droite ! J'ai tout fait pour que tu sois présente le

jour de ma soutenance, j'espère que tu trouveras également un jour adéquat pour que je puisse faire partie de l'assistance quand ton tour viendra !

Je tiens à remercier Soline dont l'implication dans l'équipe a été remarquable et dont l'aide, aussi bien pour l'entrainement des animaux que pour les analyses m'a permis d'avancer plus sereinement. Je garderai aussi en mémoire le travail d'équipe lors des longues journées d'acquisition et surtout la période mémorable de construction du nouveau box d'entrainement. Bon courage pour la suite !

Je n'oublie évidemment pas de remercier ma famille et tout particulièrement mes parents et ma sœur dont le soutien et l'aide sont des repères extrêmement forts pour moi, et ceci malgré la distance. Christelle, merci pour tout, ces derniers mois ont été intenses et tu m'as permis, par ta compréhension et ton soutien, de m'épanouir aussi dans mes activités professionnelles que personnelles. Je vais essayer de ne pas m'engager dans trop d'activités, c'est promis !

Enfin, je ne peux terminer sans mentionner Zira, Toumaï et Elak avec lesquels j'ai passé de nombreuses heures. Les interactions que nous avons pu avoir ont été riches d'apprentissage : la patience et la persévérance dont il a fallu faire preuve au quotidien me seront utiles devant mes nouveaux élèves !

TABLE OF CONTENTS

TITRE en français

Bases neurales de la représentation de soi chez le primate non-humain, par une approche d'imagerie par résonance magnétique fonctionnelle (IRMf).

RESUME en français

L'objectif de cette thèse est d'identifier les bases neurales de la représentation de soi chez le primate non-humain, par une approche d'imagerie par résonnance magnétique fonctionnelle. Nous avons pour cela étudié la convergence multimodale 1) à l'échelle de l'aire par la description de la cartographie du sillon intraparietal dans un contexte de stimulations auditives, tactiles et visuelles et 2) à l'échelle du cerveau entier où nous décrivons précisément les sites de convergence visuo-tactile au niveau cortical. Nous avons également étudié le phénomène d'intégration multisensorielle dans un contexte visuo-tactile dynamique, pour lequel nous montrons que les effets comportementaux (étude psychophysique menée chez l'homme) et le réseau d'activations cortical sont maximisés quand le stimulus visuel prédit le stimulus tactile plutôt que lors de leur présentation simultanée. Enfin, nous avons étudié la représentation de l'espace en caractérisant les bases neurales de l'espace proche et de l'espace lointain à partir d'un dispositif expérimental naturaliste et nous montrons l'existence de deux réseaux corticaux qui traitent séparément les informations appartenant à l'espace proche et à l'espace lointain.

TITRE en anglais

Neural Basis of Self-Representation in the Non-Human Primate thanks to Functional Magnetic Resonance Imaging (fMRI)

RESUME en anglais

The aim of this thesis is to investigate the neural basis of self-representation in the non-human primate. We studied the multimodal convergence both 1) at the area level precisely mapping auditory, tactile and visual convergence in the intraparietal sulcus and 2) at the whole brain level capturing the spatial pattern of visuo-tactile cortical convergence. We also investigated the neural network subserving multisensory integration in a dynamical visuo-tactile context, showing that the strongest behavioral and cortical are obtained when the visual stimuli is predictive of the tactile stimulus rather than during simultaneous presentations. Finally, we studied the representation of space by characterizing the neural bases of near space and far space in a real naturalistic environment, thus providing the neural grounds for the observed behavioral and neuropsychological dissociation between near and far space processing.

DISCIPLINE : Neurosciences

MOTS-CLES : Imagerie par Résonance Magnétique Nucléaire (IRMf), aire VIP, convergence multisensorielle, intégration multisensorielle, psychophysique, singe macaque, espace.

Centre de Neuroscience Cognitive, UMR 5229
CNRS- Université Claude Bernard Lyon 1
67 boulevard Pinel - 69675 Bron cedex

Abbreviations

Cortical areas

MIP	medial intraparietal area
MST	medial superior temporal area
MT	medial temporal area
PEci	area PE, cingulate part
PGm	area PG, medial area
Pi	parainsular cortex
PIP	posterior intraparietal area
PMZ	paramotor zone
ProM	promotor area
PV	parietoventral cortex
SII	secondary somatosensory cortex
VIP	ventral intraparietal area
V1v	visual area V1, ventral part
V1c	visual area V1, central part
V1d	visual area V1, dorsal part
V2v	visual area V2, ventral part
V2d	visual area V2, dorsal part
V3	visual area V3
V3A	visual area V3A
1, 2	somatosensory areas 1 and 2
3a, 3b	somatosensory areas 3a and 3b
6Vam	area 6Va, medial part
6Vb	ventral premotor area 6Vb

7b somatosensory area 7b

8as area 8as

11 orbitofrontal area 11

13 orbitofrontal area 13

24d cingulate area 24d

46p area 46, posterior part

Cortical sulci

AS arcuate sulcus

CgS cingulate sulcus

CeS central sulcus

IOS inferior occipital sulcus

IPS intraparietal sulcus

LaS lateral (Sylvian) sulcus

LuS lunate sulcus

OTS occipital temporal sulcus

POS parieto-occipital sulcus

PS principal sulcus

STS superior temporal sulcus

Manuscript organization

The manuscript begins with an introduction whose aim is to give an overview of the field of multisensory convergence (introducing Chapters 1 and 2) and multisensory integration (introducing Chapters 3 and 4).

The result section is organized in seven independent chapters, corresponding to published, submitted or in progress manuscripts. Chapter 1 presents the result of the mapping of visual, tactile and auditory modalities within the intraparietal sulcus. Chapter 2 is focused on the visuo-tactile convergence at the whole brain level. Experiments conducted in Chapter 3 present human psychophysical results that demonstrate that tactile detection is enhanced by visual predictive cues. Using the same stimuli, we investigated in Chapter 4 the neural basis of multisensory integration and cross-modal impact prediction thanks to fMRI in the non-human primate in a passive fixation task. In Chapter 5, we described the cortical networks of near space and far space in the non-human primate. Last, Chapter 6 investigates the neural correlates of blink events and describes the cortical blink-related activations independently of the sensory context.

A general discussion, conclusions and perspectives section wraps up the thesis manuscript.

INTRODUCTION

I. Multisensory convergence

Advances in neurosciences in the last decades have repeatedly challenged our views on the organization of cortical sensory processing. Early anatomical (Kuypers et al. 1965) and lesion studies (Massopust et al. 1965) led to the description of segregated anatomical pathways, each processing a specific sensory modality. Amongst the different sensory modalities, primary visual processing was described to take place in occipital striate cortex (area V1), primary somatosensory processing in central sulcus (primary somatosensory cortex, S1) and primary auditory processing in the temporal plane of lateral sulcus (area A1).

In 1991, Felleman and Van Essen (Felleman and Van Essen 1991) refined this view, proposing a massively parallel, hierarchical, processing organization of the visual system, in which the initial sensory stages are performed, by low level unimodal sensory areas, while later processing stages are performed by multisensory higher-order associative regions (also called multimodal or cross-modal regions, Mesulam 1998), such as the temporal cortex (Beauchamp, Lee, et al. 2004; Barraclough et al. 2005) or the parietal cortex (Duhamel et al. 1998; Avillac et al. 2005; Schlack et al. 2005; Sereno and Huang 2006; Guipponi et al. 2013).

In this section, we will first define what multisensory convergence is. We will then describe the major cortical and subcortical sites where this phenomenon takes place. Finally, based on recent anatomical, electrophysiological and imaging studies, we will nuance the classical view of primary unisensory processing areas which appear to be highly modulated by other sensory modalities.

A. Definition of multisensory convergence

A *multisensory convergence area* is a brain region which receives afferent connections from different sensory modalities (Pandya and Kuypers 1969; Jones and Powell 1970; Meredith 2002).

Let's take an example to illustrate this definition. In the context of speech processing, salient information you perceive from the environment is the sight of the person who speaks and the sound of his/her voice. If the visual information is processed in the occipital cortex and the auditory information in the temporal cortex, putative region(s) of multisensory speech processing would receive afferent connections from visual and auditory primary cortices. Such a multisensory convergence has been described in the superior temporal sulcus (Wright et al. 2003).

B. Multisensory convergence in associative areas

Multisensory convergence has been described in numerous species including rodents (Toldi et al. 1986; Di et al. 1994; Barth et al. 1995; Brett-Green et al. 2003, 2004), cats (Berman and Cynader 1972; Minciacchi et al. 1987; Wallace et al. 1992; Yaka et al. 2002), monkeys and humans. Monkey and human convergence areas are detailed in the following subsections.

In rodents, Toldi and colleagues for instance mapped the acoustic, somatosensory and visual areas of the rat cerebral cortex (Toldi et al. 1986). They identified for each pair of modalities sensory convergence areas between the cortical representations of each unimodal domains and speculated that such areas would subserve real physiological interactions between the different sensory systems. Interestingly, this result tends to be generally applicable: unimodal regions would be surrounded by transition zones which contain multisensory neurons (Wallace et al. 2004).

In cats, multisensory convergence is described in the anterior ectosylvian sulcus (AES) and the lateral bank of the lateral suprasylvian sulcus. In both regions, no systematic spatial correspondence was found between the sensory receptive fields (Minciacchi et al. 1987; Yaka et al. 2002).

1. **Convergence in associative areas in monkeys**

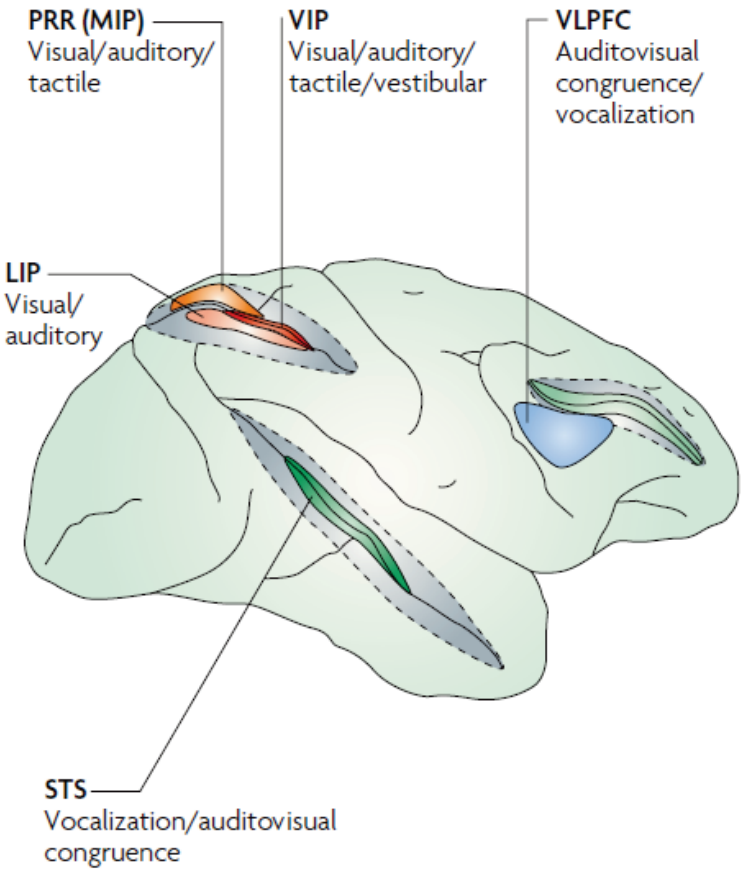

Figure 1. Multisensory regions in monkeys, extracted from (Stein and Stanford 2008). Posterior parietal multisensory convergence areas are illustrated here with Lateral Intraparietal area (LIP), Medial Intraparietal area (MIP) and Ventral Intraparietal area (VIP), temporal areas with the Superior Temporal Sulcus (STS) and frontal areas with the ventro-lateral prefrontal cortex (VLPFC).

1.1 Parietal cortex

Most of the studies about the multisensory convergence have focused on the posterior parietal cortex (Pandya and Kuypers 1969; Jones and Powell 1970; Hyvärinen and Poranen 1974; Hyvärinen 1981; Pandya and Seltzer 1982; Seltzer and Pandya 1986), where sensory information from different modalities converges: afferent inputs from visual extrastriate areas (Maunsell and van Essen 1983; Ungerleider and Desimone 1986), somatosensory cortex (Seltzer and Pandya 1980; Disbrow et al. 2003), auditory cortex (Lewis and Van Essen 2000) and vestibular nuclei (Faugier-Grimaud and Ventre 1989; Akbarian et al. 1994) result in visual (Vanduffel et al. 2001; Bremmer, Duhamel, et al. 2002; Zhang and Britten 2004), tactile (Duhamel et al. 1998; Avillac et al. 2005, 2007; Rozzi et al. 2008), auditory (Mazzoni et al. 1996; Grunewald et al. 1999; Schlack et al. 2005) and vestibular (Bremmer, Klam, et al. 2002; Chen et al. 2011) neuronal responses.

1.2 Superior Temporal Sulcus

The Superior Temporal Sulcus (STS) is also an important site of multisensory convergence. Anatomical studies identified visual, auditory and somatosensory inputs targeting this region (Jones and Powell 1970; Seltzer and Pandya 1978; Schroeder and Foxe 2002). The most described multisensory area in the STS is the superior temporal polysensory area (STP). The totality of STP neurons is visual responsive, half of them are also auditory or tactile responsive (Bruce et al. 1981; Beauchamp et al. 2008) and a small proportion are responsive to the three sensory modalities (Benevento et al. 1977; Desimone and Gross 1979; Leinonen et al. 1980; Bruce et al. 1981; Hikosaka et al. 1988; Watanabe and Iwai 1991). STP is connected to multisensory areas of fronto-lateral, orbitofrontal and cingulate cortices (Bruce et al. 1981).

1.3 Frontal and prefrontal cortex

In the frontal cortex, periarcuate region has been extensively studied for its multisensory properties (Rizzolatti et al. 1981a, 1981b; Fogassi et al. 1992, 1996; Graziano et al. 1997, 1999; Graziano and Gandhi 2000; Graziano and Cooke 2006). This region, referred to as the ventral premotor area (PMv) is responsive to visual, tactile and auditory stimulations. If unimodal visual neurons have been described rostral to the arcuate sulcus, both somatosensory and bimodal visuo-somatosensory neurons are located caudal to the arcuate sulcus (Rizzolatti et al. 1981a, 1981b).A small proportion of bimodal visuo-tactile neurons also respond to auditory stimulations and can consequently been classified as trimodal (Graziano et al. 1999). The part of the ventral premotor area located in the precentral gyrus has been called polysensory zone (PZ) or paramotor zone (PMZ). This region is anatomically connected to area VIP for the tactile and visual inputs (Luppino et al. 1999). Auditory afferents might come from area 7b (Graziano et al. 1999).

The prefrontal cortex is a key component of working memory and receives visual and auditory inputs the convergence of which has been found at the neuronal scale (Watanabe 1992).

More anteriorly, the orbitofrontal cortex has also been characterized as a site of multisensory convergence receiving visual, tactile, gustatory and olfactory inputs (Barbas 1993; Rolls and Baylis 1994; Rolls 2004).

1.4 Insular cortex

Insular cortex, located in the depth of the lateral sulcus, is responsive to olfactory, gustatory, somatosensory, visual and auditory stimulations (Mufson and Mesulam 1984; Augustine 1996). Additionally, bimodal neurons responsive both to gustatory and tactile stimulations on the tongue are found in the insular cortex (Scott et al. 1994). Bimodal visuo-auditory neurons have been found thanks to single-cell recordings (Benevento et al. 1977).

2. Convergence in associative areas in humans

Convergence in human cortical areas has been studied thanks to non-invasive neuroimaging techniques (Downar et al. 2000; Bremmer et al. 2001; Calvert 2001; Wright et al. 2003; Beauchamp, Lee, et al. 2004; van Atteveldt et al. 2004; Noesselt et al. 2007) and behavioral deficits of patients with lesions in these areas (Theuber 1966). The main human multisensory regions are inferior prefrontal cortex, premotor cortex, posterior parietal cortex and posterior superior temporal sulcus (Figure 2, Stein and Stanford 2008). Multisensory regions thus appear to be very similar between man and monkey.

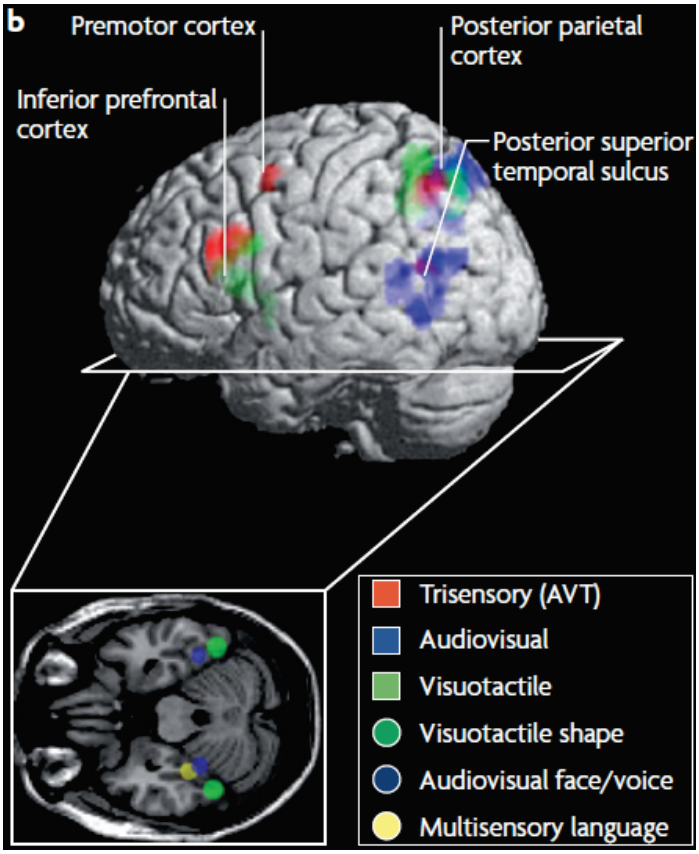

Figure 2. Multisensory regions in humans, extracted from (Stein and Stanford 2008).

STS has been characterized as multisensory by its responses to visual and auditory stimulations in numerous studies (see (Beauchamp 2005a) for a review). This brain region

responds to simple stimuli, such as visual gratings, but also to meaningful stimuli, such as moving people or objects (Beauchamp et al. 2002). Wright and colleagues have investigated anterior STS activations with animated characters speaking single words (Wright et al. 2003). Somatosensory responses have also been reported in STS (Disbrow et al. 2001; Golaszewski et al. 2002; Burton et al. 2006), and multisensory STS region responding to auditory, visual and somatosensory stimulations has been described by Beauchamp and colleagues few years later (Beauchamp et al. 2008).

Frontal cortexalso exhibits multisensory regions, such as the ventral premotor cortex (Bremmer et al. 2001; Macaluso and Driver 2001), ventromedial prefrontal cortex (Bushara et al. 2001; Calvert 2001), dorsolateral prefrontal cortex (Banati et al. 2000; Lewis et al. 2000; Bremmer et al. 2001; Bushara et al. 2003), as well as anterior cingulate cortex (Banati et al. 2000; Downar et al. 2000, 2002; Calvert 2001; Laurienti et al. 2003).

Multisensory processing has been well studied in parietal region (Downar et al. 2000; Bremmer et al. 2001; Culham and Kanwisher 2001; Sereno and Huang 2006; Huang et al. 2012), characterizing visuo-auditory convergence (Calvert et al. 2000; Lewis et al. 2000; Bushara et al. 2001), visuo-somatosensory convergence relative to the hand, arm or face (Bremmer et al. 2001; Macaluso and Driver 2001; Macaluso et al. 2003; Grefkes and Fink 2005) and even trimodal visuo-tactile-auditory convergence (Bremmer et al. 2001).

Anterior part of the insula is also a multisensory convergence site (Banati et al. 2000; Downar et al. 2000, 2002; Lewis et al. 2000; Bushara et al. 2001, 2003; Calvert et al. 2001).

C. Multisensory convergence in sub-cortical regions

Sub-cortical multisensory convergence has been investigated through rat, ferret, cat, monkey and human.

The superior colliculus, which is involved in attention and gaze orientation, receives multisensory inputs in all the above mentioned species (Stein and Meredith 1993; Wallace et al. 1996; Bell et al. 2001, 2003; Bushara et al. 2001; Calvert et al. 2001; Meredith et al. 2001; Skaliora et al. 2004) through bottom-up (*e.g.* the retina, Beckstead and Frankfurter 1983) as well as top-down projections (*i.e.* the cortex, Meredith and Clemo 1989).

The macaque putamen is also multisensory site (Graziano and Gross 1993) through its direct connections with area 7b (Weber and Yin 1984; Cavada and Goldman-Rakic 1991) and ventral premotor area (PMv, Künzle 1978).

Posterior thalamus (Steriade et al. 1997; Bushara et al. 2001), locus coeruleus (Grant et al. 1988), inferior colliculus (Tawil et al. 1983; Groh et al. 2001), basal ganglia (Wilson et al. 1983), amygdala and hippocampus (Turner et al. 1980) also exhibit multisensory properties.

D. Multisensory convergence in primary areas

Traditionally, primary sensory cortices, such as the primary auditory area A1, somatosensory area S1, or visual area V1, are considered to be unimodal. As a consequence, neuronal activity in each of these primary sensory areas is supposed to be exclusively elicited by its own sensory modality (Mesulam 1998). These areas are considered to represent both the highest processing level in their modality-specific ascending pathways and the lowest level of cortical processing. Information is, in this point of view, further treated in higher order areas, such as multimodal associative areas (Mesulam 1998; Kaas and Collins 2001).

In the last decade, an increasing number of studies have challenged this traditional concept of unimodal primary sensory cortices describing corticocortical and subcortical connections to other modalities (Figure 3; Ghazanfar and Schroeder 2006; Scheich et al. 2007).

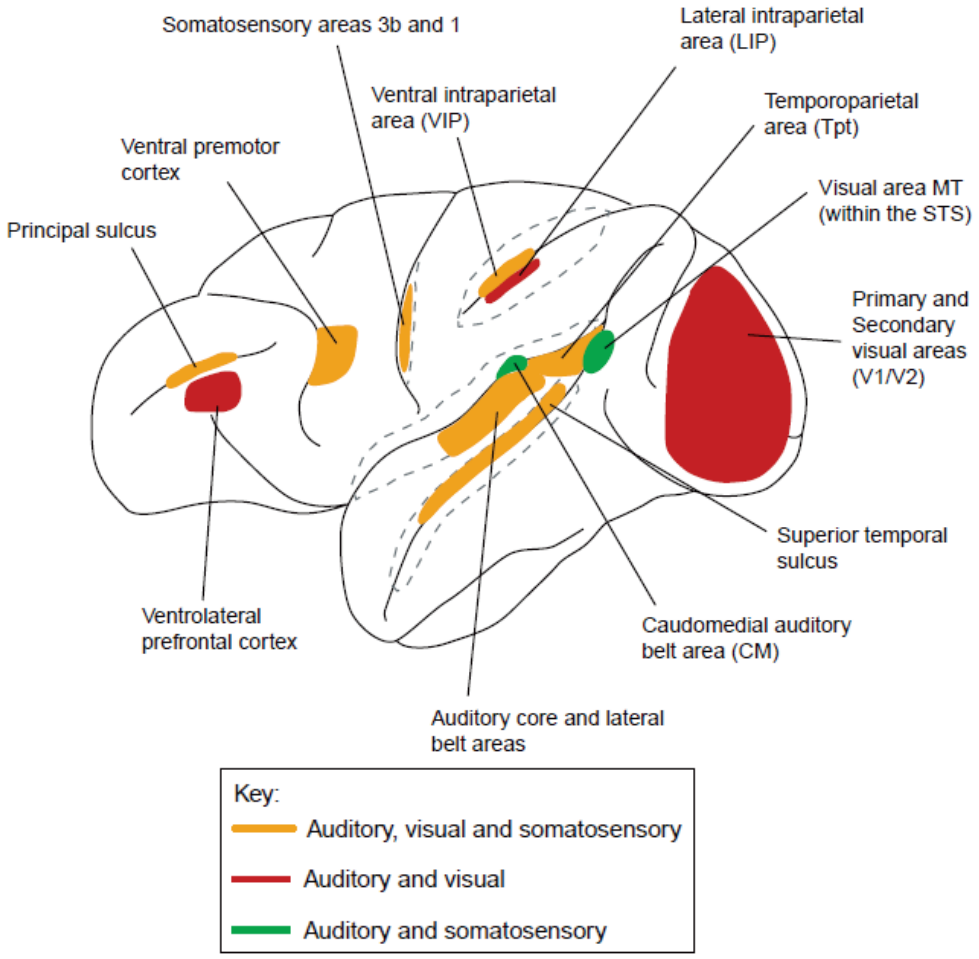

Figure 3. Multisensory regions in the primate brain, extracted from (Ghazanfar and Schroeder 2006). Colored areas represent regions where anatomical and/or electrophysiological data have demonstrated multisensory convergence.

The example of the auditory cortex can be illustrated by physiological and anatomical studies. For instance, neuronal activity is auditory cortex can be elicited or modulated by visual stimulations (Cahill et al. 1996; Werner-Reiss et al. 2003; Brosch et al. 2005; Ghazanfar et al. 2005; Bizley et al. 2007) or by tactile stimulations (Wallace et al. 2004; Brosch et al. 2005). Heteromodal connections exist between auditory and visual cortices (Falchier et al. 2002; Rockland and Ojima 2003; Cappe and Barone 2005) as well as between

auditory and tactile cortices (Cappe and Barone 2005; Budinger et al. 2006; de la Mothe et al. 2006; Smiley et al. 2007).

We took the example of the auditory cortex but evidence between tactile and visual cortices have also been described (Wallace et al. 2004).

The contribution of these heteromodal projections to the modulation of the response of early sensory neurons is confirmed both by single cell recording studies (Schroeder and Foxe 2005; Vasconcelos et al. 2011; Iurilli et al. 2012) and functional neuroimaging studies (Sathian et al. 1997; Macaluso et al. 2000; Amedi et al. 2001). On the basis of the growing evidence for pervasive multisensory influences at all levels of cortical processing, Ghazanfar and Schroeder question, in a recent review, whether multisensory processing could actually be an essential property of neocortex (Ghazanfar and Schroeder 2006).

E. Problematic and introduction to Chapters 1 and 2

Despite the accumulated knowledge about the parietal cortex and its functions, few functional neuroimaging studies have addressed multisensort convergence in humans (Bremmer et al. 2001; Sereno and Huang 2006). In particular, no such data are available in the non-human primate. To bridge this gap and allow direct transfer of accumulated knowledge on multimodal parietal functions, from single-cell recording studies in the macaque, to observations derived from human imaging studies, we conducted a multimodal mapping of the intraparietal sulcus in the macaque monkey thanks to functional magnetic resonance imaging (fMRI). This study is presented in Chapter 1 in which we describe the spatial extent of visual, somatosensory and auditory modalities.

In Chapter 2, we focus on visuo-tactile convergence and we investigate the whole brain spatial pattern of convergence in a context of static visual stimulations and tactile stimulations delivered either at the center of the face, at the periphery of the face, or on shoulders. This

allows us to capture the extent of this heteromodal convergence and bring about novel observation about the specificity of this convergence to the sensory context.

II. Integration of sensory inputs

For several centuries multisensory perception has raised interest in the scientific community (Molyneux, 1688; James, 1890). The phenomenon was first described behaviorally and demonstrated how effectively the senses merge the information to enhance the salience of biologically meaningful events. For few decades, electrophysiological and imaging techniques have been providing tools to investigate the neural bases of this process.

The convergence of inputs is related to spatially common responses to stimuli presented in isolation. The phenomenon studied in this section is relative to the simultaneous presentation of stimuli from different sensory modalities. The consequences of simultaneous presentation of sensory modalities could be described at the behavioral, single-cell or brain levels. We will consider successively each of these aspects in the following sub-sections to introduce the experiments presented in Chapters 3 and 4.

A. Behavioral evidence of multisensory integration

1. Ventriloquism

One of the examples which illustrates ventriloquism is the voices coming from speakers we attribute to the characters seen on the film screen. The auditory modality is altered by the predominant visual information (Driver 1996). This illusionary phenomenon is dependent on spatial and temporal factors (Lewald and Guski 2003): the temporal asynchrony does not exceed 100ms. The better the illusion, the harder the localization of the sound (Jack and Thurlow 1973; Slutsky and Recanzone 2001). The explanation for a visual capture instead of

a tactile capture is that the visual modality has a better spatial sharpness (Welch and Warren 1980; Ernst and Bülthoff 2004).

2. McGurk effect

In a noisy environment, speech understanding is increased when the speaker is both heard and seen (Sumby and Pollack 1954). However, an illusory percept could appear when what is heard is different from what is seen (McGurk and MacDonald 1976): an auditory "ba" presented with the mouth movements of "ga" is perceived by the subject (seeing and listening) as a completely different syllable, "da". This illusion has been called the McGurk effect and is an evidence of multisensory integration of auditory and visual modalities. Interestingly, this illusion is not experienced by all individuals (Gentilucci and Cattaneo 2005). Left STS is proposed to be a key structure for explaining interindividual differences in speech perception (Nath and Beauchamp 2012).

3. Multisensory detection

Bimodal target presentation in comparison to unimodal presentation decreases both reaction times and detection thresholds.

3.1 Decrease in reaction times

In detection tasks, reaction times are dramatically decreased in bimodal presentation context (Todd 1912; Hershenson 1962; Miller 1982; Welch and Warren 1986; Schröger and Widmann 1998; Giard and Peronnet 1999; Taylor et al. 1999). Saccadic reaction times (Hughes et al. 1994; Frens et al. 1995; Harrington and Peck 1998; Colonius and Arndt 2001; Corneil et al. 2002) or manual reaction times (Hughes et al. 1994) are decreased to detect visuo-auditory or visuo-tactile targets in comparison with unisensory targets (Groh and Sparks 1996; Forster et al. 2002; Amlôt et al. 2003; Diederich et al. 2003). Mathematical models proposed by Colonius and colleagues demonstrate that a purely statistical facilitation

effect without any integrative processes at the neuronal level does not explain the behavioral results (Colonius and Arndt 2001). The alternative proposal suggests that the unimodal sensory information is integrated in specific brain areas, which is consistent with experimental studies both in human and animal models (Stein and Meredith 1993).

3.2 Decrease in detection thresholds

Detection threshold can be decreased in bimodal target presentation condition in comparison with unimodal stimulations (London 1954; Welch and Warren 1986). For instance, in a visual target detection task in which the visual salience is degraded as well as the time of presentation, the presence of an auditory stimulus in conjunction with the visual target decreases its detection threshold (Frassinetti et al. 2002; Bolognini et al. 2005).

B. Neurophysiological approach

At the neuronal level, three different classes of neurons can be defined. The first class is the unimodal neurons: those neurons respond exclusively to a single sensory modality. In other words, their activity is above the baseline only when the modality the neuron is responsive to is played. The second class of neurons is bimodal (or trimodal etc.) neurons: those neurons have the particularity to produce an activity above the baseline in a context of more than a single sensory modality (Meredith and Stein 1983; Stein and Stanford 2008). In the second class of neurons, further investigations can be led to characterize the behavior of those neurons when the modalities the neuron is responsive to are played. Multimodal responsiveness at the single cell level defines multisensory convergence but not integration (Stein et al. 2009). If the neuron produces an activity which is different from the maximum activity produced with either unisensory stimulus (most usually used criterion, called maximum criterion), integration is supposed to take place. If the activity is greater than the maximum criterion, the neuron performs a multisensory enhancement. If the activity is lower

than the maximum criterion, the neuron is performing a multisensory suppression. One particular case of multisensory enhanced neuron is the superadditivity: it corresponds to an activity which is greater than the sum of the unisensory activities. The third class of neurons is the subthreshold neurons: those neurons are responsive to a single sensory modality but their activity is characterized by a multisensory enhancement in multisensory context (Allman and Meredith 2007; Allman et al. 2008; Meredith and Allman 2009).

C. fMRI approach

1. Searching for equivalence between fMRI and electrophysiological recordings

Blood Oxygenation level-dependent (BOLD) activation is the result of the vasculature flow which is increasing in an active region. The main issue with such a technique is its spatial and temporal resolutions compared with electrophysiological recordings. As a technique based on hemodynamic flow, the temporal resolution is second-based. Additionally the spatial resolution is around 0.5 mm^3, which is big enough to contain several thousands of neurons. As a consequence, the BOLD signal is the resultant response of thousands of neurons for each voxel.

One of the questions raised by the study of multisensory integration is how far we can compare fMRI results with electrophysiological recordings. Clear links between both techniques have been provided (Attwell and Iadecola 2002; Logothetis and Wandell 2004). Nevertheless, fMRI is recording the indirect activity of thousands of neurons whereas electrophysiology records the activity of single neurons. This difference is at the basis of the main issues to compare results between these techniques. Accumulated evidence have shown that the populations within multisensory brain regions are highly heterogeneous, that is to say contain a mixture of unisensory neurons from different sensory modalities in addition to bimodal and subthreshold multisensory neurons (Benevento et al. 1977; Bruce et al. 1981;

Meredith and Stein 1983, 1986; Hikosaka et al. 1988; Barraclough et al. 2005; Allman and Meredith 2007; Allman et al. 2008; Stein and Stanford 2008). As a consequence, the fMRI response of each voxel results from the combination of heterogeneous neuronal responses.

2. The use of superadditivity criterion

Based on electrophysiological studies, multisensory integration with fMRI has first been investigated with the superadditivity criterion (Calvert et al. 2000). With such a criterion, a region can be characterized as being multisensory once bimodal BOLD response is greater than the sum of unimodal BOLD responses (Figure 4). In this pioneer study, Calvert and colleagues used auditory (voices) and visual (video of speaking people) stimulations and showed that an area located in the superior temporal sulcus exhibited a bimodal BOLD response greater than the sum of unimodal BOLD responses.

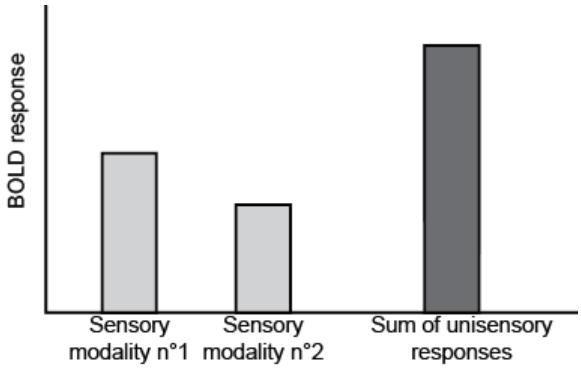

Figure 4. Superadditivity criterion to access multisensory integration.

The use of superadditivity criterion is based on 1) BOLD activation is a time-invariant system and 2) the null-hypothesis to be rejected is that the neuronal population does not contain multisensory neurons (Meredith and Stein 1983; Calvert et al. 2000, 2001). The first criterion means that the modulation of bimodal stimulation is the sum of BOLD responses to unimodal stimulations (Boynton et al. 1996; Dale and Buckner 1997; Heeger and Ress 2002).

The criterion of superadditivity consequently stands that a region is multisensory once the multimodal stimulation leads to an activity greater than the sum of unimodal stimulation (*i.e.* in the case of any multimodal neurons).

Although superadditivity allowed to describe multisensory regions (Calvert et al. 2000, 2001), other studies did not find multisensory positive results in well-known multisensory regions using the same criterion (Beauchamp, Argall, et al. 2004; Beauchamp, Lee, et al. 2004; Beauchamp 2005b; Laurienti et al. 2005; Stevenson et al. 2007). Such findings led researchers to propose alternative criteria.

3. The maximum criterion

One of the alternative criteria of superadditivity is the maximum criterion. One region is characterized as multisensory once the BOLD response in bimodal stimulation context is greater than the maximal unimodal BOLD response (Figure 5).

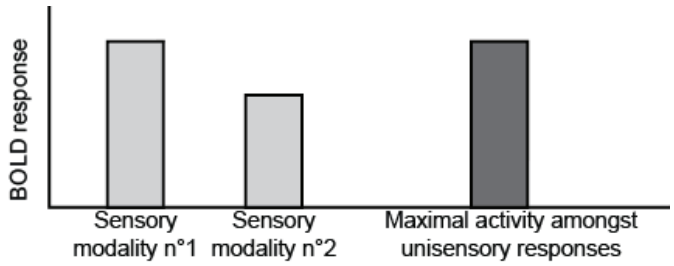

Figure 5. Maximum criterion to access multisensory integration.

In a context of auditory, visual, and auditory-visual object recognition task, Beauchamp discussed the use of different statistical criteria to investigate which ones allow to classify the STS region (which has been described to be a major site of auditory-visual integration) as multisensory (Beauchamp 2005b).

The maximum criterion is more liberal than the superadditivity criterion. Consequently, it could lead to false-positive results. Let's imagine that a region contains only unisensory

neurons. If the BOLD response obtained in bimodal stimulation context is greater than the maximum criterion, then this region would have been wrongly classified as integrating unimodal inputs.

In such a context, several models have been proposed to define the appropriate criterion to identify a multisensory region.

4. Overview of the different BOLD activation models

James and Stevenson review the different models available (Figure 6, James and Stevenson 2012).

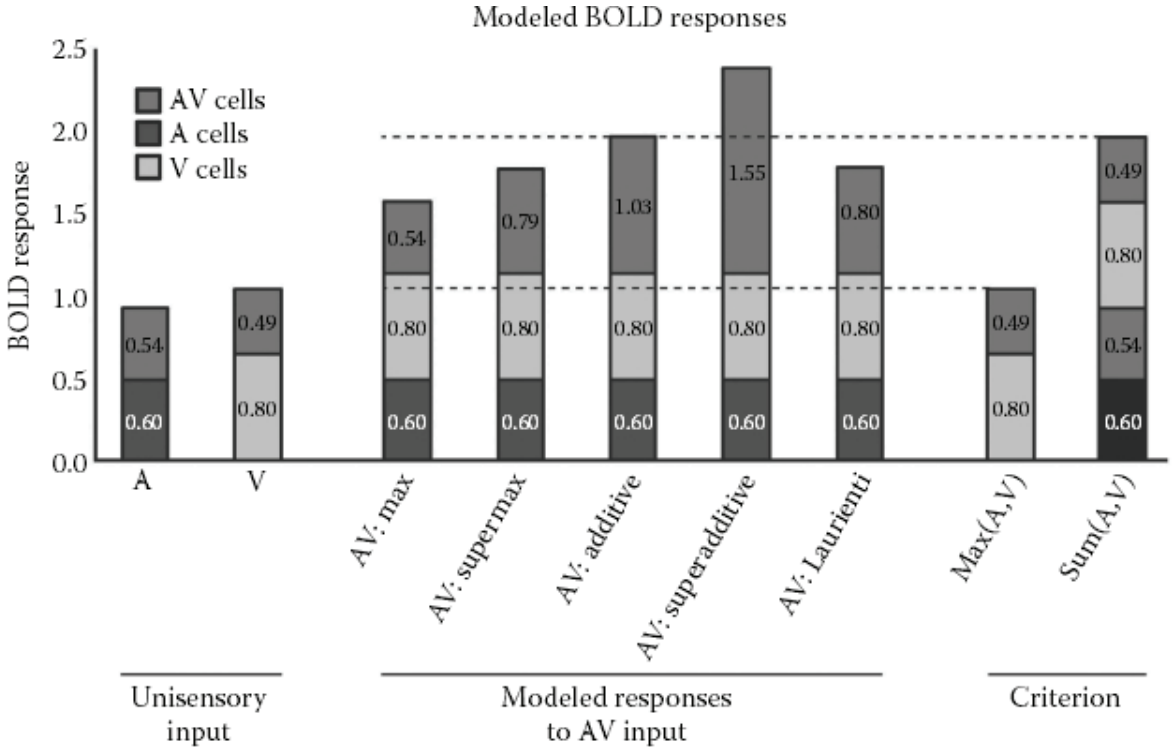

Figure 6. Models of BOLD activation with multisensory stimulation, extracted from (James and Stevenson 2012).

The first column of the figure is the response to auditory stimulations, the second column the response to visual stimulations. For each column, the BOLD response presented is the sum of contributions of unimodal neurons (either auditory or visual) and bimodal neurons

(auditory-visual neurons). The last two columns represent the criteria detailed in II.C.2 and II.C.3). The columns 3 to 7 present the modeled BOLD responses the simulation of which have been based on statistics of recorded spike counts in the superior colliculus (Laurienti et al. 2005). The differences between models are solely based on the bimodal neurons' contribution described as follows:

- The maximum model: the bimodal neurons' contribution corresponds to the maximum value of bimodal activity with unimodal visual or auditory stimulation.
- The super maximum model: it is also based on the maximum value of bimodal activity with unimodal visual or auditory stimulation, which has been additionally weighted by a 150% factor.
- The Additive model: the bimodal cells' contribution is calculated from the sum of bimodal activities in unisensory visual and auditory stimulations.
- The superadditive model: it is also based on the sum of bimodal activities in unisensory visual and auditory stimulations, which has been additionally weighted by a 150% factor.
- The Laurienti model: the contribution of bimodal neurons is calculated from recorded impulse counts.

If we take the Laurienti model as true because it is based on recorded data, the criterion based on the sum of unisensory BOLD activation (Figure 6, last column) is clearly too conservative, which has also been reported in several studies (Beauchamp, Argall, et al. 2004; Beauchamp, Lee, et al. 2004; Beauchamp 2005b; Laurienti et al. 2005; Stevenson et al. 2007). On the other hand, the maximum criterion appears too liberal.

The reasons Laurienti and colleagues (Laurienti et al. 2005) proposed to explain that the bimodal BOLD response does not exceed the sum of unisensory BOLD responses is: 1) the proportion of bimodal neurons is weak in comparison to unisensory neurons; 2) amongst the

bimodal neurons, only some of them are superadditive and 3) the bimodal superadditive neurons have relatively low impulse counts compared to the other neurons.

In reference to Laurienti and colleagues' statistics, the appropriate criterion would be between the maximum unisensory BOLD response and the sum of unisensory BOLD responses.

D. Problematic and introduction to Chapters 3 and 4

Based on the results collected in Chapters 1 and 2 in which we report the multisensory convergence mapping of the intraparietal sulcus and the visuo-tactile convergence network at the whole brain scale, we designed an fMRI protocol to investigate visuo-tactile multisensory integration (Chapter 4). Monkeys were exposed separately to visual looming stimuli (cones coming towards their face), or to tactile airpuffs at the location predicted to the visual cone trajectory, or to these visuo-tactile stimuli presented together. We manipulated the spatial congruence between the visual and tactile stimuli (airpuff delivered at the predicted side of the face, or on the opposite side of the face) and the temporal asynchrony between the visual and tactile stimuli (airpuff delivered at the predicted time of the impact *i.e.* after a short delay following the video presentation, or at the same time). Amongst the problematic raised by this experiment, we were wondering 1) which areas of our identified visuo-tactile convergence network would exhibit an integrative profile and 2) whether the best integrative window would be obtained for simultaneous visuo-tactile presentation or for tactile stimulation delivered at the predicted time of the cone trajectory. This fMRI experiment was run in parallel with a human psychophysical experiment presented in Chapter 3. In this study, we used the same stimuli (with manipulation of spatial and temporal congruencies) as in the fMRI experiment and we investigate the behavioral benefits of predictive visual cues on tactile detection.

Bibliography

Akbarian S, Grüsser OJ, Guldin WO. 1994. Corticofugal connections between the cerebral cortex and brainstem vestibular nuclei in the macaque monkey. J Comp Neurol. 339:421–437.

Allman BL, Keniston LP, Meredith MA. 2008. Subthreshold auditory inputs to extrastriate visual neurons are responsive to parametric changes in stimulus quality: sensory-specific versus non-specific coding. Brain Res. 1242:95–101.

Allman BL, Meredith MA. 2007. Multisensory processing in "unimodal" neurons: cross-modal subthreshold auditory effects in cat extrastriate visual cortex. J Neurophysiol. 98:545–549.

Amedi A, Malach R, Hendler T, Peled S, Zohary E. 2001. Visuo-haptic object-related activation in the ventral visual pathway. Nat Neurosci. 4:324–330.

Amlôt R, Walker R, Driver J, Spence C. 2003. Multimodal visual-somatosensory integration in saccade generation. Neuropsychologia. 41:1–15.

Attwell D, Iadecola C. 2002. The neural basis of functional brain imaging signals. Trends Neurosci. 25:621–625.

Augustine JR. 1996. Circuitry and functional aspects of the insular lobe in primates including humans. Brain Res. 22:229–244.

Avillac M, Ben Hamed S, Duhamel J-R. 2007. Multisensory integration in the ventral intraparietal area of the macaque monkey. J Neurosci. 27:1922–1932.

Avillac M, Denève S, Olivier E, Pouget A, Duhamel J-R. 2005. Reference frames for representing visual and tactile locations in parietal cortex. Nat Neurosci. 8:941–949.

Banati RB, Goerres GW, Tjoa C, Aggleton JP, Grasby P. 2000. The functional anatomy of visual-tactile integration in man: a study using positron emission tomography. Neuropsychologia. 38:115–124.

Barbas H. 1993. Organization of cortical afferent input to orbitofrontal areas in the rhesus monkey. Neuroscience. 56:841–864.

Barraclough NE, Xiao D, Baker CI, Oram MW, Perrett DI. 2005. Integration of visual and auditory information by superior temporal sulcus neurons responsive to the sight of actions. J Cogn Neurosci. 17:377–391.

Barth DS, Goldberg N, Brett B, Di S. 1995. The spatiotemporal organization of auditory, visual, and auditory-visual evoked potentials in rat cortex. Brain Res. 678:177–190.

Beauchamp MS. 2005a. See me, hear me, touch me: multisensory integration in lateral occipital-temporal cortex. Curr Opin Neurobiol. 15:145–153.

Beauchamp MS. 2005b. Statistical Criteria in fMRI Studies of Multisensory Integration. Neuroinformatics. 3:093–114.

Beauchamp MS, Argall BD, Bodurka J, Duyn JH, Martin A. 2004. Unraveling multisensory integration: patchy organization within human STS multisensory cortex. Nat Neurosci. 7:1190–1192.

Beauchamp MS, Lee KE, Argall BD, Martin A. 2004. Integration of auditory and visual information about objects in superior temporal sulcus. Neuron. 41:809–823.

Beauchamp MS, Lee KE, Haxby JV, Martin A. 2002. Parallel visual motion processing streams for manipulable objects and human movements. Neuron. 34:149–159.

Beauchamp MS, Yasar NE, Frye RE, Ro T. 2008. Touch, sound and vision in human superior temporal sulcus. Neuroimage. 41:1011–1020.

Beckstead RM, Frankfurter A. 1983. A direct projection from the retina to the intermediate gray layer of the superior colliculus demonstrated by anterograde transport of horseradish peroxidase in monkey, cat and rat. Exp Brain Res. 52:261–268.

Bell AH, Corneil BD, Meredith MA, Munoz DP. 2001. The influence of stimulus properties on multisensory processing in the awake primate superior colliculus. Can J Exp Psychol Rev. 55:123–132.

Bell AH, Corneil BD, Munoz DP, Meredith MA. 2003. Engagement of visual fixation suppresses sensory responsiveness and multisensory integration in the primate superior colliculus. Eur J Neurosci. 18:2867–2873.

Benevento LA, Fallon J, Davis BJ, Rezak M. 1977. Auditory--visual interaction in single cells in the cortex of the superior temporal sulcus and the orbital frontal cortex of the macaque monkey. Exp Neurol. 57:849–872.

Berman N, Cynader M. 1972. Comparison of receptive-field organization of the superior colliculus in Siamese and normal cats. J Physiol. 224:363–389.

Bizley J, Nodal F, Nelken I, King A: Investigating auditory-visual interactions in ferret auditory cortex. 28th Midwinter research meeting Association for Research in Otolaryngology 2005: 351.

Bizley JK, Nodal FR, Bajo VM, Nelken I, King AJ. 2007. Physiological and anatomical evidence for multisensory interactions in auditory cortex. Cereb Cortex. 17:2172–2189.

Bolognini N, Frassinetti F, Serino A, Làdavas E. 2005. “Acoustical vision” of below threshold stimuli: interaction among spatially converging audiovisual inputs. Exp Brain Res. 160:273–282.

Boynton GM, Engel SA, Glover GH, Heeger DJ. 1996. Linear systems analysis of functional magnetic resonance imaging in human V1. J Neurosci. 16:4207–4221.

Bremmer F, Duhamel J-R, Ben Hamed S, Graf W. 2002. Heading encoding in the macaque ventral intraparietal area (VIP). Eur J Neurosci. 16:1554–1568.

Bremmer F, Klam F, Duhamel J-R, Ben Hamed S, Graf W. 2002. Visual-vestibular interactive responses in the macaque ventral intraparietal area (VIP). Eur J Neurosci. 16:1569–1586.

Bremmer F, Schlack A, Shah NJ, Zafiris O, Kubischik M, Hoffmann K, Zilles K, Fink GR. 2001. Polymodal motion processing in posterior parietal and premotor cortex: a human fMRI study strongly implies equivalencies between humans and monkeys. Neuron. 29:287–296.

Brett-Green B, Fifková E, Larue DT, Winer JA, Barth DS. 2003. A multisensory zone in rat parietotemporal cortex: intra- and extracellular physiology and thalamocortical connections. J Comp Neurol. 460:223–237.

Brett-Green B, Paulsen M, Staba RJ, Fifková E, Barth DS. 2004. Two distinct regions of secondary somatosensory cortex in the rat: topographical organization and multisensory responses. J Neurophysiol. 91:1327–1336.

Brosch M, Selezneva E, Scheich H. 2005. Nonauditory events of a behavioral procedure activate auditory cortex of highly trained monkeys. J Neurosci. 25:6797–6806.

Bruce C, Desimone R, Gross CG. 1981. Visual properties of neurons in a polysensory area in superior temporal sulcus of the macaque. J Neurophysiol. 46:369–384.

Budinger E, Heil P, Hess A, Scheich H. 2006. Multisensory processing via early cortical stages: Connections of the primary auditory cortical field with other sensory systems. Neuroscience. 143:1065–1083.

Burton H, McLaren DG, Sinclair RJ. 2006. Reading embossed capital letters: an fMRI study in blind and sighted individuals. Hum Brain Mapp. 27:325–339.

Bushara KO, Grafman J, Hallett M. 2001. Neural correlates of auditory-visual stimulus onset asynchrony detection. J Neurosci. 21:300–304.

Bushara KO, Hanakawa T, Immisch I, Toma K, Kansaku K, Hallett M. 2003. Neural correlates of cross-modal binding. Nat Neurosci. 6:190–195.

Cahill L, Ohl F, Scheich H. 1996. Alteration of auditory cortex activity with a visual stimulus through conditioning: a 2-deoxyglucose analysis. Neurobiol Learn Mem. 65:213–222.

Calvert GA. 2001. Crossmodal processing in the human brain: insights from functional neuroimaging studies. Cereb Cortex. 11:1110–1123.

Calvert GA, Campbell R, Brammer MJ. 2000. Evidence from functional magnetic resonance imaging of crossmodal binding in the human heteromodal cortex. Curr Biol. 10:649–657.

Calvert GA, Hansen PC, Iversen SD, Brammer MJ. 2001. Detection of audio-visual integration sites in humans by application of electrophysiological criteria to the BOLD effect. Neuroimage. 14:427–438.

Cappe C, Barone P. 2005. Heteromodal connections supporting multisensory integration at low levels of cortical processing in the monkey. Eur J Neurosci. 22:2886–2902.

Cavada C, Goldman-Rakic PS. 1991. Topographic segregation of corticostriatal projections from posterior parietal subdivisions in the macaque monkey. Neuroscience. 42:683–696.

Chen A, DeAngelis GC, Angelaki DE. 2011. Representation of vestibular and visual cues to self-motion in ventral intraparietal cortex. J Neurosci. 31:12036–12052.

Colonius H, Arndt P. 2001. A two-stage model for visual-auditory interaction in saccadic latencies. Percept Psychophys. 63:126–147.

Corneil BD, Van Wanrooij M, Munoz DP, Van Opstal AJ. 2002. Auditory-visual interactions subserving goal-directed saccades in a complex scene. J Neurophysiol. 88:438–454.

Culham JC, Kanwisher NG. 2001. Neuroimaging of cognitive functions in human parietal cortex. Curr Opin Neurobiol. 11:157–163.

Dale AM, Buckner RL. 1997. Selective averaging of rapidly presented individual trials using fMRI. Hum Brain Mapp. 5:329–340.

De la Mothe LA, Blumell S, Kajikawa Y, Hackett TA. 2006. Cortical connections of the auditory cortex in marmoset monkeys: core and medial belt regions. J Comp Neurol. 496:27–71.

Desimone R, Gross CG. 1979. Visual areas in the temporal cortex of the macaque. Brain Res. 178:363–380.

Di S, Brett B, Barth DS. 1994. Polysensory evoked potentials in rat parietotemporal cortex: combined auditory and somatosensory responses. Brain Res. 642:267–280.

Diederich A, Colonius H, Bockhorst D, Tabeling S. 2003. Visual-tactile spatial interaction in saccade generation. Exp Brain Res. 148:328–337.

Disbrow E, Litinas E, Recanzone GH, Padberg J, Krubitzer L. 2003. Cortical connections of the second somatosensory area and the parietal ventral area in macaque monkeys. J Comp Neurol. 462:382–399.

Disbrow E, Roberts T, Poeppel D, Krubitzer L. 2001. Evidence for interhemispheric processing of inputs from the hands in human S2 and PV. J Neurophysiol. 85:2236–2244.

Downar J, Crawley AP, Mikulis DJ, Davis KD. 2000. A multimodal cortical network for the detection of changes in the sensory environment. Nat Neurosci. 3:277–283.

Downar J, Crawley AP, Mikulis DJ, Davis KD. 2002. A cortical network sensitive to stimulus salience in a neutral behavioral context across multiple sensory modalities. J Neurophysiol. 87:615–620.

Driver J. 1996. Enhancement of selective listening by illusory mislocation of speech sounds due to lip-reading. Nature. 381:66–68.

Duhamel JR, Colby CL, Goldberg ME. 1998. Ventral intraparietal area of the macaque: congruent visual and somatic response properties. J Neurophysiol. 79:126–136.

Ernst MO, Bülthoff HH. 2004. Merging the senses into a robust percept. Trends Cogn Sci. 8:162–169.

Falchier A, Clavagnier S, Barone P, Kennedy H. 2002. Anatomical evidence of multimodal integration in primate striate cortex. J Neurosci. 22:5749–5759.

Faugier-Grimaud S, Ventre J. 1989. Anatomic connections of inferior parietal cortex (area 7) with subcortical structures related to vestibulo-ocular function in a monkey (Macaca fascicularis). J Comp Neurol. 280:1–14.

Felleman DJ, Van Essen DC. 1991. Distributed hierarchical processing in the primate cerebral cortex. Cereb Cortex. 1:1–47.

Fogassi L, Gallese V, di Pellegrino G, Fadiga L, Gentilucci M, Luppino G, Matelli M, Pedotti A, Rizzolatti G. 1992. Space coding by premotor cortex. Exp Brain Res. 89:686–690.

Fogassi L, Gallese V, Fadiga L, Luppino G, Matelli M, Rizzolatti G. 1996. Coding of peripersonal space in inferior premotor cortex (area F4). J Neurophysiol. 76:141–157.

Forster B, Cavina-Pratesi C, Aglioti SM, Berlucchi G. 2002. Redundant target effect and intersensory facilitation from visual-tactile interactions in simple reaction time. Exp Brain Res. 143:480–487.

Frassinetti F, Bolognini N, Làdavas E. 2002. Enhancement of visual perception by crossmodal visuo-auditory interaction. Exp Brain Res. 147:332–343.

Frens MA, Van Opstal AJ, Van der Willigen RF. 1995. Spatial and temporal factors determine auditory-visual interactions in human saccadic eye movements. Percept Psychophys. 57:802–816.

Gentilucci M, Cattaneo L. 2005. Automatic audiovisual integration in speech perception. Exp Brain Res. 167:66–75.

Ghazanfar AA, Maier JX, Hoffman KL, Logothetis NK. 2005. Multisensory integration of dynamic faces and voices in rhesus monkey auditory cortex. J Neurosci Off J Soc Neurosci. 25:5004–5012.

Ghazanfar AA, Schroeder CE. 2006. Is neocortex essentially multisensory? Trends Cogn Sci. 10:278–285.

Giard MH, Peronnet F. 1999. Auditory-visual integration during multimodal object recognition in humans: a behavioral and electrophysiological study. J Cogn Neurosci. 11:473–490.

Golaszewski SM, Siedentopf CM, Baldauf E, Koppelstaetter F, Eisner W, Unterrainer J, Guendisch GM, Mottaghy FM, Felber SR. 2002. Functional magnetic resonance imaging of the human sensorimotor cortex using a novel vibrotactile stimulator. Neuroimage. 17:421–430.

Grant SJ, Aston-Jones G, Redmond DE Jr. 1988. Responses of primate locus coeruleus neurons to simple and complex sensory stimuli. Brain Res. 21:401–410.

Graziano MS, Gandhi S. 2000. Location of the polysensory zone in the precentral gyrus of anesthetized monkeys. Exp Brain Res. 135:259–266.

Graziano MS, Gross CG. 1993. A bimodal map of space: somatosensory receptive fields in the macaque putamen with corresponding visual receptive fields. Exp Brain Res. 97:96–109.

Graziano MS, Hu XT, Gross CG. 1997. Visuospatial properties of ventral premotor cortex. J Neurophysiol. 77:2268–2292.

Graziano MSA, Cooke DF. 2006. Parieto-frontal interactions, personal space, and defensive behavior. Neuropsychologia. 44:2621–2635.

Graziano MSA, Reiss LAJ, Gross CG. 1999. A neuronal representation of the location of nearby sounds. Nature. 397:428–430.

Grefkes C, Fink GR. 2005. The functional organization of the intraparietal sulcus in humans and monkeys. J Anat. 207:3–17.

Groh JM, Sparks DL. 1996. Saccades to somatosensory targets. I. behavioral characteristics. J Neurophysiol. 75:412–427.

Groh JM, Trause AS, Underhill AM, Clark KR, Inati S. 2001. Eye position influences auditory responses in primate inferior colliculus. Neuron. 29:509–518.

Grunewald A, Linden JF, Andersen RA. 1999. Responses to auditory stimuli in macaque lateral intraparietal area. I. Effects of training. J Neurophysiol. 82:330–342.

Guipponi O, Wardak C, Ibarrola D, Comte J-C, Sappey-Marinier D, Pinède S, Ben Hamed S. 2013. Multimodal convergence within the intraparietal sulcus of the macaque monkey. J Neurosci. 33:4128–4139.

Harrington LK, Peck CK. 1998. Spatial disparity affects visual-auditory interactions in human sensorimotor processing. Exp Brain Res. 122:247–252.

Heeger DJ, Ress D. 2002. What does fMRI tell us about neuronal activity? Nat Rev Neurosci. 3:142–151.

Hershenson M. 1962. Reaction time as a measure of intersensory facilitation. J Exp Psychol. 63:289–293.

Hikosaka K, Iwai E, Saito H, Tanaka K. 1988. Polysensory properties of neurons in the anterior bank of the caudal superior temporal sulcus of the macaque monkey. J Neurophysiol. 60:1615–1637.

Huang R-S, Chen C, Tran AT, Holstein KL, Sereno MI. 2012. Mapping multisensory parietal face and body areas in humans. Proc Natl Acad Sci. 109:18114–18119.

Hughes HC, Reuter-Lorenz PA, Nozawa G, Fendrich R. 1994. Visual-auditory interactions in sensorimotor processing: saccades versus manual responses. J Exp Psychol Hum Percept Perform. 20:131–153.

Hyvärinen J. 1981. Regional distribution of functions in parietal association area 7 of the monkey. Brain Res. 206:287–303.

Hyvärinen J, Poranen A. 1974. Function of the parietal associative area 7 as revealed from cellular discharges in alert monkeys. Brain J Neurol. 97:673–692.

Iurilli G, Ghezzi D, Olcese U, Lassi G, Nazzaro C, Tonini R, Tucci V, Benfenati F, Medini P. 2012. Sound-driven synaptic inhibition in primary visual cortex. Neuron. 73:814–828.

Jack CE, Thurlow WR. 1973. Effects of degree of visual association and angle of displacement on the "ventriloquism" effect. Percept Mot Skills. 37:967–979.

James TW, Stevenson RA. 2012. The Use of fMRI to Assess Multisensory Integration. In: Murray MM, Wallace MT, editors. The Neural Bases of Multisensory Processes. Frontiers in Neuroscience. Boca Raton (FL): CRC Press.

James W. The principles of psychology. New York : Henry Holt & Co ; 1890.

Jones EG, Powell TP. 1970. Connexions of the somatic sensory cortex of the rhesus monkey. 3. Thalamic connexions. Brain J Neurol. 93:37–56.

Kaas JH, Collins CE. 2001. The organization of sensory cortex. Curr Opin Neurobiol. 11:498–504.

Künzle H. 1978. An autoradiographic analysis of the efferent connections from premotor and adjacent prefrontal regions (areas 6 and 9) in macaca fascicularis. Brain Behav Evol. 15:185–234.

Kuypers HG, Szwarcbart MK, Mishkin, M M, Rosvold HE. 1965. Occipitotemporal corticocortical connections in the rhesus monkey. Exp Neurol. 11:245–262.

Laurienti PJ, Perrault TJ, Stanford TR, Wallace MT, Stein BE. 2005. On the use of superadditivity as a metric for characterizing multisensory integration in functional neuroimaging studies. Exp Brain Res. 166:289–297.

Laurienti PJ, Wallace MT, Maldjian JA, Susi CM, Stein BE, Burdette JH. 2003. Cross-modal sensory processing in the anterior cingulate and medial prefrontal cortices. Hum Brain Mapp. 19:213–223.

Leinonen L, Hyvärinen J, Sovijärvi AR. 1980. Functional properties of neurons in the temporo-parietal association cortex of awake monkey. Exp Brain Res. 39:203–215.

Lewald J, Guski R. 2003. Cross-modal perceptual integration of spatially and temporally disparate auditory and visual stimuli. Brain Res. 16:468–478.

Lewis JW, Beauchamp MS, DeYoe EA. 2000. A comparison of visual and auditory motion processing in human cerebral cortex. Cereb Cortex. 10:873–888.

Lewis JW, Van Essen DC. 2000. Corticocortical connections of visual, sensorimotor, and multimodal processing areas in the parietal lobe of the macaque monkey. J Comp Neurol. 428:112–137.

Logothetis NK, Wandell BA. 2004. Interpreting the BOLD signal. Annu Rev Physiol. 66:735–769.

London ID. 1954. Research on sensory interaction in the Soviet Union. Psychol Bull. 5:531–568.

Luppino G, Murata A, Govoni P, Matelli M. 1999. Largely segregated parietofrontal connections linking rostral intraparietal cortex (areas AIP and VIP) and the ventral premotor cortex (areas F5 and F4). Exp Brain Res. 128:181–187.

Macaluso E, Driver J. 2001. Spatial attention and crossmodal interactions between vision and touch. Neuropsychologia. 39:1304–1316.

Macaluso E, Driver J, Frith CD. 2003. Multimodal spatial representations engaged in human parietal cortex during both saccadic and manual spatial orienting. Curr Biol. 13:990–999.

Macaluso E, Frith CD, Driver J. 2000. Modulation of human visual cortex by crossmodal spatial attention. Science. 289:1206–1208.

Massopust, L.C., Barnes, H.W., and Verdura, J. Auditory frequency discrimination in cortically ablated monkeys. J. Aud. Res. 5: 85-93, 1965.

Maunsell JH, van Essen DC. 1983. The connections of the middle temporal visual area (MT) and their relationship to a cortical hierarchy in the macaque monkey. J Neurosci. 3:2563–2586.

Mazzoni P, Bracewell RM, Barash S, Andersen RA. 1996. Spatially tuned auditory responses in area LIP of macaques performing delayed memory saccades to acoustic targets. J Neurophysiol. 75:1233–1241.

McGurk H, MacDonald J. 1976. Hearing lips and seeing voices. Nature. 264:746–748.

Meredith MA. 2002. On the neuronal basis for multisensory convergence: a brief overview. Brain Res. 14:31–40.

Meredith MA, Allman BL. 2009. Subthreshold multisensory processing in cat auditory cortex. Neuroreport. 20:126–131.

Meredith MA, Clemo HR. 1989. Auditory cortical projection from the anterior ectosylvian sulcus (Field AES) to the superior colliculus in the cat: an anatomical and electrophysiological study. J Comp Neurol. 289:687–707.

Meredith MA, Miller LK, Ramoa AS, Clemo HR, Behan M. 2001. Organization of the neurons of origin of the descending pathways from the ferret superior colliculus. Neurosci Res. 40:301–313.

Meredith MA, Stein BE. 1983. Interactions among converging sensory inputs in the superior colliculus. Science. 221:389–391.

Meredith MA, Stein BE. 1986. Visual, auditory, and somatosensory convergence on cells in superior colliculus results in multisensory integration. J Neurophysiol. 56:640–662.

Mesulam MM. 1998. From sensation to cognition. Brain J Neurol. 121 (Pt 6):1013–1052.

Miller J. 1982. Divided attention: evidence for coactivation with redundant signals. Cognit Psychol. 14:247–279.

Minciacchi D, Tassinari G, Antonini A. 1987. Visual and somatosensory integration in the anterior ectosylvian cortex of the cat. Brain Res. 410:21–31.

Molyneux W. Letter to John Locke. In: de Beer E.S, editor. The correspondence of John Locke. Oxford: Clarendon Press; 1688.

Mufson EJ, Mesulam MM. 1984. Thalamic connections of the insula in the rhesus monkey and comments on the paralimbic connectivity of the medial pulvinar nucleus. J Comp Neurol. 227:109–120.

Nath AR, Beauchamp MS. 2012. A neural basis for interindividual differences in the McGurk effect, a multisensory speech illusion. Neuroimage. 59:781–787.

Noesselt T, Rieger JW, Schoenfeld MA, Kanowski M, Hinrichs H, Heinze H-J, Driver J. 2007. Audiovisual temporal correspondence modulates human multisensory superior temporal sulcus plus primary sensory cortices. J Neurosci. 27:11431–11441.

Pandya DN, Kuypers HG. 1969. Cortico-cortical connections in the rhesus monkey. Brain Res. 13:13–36.

Pandya DN, Seltzer B. 1982. Intrinsic connections and architectonics of posterior parietal cortex in the rhesus monkey. J Comp Neurol. 204:196–210.

Rizzolatti G, Scandolara C, Matelli M, Gentilucci M. 1981a. Afferent properties of periarcuate neurons in macaque monkeys. II. Visual responses. Behav Brain Res. 2:147–163.

Rizzolatti G, Scandolara C, Matelli M, Gentilucci M. 1981b. Afferent properties of periarcuate neurons in macaque monkeys. I. Somatosensory responses. Behav Brain Res. 2:125–146.

Rizzolatti G, Scandolara C, Matelli M, Gentilucci M. 1981c. Afferent properties of periarcuate neurons in macaque monkeys. II. Visual responses. Behav Brain Res. 2:147–163.

Rockland KS, Ojima H. 2003. Multisensory convergence in calcarine visual areas in macaque monkey. Int J Psychophysiol. 50:19–26.

Rolls ET. 2004. Convergence of sensory systems in the orbitofrontal cortex in primates and brain design for emotion. Anat Rec A Discov Mol Cell Evol Biol. 281:1212–1225.

Rolls ET, Baylis LL. 1994. Gustatory, olfactory, and visual convergence within the primate orbitofrontal cortex. J Neurosci Off J Soc Neurosci. 14:5437–5452.

Rozzi S, Ferrari PF, Bonini L, Rizzolatti G, Fogassi L. 2008. Functional organization of inferior parietal lobule convexity in the macaque monkey: electrophysiological

characterization of motor, sensory and mirror responses and their correlation with cytoarchitectonic areas. Eur J Neurosci. 28:1569–1588.

Sathian K, Zangaladze A, Hoffman JM, Grafton ST. 1997. Feeling with the mind's eye. Neuroreport. 8:3877–3881.

Scheich H, Brechmann A, Brosch M, Budinger E, Ohl FW. 2007. The cognitive auditory cortex: task-specificity of stimulus representations. Hear Res. 229:213–224.

Schlack A, Sterbing-D'Angelo SJ, Hartung K, Hoffmann K-P, Bremmer F. 2005. Multisensory space representations in the macaque ventral intraparietal area. J Neurosci. 25:4616–4625.

Schroeder CE, Foxe J. 2005. Multisensory contributions to low-level, "unisensory" processing. Curr Opin Neurobiol. 15:454–458.

Schroeder CE, Foxe JJ. 2002. The timing and laminar profile of converging inputs to multisensory areas of the macaque neocortex. Brain Res. 14:187–198.

Schröger E, Widmann A. 1998. Speeded responses to audiovisual signal changes result from bimodal integration. Psychophysiology. 35:755–759.

Scott TR, Plata-Salamán CR, Smith-Swintosky VL. 1994. Gustatory neural coding in the monkey cortex: the quality of saltiness. J Neurophysiol. 71:1692–1701.

Seltzer B, Pandya DN. 1978. Afferent cortical connections and architectonics of the superior temporal sulcus and surrounding cortex in the rhesus monkey. Brain Res. 149:1–24.

Seltzer B, Pandya DN. 1980. Converging visual and somatic sensory cortical input to the intraparietal sulcus of the rhesus monkey. Brain Res. 192:339–351.

Seltzer B, Pandya DN. 1986. Posterior parietal projections to the intraparietal sulcus of the rhesus monkey. Exp Brain Res Exp Hirnforsch Expérimentation Cérébrale. 62:459–469.

Sereno MI, Huang R-S. 2006. A human parietal face area contains aligned head-centered visual and tactile maps. Nat Neurosci. 9:1337–1343.

Skaliora I, Doubell TP, Holmes NP, Nodal FR, King AJ. 2004. Functional topography of converging visual and auditory inputs to neurons in the rat superior colliculus. J Neurophysiol. 92:2933–2946.

Slutsky DA, Recanzone GH. 2001. Temporal and spatial dependency of the ventriloquism effect. Neuroreport. 12:7–10.

Smiley JF, Hackett TA, Ulbert I, Karmas G, Lakatos P, Javitt DC, Schroeder CE. 2007. Multisensory convergence in auditory cortex, I. Cortical connections of the caudal superior temporal plane in macaque monkeys. J Comp Neurol. 502:894–923.

Stein BE, Meredith MA. 1993. The merging of the senses. Cambridge, Mass.: MIT Press.

Stein BE, Stanford TR. 2008. Multisensory integration: current issues from the perspective of the single neuron. Nat Rev Neurosci. 9:255–266.

Stein BE, Stanford TR, Ramachandran R, Perrault TJ Jr, Rowland BA. 2009. Challenges in quantifying multisensory integration: alternative criteria, models, and inverse effectiveness. Exp Brain Res. 198:113–126.

Steriade M, Jones EG, McCormick DA. 1997. Thalamus. Amsterdam: Elsevier.

Stevenson RA, Geoghegan ML, James TW. 2007. Superadditive BOLD activation in superior temporal sulcus with threshold non-speech objects. Exp Brain Res. 179:85–95.

Sumby WH, Pollack I. 1954. Visual contribution to speech intelligibility in noise. Journal of Acoustical Society of America 26(2), 212–215.

Tawil RN, Saadé NE, Bitar M, Jabbur SJ. 1983. Polysensory interactions on single neurons of cat inferior colliculus. Brain Res. 269:149–152.

Taylor TL, Klein RM, Munoz DP. 1999. Saccadic performance as a function of the presence and disappearance of auditory and visual fixation stimuli. J Cogn Neurosci. 11:206–213.

Teuber, H.L. 1966. Alterations of perception after brain injury. In Brain and Conscious Experience. (Eccles, J.C., ed), 182–216, Springer.

Todd JW. 1912. Reaction to multiple stimuli. In: Archives of psychology, n°25 (Woodworth RS, ed). New York: The Science Press.

Toldi J, Fehér O, Wolff JR. 1986. Sensory interactive zones in the rat cerebral cortex. Neuroscience. 18:461–465.

Turner BH, Mishkin M, Knapp M. 1980. Organization of the amygdalopetal projections from modality-specific cortical association areas in the monkey. J Comp Neurol. 191:515–543.

Ungerleider LG, Desimone R. 1986. Cortical connections of visual area MT in the macaque. J Comp Neurol. 248:190–222.

Van Atteveldt N, Formisano E, Goebel R, Blomert L. 2004. Integration of letters and speech sounds in the human brain. Neuron. 43:271–282.

Vanduffel W, Fize D, Mandeville JB, Nelissen K, Van Hecke P, Rosen BR, Tootell RB, Orban GA. 2001. Visual motion processing investigated using contrast agent-enhanced fMRI in awake behaving monkeys. Neuron. 32:565–577.

Vasconcelos N, Pantoja J, Belchior H, Caixeta FV, Faber J, Freire MAM, Cota VR, Anibal de Macedo E, Laplagne DA, Gomes HM, Ribeiro S. 2011. Cross-modal responses in the primary visual cortex encode complex objects and correlate with tactile discrimination. Proc Natl Acad Sci. 108:15408–15413.

Wallace MT, Meredith MA, Stein BE. 1992. Integration of multiple sensory modalities in cat cortex. Exp Brain Res. 91:484–488.

Wallace MT, Ramachandran R, Stein BE. 2004. A revised view of sensory cortical parcellation. Proc Natl Acad Sci. 101:2167–2172.

Wallace MT, Wilkinson LK, Stein BE. 1996. Representation and integration of multiple sensory inputs in primate superior colliculus. J Neurophysiol. 76:1246–1266.

Watanabe J, Iwai E. 1991. Neuronal activity in visual, auditory and polysensory areas in the monkey temporal cortex during visual fixation task. Brain Res. 26:583–592.

Watanabe M. 1992. Frontal units of the monkey coding the associative significance of visual and auditory stimuli. Exp Brain Res. 89:233–247.

Weber JT, Yin TC. 1984. Subcortical projections of the inferior parietal cortex (area 7) in the stump-tailed monkey. J Comp Neurol. 224:206–230.

Welch RB, Warren DH. 1980. Immediate perceptual response to intersensory discrepancy. Psychol Bull. 88:638–667.

Welch RB, Warren DH. 1986. Intersensory interactions. In: Handbook of perception and human performance (Kaufman KR, Thomal JP, ed), pp 25-21 to 25-36. New York: Wiley-Interscience.

Werner-Reiss U, Kelly KA, Trause AS, Underhill AM, Groh JM. 2003. Eye position affects activity in primary auditory cortex of primates. Curr Biol. 13:554–562.

Wilson JS, Hull CD, Buchwald NA. 1983. Intracellular studies of the convergence of sensory input on caudate neurons of cat. Brain Res. 270:197–208.

Wright TM, Pelphrey KA, Allison T, McKeown MJ, McCarthy G. 2003. Polysensory interactions along lateral temporal regions evoked by audiovisual speech. Cereb Cortex. 13:1034–1043.

Yaka R, Notkin N, Yinon U, Wollberg Z. 2002. Visual, auditory and bimodal activity in the banks of the lateral suprasylvian sulcus in the cat. Neurosci Behav Physiol. 32:103–108.

Zhang T, Britten KH. 2004. Clustering of selectivity for optic flow in the ventral intraparietal area. Neuroreport. 15:1941–1945.

RESULTS

Chapter 1

Multimodal Convergence within the Intraparietal Sulcus of the Macaque Monkey

Published in Journal of Neurosciences, February 27, 2013 – 33(9):4128-4139

Systems/Circuits

Multimodal Convergence within the Intraparietal Sulcus of the Macaque Monkey

Olivier Guipponi,[1]* Claire Wardak,[1]* Danielle Ibarrola,[2] Jean-Christophe Comte,[2] Dominique Sappey-Marinier,[2] Serge Pinède,[1] and Suliann Ben Hamed[1]

[1]Centre de Neuroscience Cognitive, CNRS UMR 5229, 69675 Bron cedex, Université Claude Bernard Lyon, France, and [2]Centre d'Exploration et de Recherche Médicale par Emission de Positons, Imagerie du vivant, 69677 Bron cedex, France

The parietal cortex is highly multimodal and plays a key role in the processing of objects and actions in space, both in human and nonhuman primates. Despite the accumulated knowledge in both species, we lack the following: (1) a general description of the multisensory convergence in this cortical region to situate sparser lesion and electrophysiological recording studies; and (2) a way to compare and extrapolate monkey data to human results. Here, we use functional magnetic resonance imaging (fMRI) in the monkey to provide a bridge between human and monkey studies. We focus on the intraparietal sulcus (IPS) and specifically probe its involvement in the processing of visual, tactile, and auditory moving stimuli around and toward the face. We describe three major findings: (1) the visual and tactile modalities are strongly represented and activate mostly nonoverlapping sectors within the IPS. The visual domain occupies its posterior two-thirds and the tactile modality its anterior one-third. The auditory modality is much less represented, mostly on the medial IPS bank. (2) Processing of the movement component of sensory stimuli is specific to the fundus of the IPS and coincides with the anatomical definition of monkey ventral intraparietal area (VIP). (3) A cortical sector within VIP processes movement around and toward the face independently of the sensory modality. This amodal representation of movement may be a key component in the construction of peripersonal space. Overall, our observations highlight strong homologies between macaque and human VIP organization.

Introduction

The parietal cortex is considered to be an "association" cortex that receives convergent multimodal sensory inputs. This view, initially based on anatomical evidence, is confirmed by single-cell electrophysiological recordings. Briefly, the parietal cortex receives visual afferents from the extrastriate visual cortex (Maunsell and van Essen, 1983; Ungerleider and Desimone, 1986). In agreement with this, visual neurons are recorded from several parietal regions, coding the location and structure of visual items as well as their movement in 3D space with respect to the subject. These neurons can have a preference for large field dynamic visual stimuli, such as expanding or contracting optic flow patterns or moving bars (Schaafsma and Duysens, 1996; Bremmer et al., 2002a; Zhang et al., 2004), or smaller moving visual stimuli (Vanduffel et al., 2001). The parietal cortex also receives monosynaptic afferents from the somatosensory cortex (Seltzer and Pandya, 1980; Disbrow et al., 2003). Accordingly, tactile neuronal responses have been documented in this region (Duhamel et al., 1998; Avillac et al., 2005). A light auditory input to the parietal cortex has also been described from the caudomedial auditory belt (Lewis and Van Essen, 2000a), corroborating the description of parietal neurons responsive to auditory stimulations (Mazzoni et al., 1996; Grunewald et al., 1999; Schlack et al., 2005). Last but not least, the parietal cortex also receives vestibular afferents from several cortical regions with direct input from vestibular nuclei (Faugier-Grimaud and Ventre, 1989; Akbarian et al., 1994) and accordingly contains neurons that are modulated by vestibular information (Bremmer et al., 2002b; Chen et al., 2011).

This heavily multimodal convergence within the parietal cortex appears to serve two key functions: on the one hand, the processing of space and objects in space and on the other hand the preparation of oriented actions in space (i.e., sensorimotor transformation). These functions are documented by lesion, fMRI, and single-cell recording studies (Colby and Goldberg, 1999; Bremmer et al., 2002b; Andersen and Cui, 2009; Orban, 2011).

Despite this accumulated knowledge on parietal functions, little effort has been directed toward functional neuroimaging of multimodal convergence within this cortex (Bremmer et al., 2001; Sereno and Huang, 2006). In particular, no such data are available in the nonhuman primate. This prevents a direct transfer of accumulated knowledge on multimodal parietal functions, from the single-cell recording studies in the macaque, to observations derived from the human studies. Here, we propose to bridge this gap, thanks to nonhuman primate fMRI. More pre-

Received March 21, 2012; revised Dec. 6, 2012; accepted Jan. 9, 2013.

Author contributions: C.W. and S.B.H. designed research; O.G., C.W., and S.B.H. performed research; D.I., J.-C.C., D.S.-M., and S.P. contributed unpublished reagents/analytic tools; O.G., C.W., and S.B.H. analyzed data; O.G., C.W., and S.B.H. wrote the paper.

This work was supported by the Agence Nationale de la Recherche (Grant ANR-05-JCJC-0230-01), and by the Fondation pour la Recherche Médicale to S.P. We thank J.R. Duhamel and S. Wirth for helpful comments on the manuscript; W. Vanduffel, J. Mandeville (JIP software), N. Richard, E. Metereau, and S. Maurin for technical support; E. Åstrand for her continuous support; and J.L. Charieau and F. Herant for animal care.

The authors declare no competing financial interests.

*O.G. and C.W. contributed equally to this work.

Correspondence should be addressed to Dr. Suliann Ben Hamed, Centre de Neuroscience Cognitive, CNRS UMR 5229, Université Claude Bernard Lyon I, 67 BdPinel, 69675 Bron cedex, France. E-mail: benhamed@isc.cnrs.fr.

DOI:10.1523/JNEUROSCI.1421-12.2013

 0270-6474/13/334128-12$15.00/0

cisely, we focus on the intraparietal sulcus (IPS). This region has distinctive functions compared with the parietal convexity and is proposed to be involved in the construction of a multisensory representation of space (Bremmer, 2011). In particular, a subregion of the IPS is thought to code peripersonal space thanks to the processing of moving stimuli toward the subject (Graziano and Cooke, 2006). We specifically probe the involvement of the IPS in the processing of visual, tactile, and auditory moving stimuli around and toward the face.

Materials and Methods

Subjects and materials

Two rhesus monkeys (female M1, male M2, 5–7 years old, 5–7 kg) participated to the study. The animals were implanted with a plastic MRI compatible headset covered by dental acrylic. The anesthesia during surgery was induced by Zoletil (tiletamine-zolazepam, Virbac, 5 mg/kg) and followed by isoflurane (Belamont, 1–2%). Postsurgery analgesia was ensured thanks to Temgesic (buprenorphine, 0.3 mg/ml, 0.01 mg/kg). During recovery, proper analgesic and antibiotic coverage was provided. The surgical procedures conformed to European and National Institutes of Health guidelines for the care and use of laboratory animals.

During the scanning sessions, monkeys sat in a sphinx position in a plastic monkey chair positioned within a horizontal magnet (1.5-T MR scanner Sonata; Siemens) facing a translucent screen placed 90 cm from the eyes. Their head was restrained and equipped with MRI-compatible headphones customized for monkeys (MR Confon). A radial receive-only surface coil (10 cm diameter) was positioned above the head. Eye position was monitored at 120 Hz during scanning using a pupil-corneal reflection tracking system (Iscan). Monkeys were rewarded with liquid dispensed by a computer-controlled reward delivery system (Crist) thanks to a plastic tube coming to their mouth. The task, all the behavioral parameters, and the sensory stimulations were monitored by two computers running with Matlab and Presentation. Visual stimulations were projected onto the screen with a Canon XEED SX60 projector. Auditory stimulations were dispensed with an MR Confon. Tactile stimulations were delivered through Teflon tubing and 6 articulated plastic arms connected to distant air pressure electro-valves. Monkeys were trained in a mock scan environment approaching to the best the actual MRI scanner setup.

Task and stimuli

The animals were trained to maintain fixation on a red central spot ($0.24° \times 0.24°$) while stimulations (visual, auditory, or tactile) were delivered. The monkeys were rewarded for staying within a $2° \times 2°$ tolerance window centered on the fixation spot. The reward delivery was scheduled to encourage long fixation without breaks (i.e., the interval between successive deliveries was decreased and their amount was increased, up to a fixed limit, as long as the eyes did not leave the window). The different modalities were tested in independent interleaved runs (see below for the organization of the runs).

Visual stimulations. Large field ($32° \times 32°$) visual stimulations consisted of white bars ($3.2° \times 24.3°$, horizontal, vertical, or 45° oblique) or white random dots on a black background (see Fig. 1*A* for an example). Three conditions were tested in blocks of 10 pulses (TR = 2.08 s): (1) coherent movement, with bars moving in one of the 8 cardinal directions or expanding or contracting random dots pattern (with 5 possible optic flow origins: center, top left (−8°, 8°), top right, lower left and lower right); each coherent movement sequence lasted 850 ms, and 24 such sequences were pseudo-randomly presented in a given coherent movement block; (2) scrambled movement, in which the different frames of a given coherent movement sequence were randomly reorganized so that no coherent movement component was left; each scrambled movement sequence lasted 850 ms, and 24 such sequences were presented in a given scrambled movement block; these matched the 24 coherent movement sequences of the coherent movement block from which they were derived; this provides precise visual controls of the coherent movement blocks; (3) static, in which individual frames randomly picked from the coherent movement visual stimuli sequences, were presented for 250 ms; these matched the coherent movement sequences of the coherent movement block they were derived from so as to provide precise visual controls of the coherent movement blocks. As a result, within a given block, 850 ms portions of the different stimuli (bars/dots/directions/origins) of a same category (coherent/scrambled/static) were pseudo-randomly interleaved. All of these stimulations were optimized for area ventral intraparietal area (VIP) as we used large field visual stimuli, moving at 100°/s in the coherent movement condition (Bremmer et al., 2002a).

Auditory stimulations. In both monkeys, we used coherent movement complex auditory stimuli moving in near space around the head (binaural, 3D holographic sounds, http://gprime.net/flash.php/soundimmersion, http://onemansblog.com/2007/05/13/get-your-virtual-haircut-and-other-auditory-illusions/, durations ranging between 1.7 and 11.5 s). We selected the stimuli evoking the best movement perception and localization among a group of 12 human subjects (average age, 45.5 years). Scrambled stimulations were obtained by cutting the movement sounds in 100 ms or 300 ms segments and randomly mixing them. Static stimulations consisted of auditory stimuli evoking a stable stimulus in space (selected from the same 3D holographic sounds database and evaluated by the same group of subjects as the coherent movement auditory sounds). In M2, we also used pure-tones auditory stimulations (generated in Goldwave, at 300, 500, and 800 Hz). Coherent movement stimulations consisted of two kinds of movement: (1) 2.0 s long sounds simulating far away to near movements (linear increase in signal amplitude + Doppler effect) or the opposite (linear decrease in sound amplitude); and (2) sound moving between the left and the right ear (3.5 s stimuli, corresponding to two back-and-forth cycles, thanks to opposite amplitude variations between the two binaural sounds and a 1 Hz stimulus frequency binaural offset). Human subject rating of these stimuli was less consistent than that for complex sounds, subjects usually describing stimuli moving within the head. Scrambled stimulations were obtained as for complex scrambled stimuli. Static stimuli consisted of constant left ear or right ear stimulations. Within a given block, 2 s and 3.5 s stimulations of a given category (coherent/scrambled/static) were pseudo-randomly interleaved.

Tactile stimulations. They consisted of air puffs delivered to three different locations on the left and the right of the animals' body (see Fig. 1*A* for a schematic representation): (1) center of the face, close to the nose and the mouth; (2) periphery of the face, above the eyebrows; and (3) shoulders. The intensity of the stimulations ranged from 0.5 bars (center/periphery) and 1 bar (shoulders), to adjust for the larger distance between the extremity of the stimulation tubes and the skin, as well as for the difference in hair density. Within a given block, left and right stimulations were pseudo-randomly interleaved, each stimulation lasting between 400 and 500 ms and the interstimulation interval between 500 and 1000 ms.

Functional time series (runs) were organized as follows: a 10-volume block of pure fixation (baseline) was followed by a 10-volume block of category 1, a 10-volume block of category 2, and a 10-volume block of category 3; this sequence was played four times, resulting in a 160-volume run. The blocks for the 3 categories were presented in 6 counterbalanced possible orders. A retinotopy localizer was run independently in the two monkeys using exactly the stimulations of Fize et al. (2003). This localizer is not effective in driving VIP specifically or identifying a reliable topographical organization in this region (except for a relative overrepresentation of the upper with respect to the lower visual field). Here, it is used to locate the central representation of the lateral intraparietal area (LIP) within each hemisphere, in both animals.

Scanning

Before each scanning session, a contrast agent, monocrystalline iron oxide nanoparticle (Sinerem, Guerbet or Feraheme, AMAG), was injected into the animal's femoral/saphenous vein (4–10 mg/kg). For the sake of clarity, the polarity of the contrast agent MR signal changes, which are negative for increased blood volumes, was inverted. We acquired gradient-echo echoplanar (EPI) images covering the whole brain (1.5 T; repetition time [TR] 2.08 s; echo time [TE] 27 ms; 32 sagittal slices; $2 \times 2 \times 2$ mm voxels). During each scanning session, the runs of different modalities and different orders were pseudo-randomly intermixed. A

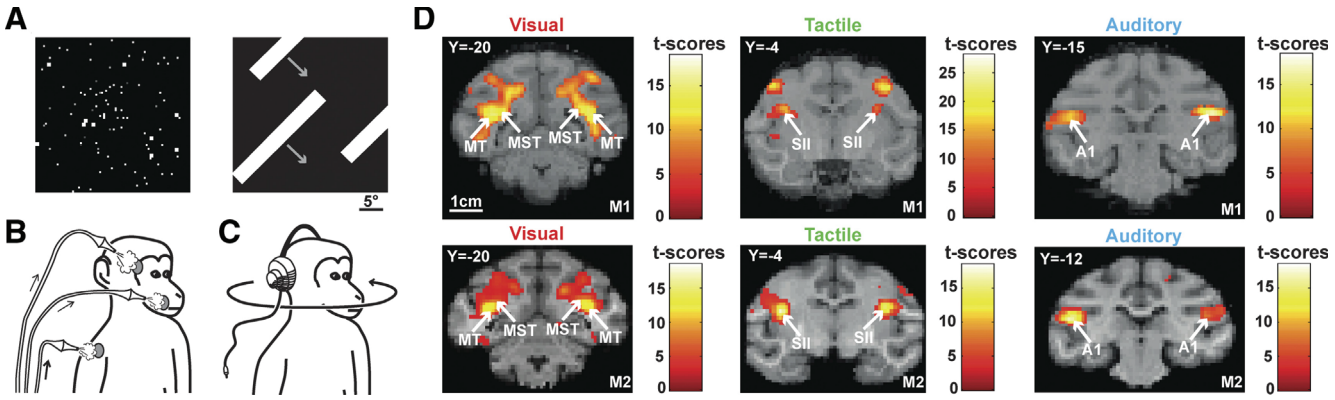

Figure 1. Stimulations for the three sensory modalities and their corresponding primary activations. ***A***, Two examples of visual stimuli: coherent optic flows and moving bars. The main condition of interest, coherent movement, was mixed with two control conditions (scrambled and static stimulations) and a baseline condition (fixation only). ***B***, Schematics of the tactile stimulations: air puffs were delivered to the center of the face, the periphery of the face, or the shoulders, both on the left and right sides of the monkeys. ***C***, Schematics of the auditory stimulations: moving sounds were delivered to the monkeys via a headset. We used the same conditions as for the visual modality. ***D***, Statistical parametric maps (SPMs) showing the primary activations obtained for the three sensory modalities. The visual activations (left column) are specific for visual motion and correspond to the conjunction analysis of two contrasts (coherent movement vs scrambled and coherent movement vs static; $p < 0.05$, FWE-corrected level, masked to display only positive signal change relative to the fixation baseline). The tactile activations (middle column) correspond to stimulations to the center of the face relative to the fixation baseline ($p < 0.05$, FWE-corrected level). The auditory activations (right column) correspond to coherent movement relative to the fixation baseline ($p < 0.05$, FWE-corrected level). These results are presented individually for each monkey and displayed on coronal sections of each anatomy (M1 for the top, and M2 for the lower ones). MT, Medial temporal area; MST, medial superior temporal area; SII, secondary somatosensory area; A1, primary auditory area.

total of 40 (34) runs was acquired for visual stimulations in M1 (M2), 36 (40) runs for tactile stimulations, and 37 (42) runs for complex auditory stimulations (plus 40 runs for pure-tones auditory stimulations in M2). Fifty-seven (45) runs were obtained for the retinotopy localizer were obtained in independent sessions for M1 (M2).

Analysis

The analyzed runs were selected based on the quality of the monkeys' fixation (>85% within the tolerance window): a total of 23 (25) runs were selected for visual stimulations in M1 (M2), 20 (32) for tactile stimulations, 26 (32) for complex auditory stimulations (and 34 for pure-tones auditory stimulations in M2) and 20 (24) for the retinotopy localizer. Time series were analyzed using SPM8 (Wellcome Department of Cognitive Neurology, London, United Kingdom). For spatial preprocessing, functional volumes were first realigned and rigidly coregistered with the anatomy of each individual monkey (T1-weighted MPRAGE 3D 0.6×0.6×0.6 mm or 0.5×0.5×0.5 mm voxel acquired at 1.5T) in stereotactic space. The JIP program (Mandeville et al., 2011) was used to perform a nonrigid coregistration (warping) of a mean functional image onto the individual anatomies. Fixed-effect individual analyses were performed for each sensory modality in each monkey, with a level of significance set at $p < 0.05$ corrected for multiple comparisons (familywise error [FWE], $t > 4.89$) unless stated otherwise. We also performed conjunction analyses (statistical levels set at $p < 0.05$ at corrected level unless stated otherwise). In all analyses, realignment parameters, as well as eye movement traces, were included as covariates of no interest to remove eye movement and brain motion artifacts. When coordinates are provided, they are expressed with respect to the anterior commissure. We also performed ROI analyses using MarsBar toolbox (Brett et al., 2002). The ROIs were defined based on the conjunction analyses results. The significance threshold for the t tests was set at $p < 0.05$ (one-tailed). Results are displayed on coronal sections from each individual anatomy or on individual flattened maps obtained with Caret (Van Essen et al., 2001; http://www.nitrc.org/projects/caret/). We also mapped each individual anatomy onto the F6 monkey atlas of Caret to visualize the obtained activations against the anatomical subdivisions described by Lewis et al. (2000, 2005) within the intraparietal sulcus IPS.

Test-retest analyses are performed to evaluate the robustness of the reported activations (see Figs. 4 and 6). For each monkey, the runs of the sensory modality of interest are divided into two equal groups as follows. The runs are ordered from the first run to be recorded to the last. A first group (called the ODD test-retest group) is composed of all the odd runs in the acquisition sequence (first, third, fifth, seventh, etc.). A second group (called the EVEN test-retest group) is composed by all the even runs in the acquisition sequence (second, fourth, sixth, eighth, etc.). The percentage of signal change (PSC) in the contrast of interest is calculated for all the runs, only the ODD runs and only the EVEN runs independently.

ANOVA. A two-way ANOVA is performed when necessary to investigate whether two ROIs have similar response profiles or not. PSCs are extracted for each ROI for the contrasts of interest. The two-way ANOVA takes the contrasts of interest as first factor and the ROI identity as second factor. A main contrast effect indicates that all contrasts do not activate the ROIs to the same extent, irrespective of ROI identity. A main ROI effect indicates that the overall activation between the two ROIs is different, irrespective of what contrast is considered. An interaction effect indicates that the two ROIs are activated in different ways by each contrast of interest.

Potential covariates. In all analyses, realignment parameters, as well as eye movement traces, were included as covariates of no interest to remove eye movement and brain motion artifacts. However, some of the stimulations might have induced a specific behavioral pattern biasing our analysis, not fully accounted for by the aforementioned regressors. For example, large field coherent fast-moving stimuli might have induced an eye nystagmus, air puffs to the face might have evoked facial mimics (as well as some imprecision in the point of impact of the air puff) and spatially localized auditory stimuli might have induced an overt orienting behavior (microsaccades and saccades, offset fixation). Although we cannot completely rule out this possibility, our experimental setup allows to minimize its impact. First, monkeys worked head-restrained (to maintain the brain at the optimal position within the scanner, to minimize movement artifacts on the fMRI signal, and to allow for a precise monitoring of their eye movements). As a result, the tactile stimulations to the center and to the periphery of the face were stable in a given session. When drinking the liquid reward, small lip movements occurred. These movements thus correlated with reward timing and were on average equally distributed over the different sensory runs and the different conditions within each run (we checked that the monkeys had equal performance among the different conditions within a given run). The center of the face air puffs were placed on the cheeks on each side of the monkey's nose at a location that was not affected by the lip movements. Peripheral body stimulation air puffs were directed to the shoulders, at a location that was not affected by possible arms movements by the monkey. This was possible because the monkey chair tightly fit the monkey's width. Second, monkeys were required to maintain their gaze on a small fixation point, within a tolerance window of 2° × 2°. This was

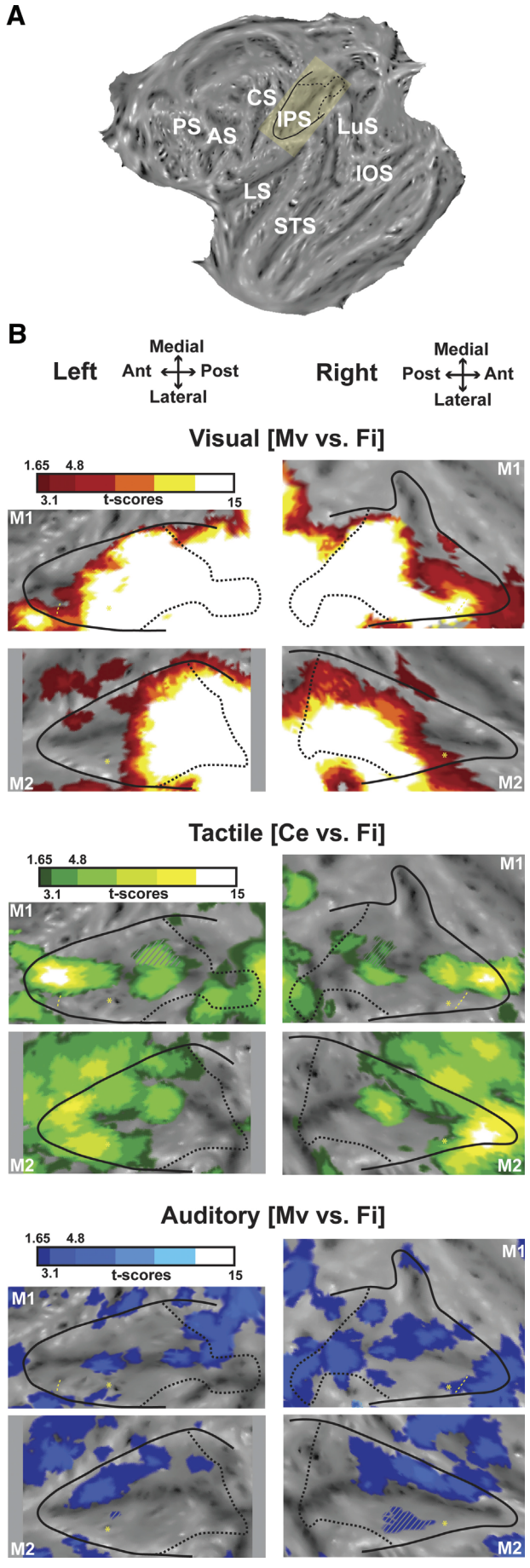

controlled online and was used to motivate the animal to maximize fixation rates (as fixation disruptions, such as saccades or drifts, affected the reward schedule). Eye traces were also analyzed offline for the selection of the runs to include in the analysis (good fixation for 85% of the run duration, with no major fixation interruptions). A statistical analysis indicates that the monkeys' performance was not significantly different across the visual, tactile, or auditory runs (one-way ANOVA: M1, $p = 0.75$; M2, $p = 0.65$). This suggests that the overall oculomotor behavior was constant across types of runs. Small systematic changes taking place within the tolerance window could have affected our data, such as small saccades, microsaccades, or other differences in eye position variance. When eye position is used as a regressor for fMRI signal, changes in the fMRI signal can be specifically located in LIP and the FEF (this analysis is used to delineate the anterior limit of LIP in monkey M1). Microsaccades are expected to activate the same regions as saccades. The fact that LIP is not activated in the contrasts presented in Figures 5 and 6 indicates that microsaccade and small saccade patterns were similar across conditions.

Results

Monkeys were exposed to visual (Fig. 1*A*), tactile (Fig. 1*B*), or auditory (Fig. 1*C*) stimulations, while fixating a central point, in independent time series. Based on prior studies, we used large field visual stimuli (expanding and contracting optic flow stimuli and moving bars) (Bremmer et al., 2002b), tactile stimuli to the face and upper body (Duhamel et al., 1998), and rich auditory stimuli moving in space (complex sounds have been shown to produce more robust cortical activations outside the primary auditory cortex, Blauert, 1997; than pure tones as used by Schlack et al., 2005). These stimulations were effective in activating the primary areas involved in their processing: all the visual stimuli activated the primary visual areas, and coherent movement specifically activated areas MT and MST (Fig. 1*D*, left); the three tactile stimulations activated area SII (Fig. 1*D*, middle, center of the face stimulation); and all the auditory stimuli activated the primary auditory cortex and the auditory belt (Fig. 1*D*, right, coherent movement stimuli).

In this paper, we specifically focus on the IPS. However, other cortical regions in both hemispheres of both monkeys were also robustly activated ($p < 0.05$, FWE-corrected level) by our stimulations: the occipital cortex (visual stimulations: striate and extrastriate areas), temporal cortex (visual: superior temporal

←

Figure 2. Visual, tactile, and auditory modalities within the intraparietal sulcus. ***A***, Localization of the IPS on the flattened representation of the cortex obtained with Caret (monkey M1, left hemisphere). The yellow inset corresponds to the IPS, which was slightly rotated to be depicted as horizontal in ***B*** and in the following figures. Black solid line indicates the limit between the convexity and the banks of the IPS; and black dashed line, projection on the flat map of the most posterior coronal section of the IPS, just before the annectant gyrus can be identified. AS, Arcuate sulcus; CS, central sulcus; IOS, inferior occipital sulcus; IPS, intraparietal sulcus; LS, lateral sulcus; LuS, lunate sulcus; PS, principal sulcus; STS, superior temporal sulcus. ***B***, Activations presented on the flattened IPS for (1) the visual modality (top panels), showing the coherent movement versus fixation contrast (red represents *t* score scale, color transitions being adjusted to *t* scores = 1.65 at $p < 0.05$, uncorrected level; *t* scores = 3.1 at $p < 0.001$, uncorrected level and *t* scores = 4.8 at $p < 0.05$, FWE-corrected level); (2) the tactile modality (middle panels), showing the center of the face versus fixation contrast (green color *t* score scale, color transitions as in 1); and (3) the auditory modality (lower panels), showing the coherent movement versus fixation contrast (blue represents *t* score scale, color transitions as in 1). The hyphenated yellow line corresponds to the anterior boundary of M1 eye movements' regressors extracted from the visual analysis. This limit corresponds to the anterior boundary of the LIP (Durand et al., 2007); nothing reliable was obtained in M2. Yellow asterisk indicates local maximal activation for the central visual field compared with the peripheral visual field, assessed with the retinotopic localizer, and corresponds to the central representation located in anterior LIP (Ben Hamed et al., 2001; Fize et al., 2003; Arcaro et al., 2011). Gray hyphenated areas represent activations spilling over the other bank of the IPS. Top (respectively lower) panels correspond to flat maps of M1 (respectively M2). A, Anterior; L, lateral; M, medial; P, posterior.

sulcus; auditory: different parts of the temporoparietal cortex), cingulate cortex (visual: anterior and posterior cingulate), frontal cortex (visual: anterior arcuate sulcus, principal sulcus and convexity; tactile: central sulcus, premotor cortex and ventrolateral prefrontal cortex), and parietal cortex outside of the IPS (visual: inferior parietal convexity; tactile: superior and inferior parietal convexities).

Visual, tactile, and auditory processing within the IPS

Because the parietal cortex is a site of multisensory convergence, we first studied how each modality activated the IPS (Fig. 2*A*). Figure 2*B* shows, for each monkey, the results for the main stimulation conditions contrasted with the fixation baseline. For the visual and auditory modalities, the main stimulation condition is the coherent movement. These coherent movement versus fixation contrasts extract the activations that are related both to the stimulation onset (visual onset of the large-field visual stimuli or auditory onset of the rich moving sounds) as well as to the coherent movement component that builds up within a given coherent movement sequence. They capture both movement-selective and nonselective IPS domains. For the tactile modality, the main condition is the center of the face stimulation, as it is the one eliciting the strongest activation in the IPS for both monkeys (Fig. 3).

Two major results can be highlighted. First, the three sensory modalities do not activate the IPS with the same robustness: the visual (t score for the principal local maximum: $t = 41.4/42.6$ and $t = 29.4/29.9$, left/right, in M1 and M2, respectively) and tactile ($t = 14.4/13.1$ and $t = 9.7/13.4$) modalities activate a large region at corrected level, whereas no auditory activation can be observed at this criterion (t score for the principal local maximum: $t = 3.8/4.1$ and $t = 3.1/5.2$ in M1 and M2, respectively). To check that the weak auditory activations that we observe are not specific to the 3D holographic binaural sound stimuli we chose, we presented monkey M2 with pure tone auditory stimuli as in Bremmer et al. (2001). These pure tones hardly elicited any activation within the IPS (t score for the principal local maximum: $t = 2.46/1.35$, data not shown). Thus, in the next analyses, we will present the auditory results for the 3D holographic sound stimuli at a lower statistical level ($p < 0.05$, uncorrected).

Second, we observed a clear topography: the visual stimulations mainly activated the posterior two-thirds of the IPS,

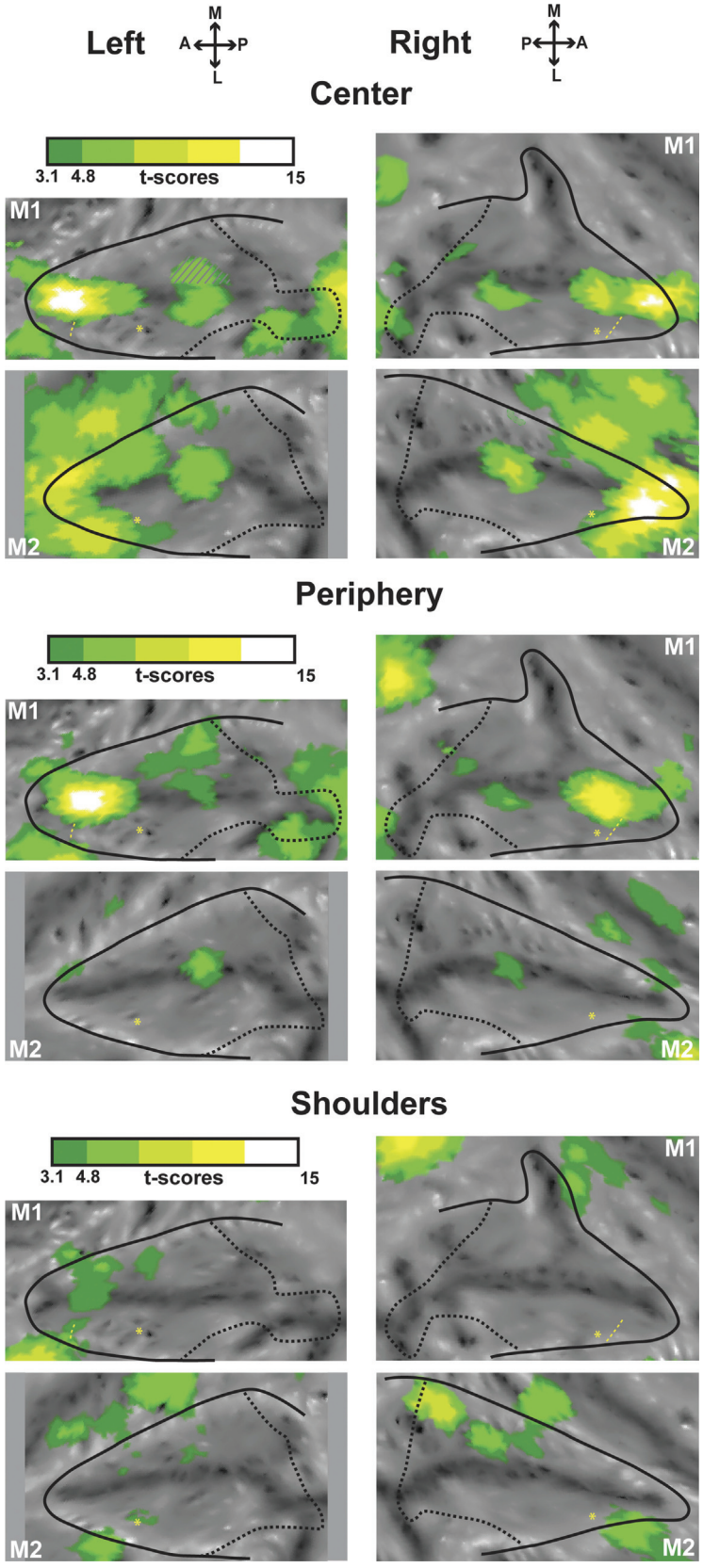

Figure 3. Tactile activations for the center of the face, periphery of the face, and shoulders presented on flap maps of the intraparietal sulcus. The center of the face (top panels for left and right sides), periphery of the face (middle panels), and shoulder (lower panels) activations correspond, respectively, to the center of the face versus fixation, periphery of the face versus fixation, and shoulder versus fixation contrasts. For other conventions, see Figure 2.

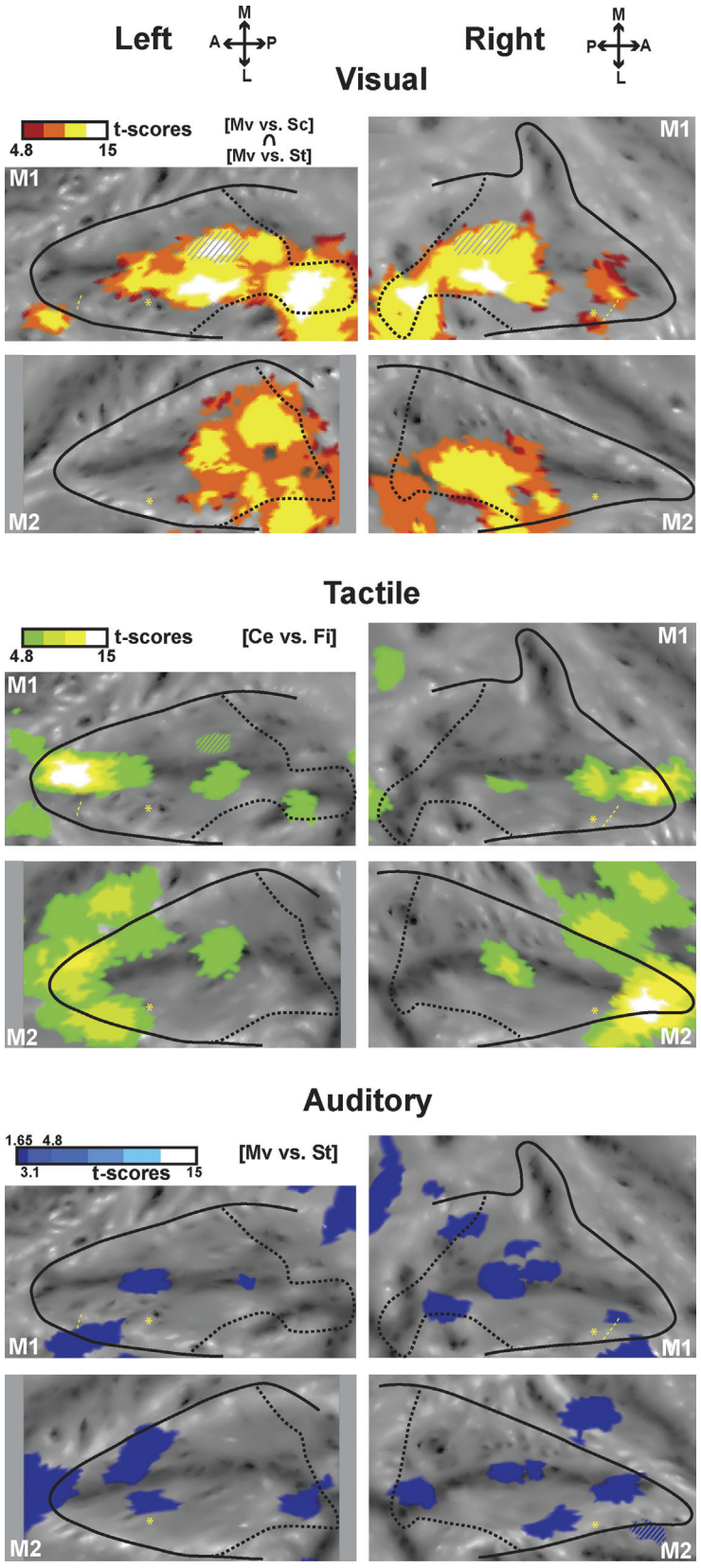

Figure 4. Motion processing regions within the intraparietal sulcus. SPMs of the visual (top panels, red scale) conjunction analysis (coherent movement vs scrambled and coherent movement vs static contrasts) are hot color-coded and displayed on the individual flat maps of the IPS ($p < 0.05$, FWE-corrected level, masked to display only positive signal change relative to the fixation baseline). Tactile activations (center of the face vs fixation contrast, green scale, $p < 0.05$, FWE-corrected level) are displayed on the middle panels. Auditory activations are displayed on the bottom (conjunction of the coherent movement vs static contrasts for the even and odd groups of runs) (test-retest analysis; $p < 0.05$ at uncorrected level). For other conventions, see Figure 2.

whereas the tactile stimulations activated the anterior third. This topography is very stable, as can be seen by comparing the activations at corrected and uncorrected levels. The auditory activations were more patchy and variable in between animals and hemispheres but were mainly concentrated on the medial bank.

Movement processing toward and around the face within the IPS

The parietal cortex is also involved in the processing of stimuli moving with respect to the subject (Duhamel et al., 1997, 1998). Here, we studied how the movement component of the sensory stimulations we used specifically activated the IPS. We thus contrasted, for the visual modality, the coherent movement condition both with the scrambled movement and static conditions (coherent movement vs scrambled and coherent movement vs static; Fig. 4, top). Using both these contrasts allows to subtract visual onset and local motion cues so as to reveal activations specific to large field movement toward and around the face or self-motion. In contrast to the widespread activations elicited compared with the fixation baseline (Fig. 2*B*), these specific visual coherent movement activations were found at the fundus of the IPS.

Ideally, auditory movement activations should also be defined by contrasting the coherent movement condition both to the scrambled movement and static conditions, as done for the visual activations. However, the scrambled sounds activated the IPS nearly as much as the coherent sounds (see, for example, the PSC histograms in Fig. 5), possibly because they retained some degree of sound motion (they corresponded to a random rearrangement of small fragments of the coherent motion complex sounds). We thus only used the coherent movement versus static contrast. We observed activations in the fundus of the IPS overlapping with the visual movement activations, only at very low t score levels (t score between 1.73 and 2.53, <4.8, which corresponds to $p < 0.05$, FWE-corrected level, and <3.1, which corresponds to $p < 0.001$, uncorrected level). To assess the reliability of these auditory activations, we performed a test-retest analysis (separating the runs in EVEN and ODD groups). We show in Figure 4 (bottom) the conjunction analysis ($p < 0.05$, uncorrected level) for the coherent movement versus static contrasts in these EVEN and ODD groups, thus revealing only the weak but reproducible auditory activations. Con-

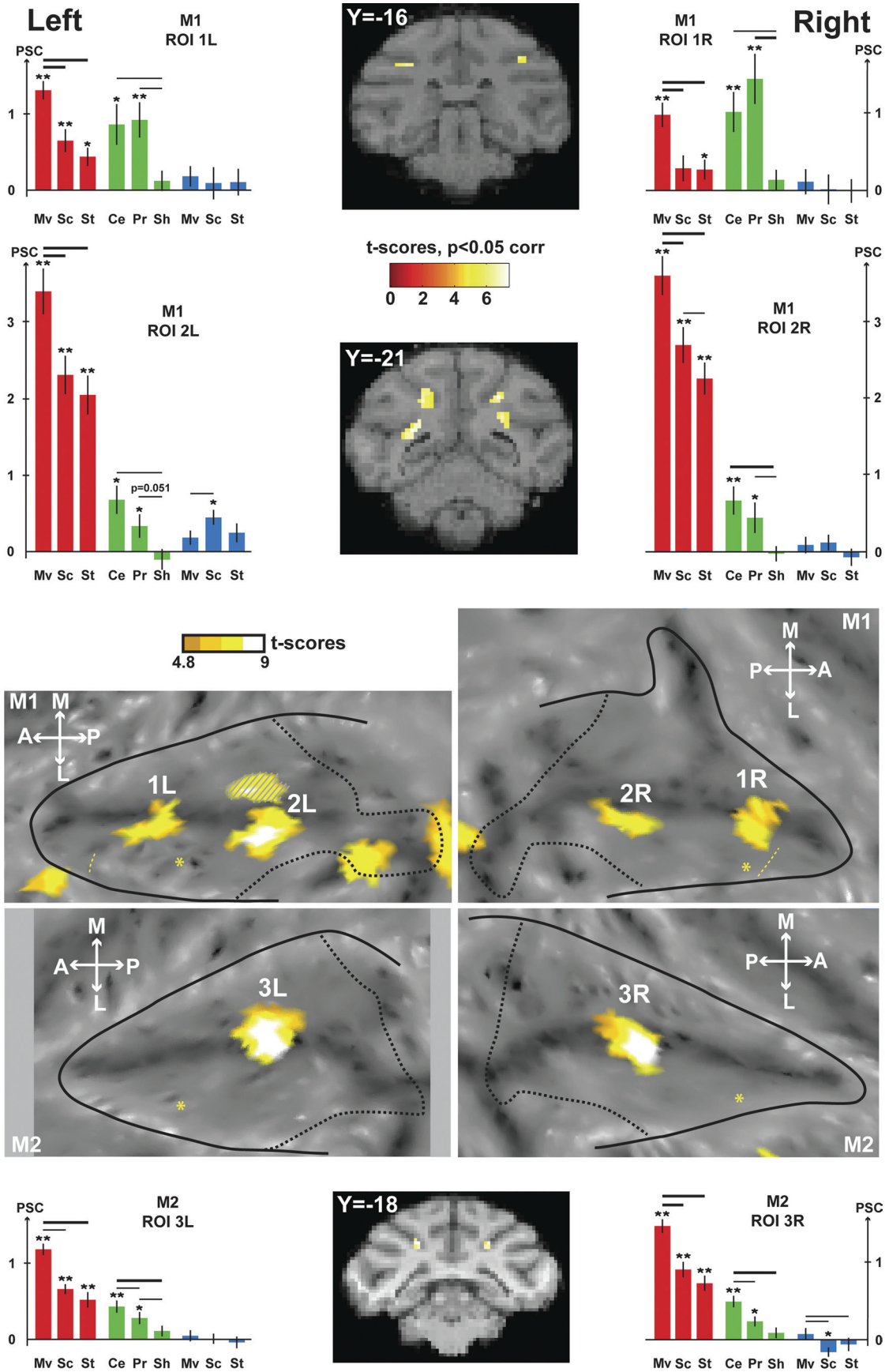

Figure 5. VT movement-specific conjunction analyses. The contrasts used for the conjunction are the visual contrasts (coherent movement vs scrambled and coherent movement vs static) and the tactile contrast (center of the face vs fixation). The activations are masked by the visual contrast (coherent movement vs fixation) so as to display only positive signal change relative to the fixation baseline. The VT conjunction ($p < 0.05$, FWE-corrected level) is shown on the flat maps of the two individual monkeys, and SPMs are displayed on two coronal (*Figure legend continues.*)

firming our previous observations, auditory regions processing movement were mainly found at the fundus of the IPS in three of four hemispheres (two regions in both hemispheres of monkey M1 and one region in the right hemisphere of monkey M2).

Together, this suggests that processing moving visual or auditory stimuli recruited overlapping regions in the fundus of the IPS. Interestingly, these regions also overlapped with tactile regions activated by stimulations to the center of the face (Fig. 4, middle), signing a region of multisensory convergence. In this context, air puff stimulations can be viewed as the dynamic impact of an object approaching the face. We did not specifically test for dynamic versus stationary tactile stimulations (the latter being quite challenging to produce). We rather focused on face specificity with respect to other body parts (the fundus of the IPS being known to preferentially represent the face) (Duhamel et al., 1998). We thus cannot conclude whether the tactile activations we observe at the fundus of the IPS are induced by the stationary or the movement components of the tactile stimulations to the face (air puffs to the face, including both aspects). If we extrapolate recording results from Duhamel et al. (1998), who showed that 30% of VIP tactile cells have no direction selectivity, this would mean that 70% of the tactile fMRI signal we observe is driven by the dynamic component of the air puffs, whereas the remaining 30% is driven by the purely stationary component of tactile face stimulation (see discussion on this point).

Convergence of multimodal movement processing signals within the IPS as a putative definition of the VIP

In the next step, we looked for the multimodal regions at the fundus of the IPS that are specific to movement processing, thanks to conjunction analyses. Both the visual and the tactile modalities activated very robustly the IPS. As a result, the most reliable sensory convergence was the visuo-tactile one (Fig. 5, VT, coronal sections, orange to white areas on the flat maps). Two bilateral regions were observed at the fundus of the IPS in M1 [anterior, 1L (−14, −16, 10), t score = 6.12 and 1R (16, −16, 12), t score = 5.98; posterior, 2L (−9, −22, 9), t score = 6.61 and 2R (10, −22, 10), t score = 7.12); and one bilateral region was observed in M2 (3L (−9, −16, 9), t score = 6.86 and 3R (10, −16, 9), t score = 6.64]. An ROI analysis based on these VT conjunction results (Fig. 5, red and green histograms) showed that these bimodal regions were dominated by the visual input and specifically its movement component, and were more activated by the face tactile stimulations than by the shoulder stimulations (Fig. 3). Auditory stimulations elicited almost no responses in these regions (Fig. 5, blue histograms).

The visual, auditory, and tactile conjunction analysis was performed at a lower statistical level ($p < 0.05$ at uncorrected level, conjunction of four contrasts). In M1, we observed again two bilateral regions at the fundus of the IPS for the visuo-auditory-tactile (VAT) conjunction (Fig. 6*A*, purple to white color scale): M1 anterior, left (−12, −16, 9), t score = 2.64, right (22, −15, 11), t score = 2.11; M1 posterior, left (−9, −20, 7), t score = 1.70, right (7, −20, 9), t score = 2.33. In M2, one bilateral trimodal region was identified, again at the fundus of the IPS (Fig. 6*A*, purple to white color scale): M2, left (−10, −18, 8), t score = 2.21, right (8, −17, 7), t score = 2.63. These VAT regions were used to define another set of ROIs (Fig. 6*A*, histograms), in which the PSC profiles were very similar to the VT profiles but lower for all conditions, except the auditory ones. Notably, the PSC for auditory movement was significantly different from that for static auditory stimuli for all ROIs, both in monkey M1 and monkey M2. In monkey M2, one additional VAT conjunction region is observed on the medial bank of the IPS. As no VT region is identified at corrected level in this monkey, and no VT or VAT convergence is observed in the medial bank of the IPS in monkey M1, this observation will not be considered in the following sections.

To evaluate the robustness of the VAT conjunction analysis, we performed test-retest analyses (Fig. 6*B*). ODD and EVEN groups of runs were selected independently from the visual, tactile, and auditory runs. PSC were calculated for the relevant contrasts (coherent movement vs scrambled and coherent movement vs static for the visual modality, center of the face vs fixation for the tactile modality, and coherent movement vs static for the auditory modality), for each of the ROIs identified by the VAT conjunction analysis (2 ROIs per hemisphere in monkey M1 and 1 ROI per hemisphere in monkey M2), on all the runs, on the ODD test-retest dataset and on the EVEN test-retest dataset. All PSC changes are significant at $p < 0.05$ or at $p < 0.001$, except for the auditory contrasts calculated in the left ROI of monkey M2, for which PSC reaches significance for all the runs together, are close to significance for the EVEN test-retest dataset ($p = 0.07$) but not significant for the ODD test-retest dataset.

In the following section, we address the fact that, in monkey M1, two multimodal regions are observed in the fundus of the IPS, whereas only one multimodal region was found in monkey M2. First, we tested the robustness of the spatial disjunction between these two VAT regions in monkey M1. To this end, we defined two cubic ROIs of 8 contiguous voxels lying in the fundus of the right and left IPS, respectively, just between the two multimodal regions of each hemisphere. Percentage signal changes remained far from significance for both ROIs, for all tested contrasts (tactile [center of the face vs fixation], visual [coherent movement vs scrambled], visual [coherent movement vs static], auditory [coherent movement vs static]), on all data as well as on a test-retest analysis considering first the ODD runs of each modality then the EVEN runs of each modality. Second, we compared the activation profiles within these ROIs (VT ROIs 1 and 2 in Fig. 5 and VAT ROIs 1′ and 2′ in Fig. 6) to evaluate whether these two regions were functionally different or not. Although the PSC for the center of the face tactile stimulation and for the visual coherent movement were similar in the anterior ROI, the response to visual movement was significantly higher than the tactile one in the posterior ROI: pooled left and right data, two-way ANOVA, conditions × ROIs, interaction $p < 2 \times 10^{-14}$ for the VT ROI and $p < 7 \times 10^{-5}$ for the VAT ROI; Holm-Sidak *post hoc* test, $p > 0.25$ for the visual versus tactile comparison in the anterior VT ROI (respectively $p > 0.1$ for the anterior VAT ROI) and $p < 10^{-15}$ for the visual versus tactile comparison in the posterior VT ROI (respectively $p < 10^{-7}$ for the posterior VAT ROI). This was the only distinctive feature we could identify between these two regions. In particular, there was no difference in the relative strength of the tactile responses to the center and to the periphery of the face between the anterior and posterior ROIs (interaction for the two-way ANOVA, condition × ROI, $p = 0.11$ and $p = 0.58$, for the VT and the VAT ROIs, respectively), or any

←

(*Figure legend continued.*) sections in M1 and one coronal section in M2. Histograms show the PSC (mean ± SE) within the ROIs defined by the VT conjunction (1L/1R and 2L/2R for M1, 3L/3R for M2) for each individual condition of the visual runs (red: Mv, Coherent movement; Sc, scrambled; St, static), the tactile runs (green: Ce, Center of the face; Pr, periphery of the face; Sh, shoulders), and the auditory runs (blue). t tests were performed on the PSC for each condition (**$p < 0.001$, *$p < 0.05$), and in-between conditions (thick line: $p < 0.001$; thin line: $p < 0.05$). For other conventions, see Figure 2.

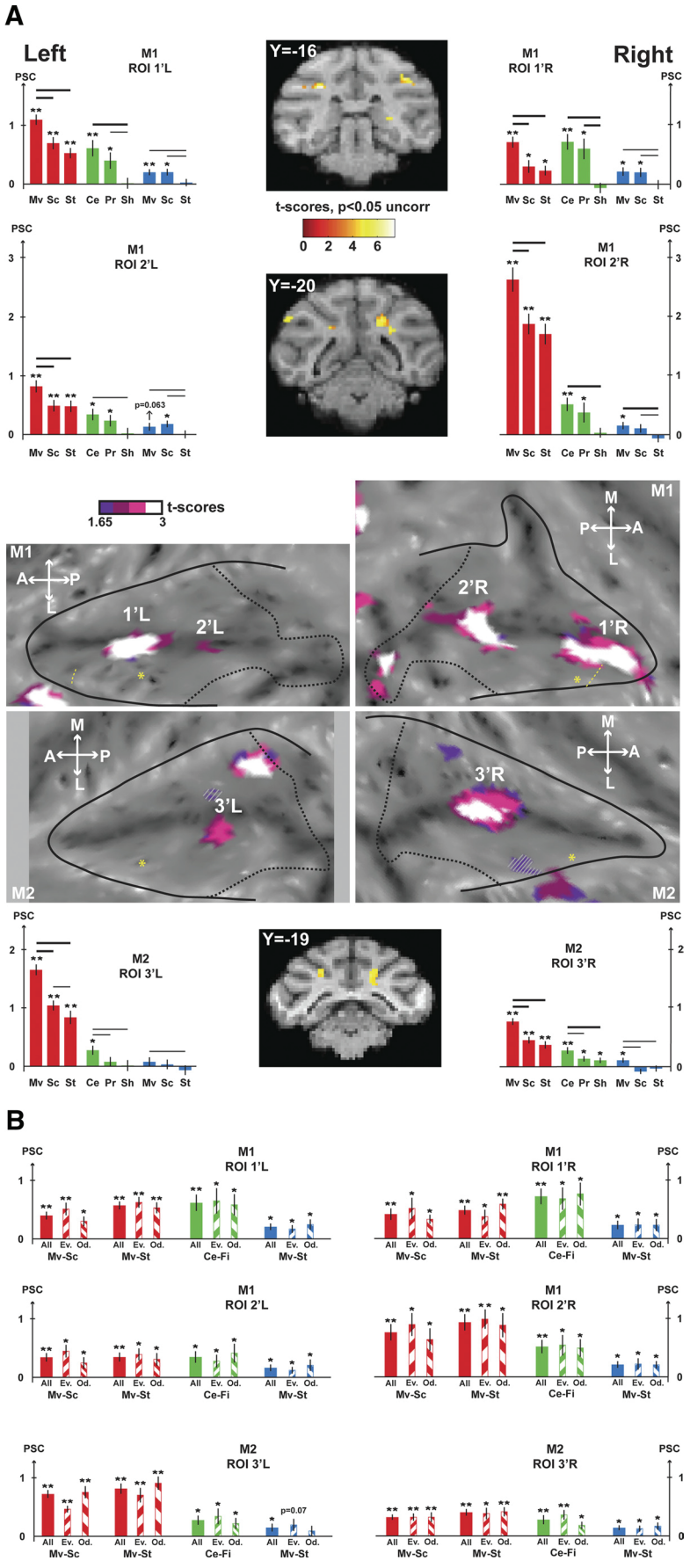

Figure 6. VAT movement-specific conjunction analyses. ***A***, The contrasts used for the conjunction are the visual contrasts (coherent movement vs scrambled and coherent movement vs static), the tactile contrast (center of the face vs fixation), and the auditory contrast (coherent movement vs static). The VAT conjunction is shown at the uncorrected level ($p < 0.05$). The activations are masked by the visual contrast (coherent movement vs fixation) so as to display only positive signal change relative to the fixation baseline. For other conventions, see Figure 5. ***B***, Test-retest analyses performed on VAT ROIs (1′L/1′R and 2′L/2′R for M1, 3′L/3′R for M2). For each region of interest, histograms show the PSC (mean ± SE) for the contrasts of interest used to define the VAT conjunction (visual contrasts: Mv-Sc, coherent movement vs scrambled; Mv-St, coherent movement vs static; tactile contrasts: Ce-Fi, center of the face vs fixation; auditory contrast: Mv-St, coherent movement vs static). For each sensory modality and each contrast, PSC of the whole dataset (full colored bars) and even/odd subsets (135°/45° hatched colored bars) are presented. *t* tests were performed on the PSC for each condition (**$p < 0.001$; *$p < 0.05$).

difference in the retinotopy localizer-induced activations (similar activation profiles in the anterior and posterior ROIs for central visual stimulation, horizontal meridian, vertical meridian, superior peripheral stimulation and inferior visual stimulation, stimulations as in Fize et al., 2003; data not shown, interaction for the two-way ANOVA, condition × ROI, $p = 0.39$ and $p = 0.76$ for the VT and the VAT ROIs, respectively). In conclusion, these anterior and posterior regions of monkey M1 IPS fundus have similar activation profiles, the only difference being that the posterior regions are more activated by the visual stimuli than by the tactile stimuli, consistent with the observation that the visual modality dominates the posterior portion of the IPS (Fig. 2).

The regions of convergence for multimodal movement processing signals identified above (ROIs and VAT ROIs in all 4 hemispheres) consistently fall in the fundus of the IPS at a location compatible with the described localization of area VIP based on anatomical and connectivity data (Lewis and Van Essen, 2000a). To confirm this, we projected the individual results of each monkey on a common atlas (F6 atlas in Caret), together with the boundaries of the intraparietal areas as defined by Lewis and Van Essen (2000a, 2000b) (Fig. 7). Interestingly, the VT and VAT regions mainly fall within what has been described as VIPl, at the fundus of the IPS, without however encompassing its whole anteroposterior extent. In monkey M1, the anterior region, which is functionally undistinguishable from the posterior region (except for a slight difference in the ratio between the visual and tactile levels of activation), extends anteriorly to the boundaries of area VIP, in what is identified in the F6 atlas as anterior intraparietal area (AIP). However, given

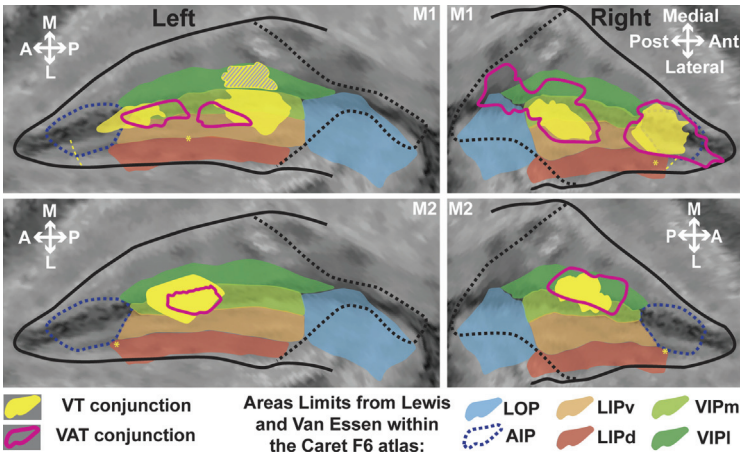

Figure 7. Projection of the VT and VAT conjunction results onto the F6 Caret atlas. Only the activations at the fundus of the IPS are represented. The boundaries of relevant IPS subdivisions as defined in the F6 atlas from Lewis and Van Essen (2000a, 2000b) are color shaded. See main text for a discussion of the boundaries of the AIP (dotted blue lines). For other conventions, see Figure 2.

the reported physiological properties of area AIP (Sakata and Taira, 1994; Murata et al., 2000), it appears that the IPS cytoarchitectonic organization of monkey M1 is not perfectly captured by its coregistration onto the F6 atlas. As a result, we think that this anterior ROI actually belongs to VIP. Corroborating this fact, this ROI never extends anteriorly to the anterior border of area LIP in either hemisphere (as defined by the eye movement activation anterior limit, $p < 0.05$, FWE-corrected level). This is in agreement with most electrophysiological and anatomical studies that describe the anterior border of VIP as matching that of LIP (Sakata and Taira, 1994; Luppino et al., 1999; Murata et al., 2000; Borra et al., 2008). The proposed location of AIP in the F6 atlas is also questionable as this area is rarely described as encompassing the fundus of anterior IPS (Luppino et al., 1999; Lewis and Van Essen, 2000a, 2000b).

The dual VT and VAT regions observed in monkey M1 strongly suggest an interindividual variability in IPS multisensory convergence patterns between monkeys M1 and M2. In the following, we consider sequentially the following: (1) within individual interhemispheric size variability, (2) interindividual size variability, (3) within individual interhemispheric spatial variability, and (4) interindividual spatial variability. The projection surface of the significant voxels onto the flat map (Fig. 7) does not allow to precisely address these questions, and a voxel count is more appropriate as it reflects the volume of cortex specifically recruited in the contrast of interest (VT ROIs; M1, anterior ROI, right: 31 voxels; left: 49 voxels; posterior ROI, right: 65 voxels; left: 132 voxels, including mirror activations on medial bank; M2, right: 53 voxels; left: 86 voxels). An interhemispheric size variability can be noted, ranging between a 30% and a 60% size difference (only an approximation of this measure can be derived for the posterior ROI of monkey M1). The interindividual size variability ranges between 50% (left hemisphere) and 80% (right hemisphere), thus slightly surpassing intraindividual variability. This observation is in agreement with reports of higher interindividual variability in area size compared with intraindividual variability, and specifically in higher-order areas, such as VIP (for review, see Krubitzer and Seelke, 2012). From a spatial perspective, the identified convergence regions within each hemisphere in a given animal are positioned symmetrically with respect to each other, as can be seen from the coronal sections of Figures 5 and 6. In contrast, their location in monkey M2 appears to fall just in between the two convergence regions identified in monkey M1, indicating a high degree of interindividual variability. Overall, the same analysis applies to the VAT convergence regions, although both their intraindividual and interindividual variability appear to be more important than that of the VT convergence. This is most probably because, although the VT convergence analysis is affected by the variability of visual and tactile projections within the IPS, the VAT convergence analysis is affected by the variability of all of the visual, tactile, and auditory projections within the IPS. The intraindividual and interindividual variability we observe in the VT and VAT convergence patterns is the result of the variability of visual and tactile projections within the IPS as described from anatomical studies (Fig. 4) (e.g., Lewis and Van Essen, 2000a). Overall, this depicts a patchy topographic organization of VT VIP domains.

Discussion

fMRI allows us to capture the spatial extent of the visual, tactile, and auditory domains within the IPS as well as their regions of overlap. In particular, we highlight a heterogeneous region involved in the processing of the movement component of these different sensory modalities. This region corresponds to area VIP as defined by its cytoarchitectonic limits. We further describe, within VIP, a region specifically dedicated to the amodal processing of movement (i.e., irrespective of the sensory domain by which it is determined).

Sensory domains within the IPS

Posterior IPS is strongly recruited by large field moving visual patterns (coherent movement vs fixation contrast; Fig. 2). This activation extends from the parieto-occipital pole and the inferior parietal gyrus to two-thirds into the IPS and up its medial and lateral banks. This activation covers area LIP, in agreement with single-cell recording studies describing complex neuronal responses to moving visual patterns (Eskandar and Assad, 1999, 2002; Williams et al., 2003) and fMRI (Vanduffel et al., 2001). It also covers area medial intraparietal area (MIP), although the visual responses in this cortical area are strongest when associated with a coordinated hand movement (Eskandar and Assad, 2002; Grefkes and Fink, 2005). Finally, VIP is also robustly activated, in agreement with its functional involvement in the processing of large field visual stimuli (Bremmer et al., 2002a, 2002b). Within this visual IPS, we further identify a visual movement-specific territory (coherent movement vs scrambled and coherent movement vs static contrasts; Fig. 5), grossly encompassing the posterior half of the IPS fundus. This region is consistently larger than the fundal IPS region activated by the random dot patterns used by Vanduffel et al. (2001) to identify VIP, most probably the result of the high speed (100°/s vs 2–6°/s) and large aperture (60° vs 14°) of our stimuli.

Tactile stimulations to the face activate the anterior inferior parietal gyrus extending down into the IPS fundus. Tactile stimulations to the center of the face produce higher IPS activations than tactile stimulations to the periphery of the face, although both are colocalized (Fig. 3). Shoulder tactile stimulations produce very low IPS activations, specific to the upper medial bank (in agreement with early descriptions of somatosensory responses in this region; for review, see Hyvärinen, 1982), confirming the overrepresentation of the face with respect to other body parts within the IPS fundus as described by single-cell recording studies (Duhamel et

al., 1998). Contrary to the two other modalities, we did not specifically test for tactile movement. However, because of the reported characteristics of tactile neurons in the fundus of the IPS (Duhamel et al., 1998), we think that our tactile activations are part of the global processing of movement around and toward the face (70% of VIP's tactile cells have tactile direction selectivity, which could be driven by the dynamic component of air puffs in our experiment; the other 30% of cells respond to stationary tactile stimulations touching the face or moving away from it, in congruence to their visual response to proceeding/receding optic flow).

The auditory IPS activations are weak, consistent with Joly et al. (2011) and with the known light connections from the caudomedial auditory belt (Lewis and Van Essen, 2000a). Auditory responses have been described in area VIP in naive animals (Schlack et al., 2005), using broadband auditory noise stimuli that are known to allow for a better sound localization ability than stimuli with narrower bandwidths (Blauert, 1997). Auditory responses have also been recorded, during spatially guided behavior, both in area LIP and in the parietal reach region (Mazzoni et al., 1996; Stricanne et al., 1996; Cohen et al., 2002; Gifford and Cohen, 2005). However, these activities have been shown to be nonexistent in naive animals, only arising after behavioral training (Grunewald et al., 1999; Linden et al., 1999). We thus predict that our activations would be stronger in animals trained to perform an auditory-motor behavior (Mullette-Gillman et al., 2005, 2009).

Functional definition of the ventral parietal area VIP

In the present work, we were specifically interested in the IPS regions that were functionally specialized for processing moving stimuli independent of which sensory modality in which they were presented. A single domain dedicated to movement could be identified, situated at the fundus of the IPS, coinciding within the VIP, as defined by Lewis and Van Essen (2000a, 2000b). This area is monosynaptically connected with the medial temporal area MT (Maunsell and van Essen, 1983; Ungerleider and Desimone, 1986) and with the somatosensory cortex (Seltzer and Pandya, 1980; Lewis and Van Essen, 2000a). Weak but direct connections with the caudo-medial auditory belt have also been described (Lewis and Van Essen, 2000a). From a functional point of view, area VIP was initially defined based on its neuronal responses to visual stimuli approaching the face (Colby et al., 1993) or representing relative movement of the subject with its environment (Bremmer et al., 2002a, 2002b). In addition to unimodal visual neurons, VIP also hosts neurons that are modulated by VT (Duhamel et al., 1998; Avillac et al., 2005) and visuo-vestibular stimulations (Bremmer et al., 2002b; Chen et al., 2011).

Although the extent of the motion-specific visual region we describe matches closely the expected cytoarchitectonically defined VIP (joint VIPl and VIPm of Lewis and Van Essen, 2000b), both the VT and VAT conjunctions cover only part of this region, sometimes extending into ventral LIP (Fig. 7). Although spatially contiguous, these multimodal regions only partially overlap. We thus provide functional evidence for a multimodal associative definition of area VIP, spatially more restrictive than its motion-specific definition. Our data support a patchy organization of this IPS region, although higher-resolution fMRI acquisitions will be required to directly address this point. In addition, because the vestibular modality has not been tested, we do not know where visuo-vestibular convergence regions would fall in the fundus of the IPS with respect to the reported multimodal convergence regions and whether a purely visual region will be found to coexist next to multimodal patches. The recordings of Chen et al. (2011) suggest that visuo-vestibular convergence should be found all throughout the fundus of the IPS (their Fig. 1) as they report that up to 97% of the cells recorded in this region respond to rotational vestibular stimulations while at the same time 98% of them respond to translational or rotational visual stimulations (Table 1 in Chen et al., 2011).

In addition to multisensory convergence, VIP has also been described as a cortical site of multisensory integration (Bremmer et al., 2002b; Avillac et al., 2007; Chen et al., 2011). While we expect that the VIP patches we identify will be performing multisensory integration across the dominant sensory modalities by which they are activated, it is not clear whether they will also be influenced by sensory signals from contiguous patches. Indeed, in Avillac et al. (2007), we describe visual unimodal neurons within VIP whose responses are modulated by tactile stimulation. Only electrophysiological recordings performed in fMRI-identified patches will allow to test whether multisensory integration is processed locally or at the level of the whole area.

It is important to note that the multimodal convergence we describe here is dependent on the stimulation characteristics and as such does not reflect the entirety of multisensory convergence patterns within the IPS. For example, multisensory convergence is also expected to be found in areas MIP and AIP. However, whereas our visual stimuli robustly activate the medial bank of the IPS, the tactile stimulations we used do not. Hand or arm tactile stimulations would have been more suited to map multisensory convergence in MIP (for review, see Grefkes and Fink, 2005). Conversely, whereas our tactile stimulations robustly activate the anterior most part of the IPS, the visual stimuli we use are clear not optimal for this region. Objects with 3D structure or small 2D objects would have allowed describing multisensory convergence in area AIP (Durand et al., 2007).

Comparison with human studies

Our present observations in the macaque monkey reveal several similarities of interest with human fMRI studies identifying VIP on the basis of its multimodality. Bremmer et al. (2001) identify human VIP based on a conjunction analysis of visual, auditory, and face tactile stimulations. The group results reveal a unitary human VIP, whereas the single subject activations suggest that the patchy organization that we describe here might be a shared functional trait between humans and nonhuman primates. In another study, Sereno and Huang (2006) highlight an important interindividual and intraindividual variability in the location and extent of human VIP within the parietal cortex. In addition, their subject 2 (Fig. 5 of Sereno and Huang, 2006) has a doubled representation of both its somatosensory and visual maps. This is similar to our monkey M1 in which we describe two disjoint sites of VAT conjunction, suggesting that such a duplication of cortical maps might be more under the dependence of ontogenetic rather than phylogenetic factors.

References

Akbarian S, Grüsser OJ, Guldin WO (1994) Corticofugal connections between the cerebral cortex and brainstem vestibular nuclei in the macaque monkey. J Comp Neurol 339:421–437. CrossRef Medline

Andersen RA, Cui H (2009) Intention, action planning, and decision making in parietal-frontal circuits. Neuron 63:568–583. CrossRef Medline

Arcaro MJ, Pinsk MA, Li X, Kastner S (2011) Visuotopic organization of macaque posterior parietal cortex: a functional magnetic resonance imaging study. J Neurosci 31:2064–2078. CrossRef Medline

Avillac M, Denève S, Olivier E, Pouget A, Duhamel JR (2005) Reference frames for representing visual and tactile locations in parietal cortex. Nat Neurosci 8:941–949. CrossRef Medline

Avillac M, Ben Hamed S, Duhamel JR (2007) Multisensory integration in the ventral intraparietal area of the macaque monkey. J Neurosci 27:1922–1932. CrossRef Medline

Ben Hamed S, Duhamel JR, Bremmer F, Graf W (2001) Representation of

the visual field in the lateral intraparietal area of macaque monkeys: a quantitative receptive field analysis. Exp Brain Res 140:127–144. CrossRef Medline

Blauert J (1997) Spatial hearing. Cambridge, MA: MIT.

Borra E, Belmalih A, Calzavara R, Gerbella M, Murata A, Rozzi S, Luppino G (2008) Cortical connections of the macaque anterior intraparietal (AIP) area. Cereb Cortex 18:1094–1111. CrossRef Medline

Bremmer F (2011) Multisensory space: from eye-movements to self-motion. J Physiol 589:815–823. CrossRef Medline

Bremmer F, Schlack A, Shah NJ, Zafiris O, Kubischik M, Hoffmann K, Zilles K, Fink GR (2001) Polymodal motion processing in posterior parietal and premotor cortex: a human fMRI study strongly implies equivalencies between humans and monkeys. Neuron 29:287–296. CrossRef Medline

Bremmer F, Duhamel JR, Ben Hamed S, Graf W (2002a) Heading encoding in the macaque ventral intraparietal area (VIP). Eur J Neurosci 16:1554–1568. CrossRef Medline

Bremmer F, Klam F, Duhamel JR, Ben Hamed S, Graf W (2002b) Visual-vestibular interactive responses in the macaque ventral intraparietal area (VIP). Eur J Neurosci 16:1569–1586. CrossRef Medline

Brett M, Anton JL, Valabregue R, Poline JB (2002) Region of interest analysis using an SPM toolbox [abstract]. Presented at the 8th International Conference on Functional Mapping of the Human Brain, Sendai, Japan, June 2–6, 2002.

Chen A, DeAngelis GC, Angelaki DE (2011) Representation of vestibular and visual cues to self-motion in ventral intraparietal cortex. J Neurosci 31:12036–12052. CrossRef Medline

Cohen YE, Batista AP, Andersen RA (2002) Comparison of neural activity preceding reaches to auditory and visual stimuli in the parietal reach region. Neuroreport 13:891–894. CrossRef Medline

Colby CL, Goldberg ME (1999) Space and attention in parietal cortex. Annu Rev Neurosci 22:319–349. CrossRef Medline

Colby CL, Duhamel JR, Goldberg ME (1993) Ventral intraparietal area of the macaque: anatomic location and visual response properties. J Neurophysiol 69:902–914. Medline

Disbrow E, Litinas E, Recanzone GH, Padberg J, Krubitzer L (2003) Cortical connections of the second somatosensory area and the parietal ventral area in macaque monkeys. J Comp Neurol 462:382–399. CrossRef Medline

Duhamel JR, Bremmer F, Ben Hamed S, Graf W (1997) Spatial invariance of visual receptive fields in parietal cortex neurons. Nature 389:845–848. CrossRef Medline

Duhamel JR, Colby CL, Goldberg ME (1998) Ventral intraparietal area of the macaque: congruent visual and somatic response properties. J Neurophysiol 79:126–136. Medline

Durand JB, Nelissen K, Joly O, Wardak C, Todd JT, Norman JF, Janssen P, Vanduffel W, Orban GA (2007) Anterior regions of monkey parietal cortex process visual 3D shape. Neuron 55:493–505. CrossRef Medline

Eskandar EN, Assad JA (1999) Dissociation of visual, motor and predictive signals in parietal cortex during visual guidance. Nat Neurosci 2:88–93. CrossRef Medline

Eskandar EN, Assad JA (2002) Distinct nature of directional signals among parietal cortical areas during visual guidance. J Neurophysiol 88:1777–1790. CrossRef Medline

Faugier-Grimaud S, Ventre J (1989) Anatomic connections of inferior parietal cortex (area 7) with subcortical structures related to vestibulo-ocular function in a monkey (Macaca fascicularis). J Comp Neurol 280:1–14. CrossRef Medline

Fize D, Vanduffel W, Nelissen K, Denys K, Chef d'Hotel C, Faugeras O, Orban GA (2003) The retinotopic organization of primate dorsal V4 and surrounding areas: a functional magnetic resonance imaging study in awake monkeys. J Neurosci 23:7395–7406. Medline

Gifford GW 3rd, Cohen YE (2005) Spatial and non-spatial auditory processing in the lateral intraparietal area. Exp Brain Res 162:509–512. CrossRef Medline

Graziano MS, Cooke DF (2006) Parieto-frontal interactions, personal space, and defensive behavior. Neuropsychologia 44:2621–2635. CrossRef Medline

Grefkes C, Fink GR (2005) The functional organization of the intraparietal sulcus in humans and monkeys. J Anat 207:3–17. CrossRef Medline

Grunewald A, Linden JF, Andersen RA (1999) Responses to auditory stimuli in macaque lateral intraparietal area: I. Effects of training. J Neurophysiol 82:330–342. Medline

Hyvärinen J (1982) Posterior parietal lobe of the primate brain. Physiol Rev 62:1060–1129. Medline

Joly O, Ramus F, Pressnitzer D, Vanduffel W, Orban GA (2012) Interhemispheric differences in auditory processing revealed by fMRI in awake rhesus monkeys. Cereb Cortex 22:838–853. CrossRef Medline

Krubitzer LA, Seelke AM (2012) Cortical evolution in mammals: the bane and beauty of phenotypic variability. Proc Natl Acad Sci U S A 26;109 [Suppl 1]:10647–10654. CrossRef Medline

Lewis JW, Van Essen DC (2000a) Corticocortical connections of visual, sensorimotor, and multimodal processing areas in the parietal lobe of the macaque monkey. J Comp Neurol 428:112–137. CrossRef Medline

Lewis JW, Van Essen DC (2000b) Mapping of architectonic subdivisions in the macaque monkey, with emphasis on parieto-occipital cortex. J Comp Neurol 428:79–111. CrossRef Medline

Lewis JW, Beauchamp MS, DeYoe EA (2000) A comparison of visual and auditory motion processing in human cerebral cortex. Cereb Cortex 10:873–888. CrossRef Medline

Lewis JW, Brefczynski JA, Phinney RE, Janik JJ, DeYoe EA (2005) Distinct cortical pathways for processing tool versus animal sounds. J Neurosci 25:5148–5158. CrossRef Medline

Linden JF, Grunewald A, Andersen RA (1999) Responses to auditory stimuli in macaque lateral intraparietal area: II. Behavioral modulation. J Neurophysiol 82:343–358. Medline

Luppino G, Murata A, Govoni P, Matelli M (1999) Largely segregated parietofrontal connections linking rostral intraparietal cortex (areas AIP and VIP) and the ventral premotor cortex (areas F5 and F4). Exp Brain Res 128:181–187. CrossRef Medline

Mandeville JB, Choi JK, Jarraya B, Rosen BR, Jenkins BG, Vanduffel W (2011) FMRI of cocaine self-administration in macaques reveals functional inhibition of basal ganglia. Neuropsychopharmacology 36:1187–1198. CrossRef Medline

Maunsell JH, van Essen DC (1983) The connections of the middle temporal visual area (MT) and their relationship to a cortical hierarchy in the macaque monkey. J Neurosci 3:2563–2586. Medline

Mazzoni P, Bracewell RM, Barash S, Andersen RA (1996) Spatially tuned auditory responses in area LIP of macaques performing delayed memory saccades to acoustic targets. J Neurophysiol 75:1233–1241. Medline

Mullette-Gillman OA, Cohen YE, Groh JM (2005) Eye-centered, head-centered, and complex coding of visual and auditory targets in the intraparietal sulcus. J Neurophysiol 94:2331–2352. CrossRef Medline

Mullette-Gillman OA, Cohen YE, Groh JM (2009) Motor-related signals in the intraparietal cortex encode locations in a hybrid, rather than eye-centered reference frame. Cereb Cortex 19:1761–1775. CrossRef Medline

Murata A, Gallese V, Luppino G, Kaseda M, Sakata H (2000) Selectivity for the shape, size, and orientation of objects for grasping in neurons of monkey parietal area AIP. J Neurophysiol 83:2580–2601. Medline

Orban GA (2011) The extraction of 3D shape in the visual system of human and nonhuman primates. Annu Rev Neurosci 34:361–388. CrossRef Medline

Sakata H, Taira M (1994) Parietal control of hand action. Curr Opin Neurobiol 4:847–856. CrossRef Medline

Schaafsma SJ, Duysens J (1996) Neurons in the ventral intraparietal area of awake macaque monkey closely resemble neurons in the dorsal part of the medial superior temporal area in their responses to optic flow patterns. J Neurophysiol 76:4056–4068. Medline

Schlack A, Sterbing-D'Angelo SJ, Hartung K, Hoffmann KP, Bremmer F (2005) Multisensory space representations in the macaque ventral intraparietal area. J Neurosci 25:4616–4625. CrossRef Medline

Seltzer B, Pandya DN (1980) Converging visual and somatic sensory cortical input to the intraparietal sulcus of the rhesus monkey. Brain Res 192:339–351. CrossRef Medline

Sereno MI, Huang RS (2006) A human parietal face area contains aligned head-centered visual and tactile maps. Nat Neurosci 9:1337–1343. CrossRef Medline

Stricanne B, Andersen RA, Mazzoni P (1996) Eye-centered, head-centered, and intermediate coding of remembered sound locations in area LIP. J Neurophysiol 76:2071–2076. Medline

Ungerleider LG, Desimone R (1986) Cortical connections of visual area MT in the macaque. J Comp Neurol 248:190–222. CrossRef Medline

Van Essen DC, Drury HA, Dickson J, Harwell J, Hanlon D, Anderson CH (2001) An integrated software suite for surface-based analyses of cerebral cortex. J Am Med Inform Assoc 8:443–459. CrossRef Medline

Vanduffel W, Fize D, Mandeville JB, Nelissen K, Van Hecke P, Rosen BR, Tootell RB, Orban GA (2001) Visual motion processing investigated using contrast agent-enhanced fMRI in awake behaving monkeys. Neuron 32:565–577. CrossRef Medline

Williams ZM, Elfar JC, Eskandar EN, Toth LJ, Assad JA (2003) Parietal activity and the perceived direction of ambiguous apparent motion. Nat Neurosci 6:616–623. CrossRef Medline

Zhang T, Heuer HW, Britten KH (2004) Parietal area VIP neuronal responses to heading stimuli are encoded in head-centered coordinates. Neuron 42:993–1001. CrossRef Medline

Chapter 2

Evidence for a Widespread Stimulus-Dependent Visuo-Tactile Convergence Network in the Macaque Monkey

Evidence for a widespread stimulus-dependent visuo-tactile convergence network in the macaque monkey

Abbreviated title: Visuo-tactile convergence in the macaque monkey

Authors: Olivier Guipponi[1], Soline Odouard[1], Claire Wardak[1], Suliann Ben Hamed[1]

1. Centre de Neuroscience Cognitive, CNRS UMR 5229, 67 Bd Pinel, 69675 Bron cedex, Université Claude Bernard Lyon I

Corresponding author: Suliann Ben Hamed, Centre de Neuroscience Cognitive, CNRS UMR 5229, Université Claude Bernard Lyon I, 67 Bd Pinel, 69675 Bron cedex, France, benhamed@isc.cnrs.fr

Abstract

Advances in neurosciences in the last decades have repeatedly challenged our views on the organization of cortical sensory processing. In particular, the proposal that sensory processing is achieved in segregated anatomical pathways has been profoundly revisited following the description of cross-modal connections both at higher and at lower processing levels. However, the spatial cortical extent of the functional influence of these connections has been missing. In the present study, we use functional magnetic resonance imaging to map, in the non-human primate brain, the cortical regions which are activated both by visual stimulation and tactile stimulations. This allows us to capture the spatial pattern of visuo-tactile cortical convergence, the extent of which has been overlooked by previous studies, both in low-level visual and somatosensory areas and in multiple higher-order associative temporal, parietal, prefrontal, cingulate and orbito-frontal areas. We also show that the profile of this visuo-tactile convergence is functionally shaped by the physical properties of the stimuli used for the mapping, suggesting that visuo-tactile convergence could actually be even more prevailing than what we describe. Last, functional connectivity within this large visuo-tactile convergence network appears to change between the tactile and the visual stimulation context, suggesting that this network could be dynamically tuned by the sensory context as well as possibly by the behavioral context.

Key words: visual, tactile, fMRI, macaque, convergence, functional connectivity.

Introduction

Advances in neurosciences in the last decades have repeatedly challenged our views on the organization of cortical sensory processing. Early anatomical (Kuypers et al. 1965) and lesion studies (Massopust et al. 1965) led to the description of segregated anatomical pathways, each processing a specific sensory modality. In 1991, Felleman and Van Essen (Felleman and Van Essen 1991) refined this view, proposing a massively parallel, hierarchical, processing organization of the visual system, in which the initial sensory stages are performed, by low level unimodal sensory areas, while later processing stages are performed by multisensory higher-order associative region, such as the temporal cortex (Beauchamp et al. 2004; Barraclough et al. 2005) or the parietal cortex (Duhamel et al. 1998; Avillac et al. 2005; Schlack et al. 2005; Sereno and Huang 2006; Guipponi et al. 2013). The subsequent description of heteromodal connection in early sensory processing areas (*e.g.* auditory projection onto visual cortex or vice-versa: Falchier et al. 2002; Rockland and Ojima 2003; Cappe and Barone 2005; somatosensory projections onto auditory cortex or vice-versa: Cappe and Barone 2005; Budinger et al. 2006; de la Mothe et al. 2006; Smiley et al. 2007; visual projections onto somatosensory cortex: Wallace et al. 2004) further nuanced this view, suggesting that multisensory processing takes place at earlier processing stages than commonly admitted. The contribution of these heteromodal projections to the modulation of the response of early sensory neurons is confirmed both by single cell recording studies (Schroeder and Foxe 2005; Vasconcelos et al. 2011; Iurilli et al. 2012) and functional neuroimaging studies (Sathian et al. 1997; Macaluso et al. 2000; Amedi et al. 2001). On the basis of the growing evidence for pervasive multisensory influences at all levels of cortical processing, Ghazanfar and Schroeder (Ghazanfar and Schroeder 2006) question, in a recent review, whether multisensory processing could actually be an essential property of neocortex.

Here, functional magnetic resonance imaging (fMRI) in the non-human primate allows us to capture the spatial pattern of visuo-tactile cortical convergence, the extent of which has been overlooked by previous studies, both in low-level visual and somatosensory areas and in multiple higher-order associative areas. In particular, we show that the profile of this visuo-tactile convergence is functionally shaped by the physical properties of the stimuli used for the mapping as well as by the general stimulation context.

Material and Methods

Subjects and materials

Two rhesus monkeys (female M1, male M2, 5-7 years old, 5-7 kg) participated to the study. The animals were implanted with a plastic MRI compatible headset covered by dental acrylic. The anesthesia during surgery was induced by Zoletil (Tiletamine-Zolazepam, Virbac, 15 mg/kg) and followed by Isoflurane (Belamont, 1-2%). Post-surgery analgesia was ensured thanks to Temgesic (buprenorphine, 0.3 mg/ml, 0.01 mg/kg). During recovery, proper analgesic and antibiotic coverage were provided. The surgical procedures conformed to European and National Institutes of Health guidelines for the care and use of laboratory animals.

During the scanning sessions, monkeys sat in a sphinx position in a plastic monkey chair positioned within a horizontal magnet (1.5-T MR scanner Sonata; Siemens, Erlangen, Germany) facing a translucent screen placed 90 cm from the eyes. Their head was restrained and equipped with MRI-compatible headphones customized for monkeys (MR Confon GmbH, Magdeburg, Germany). A radial receive-only surface coil (10-cm diameter) was positioned above the head. Eye position was monitored at 120 Hz during scanning using a pupil-corneal reflection tracking system (Iscan®, Cambridge, MA). Monkeys were rewarded with liquid dispensed by a computer-controlled reward delivery system (Crist®) thanks to a plastic tube coming to their mouth. The task, all the behavioral parameters as well as the sensory stimulations were controlled by two computers running with Matlab® and Presentation®. The fixation point the monkeys were instructed to fixate, as well as the visual stimuli, were projected onto a screen with a Canon XEED SX60 projector. Tactile stimulations were delivered through Teflon tubing and 6 articulated plastic arms connected to

distant air pressure electro-valves. Monkeys were trained in a mock scan environment approaching to the best the actual MRI scanner setup.

Task and stimuli

The animals were trained to maintain fixation on a red central spot (0.24°x0.24°) while stimulations (visual or tactile) were delivered. The monkeys were rewarded for staying within a 2°x2° tolerance window centered on the fixation spot. The reward delivery was scheduled to encourage long fixation without breaks (*i.e.* the interval between successive deliveries was decreased and their amount was increased, up to a fixed limit, as long as the eyes did not leave the window). The two sensory modalities were tested in independent interleaved runs (see below for the organization of the runs). Stimulation strength was maximized in order to saturate the evoked neuronal response and induce an unambiguously strong percept for all types of stimuli.

Visual stimulations. Large field (32°x32°) visual stimulations consisted in white bars (3.2°x24.3°, horizontal, vertical, or 45° oblique) or white random dots on a black background (Fig.1A). Three conditions were tested in blocks of 10 pulses (TR = 2.08 sec): 1) ***coherent movement***, with bars moving in one of the 8 cardinal directions or expanding or contracting random dots pattern (with 5 possible optic flow origins: center, upper left (-8°, 8°), upper right, lower left and lower right); each coherent movement sequence lasted 850ms and 24 such sequences were pseudo-randomly presented in a given coherent movement block; 2) ***scrambled movement***, in which the different frames of a given coherent movement sequence were randomly reorganized; 3) ***static***, in which individual frames randomly picked from the coherent movement visual stimuli sequences, were presented for 250ms. As a result, within a given block, 850ms portions of the different stimuli (bars/dots/directions/origins) of a same category (coherent/scrambled/static) were pseudo-randomly interleaved. The movement

related activations were reported for the parietal cortex in a previous paper (Guipponi, Wardak et al. 2013). In the present paper, we focus on the static stimulations only, so that the visual stimulation vs. fixation contrast corresponds to static visual stimuli compared to the fixation.

Tactile stimulations. They consisted in air puffs delivered to three different locations on the left and the right of the animals' body (Fig. 1B): 1) ***center*** of the face, close to the nose and the mouth; 2) ***periphery*** of the face, above the eyebrows; 3) ***shoulders*** (*cf.* Guipponi, Wardak et al., 2013).

Functional time series (runs) were organized as follows: a 10-volume block of pure fixation (baseline) was followed by a 10-volume block of stimulation category 1, a 10-volume block of stimulation category 2, and a 10-volume block of stimulation category 3; this sequence was played four times, resulting in a 160-volume run. The blocks for the 2 categories were presented in 6 counterbalanced possible orders. A ***retinotopy*** localizer was run independently in the two monkeys using exactly the stimulations of Fize and colleagues (Fize et al., 2003). This localizer is used to localize the central and peripheral representations of visual areas within each hemisphere, in both animals. Moreover, ***resting state*** runs consisted in 284-volume blocks of pure fixation for M1 and under anesthesia for M2 (Zoletil, 20 mg/kg).

Scanning

Before each scanning session, a contrast agent, monocrystalline iron oxide nanoparticle (Sinerem, Guerbet or Feraheme, AMAG, Vanduffel et al., 2001), was injected into the animal's femoral/saphenous vein (4-10 mg/kg). For the sake of clarity, the polarity of the contrast agent MR signal changes, which are negative for increased blood volumes, was

inverted. We acquired gradient-echo echoplanar (EPI) images covering the whole brain (1.5 T; repetition time (TR) 2.08 s; echo time (TE) 27 ms; 32 sagittal slices; 2x2x2-mm voxels). During each scanning session, the runs of different modalities and different orders were pseudo-randomly intermixed. A total of 40 (34) runs was acquired for visual stimulations in M1 (/M2), 36 (40) runs for tactile stimulations. Fifty-seven (45) runs were obtained for the retinotopy localizer were obtained in independent sessions for M1 (/M2). A total of 40 (12) runs was acquired for the resting state experiment for M1 (/M2).

Analysis

A total of 23 (25) runs were selected for the visual stimulation condition, 18 (20) for the tactile stimulation condition, 20 (24) for the retinotopy localizer and 20 (12) for the resting state experiment based on the quality of the monkeys' fixation throughout each run (>85% within the tolerance window). Time series were analyzed using SPM8 (Wellcome Department of Cognitive Neurology, London, United Kingdom). For spatial preprocessing, functional volumes were first realigned and rigidly coregistered with the anatomy of each individual monkey (T1-weighted MPRAGE 3D 0.6x0.6x0.6 mm or 0.5x0.5x0.5 mm voxel acquired at 1.5T) in stereotactic space. The JIP program (Mandeville et al., 2011) was used to perform a non-rigid coregistration (warping) of a mean functional image onto the individual anatomies. The same procedure was used to coregister the functional images of monkey M1 onto the anatomy of monkey M2 (*i.e.*, realignment followed by a rigid and then a non-rigid coregistration).

Fixed effect individual analyses were performed for each sensory modality in each monkey, with a level of significance set at $p<0.05$ corrected for multiple comparisons (FWE, $t>4.89$, unless stated otherwise). We also performed conjunction analyses (statistical levels set at $p<0.05$ at corrected level, unless stated otherwise). In all analyses, realignment parameters,

as well as eye movement traces, were included as covariates of no interest to remove eye movement and brain motion artifacts. When coordinates are provided, they are expressed with respect to the anterior commissure. Fixed effect group analyses were performed for each sensory modality and for conjunction analyses with a level of significance set at $p<0.001$ ($t>3.1$) and projected onto the anatomy of monkey M2. Results are displayed on coronal sections from M2 anatomy or on M2 flattened maps obtained with Caret (Van Essen et al., 2001; http://www.nitrc.org/projects/caret/).

Regions of Interest. We performed regions of interest (ROI) analyses using MarsBar toolbox (Brett et al., 2002), based on the group conjunction analyses results. The ROIs were defined using the activations obtained at corrected level (FWE, $t>4.89$) or at uncorrected level (t-scores>3.1) when the activations failed to reach the corrected level. When the activations obtained at corrected level were too large and included several areas, we defined a geometric cubic ROI (2x2x2mm) centered on the local maximum t-score. In rare instances, we also defined ROIs from individual analyses. This was the case when the functional activations obtained in both animals for a given area didn't show up on the group analysis because they were spatially contiguous but non-overlapping.

Effective connectivity analyses. Effective connectivity methodology can be divided in two consecutive steps: 1) the extraction and transformation of the raw signal and 2) the calculation of the functional connectivity patterns between ROI. These steps are illustrated on figure 2. The physiological raw signal was extracted for each modality, each run, each ROI and each animal (MarsBar toolbox, Brett et al., 2002). This signal contains the activities evoked either by visual or by tactile stimulations, as defined by the block structure of the runs. Figure 2a shows evoked tactile activities in two ROIs located at the tip of the intraparietal sulcus (left side: 130 mm^3 and right side: 68 mm^3). Effective connectivity between two ROIs is estimated on the residual physiological signal once the evoked activities have been

removed. To do this, the beta-weights relative to each task regressor were estimated (Fig. 2c) and subtracted from the physiological signal (Fig. 2d). This operation was performed on the deconvolved signal (Fig. 2b), so as to account for the temporal shift induced by the hemodynamic monkey response function.

Residual signal correlations between pairs of ROI were estimated run per run. For each run, the resulting r-scores were transformed into z scores (Fisher's r-to-z transform). These z-scores were then averaged across runs. Between run z-score differences were assessed thanks to t-tests. The reliability of these z-score differences was challenged at different statistical levels: either corrected for multiple comparisons thanks to Holm-Bonferroni method or non-corrected for multiple comparisons ($p<0.001$ or $p<0.01$).

Potential covariates. In all analyses, realignment parameters, as well as eye movement traces, were included as covariates of no interest to remove eye movement and brain motion artifacts. However, some of the stimulations might have induced a specific behavioral pattern biasing our analysis, not fully accounted for by the above regressors. For example, air-puffs to the face might have evoked facial mimics (as well as some imprecision in the point of impact of the air puff). While we cannot completely rule out this possibility, our experimental set-up allows to minimize its impact. First, monkeys worked head-restrained (to maintain the brain at the optimal position within the scanner, to minimize movement artifacts on the fMRI signal and to allow for a precise monitoring of their eye movements). As a result, the tactile stimulations to the center were stable in a given session. When drinking the liquid reward, small lip movements occurred. These movements thus correlated with reward timing and were on average equally distributed over the different sensory runs and the different conditions within each run (we checked that the monkeys had equal performance amongst the different conditions within a given run). The center of the face air puffs were placed on the cheeks on each side of the monkey's nose at a location that was not affected by the lip

movements. Peripheral body stimulation air puffs were directed to the shoulders, at a location that was not affected by possible arms movements by the monkey. This was possible because the monkey chair tightly fit the monkey's width. Second, monkeys were required to maintain their gaze on a small fixation point, within a tolerance window of 2°x2°. This was controlled online and was used to motivate the animal to maximize fixation rates (as fixation disruptions, such as saccades or drifts, affected the reward schedule). Eye traces were also analyzed offline for the selection of the runs to include in the analysis (good fixation for 85% of the run duration, with no major fixation interruptions). A statistical analysis indicates that the monkeys' performance was not significantly different across the visual or tactile (One-way ANOVA, M1, $p=0.75$, M2, $p=0.65$). This suggests that the overall oculomotor behavior was constant across types of runs.

Results

Monkeys were exposed, in independent time series, to visual (Figure 3, upper panel, red scale, visual stimulations versus fixation contrast) or tactile (Figure 3, upper panel, green scale, center of the face tactile stimulations versus fixation contrast) stimulations, while fixating a central point. In the following, we specifically focus on the visuo-tactile conjunction network, *i.e.* on the functional network that is activated both by visual and tactile stimulations. All reported activations are identified using a group analysis. As a result, they reflect the activations that are common to both monkeys.

Unimodal visual and tactile cortical networks

Static visual stimulations massively activated the occipital striate and extrastriate areas, the temporal cortex (superior temporal sulcus), the parietal cortex (inferior and medial parietal convexity and the lateral and posterior parts of the intraparietal sulcus), the prefrontal cortex (principal and arcuate sulci) and the inferior orbitofrontal cortex.

Center of the face tactile stimulations strongly activated primary (central sulcus) and secondary (lateral sulcus) somatosensory cortices, the cingulate cortex, the parietal cortex (anterior superior and inferior parietal convexities, anterior intraparietal sulcus), the prefrontal cortex (ventro-lateral prefrontal cortex and premotor cortex) and the inferior orbitofrontal cortex.

Visuo-tactile convergence network

Figure 3 (lower panel) represents the visuo-tactile conjunction statistical maps identifying the cortical regions responding both to visual stimuli and center of the face tactile stimuli. This analysis reveals parietal activations including posterior intraparietal area PIP,

ventral intraparietal area VIP, somatosensory area 7b and parietal opercular area 7op; prefrontal activations in area 46, area 8as, medial part of area 6Va, paramotor zone PMZ; cingulate activations in area 24d; insular activations in area Pi; and orbitofrontal activations in areas 11 and 13. Interestingly, both visual and tactile stimulations also activated, bilaterally, visual striate and extrastriate areas (V1, V2, V3, V3A), medial superior temporal area MST, as well as tactile somatosensory complex SII/PV.

Regions of interest (ROIs) were extracted for all these regions as described in the methods section and the percentage of signal change induced by both the visual and the tactile stimulations was calculated. Two distinct response profiles were observed. The response of all the occipital areas, parietal areas VIP and PIP, and area MST was significantly higher for the visual modality than for the tactile modality ($p<0.05$). All the remaining regions responded equally well to either modality.

Visuo-tactile convergence is stimulus-dependent

Figure 4 reproduces the above described visuo-tactile convergence network for tactile stimulations to the center of the face (light green), together with the visuo-tactile convergence networks defined by periphery of the face (middle scale green) and shoulders (dark green) tactile stimulations. Center of the face tactile stimulations globally activate a larger visuo-tactile convergence network, only partially overlapping the visuo-tactile convergence networks defined by the periphery of the face and shoulder tactile stimulations. In particular, while some convergence regions were activated by the three types of tactile stimulations, other regions were activated by only one or two types of tactile stimulations. Importantly, within the occipital, posterior parietal and temporal visual cortex, visuo-tactile convergence prevailed in regions representing the peripheral visual field (Figure 4, dark gray shading, as defined using standard retinotopic localizers, Fize et al., 2003) rather than in those

representing the central visual field (Figure 4, white-shaded cortex), including when this convergence was defined using center of the face tactile stimulations.

Functional connectivity between visuo-tactile ROIs depends on the sensory context

The conjunction analysis presented in Figure 3 reveals the cortical sites that produce a statistically significant evoked response to both visual and center of the face tactile stimulations. In the following, we sought to quantify whether the sensory context, in addition to producing an evoked response, also affected the functional connectivity between these ROIs. We thus estimated the degree of connectivity between pairs of ROIs during visual runs, tactile runs and resting-state (simple fixation) runs, as follows. For a given run, functional connectivity between two ROIs was defined as the correlation scores between the residual signals measured in each of them, in a given sensory context, once the evoked activities have been regressed out using the beta-weight estimated in the main effect fMRI design (see material and methods section and Figure 2 for more details). As a result, for each pair of ROIs, three sets of correlation scores were obtained: *visual context* correlation scores (one for each visual run), *tactile context* correlation scores (one for each tactile run) and *resting state context* correlation scores (one for each resting state run). These correlation scores were subsequently used to define an average correlation score as well as to estimate between-condition statistical differences in functional connectivity scores. The resting state condition can be viewed as a stimulation-free baseline condition for interpreting the functional connectivity observations in the sensory stimulation conditions.

Overall functional connectivity is enhanced during visual and tactile stimulations as compared to resting-state

The upper panel of Figure 5 summarizes, for each sensory context, how overall functional connectivity varies, within the visuo-tactile convergence network, as a function of

the sensory context. The ROIs of interest are coarsely located onto a schematic primate brain (Figure 5, left panels). ROIs classically described as belonging to visual areas are indicated on a black background, ROIs classically described as belonging to tactile areas are indicated on a dark gray background, and ROIs classically described as belonging to associative areas are indicated on a light gray background. Lines link pairs of ROIs whose correlation z-score (averaged over all run, both hemispheres and both monkeys) is higher than 0.2, the thicker the line, the higher the correlation z-score. The corresponding cross-correlation z-score matrices for the visual, tactile and resting state contexts are represented in the middle panels of Figure 5. Stars highlight the pairs of ROIs the correlation z-score distributions of which are significantly different from zero ($p<0.05$, Holm-Bonferroni family-wise corrected). The overall picture that emerges is that functional connectivity within the visuo-tactile convergence network varies as a function of the sensory context the monkeys are subjected to. In particular, functional connectivity is enhanced during sensory contexts (Figure 5a-b) as compared to the resting state context (Figure 5c). In addition, a larger network appears to be recruited during the tactile context (Figure 5b) as compared to the visual context (Figure 5b). Specifically, a core visual sub-network can be identified in the resting state context (Figure 5c), the overall correlation of which increases in both sensory contexts (Figures 5a-b). This sub-network includes subregions of V1d, V1v, V2d, V3, V3A, MST, PIP and VIP. A prefrontal sub-network, hardly visible in the resting state context, also arises in the visual and tactile contexts. This prefrontal sub-network is composed of areas PMZ, 46p, 8as and 6Vam. Interestingly, the functional correlation between the prefrontal and the visual subnetworks is achieved through the MST mode mainly in the visual context, while the proportion of functional connections (z-scores > 0.2) between the two networks is highly enhanced during the tactile stimulation context. In order to better quantify these aspects, we calculated, for each pair of ROIs, the relative difference in correlation between the tactile and the visual

stimulation contexts (Figure 5d, all colored nodes reflect significant differences at $p<0.05$). The key observations provided by this analysis are described below.

Visual stimulation context enhances occipito-parietal functional connectivity

Remarkably, the visual stimulation context selectively enhances the functional connectivity z-scores between ventral intraparietal area VIP and lower visual areas V1v, V2d and V3 (Figure 5d). The visual stimulation context also reshapes the correlation patterns within the core visual sub-network described above, enhancing the overall functional connectivity z-scores with areas V1c and MST (Figure 5d). More rostral, the visual context also enhances prefrontal 8as – cingulate 24d functional correlation (Figure 5d). Last, increased correlation scores can also be noted between visual areas V1d and MST and inferior orbitofrontal area 13.

Tactile stimulation context enhances occipito-cingulate and occipito-prefrontal functional connectivity

As described above, the tactile context produces an overall higher level of functional connectivity as compared to the visual context (Figure 5d). Specifically, a selective enhancement of the functional connectivity z-scores can be seen between the core visual sub-network described above, cingulate area 24d on the one hand, and somatosensory area 2 and prefrontal area PMZ on the other hand. In addition, an enhanced connectivity within a core prefrontal network composed of somatosensory area 2, prefrontal area PMZ and prefrontal area 46p also emerges. Last, increased correlation scores are also observed between visual areas V1v and cingulate area 24d and inferior orbitofrontal area 11.

Discussion

While our observations confirm that visuo-tactile convergence takes place in expected parietal, prefrontal, cingulate and orbitofrontal cortices, we additionally demonstrate that it is ubiquitous in early sensory processing visual and tactile cortical areas. We also show that the functional connectivity within this large visuo-tactile convergence network is shaped by the sensory context and is highly dependent upon the sensory stimulation being investigated. This latter point suggests that multisensory convergence might actually be of general occurrence in lower sensory areas, its precise cortical pattern being determined by the sensory stimuli at play. In the following, we discuss the functional and physiological implications of these observations.

Multisensory convergence at early sensory processing stages

In spite of the growing evidence that multisensory convergence is not specific of higher-order associative areas, but also takes place in lower level sensory processing areas, very few accounts of the exact spatial extent of this phenomenon are available to date, if any. Here, we provide compelling evidence for widespread somatosensory functional influences within the striate and extrastriate cortex. The hemodynamic signals measured with fMRI in a given cortical region correlate with synaptic inputs rather than with spiking outputs (Logothetis et al. 2001; Logothetis and Pfeuffer 2004; Goense and Logothetis 2008; Magri et al. 2012). The observations described here thus capture the spatial range of synaptic action of these somatosensory projections onto the visual cortex. These are not expected to necessarily be at the origin of tactile spikes within the visual cortex. But they can fully account for the modulation of visual responses by tactile stimulations (Sathian et al. 1997; Macaluso et al. 2000; Amedi et al. 2001).

These influences are remarkably widespread, covering almost 50% of the visual cortex dedicated to the representation of the peripheral visual field. Surprisingly, there are very few accounts of direct anatomical projections from low level somatosensory cortices onto the visual cortex. Cappe et al. (Cappe and Barone 2005; Cappe et al. 2009) describe, in the marmoset, direct projections from visual area MTc onto somatosensory areas 1 and 3a, but no reverse projections. Clavagnier et al. (Clavagnier et al. 2004) describe projections from the multisensory superior temporal polysensory area STP onto V1, possibly at the origin of both auditory and somatosensory inputs on this area. However, STP is unlikely at the source of the entire visuo-tactile convergence we describe in visual cortex. Indeed, visuo-tactile convergence within STP represents the periphery of the face as well as the shoulders rather than the center of the face (Figure 4). Functional connectivity measures describe increased correlations between somatosensory area 2 and visual areas V1 and V2 as well as between the somatosensory complex SII/PV and visual areas V3A and MST (Figure 5). Privileged anatomical connections subserving these observations might have been missed by previous studies, in the absence of functional cues allowing to target tracer injections at relevant sites.

Interestingly, visuo-tactile convergence within the visual cortex is localized in the peripheral visual field representation, similar to what is described for the auditory projections onto areas V1 and V2 (Falchier et al. 2002; Rockland and Ojima 2003). The functional significance of this bias for the periphery of the visual field is unclear. Multisensory integration enhances perception when sensory inputs are uncertain, the combination of the several incoming information allowing to disambiguate this uncertainty (Ernst and Banks 2002; Alais and Burr 2004). When a given sensory modality provides enough information about the environment, the benefit of multisensory integration decreases both as measured behaviorally (Ernst and Banks 2002; Alais and Burr 2004) and at the neuronal level (Beauchamp 2005; Helbig et al. 2012; Fetsch et al. 2013). This principle could be at the origin

of the progressive selection, throughout evolution, of heteromodal projections specifically onto cortical regions representing the periphery of the visual field (here defined as visual stimuli beyond 1.5° of eccentricity) and in which visual information is spatially degraded (due to photoreceptor distribution on the retinal sheet and cortical magnification, both favoring center of the visual field processing). Alternatively, these somatosensory projections onto the visual cortex could be due to lifelong associative plasticity reflecting the fact that visual stimuli moving in the peripheral visual field have a high probability of subsequently resulting in a tactile stimulation onto the body (impacts during locomotion, self-touches, grooming by conspecifics etc.).

This visuo-tactile convergence provides the neural substrates for the modulation of visual cortex by tactile stimulation (Sathian et al. 1997; Macaluso et al. 2000; Amedi et al. 2001). Importantly, disrupting the visual cortex alters tactile discrimination, suggesting that this low-level sensory convergence contributes to behavior (Zangaladze et al. 1999).

Visuo-tactile convergence is also observed on the upper bank of the lateral sulcus, possibly within the SII/PV complex as well as in area 2. Its spatial extent is much smaller than what is observed in the visual cortex (Figures 3 and 4). This could reflect a major functional difference between these two low level sensory areas. Alternatively, visuo-tactile convergence within the somatosensory pathway might be specific of more complex visual stimuli than those used in the present study, such as textured stimuli potentially evoking tactile experience.

Multisensory convergence in higher-order associative cortical regions

We confirm multisensory convergence in several higher order cortical regions: the posterior parietal cortex (Hikosaka et al. 1988; Duhamel et al. 1998; Bremmer et al. 2002; Avillac et al. 2005, 2007; Schlack et al. 2005; Rozzi et al. 2008; Guipponi et al. 2013), the anteriorparietal cortex (Hikosaka et al. 1988; Huang et al. 2012), the superior temporal sulcus

(Bruce et al. 1981; Hikosaka et al. 1988; Beauchamp et al. 2004; Barraclough et al. 2005) including medial superior temporal area MST as described in humans (Beauchamp et al. 2007), the peri-arcuate prefrontal cortex (Graziano et al. 1994; Graziano et al. 1997; Graziano and Gandhi 2000; Graziano and Cooke 2006; Fogassi et al. 1996), the insular and peri-insular cortex (Augustine 1996), the cingulate cortex (Laurienti et al. 2003) as well as the inferior orbitofrontal cortex (Rolls and Baylis 1994; Rolls 2004). Each of these regions could contribute to a distinct functional aspect of the incoming visuo-tactile information (*e.g.* location, identity, texture, emotional valence etc.). Interestingly, overall, a large portion of the cortex, including both low-level sensory and higher-level associative areas, is involved in this process.

Multisensory convergence as a general property of the neocortex

We extend this view, by demonstrating that convergence patterns vary within these several cortical regions as a function of the specific stimulation type. Here, while always considering static stimulation for the visual condition, we identified visuo-tactile convergence as defined by a tactile stimulus to the center of the face, to the periphery of the face or alternatively to the shoulders. While multisensory convergence within the visual cortex is largest for tactile stimuli directed to the center of the face, this bias is less marked for the rest of the cortex. Remarkably, while convergence patterns in the orbitofrontal cortex are co-localized, elsewhere, the overlap ranges from partial (inferior precentral gyrus, ventral premotor cortex) to weak (superior temporal cortex, parietal cortex, cingulate cortex), potentially suggesting a topographical organization of these convergence maps. In particular, and consistent with the recent description of a higher-level visuo-tactile homunculus within the parietal cortex (Huang et al. 2012), we describe a parietal visuo-tactile-center-of-the-face activation in the fundus and the medial bank of the intraparietal sulcus. Medial to it and

posteriorly, we describe a parietal visuo-tactile-shoulder activation. As a result, both humans and macaques might share the same multisensory parietal organization. A gradient of multisensory convergence from center of the face to periphery of the face to shoulder can also be seen along the anterior bank of the superior temporal sulcus. A similar gradient potentially also exists along the depth of the cingulate cortex, center of the face convergence taking place within the depth of the sulcus and shoulder convergence taking place in the underneath gyrus. A study investigating visuo-tactile convergence using topographically more distant tactile stimuli (*e.g.* center of the face, arm and foot) would allow to precisely address this issue. A major prediction of this work is that by varying the nature of visual stimulus (*e.g.* small moving object, large field visual stimuli, 3D objects, textured objects etc.), that of the tactile stimuli (*e.g.* painful, hot or cold, mechanical, textured etc.) as well as the behavioral requirements (*e.g.* no task as here, detection, discrimination etc.), new visuo-tactile convergence patterns will be identified, revealing both anatomical and functional stimulus and task dependencies. In the following, we specifically address context dependencies.

Context dependent dynamical multisensory convergence

The question we ask here is whether the strength of the functional connection between some multisensory convergence regions change as a function of whether the system is expecting a visual stimulus (visual runs) or a tactile stimulus (tactile runs), as assessed by temporal correlation in the residual hemodynamic system once the evoked stimulus-related signal has been regressed out. This approach allows us to identify three key context-dependent functional hubs: multisensory ventral intraparietal area VIP, whose functional connectivity with the striate and extrastriate visual areas is enhanced by the visual context; multisensory premotor zone PMZ, whose functional connectivity with the striate and extrastriate visual areas is enhanced by the tactile context; and multisensory cingulate area

24d, whose functional connectivity with the striate and extrastriate visual areas is enhanced by the tactile context. While the contribution of area 24d to visuo-tactile processing is unclear in the light of the current literature, the identification of VIP and PMZ as potential functional visuo-tactile hubs is particularly interesting. Areas VIP and PMZ are densely interconnected (Luppino et al. 1999; Lewis and Van Essen 2000; Graziano, Taylor, Moore, et al. 2002). In addition, both areas participate in the representation of objects close to, or approaching the face (Graziano et al. 1997; Bremmer et al. 2013) and possibly in defensive behavior (Graziano, Taylor, and Moore 2002; Cooke et al. 2003). As a result, the context-dependent functional connectivity patterns described above suggests that the sensory context might actually affect information flow between this functional network and lower level visual areas. During the visual context, a visual occipito-parieto-prefrontal highway is privileged. During the tactile context, a visual occipito-prefrontal highway is privileged though overall functional connectivity is also enhanced. Vision is considered as the dominant sensory modality in diurnal primates with over 50% of their cortex involved in visual processing (Felleman and Van Essen 1991). We predict that adjusting to the sensory context allows the network to shift into a functional connectivity state that maximizes sensory processing given a set of priors defined by the context (here, visual context or tactile context). A similar change in functional connectivity is also expected during changes in the behavioral context (*e.g.* fixation as here, or sensory detection or discrimination).

The extended cortical visuo-tactile convergence network we describe here is most probably involved in multisensory integration and each of its subcomponents possibly contributes to a distinct functional aspect of multisensory integration (Werner and Noppeney 2010). In conclusion, we thus propose that multisensory convergence is a general, context-dependent, dynamical property of the neocortex, subserving 'amodal' perception and decision-making processes that are not determined by unique sensory channels.

Abbreviations

Cortical areas

MST	medial superior temporal area
Pi	parainsular cortex
PIP	posterior intraparietal area
PMZ	paramotor zone
PV	parietoventral cortex
SII	secondary somatosensory cortex
VIP	ventral intraparietal area
V1v	visual area V1, ventral part
V1c	visual area V1, central part
V1d	visual area V1, dorsal part
V2v	visual area V2, ventral part
V2d	visual area V2, dorsal part
V3	visual area V3
V3A	visual area V3A
2	somatosensory area 2
6Vam	area 6Va, medial part
7b	somatosensory area 7b
8as	area 8as
11	orbitofrontal area 11
13	orbitofrontal area 13
24d	cingulate area 24d
46p	area 46, posterior part

Cortical sulci

AS arcuate sulcus

CgS cingulate sulcus

CeS central sulcus

IOS inferior occipital sulcus

IPS intraparietal sulcus

LaS lateral (Sylvian) sulcus

LuS lunate sulcus

OTS occipital temporal sulcus

POS parieto-occipital sulcus

PS principal sulcus

STS superior temporal sulcus

Acknowledgments: We thank S. Maurin for technical support and J.L. Charieau and F. Hérant for animal care. This work was supported by Agence Nationale de la Recherche (ANR-05-JCJC-0230-01).

Bibliography

Alais D, Burr D. 2004. The ventriloquist effect results from near-optimal bimodal integration. Curr Biol. 14:257–262.

Amedi A, Malach R, Hendler T, Peled S, Zohary E. 2001. Visuo-haptic object-related activation in the ventral visual pathway. Nat Neurosci. 4:324–330.

Augustine JR. 1996. Circuitry and functional aspects of the insular lobe in primates including humans. Brain Res. 22:229–244.

Avillac M, Ben Hamed S, Duhamel J-R. 2007. Multisensory integration in the ventral intraparietal area of the macaque monkey. J Neurosci. 27:1922–1932.

Avillac M, Denève S, Olivier E, Pouget A, Duhamel J-R. 2005. Reference frames for representing visual and tactile locations in parietal cortex. Nat Neurosci. 8:941–949.

Barraclough NE, Xiao D, Baker CI, Oram MW, Perrett DI. 2005. Integration of visual and auditory information by superior temporal sulcus neurons responsive to the sight of actions. J Cogn Neurosci. 17:377–391.

Beauchamp MS. 2005. See me, hear me, touch me: multisensory integration in lateral occipital-temporal cortex. Curr Opin Neurobiol. 15:145–153.

Beauchamp MS, Lee KE, Argall BD, Martin A. 2004. Integration of auditory and visual information about objects in superior temporal sulcus. Neuron. 41:809–823.

Beauchamp MS, Yasar NE, Kishan N, Ro T. 2007. Human MST but not MT responds to tactile stimulation. J Neurosci. 27:8261–8267.

Bremmer F, Klam F, Duhamel J-R, Ben Hamed S, Graf W. 2002. Visual-vestibular interactive responses in the macaque ventral intraparietal area (VIP). Eur J Neurosci. 16:1569–1586.

Bremmer F, Schlack A, Kaminiarz A, Hoffmann K-P. 2013. Encoding of movement in near extrapersonal space in primate area VIP. Front Behav Neurosci. 7:8.

Bruce C, Desimone R, Gross CG. 1981. Visual properties of neurons in a polysensory area in superior temporal sulcus of the macaque. J Neurophysiol. 46:369–384.

Budinger E, Heil P, Hess A, Scheich H. 2006. Multisensory processing via early cortical stages: Connections of the primary auditory cortical field with other sensory systems. Neuroscience. 143:1065–1083.

Cappe C, Barone P. 2005. Heteromodal connections supporting multisensory integration at low levels of cortical processing in the monkey. Eur J Neurosci. 22:2886–2902.

Cappe C, Rouiller EM, Barone P. 2009. Multisensory anatomical pathways. Hear Res. 258:28–36.

Clavagnier S, Falchier A, Kennedy H. 2004. Long-distance feedback projections to area V1: implications for multisensory integration, spatial awareness, and visual consciousness. Cogn Affect Behav Neurosci. 4:117–126.

Cooke DF, Taylor CSR, Moore T, Graziano MSA. 2003. Complex movements evoked by microstimulation of the ventral intraparietal area. Proc Natl Acad Sci. 100:6163–6168.

De la Mothe LA, Blumell S, Kajikawa Y, Hackett TA. 2006. Cortical connections of the auditory cortex in marmoset monkeys: core and medial belt regions. J Comp Neurol. 496:27–71.

Duhamel JR, Colby CL, Goldberg ME. 1998a. Ventral intraparietal area of the macaque: congruent visual and somatic response properties. J Neurophysiol. 79:126–136.

Duhamel JR, Colby CL, Goldberg ME. 1998b. Ventral intraparietal area of the macaque: congruent visual and somatic response properties. J Neurophysiol. 79:126–136.

Ernst MO, Banks MS. 2002. Humans integrate visual and haptic information in a statistically optimal fashion. Nature. 415:429–433.

Falchier A, Clavagnier S, Barone P, Kennedy H. 2002. Anatomical evidence of multimodal integration in primate striate cortex. J Neurosci. 22:5749–5759.

Felleman DJ, Van Essen DC. 1991. Distributed hierarchical processing in the primate cerebral cortex. Cereb Cortex. 1:1–47.

Fetsch CR, DeAngelis GC, Angelaki DE. 2013. Bridging the gap between theories of sensory cue integration and the physiology of multisensory neurons. Nat Rev Neurosci. 14:429–442.

Fize D, Vanduffel W, Nelissen K, Denys K, Chef d'Hotel C, Faugeras O, Orban GA. 2003a. The retinotopic organization of primate dorsal V4 and surrounding areas: A functional magnetic resonance imaging study in awake monkeys. J Neurosci. 23:7395–7406.

Fogassi L, Gallese V, Fadiga L, Luppino G, Matelli M, Rizzolatti G. 1996. Coding of peripersonal space in inferior premotor cortex (area F4). J Neurophysiol. 76:141–157.

Ghazanfar AA, Schroeder CE. 2006. Is neocortex essentially multisensory? Trends Cogn Sci. 10:278–285.

Goense JBM, Logothetis NK. 2008. Neurophysiology of the BOLD fMRI signal in awake monkeys. Curr Biol. 18:631–640.

Graziano MS, Hu XT, Gross CG. 1997. Visuospatial properties of ventral premotor cortex. J Neurophysiol. 77:2268–2292.

Graziano MS, Yap GS, Gross CG. 1994. Coding of visual space by premotor neurons. Science. 266:1054–1057.

Graziano MSA, Taylor CSR, Moore T. 2002. Complex movements evoked by microstimulation of precentral cortex. Neuron. 34:841–851.

Graziano MSA, Taylor CSR, Moore T, Cooke DF. 2002. The cortical control of movement revisited. Neuron. 36:349–362.

Guipponi O, Wardak C, Ibarrola D, Comte J-C, Sappey-Marinier D, Pinède S, Ben Hamed S. 2013. Multimodal convergence within the intraparietal sulcus of the macaque monkey. J Neurosci. 33:4128–4139.

Helbig HB, Ernst MO, Ricciardi E, Pietrini P, Thielscher A, Mayer KM, Schultz J, Noppeney U. 2012. The neural mechanisms of reliability weighted integration of shape information from vision and touch. Neuroimage. 60:1063–1072.

Hikosaka K, Iwai E, Saito H, Tanaka K. 1988. Polysensory properties of neurons in the anterior bank of the caudal superior temporal sulcus of the macaque monkey. J Neurophysiol. 60:1615–1637.

Huang R-S, Chen C, Tran AT, Holstein KL, Sereno MI. 2012. Mapping multisensory parietal face and body areas in humans. Proc Natl Acad Sci. 109:18114–18119.

Iurilli G, Ghezzi D, Olcese U, Lassi G, Nazzaro C, Tonini R, Tucci V, Benfenati F, Medini P. 2012. Sound-driven synaptic inhibition in primary visual cortex. Neuron. 73:814–828.

Kuypers HG, Szwarcbart MK, Mishkin, M M, Rosvold HE. 1965. Occipitotemporal corticocortical connections in the rhesus monkey. Exp Neurol. 11:245–262.

Laurienti PJ, Wallace MT, Maldjian JA, Susi CM, Stein BE, Burdette JH. 2003. Cross-modal sensory processing in the anterior cingulate and medial prefrontal cortices. Hum Brain Mapp. 19:213–223.

Lewis JW, Van Essen DC. 2000. Corticocortical connections of visual, sensorimotor, and multimodal processing areas in the parietal lobe of the macaque monkey. J Comp Neurol. 428:112–137.

Logothetis NK, Pauls J, Augath M, Trinath T, Oeltermann A. 2001. Neurophysiological investigation of the basis of the fMRI signal. Nature. 412:150–157.

Logothetis NK, Pfeuffer J. 2004. On the nature of the BOLD fMRI contrast mechanism. Magn Reson Imaging. 22:1517–1531.

Luppino G, Murata A, Govoni P, Matelli M. 1999. Largely segregated parietofrontal connections linking rostral intraparietal cortex (areas AIP and VIP) and the ventral premotor cortex (areas F5 and F4). Exp Brain Res. 128:181–187.

Macaluso E, Frith CD, Driver J. 2000. Modulation of human visual cortex by crossmodal spatial attention. Science. 289:1206–1208.

Magri C, Schridde U, Murayama Y, Panzeri S, Logothetis NK. 2012. The amplitude and timing of the BOLD signal reflects the relationship between local field potential power at different frequencies. J Neurosci. 32:1395–1407.

Mandeville JB, Choi J-K, Jarraya B, Rosen BR, Jenkins BG, Vanduffel W. 2011. FMRI of cocaine self-administration in macaques reveals functional inhibition of basal ganglia. Neuropsychopharmacol. 36:1187–1198.

Massopust, L.C., Barnes, H.W., and Verdura, J. Auditory frequency discrimination in cortically ablated monkeys. J. Aud. Res. 5 : 85-93, 1965.

Rockland KS, Ojima H. 2003. Multisensory convergence in calcarine visual areas in macaque monkey. Int J Psychophysiol. 50:19–26.

Rolls ET. 2004. Convergence of sensory systems in the orbitofrontal cortex in primates and brain design for emotion. Anat Rec A Discov Mol Cell Evol Biol. 281:1212–1225.

Rolls ET, Baylis LL. 1994. Gustatory, olfactory, and visual convergence within the primate orbitofrontal cortex. J Neurosci. 14:5437–5452.

Rozzi S, Ferrari PF, Bonini L, Rizzolatti G, Fogassi L. 2008. Functional organization of inferior parietal lobule convexity in the macaque monkey: electrophysiological characterization of motor, sensory and mirror responses and their correlation with cytoarchitectonic areas. Eur J Neurosci. 28:1569–1588.

Sathian K, Zangaladze A. 2002. Feeling with the mind's eye: contribution of visual cortex to tactile perception. Behav Brain Res. 135:127–132.

Sathian K, Zangaladze A, Hoffman JM, Grafton ST. 1997. Feeling with the mind's eye. Neuroreport. 8:3877–3881.

Schlack A, Sterbing-D'Angelo SJ, Hartung K, Hoffmann K-P, Bremmer F. 2005a. Multisensory space representations in the macaque ventral intraparietal area. J Neurosci. 25:4616–4625.

Schlack A, Sterbing-D'Angelo SJ, Hartung K, Hoffmann K-P, Bremmer F. 2005b. Multisensory space representations in the macaque ventral intraparietal area. J Neurosci. 25:4616–4625.

Schroeder CE, Foxe J. 2005. Multisensory contributions to low-level, "unisensory" processing. Curr Opin Neurobiol. 15:454–458.

Sereno MI, Huang R-S. 2006. A human parietal face area contains aligned head-centered visual and tactile maps. Nat Neurosci. 9:1337–1343.

Smiley JF, Hackett TA, Ulbert I, Karmas G, Lakatos P, Javitt DC, Schroeder CE. 2007. Multisensory convergence in auditory cortex, I. Cortical connections of the caudal superior temporal plane in macaque monkeys. J Comp Neurol. 502:894–923.

Van Essen DC, Drury HA, Dickson J, Harwell J, Hanlon D, Anderson CH. 2001. An integrated software suite for surface-based analyses of cerebral cortex. J Am Med Informatics. 8:443–459.

Vasconcelos N, Pantoja J, Belchior H, Caixeta FV, Faber J, Freire MAM, Cota VR, Anibal de Macedo E, Laplagne DA, Gomes HM, Ribeiro S. 2011. Cross-modal responses in the primary visual cortex encode complex objects and correlate with tactile discrimination. Proc Natl Acad Sci. 108:15408–15413.

Wallace MT, Ramachandran R, Stein BE. 2004. A revised view of sensory cortical parcellation. Proc Natl Acad Sci. 101:2167–2172.

Werner S, Noppeney U. 2010. Distinct functional contributions of primary sensory and association areas to audiovisual integration in object categorization. J Neurosci. 30:2662–2675.

Figures

Figure 1: Visual (A, optic flows and large field moving bars) and tactile (B, air puffs to the center of the face, the periphery of the face and the shoulders) stimulations.

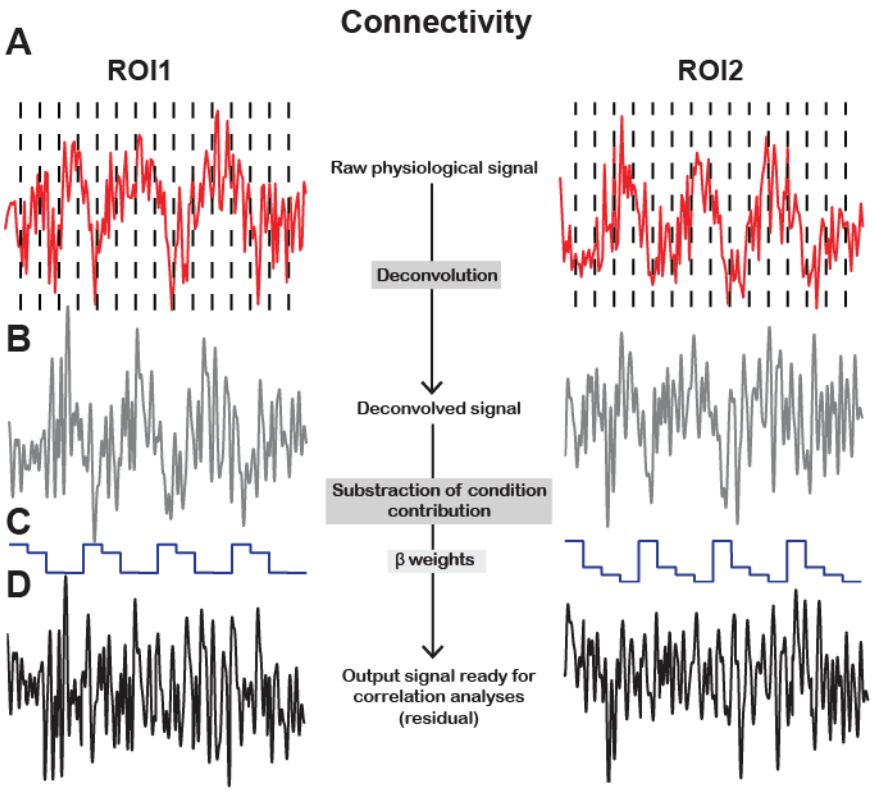

Figure 2: Effective connectivity procedure. A) Raw physiological signals are extracted in the ROI of interest (here, ROI1 and ROI2 correspond, respectively, to the left and right anterior intraparietal sulcus activation) for each modality, each run and each animal. B) Deconvolved physiological signal. C) Beta weights as defined by the main fMRI analysis. D) Residual physiological signal one the evoked activities as estimated by the beta-weights are regressed out.

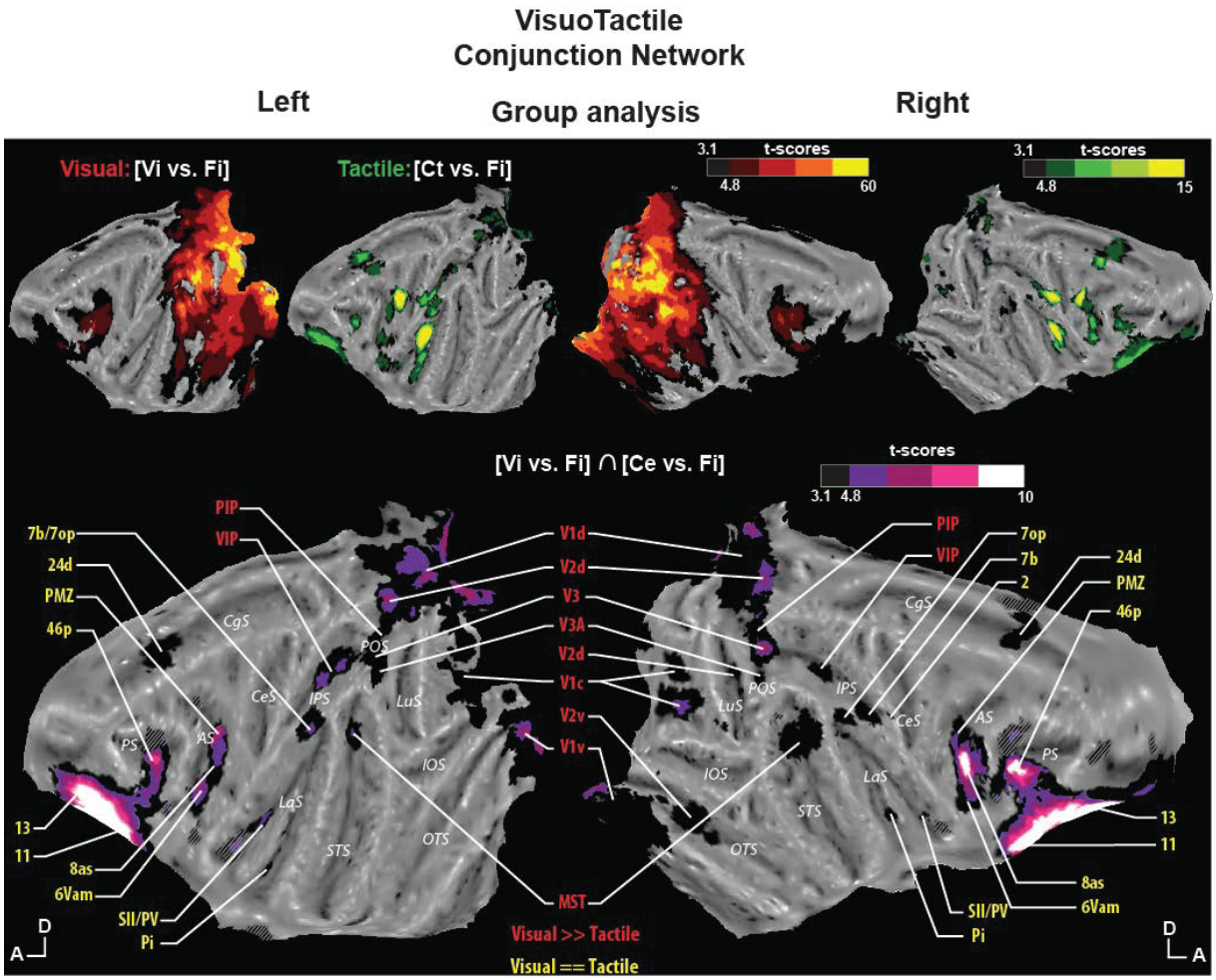

Figure 3: Visual, tactile and the corresponding VisuoTactile convergence group network. Activations are presented on the flattened representation of the reference monkey cortex obtained with Caret. The upper part of the figure shows the unimodal activations: (1) static visual stimulations versus fixation contrast (the t scores = 3.1, at $p<0.001$, uncorrected level in black and t scores = 4.8 at $p<0.05$, FWE-corrected level in the red scale); and (2) tactile center of the face stimulations versus fixation contrast (green t score scale, color transitions as in 1). The lower part of the figure shows the visuo-tactile conjunction maps (magenta t score scale, color transitions as in 1, static visual stimulation vs. fixation in conjunction with tactile stimulation to the center of the face vs. fixation). Areas are identified in red when their percentage of signal change is significantly higher in the visual condition as compared to the tactile condition and in yellow otherwise. A, Anterior; D, Dorsal; MST: medial superior temporal area; Pi: parainsular cortex; PIP: posterior intraparietal area; PMZ: paramotor zone;

PV, parietoventral cortex; SII: secondary somatosensory cortex; VIP: ventral intraparietal area; V1v: visual area V1, ventral part; V1c: visual area V1, central part; V1d: visual area V1, dorsal part; V2v: visual area V2, ventral part; V2d: visual area V2, dorsal part; V3: visual area V3; V3A: visual area V3A; 2: somatosensory area 2; 6Vam: area 6Va, medial part; 7b: somatosensory area 7b; 7op: opercular area 7; 8as: area 8as; 11: orbitofrontal area 11; 13: orbitofrontal area 13; 24d: cingulate area 24d; 46p: area 46, posterior part. Cortical sulci: AS, arcuate sulcus; CgS, cingulate sulcus; CeS, central sulcus; IOS, inferior occipital sulcus; IPS, intraparietal sulcus; LaS, lateral (Sylvian) sulcus; LuS, lunate sulcus; OTS, occipital temporal sulcus; POS, parieto-occipital sulcus; PS, principal sulcus; STS, superior temporal sulcus.

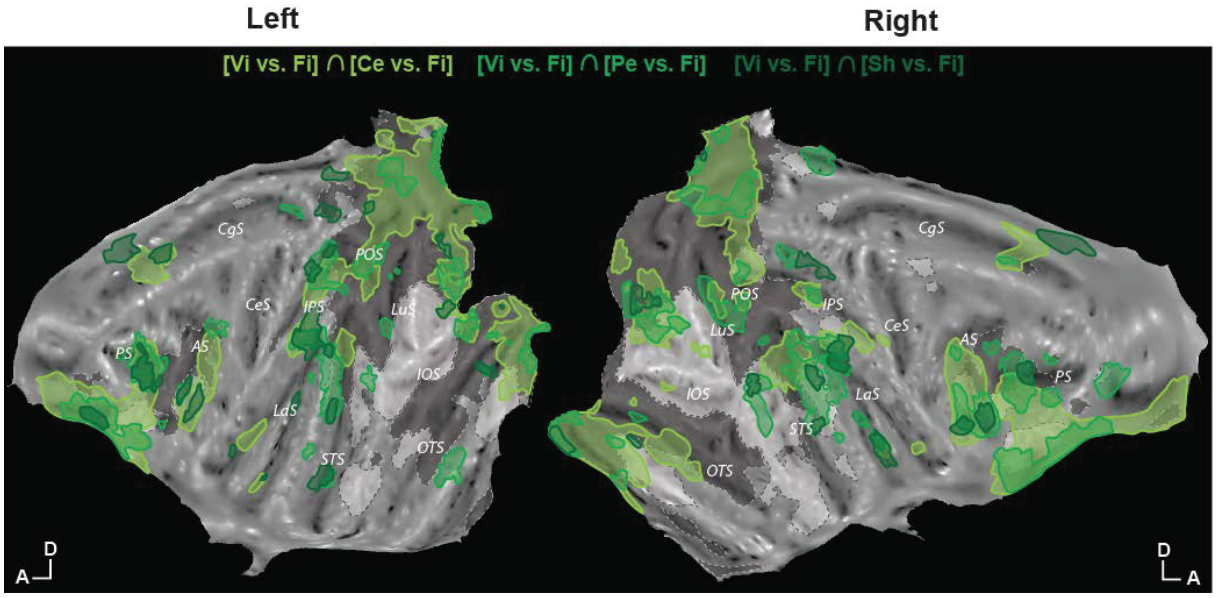

Figure 4: VisuoTactile conjunction activation maps defined with the center of the face (Ce, light green), periphery of the face (Pe, middle scale green), or shoulders (Sh, dark green) tactile stimulations and the static visual stimulations (Vi, t scores > 3.1 at $p<0.001$, uncorrected level). Peripheral (dark background, dashed white contours) and central (light background, dashed black contours) visual fields representations are also represented (t scores > 3.1 at $p<0.001$, uncorrected level). For other conventions, see Figure 3.

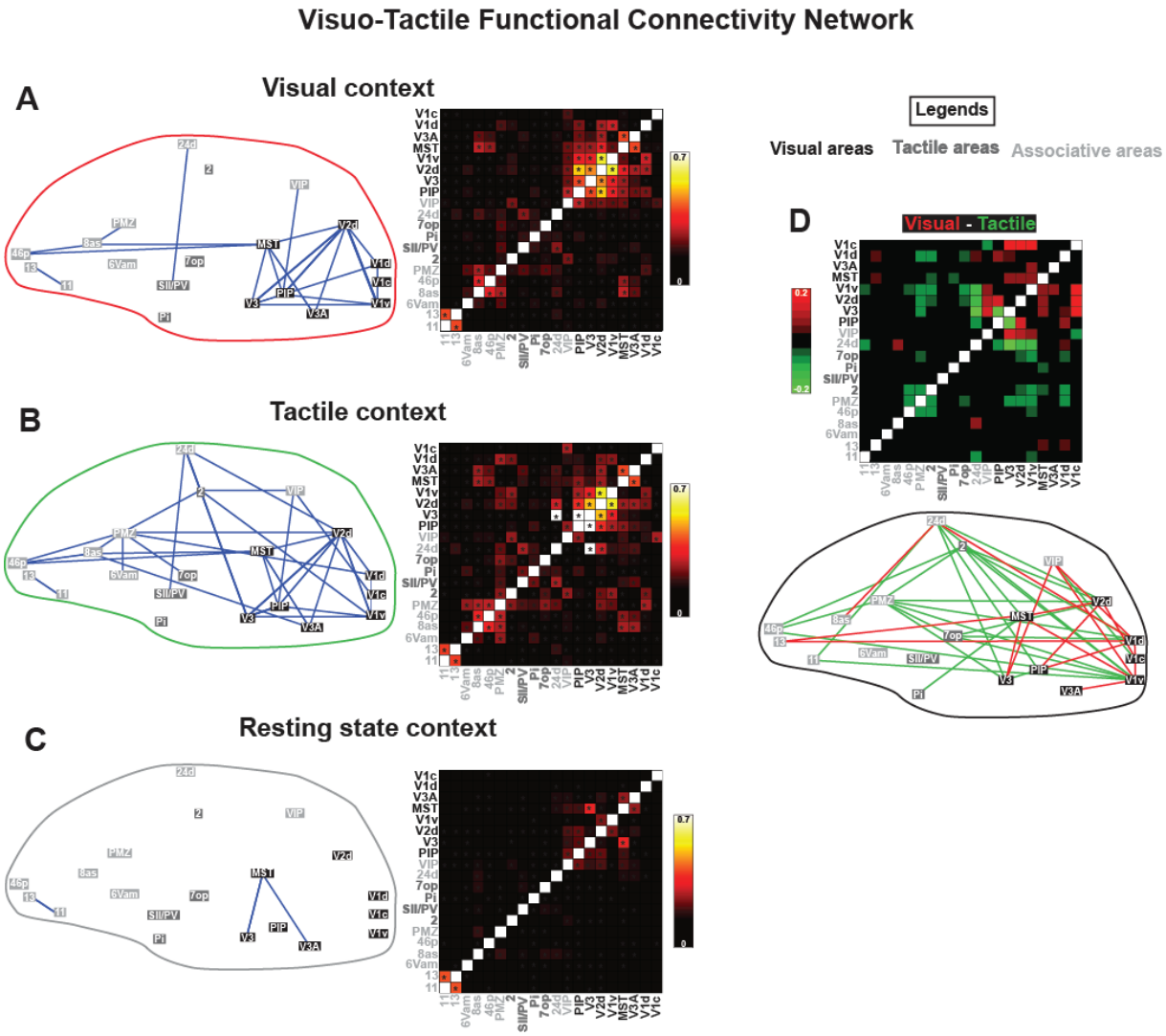

Figure 5: Effective functional connectivity assessed in the visual (A), the tactile (B) and the resting state (C) stimulation contexts. (A-C) Left, selected ROIs placed onto a schematic monkey brain representation, lines between pairs of ROIs indicating correlation z-scores higher than 0.2; Right, ROIs functional cross-correlation matrix (*, $p < 0.05$, Holm-Bonferroni corrected). D) Visual-Tactile stimulation context ROIs functional cross-correlation matrix. All as in A-C. Nomenclatures of areas are given in Figure 3.

Chapter 3

Impact Prediction by Looming Stimuli Enhances Tactile Detection

Impact prediction by looming stimuli enhances tactile detection

Abbreviated title: Multisensory integration for looming visual stimuli

Authors: Justine Cléry*[1], Olivier Guipponi*[1], Soline Odouard[1], Claire Wardak[1], Suliann Ben Hamed[1]

1. Centre de Neuroscience Cognitive, CNRS UMR 5229, 67 Bd Pinel, 69675 Bron cedex, Université Claude Bernard Lyon I

* these two authors equally contributed to the present study

Corresponding author: Suliann Ben Hamed, Centre de Neuroscience Cognitive, CNRS UMR 5229, Université Claude Bernard Lyon I, 67 Bd Pinel, 69675 Bron cedex, France, benhamed@isc.cnrs.fr

Abstract

From an ecological point of view, approaching objects are potentially more harmful than receding objects. A predator, a dominant conspecific, or a mere branch coming up at high speed can all be dangerous if one does not detect them and produce the correct escape motor repertoire fast enough. And indeed, looming stimuli trigger stereotyped defensive responses in both monkeys and human infants. In the present study, we report that, in addition to triggering a defensive motor repertoire, looming stimuli towards the face provide the nervous system with predictive cues that selectively enhance tactile sensitivity at the expected time and location of impact of the stimulus. We propose that this cross-modal predictive facilitation involves multisensory convergence areas and possibly draws on the same neuronal bases as those triggered by multi-sensory. These results challenge our current understanding of the neural bases of multisensory integration and call for reconsidering the temporal coincidence rule (Stein and Meredith, 1993).

Key words: visual, tactile, psychophysics, human, looming stimuli, multisensory integration, prediction.

Introduction

From an ecological point of view, approaching objects are potentially more harmful than receding objects. A predator, a dominant conspecific, or a mere branch coming up at high speed can all be dangerous if one does not detect them and produce the correct escape motor repertoire fast enough. And indeed, looming stimuli trigger stereotyped defensive responses in both monkeys (Schiff et al. 1962) and human infants (Ball and Tronick 1971). The time of impact of such looming stimuli to the body is highly modulated by their identity. Indeed, time-to-collision is perceived as shorter for threatening as compared to non-threatening stimuli (Vagnoni et al. 2012).Relevant to the present study, looming visual stimuli trigger pronounced orienting behavior over receding stimuli when presented with simultaneous matching auditory cues, both in non-human primates (Maier et al. 2004) and in 5-months human infants (Walker-Andrews and Lennon 1985), suggesting that stimulus dynamics with respect to the subject influences multisensory integration processes.

These observations are in agreement with the general multisensory integration framework which assumes a common source for multimodal sensory inputs (Sugita and Suzuki 2003). They further extend this framework to the case of dynamical common multimodal sources demonstrating that spatially and temporally matching auditory stimuli enhance the perception of both static (McDonald et al. 2000) and dynamic visual stimuli (Maier et al. 2004; Cappe et al. 2009; Leo et al. 2011; Parise et al. 2012). The neural substrates of this phenomenon are increasingly understood both in humans (Cappe et al. 2012; Tyll et al. 2013) and in non-human primates (Maier and Ghazanfar 2007; Maier et al. 2008). Overall, these studies derive multisensory integration principals for looming multisensory stimuli under the assumption of a causal common source.

Here, we question, whether the same principals hold in the context of prediction of impact. Indeed, while a dynamic stimulus can often be at the origin of both a visual and an auditory or a tactile cortical input, both reflecting the spatio-temporal characteristics of the stimulus relative to the subject (*e.g.* a car passing in the next by road, a mosquito walking on one's forearm etc.), a dynamic visual looming stimulus can have delayed heteromodal consequences. For example, a ball falling on the floor will produce an expected bouncing sound only at the end of its fall. Likewise, and relevant to the present work, an object approaching the face will induce a tactile stimulation at the end of its trajectory. In both cases, the heteromodal sensory consequences can be fully predicted, by the spatio-temporal dynamics of the looming stimulus.

In the following, we thus test the hypothesis that the sensitivity to a tactile stimulus is maximized by the presentation of a predictive looming visual stimulus. We demonstrate that tactile sensitivity is maximized by a temporally and spatially predictive approaching stimulus. These results challenge our current understanding of the neural bases of multisensory integration and call for reconsidering the temporal coincidence rule (Stein and Meredith, 1993).

Material and methods

The experimental protocol was approved by the local ethics committee in Biomedical Research (Comité de protection des personnes sud-est IV, N_CPP 11 / 025) and all participants gave written informed consent.

Experimental set-up

Subjects sat in a chair at 50cm from a 23-inch computer monitor. Their head was restrained by a chin rest. Their arms were placed on a table and they held a gamepad with their two hands. Vertical and horizontal eye position was monitored using a video eye-tracker (EyeLink™, sampling at 120 Hz, spatial resolution <1°). Data acquisition, eye monitoring and visual presentation were controlled by a PC running Presentation (Neurobehavioural systems, Albany, Canada).

Visual stimuli

The fixation point was a 0.06° x 0.06° yellow square (0.67 cd/m2). The screen background was set to a structured 3D environment with visual depth cues (figure 1a). Visual stimuli consisted in 8 possible video sequences of a cone, pointing towards the subject, moving within this 3D environment, originating away from and rapidly approaching the subject. The cone could originate from 8possible locations around the fixation point ((-6.8°,-1.0°), (-3.2°,-1.0°), (-2.8°, -1.0°), (-1.1°, -1.0°), (1.1°, -1.0°), (2.8°, -1.0°), (3.2°, -1.0°) and (6.8°, -1.0°)) and moved along trajectories that intersected the subject's face at 2 possible locations, on the left or right cheeks, close to the nostrils (figure 1b). Each video sequence consisted in 24 images played for a total duration of 800ms. The 3D environment, the cone and the 8 different trajectories were all constructed with the Blender software (http://www.blender.org/).

Tactile stimuli

Tactile stimuli consisted in air puffs directed to the left or right cheek of the subjects, at locations coinciding with the two possible visual cone trajectory endpoints (figure 1b), thanks to tubing placed at 2-4mm from each cheek and rigidly fixed to the chin rest. The relative position between the screen and the air puff tubing was maintained constant throughout the experiments and across subjects. The intensity of the left and right air puffs was adjusted independently, and for each subject, to achieve a 50% detection rate as estimated over a short block of 20 trials (one block for the left air puff and one block for the right air puff). The latency of air puff outlet at the tubing end following the opening of the solenoid air pressure valve was measured as a function of air puff intensity, thanks to a silicon on-chip signal conditioned pressure sensor (MPX5700 Series, Freescale™). Detection thresholds were achieved with air pressures varying between 0.05 and 0.1 bars, corresponding to average air puff latencies of220ms. All throughout the manuscript, airpuff timings correspond to when the airpuffs actually hit the face.

Experimental procedure

Subjects had to fixate a central yellow point throughout the trial. The fixation was monitored thanks to an eye tolerance window of 2° (controlled by a video eye tracker) around the fixation stimulus. One to three seconds following trial start, a visual stimulus, a tactile stimulus or a combination of both visual and tactile stimuli was presented. At the end of the trial, subjects were requested to report the detection of a tactile stimulus by a 'Yes' button press (right hand gamepad button) and respond by a 'No' button press otherwise (left hand gamepad button). In order to maximize multisensory integration, we used very weak tactile stimuli to the face (*cf.* Tactile stimuli description above). The main measure reported in the present study is a d' measure quantifying the sensitivity of each subject to tactile stimulations

as a function of the stimulation context (no stimulation, tactile stimulation alone or tactile stimulation associated with visual stimulation of specific spatial and temporal properties). This measure is based on a reliable estimate of false reports of tactile stimuli in noise (False alarms) and correct reports of tactile stimuli (Hits). Such reliability is achieved by collecting a minimum of 75 trials per stimulation context. The d' measures were estimated for the different stimulation conditions in four different experiments as follows.

Experiment 1: Influence of a predictive visual stimulus on tactile d'

Thirteen subjects participated in this study (26.7 +/- 5.2 years, 6 males and 7 females). All subjects were naive as to the purpose of the experiment except one (author S.BH.). All participants had normal or corrected-to-normal vision. Five possible trial types were presented to the subjects. Noise trials allowed to estimate their false alarm rate. The trials could either be no stimulus trials (1/6 of all trials) or visual stimulation only trials (1/3 of all trials). Signal trials allowed to estimate their Hit rate as a function of the stimulation condition. The trials could be 1) tactile stimulation only trials (1/6 of all trials, allowing to estimate d' to pure tactile stimuli), 2) visual stimulation + tactile stimulation presented midway through the visual video trials (1/6 of all trials, 360ms before video offset, allowing to estimate d' to tactile stimuli in the presence of a visual stimulus) and 3) visual stimulation + tactile stimulation presented when the visual cone is expected to impact the face and on the cheek predicted by the cone trajectory trials (1/6 of all trials, 100ms after video offset, allowing to estimate d' to tactile stimuli that is spatially and temporally predicted by a dynamical visual stimulus). Trials were presented pseudorandomly. Subjects were allowed to rest whenever they needed by closing their eyes. During these rest periods, they were instructed not to move their head in the rest chin so as not to change the distance of the air puff tubing to their face or to change eye calibration. Four hundred and fifty trials were collected in all.

Experiment 2: Influence of spatial congruence on temporal prediction

Eight subjects participated in this study (27.3 +/- 4.5 years, 3 males and 5 females). All subjects were naive as to the purpose of the experiment. All participants had normal or corrected-to-normal vision. Five possible trial types were presented to the subjects. Noise trials were as in Experiment 1. Signal trials were as follows 1) tactile stimulation only trials (1/6 of all trials, allowing to estimate d' to pure tactile stimuli), 2) visual stimulation + tactile stimulation presented when the visual cone is expected to impact the face and on the cheek predicted by the cone trajectory trials (1/6 of all trials, -100ms after video offset, allowing to estimate d' to tactile stimuli that is spatially and temporally predicted by a dynamical visual stimulus) and 3) visual stimulation + tactile stimulation presented when the visual cone is expected to impact the face but on the opposite cheek to the one predicted by the cone trajectory trials (1/6 of all trials, 100ms after video offset, allowing to estimate d' to tactile stimuli that is temporally predicted by a dynamical visual stimulus but spatially incongruent to it). Trials were presented pseudo-randomly. Subjects were allowed to rest whenever they needed by closing their eyes. Rest periods were arranged for as in Experiment 1 and 450 total trials were collected.

Experiment 3: Influence of visual stimulus trajectory on temporal prediction

Five subjects participated in this study (27.8 +/- 5.8 years, 2 males and 3 females). All subjects were naive as to the purpose of the experiment. All trial types were as in Experiment 1, except that the visual video sequences were played in reverse order such that the cones appeared to move away from the subjects rather than towards their face.

Experiment 4: Influence of the temporal offset between the visual and tactile stimuli

Six subjects participated in this study (28.8 +/- 7.1 years, 5 males and 3 females). All subjects were naive as to the purpose of the experiment except one (author S.BH.). All participants had normal or corrected-to-normal vision. Eight possible trial types were presented to the subjects. Noise trials were composed of only no stimulus trials (1/2 of all trials). Signal trials were as follows 1) tactile stimulation only trials (1/14 of all trials, allowing to estimate d' to pure tactile stimuli), 2) visual stimulation + tactile stimulation trials in which the tactile stimulus could be presented at 6 possible timings with respect to the visual stimuli (1/14 of all trials for each possible timing, possible timings being 0ms, 50ms, 100ms, 150ms, 200ms or 250ms after video offset, allowing to estimate d' to tactile stimuli for each condition). Trials were presented pseudorandomly. Subjects were allowed to rest whenever they needed by closing their eyes. Rest periods were arranged for as in Experiment 1 and 900 total trials were collected.

The above protocol contains only no stimulus noise trials. Because this most probably biased the subject's representation of the task (a tactile stimulus had a 100% probability of being presented when a visual stimulus was also presented), a second varied of this task was also run on 1 subject for now. In this protocol, eight possible trial types were presented to the subjects. Noise trials were composed of only no stimulus trials (1/10 of all trials) of visual stimulus only trials (4/10 of all trials). Signal trials were as follows 1) tactile stimulation only trials (1/10 of all trials, allowing to estimate d' to pure tactile stimuli), 2) visual stimulation + tactile stimulation trials in which the tactile stimulus could be presented at 4 possible timings with respect to the visual stimuli (1/10 of all trials for each possible timing, possible timings being -300ms, -100ms, 100ms or300ms after video offset, allowing to estimate d' to tactile stimuli for each condition).

Analysis

Data analysis was performed in Matlab™ (The MathWorks Inc., Natick, MA, USA). For each experiment, we extract, for each signal trial type (*i.e.* each trial type in which a tactile stimulus was effectively presented), and for each subject, the d' quantifying the subject's sensitivity at detecting tactile stimuli. For all experiments, we also quantified the response criterion for each such subject within a given experiment and confirmed that this criterion was independent of trial type (data not shown). Statistical effects were assessed using t-tests and one-way ANOVAs.

Results

The main experimental measures reported below are tactile d' sensitivity measures. This measure is based on the analysis of how often subjects report the presence of a tactile stimulus when none was actually presented (*i.e.* responses to noise, also referred to as false alarms) and how often they correctly report the presence of tactile stimuli when a stimulus was indeed presented (*i.e.* responses to signal, also referred as hits or correct detections). D-primes are high when stimuli can unambiguously be detected and low when they are difficult to discriminate against noise. As a result, they reflect the sensitivity of the subject to the stimulus of interest. In the following, we analyse how the sensitivity to a tactile stimulus is affected by the simultaneous presentation of a dynamical visual stimulus, as a function of the spatial and temporal characteristics of this latter stimulus relative to the tactile stimulus.

Temporal prediction against temporal simultaneity

In a first experiment, we question whether tactile detection is maximized by the simultaneous presentation of a dynamical visual stimulus approaching the face (a benefit classically attributed to multisensory integration) or whether the more ecological situation in which such a looming visual stimulus is actually predictive of the tactile stimulus further enhances tactile detection. To do so, we measured the tactile d' of subjects when the tactile stimulus was applied to one of their cheeks 1) in the absence of any visual stimulation (d'(T), Tactile only), 2) midway through the video sequence of a cone looming towards their face and predicting an impact at the very location of the tactile stimulus (d'(VT_sim), Visuo-Tactile simultaneous) or 3) following the video sequence of a cone looming towards their face at the time and location predicted by this visual stimulus (d'(VT_pr), Visuo-Tactile predictive). As expected from previous studies, d'(T) was significantly smaller than d'(VT_sim) (one-tailed t-

test, p<0.05) and d'(VT_pr) (one-tailed t-test, p< 0,005). Most interestingly d'(VT_sim) was also significantly smaller than d'(VT_pr) (one-tailed t-test, p< 0,005, figure 2). Thus maximum tactile detection is achieved when the tactile stimulus is temporally predicted by a visual stimulus looming toward the location of the tactile stimulation as compared to when visual and tactile stimuli are simultaneous. This effect did not depend on the tactile stimulation side (left or right cheek) nor on the origin of the looming visual stimulus (left or right visual field, periphery or center of the visual field).

Spatial prediction

The effect of temporal prediction reported above could actually be fully explained by temporal prediction. In this second experiment, we test whether this is the case or whether spatial prediction is also important in maximizing tactile detection. To do so, we measured the tactile d' of subjects when the tactile stimulus was applied to one of their cheeks 1) in the absence of any visual stimulation (d'(T), Tactile only), 2) following the video sequence of a cone looming towards their face at the time and location predicted by this visual stimulus (d'(VT_pr), Visuo-Tactile predictive temporally and spatially) or 3) following the video sequence of a cone looming towards their face at the time predicted by this visual stimulus but at the opposite location (d'(VT_sp), Visuo-Tactile spatially incoherent).Here again, we find that d'(T) was significantly smaller than both d'(VT_pr) (one-tailed t-test, p<0.001) and d'(VT_sp) (one-tailed t-test, p< 0,05). Most interestingly d'(VT_sp) was also significantly smaller than d'(VT_pr) (one-tailed t-test, p< 0,05, figure 3).Thus maximum tactile detection is achieved when the tactile stimulus is both temporally and spatially predicted by a visual stimulus looming toward the location of the tactile stimulation as compared to when the visual stimulus is only temporally predictive of the tactile stimulus. Again, this effect did not depend on the tactile stimulation side (left or right cheek) nor on the origin of the looming visual

stimulus (left or right visual field, periphery or center of the visual field). These observations together with those reported in the first experiment indicate that both temporal and spatial prediction contribute to enhanced target detection.

Trajectory cues

In the previous experiments, the dynamical visual stimulus was a looming cone approaching the face. The spatial and temporal prediction enhancement of tactile detection described above could be fully due to the predictive cues provided by the stimulus trajectory. Alternatively, the reported effect could reflect an attentional spatio-temporal enhancement of tactile processing at the predicted location, independent of the fact that the trajectory of the cone is predictive of an impact on the face. In order to test for this effect, we repeated the first experiment, but this time with inverted video sequences, *i.e.* with dynamical visual stimuli receding away from the subject's face. We find that d'(T) is statistically smaller than d'(VT_sim) (d' in the temporal prediction condition, with receding cone, one-tailed t-test, p=0.01) but statistically undistinguishable from d'(VT_ rec) (d' in the simultaneous visuo-tactile condition, with receding cone, one-tailed t-test, p= 0,43). In contrast with what was observed in the first experiment, d'(VT_rec) was significantly smaller than d'(VT_sim) (one-tailed t-test, p< 0,02, figure 4).This effect did not depend on the tactile stimulation side (left or right cheek) nor on the origin of the looming visual stimulus (left or right visual field, periphery or center of the visual field, stats?). These observations indicate that the effects reported in the previous experiments cannot be accounted for by general attentional perceptual enhancement effects but rather that the predictive cues contained in the looming cone trajectories are crucially contribute to enhanced tactile detection at the predicted impact location at the expected time of impact.

Temporal prediction window

In a last experiment, we sought to explore how the relative timing between the visual looming cone and the tactile stimulus modulated tactile d', by manipulating the temporal asynchrony between these two stimuli. As reported in figure 5a, all visuo-tactile conditions were associated with significantly higher d' than the tactile only condition (one-tailed t-test, $p<0.001$). Within these visuo-tactile conditions, maximum tactile d' are obtained when the tactile stimulus is applied at the estimated time of impact of the looming cone on the face (100ms, same timing as that used for the temporal prediction condition in all the previous experiments). The d' at this timing is significantly higher than that obtained for shorter temporal asynchronies (-50ms and –0ms, *i.e.* before the offset of the visual sequence, $p<0.05$). Surprisingly, the longer temporal asynchronies (+100ms and +300ms, *i.e.* before the offset of the visual sequence) remain high, suggesting that task-related priors (figure 5c). Indeed, in this task variant, noise trials were composed of only no stimulus trials. As a result, the presence of a visual stimulus was in itself predictive of the presence of a tactile stimulus at the predicted location of impact of the visual stimulus, sometime during and following the visual stimulus. Subjects were thus possibly summing up two probabilistic representations of the most probable time of tactile stimulus (figure 5b, black line): a pragmatic knowledge prior on the predicated time of impact of the looming stimulus, accumulated over a life time experience (continuous gray line) and a task-related probability of tactile target within a given trial (dashed gray line). In order to test for this, we are currently running an additional control experiment in which noise trials are composed of both no stimulus trials (in the same proportion as tactile only trials) and visual stimulus alone trials (in the same proportion as visuo-tactile trials). Less temporal asynchronies are explored in order to keep the overall trial number manageable by the subjects. The preliminary results obtained for one subject confirm that tactile d' are maximized for a temporal asynchrony of 100ms.

Discussion

This study demonstrates that visual stimuli looming towards the face provide the nervous system with predictive cues that have an effect to selectively enhance tactile sensitivity at the expected impact of the stimulus. In the following, we discuss these observations in the context of multisensory integration and we propose that they reflect an ecological specificity of somatosensory sensation, as compared to vision or audition.

Predictive cues

We identify three predictive dimensions of the visual looming stimulus that contribute to enhancing tactile sensitivity on the face:

1) Dynamic depth cues. Maximal tactile sensitivity enhancement is selectively observed for a looming stimulus while a receding stimulus hardly has any effect on tactile sensitivity (Experiment 3). Maier et al. (Maier et al. 2004) show that orienting towards a looming visual stimulus is improved when this stimulus is presented together with a looming sound as compared to when presented with a receding sound. The effect we report here is somewhat different in that we probe tactile sensitivity *100ms after* the end of the looming visual stimulus. This effect could be due to the fact that the last cone presented in the looming stimulus sequence is a large cone perceived close to the subject while the last cone presented in the receding stimulus sequence is a small cone perceived far away from the subject. This effect would thus result from a combination of size and depth cues. While we believe that both these cues most probably do contribute to modulate tactile sensitivity on the face, we predict that the additional movement direction away or towards the subject is actually the dominant cue affecting tactile detection. The exact contribution of these several depth cues remains to be quantified experimentally.

2) The estimated time of impact. Maximal d-primes are obtained for tactile stimuli presented 100ms following the disappearance of the looming stimulus, at the subjective time of impact to the face (Experiments 1 and 4), though some enhancement of the d' is also observed when the tactile stimulus is presented midway through the looming phase as compared to the d' obtained in the absence of any visual stimulus. Seminal studies demonstrate that temporal coincidence (Sugita and Suzuki 2003) and correlation (Parise et al. 2012) maximize audio-visual integration. Here, we demonstrate that maximal tactile detection is achieved, for dynamic looming visual stimuli, at the predicted time of impact.

3) The estimated position of impact. Maximal tactile sensitivity enhancement is observed when the tactile stimulus is presented at the expected location of impact of the looming stimulus on the face (Experiment 2). Visual stimuli could originate from 8 different locations in the far visual field (4 locations ipsilateral to the impact point and 4 contralateral) but predict only two possible impact locations to the face (left or right cheek). As a result, the spatial effects reported here cannot be accounted for by other aspects of the stimulus.

While we discuss the dynamic, spatial and temporal predictive cues in isolation, all of them are fully accounted for by the movement direction and speed of the looming stimulus. We can predict that the slower the stimulus the more delayed would be the predicted time of impact and hence the time at which tactile sensitivity is enhanced. Similarly, the trajectory of the looming stimulus is fully informative of the predicted time of impact. Overall, these finding raises several important questions. In particular, dynamic visual stimuli are not necessarily predictive of impact, but can be coincident with tactile stimulation (*e.g.* a mosquito swiftly moving on one's arm). Do these distinct situations call on to the same cortical functions and underlying neuronal bases (*e.g.* multisensory convergence and

integration), or on distinct cortical functions (*e.g.* multisensory integration and temporal prediction)?

Impact prediction and multisensory integration

The mere presence of a looming visual stimulus around tactile detection enhances it, including when the tactile stimulus is presented during the looming phase (Experiment 1 and 4) or when the looming stimulus predicts impact away from the tactile stimulation location (Experiment 2). This baseline effect could be due to an alerting effect of the visual stimulus, though it needs to be noted that this alerting effect is present only for looming stimuli (as receding stimuli do not induce an increase in tactile sensitivity, Experiment 3). However, given the tight correlation of tactile sensitivity modulation with the physical properties of the looming visual stimulus, this alerting component most probably builds add up on classical multisensory integration effects that are expected when a visual and a tactile stimulus are presented to the nervous system in temporal and spatial coincidence (Stein and Meredith, 1993).

Multisensory integration is a neuronal process by which the response of a neuron in spikes per second to two sensory stimuli of different modalities (say visual and tactile), presented simultaneously, is different from the sum of the spikes per second produced by this same neuron in response to each sensory stimulus presented independently (Avillac et al. 2007). The general multisensory framework assumes that maximum multisensory integration is observed when the two sensory stimuli are presented at the same location (spatially congruent) and at the same time (temporally congruent, Stein and Meredith, 1993). This leads to the notion of causal inference: a visual and an auditory signal originating at the same spatial location at the same time can most probably be attributed to a unique underlying cause (Körding et al. 2007; Shams and Beierholm 2010; Parise et al. 2012). The ecological

relevance of this framework is beyond discussion. The faint sound of leaves being moved in the bush can facilitate the detection of the hidden lion and provide the 100ms extra milliseconds necessary for survival. Likewise, seeing the lips moving provides important information to disambiguate speech, more so in a noisy environment.

Here, we consider a different situation in which the information from a given sensory modality is predicting a sensory input from a different modality. While anticipating the sound of the crash of a glass falling to the ground has little ecological relevance, anticipating an impact to the body is of vital importance. We propose that the cortical regions responsible for this multisensory impact prediction are multisensory convergence and integration regions.

The neural bases of multisensory impact prediction

Very early on, Hyvärinen and Poranen (Hyvärinen and Poranen 1974, cited in Brozzoli et al. 2012 in *The neural bases of multisensory processes*) describe the visual response of parietal neurons "as an anticipatory activation" that appears before the neuron's tactile RF is touched. However additional experimental evidence on the contribution of multisensory neurons to impact prediction is sparse. In a fMRI study in the non-human primate (Guipponi et al., in preparation (b)), we identify a cortical network whose activity is enhanced in the impact prediction condition both as compared to the classical temporal congruence condition and to a control spatial incongruence condition. This network involves both low level visual (V1, V2) and somatosensory (SII/PV) processing areas as well as well identified multisensory convergence and/or integration areas such as medial superior temporal area MST (Guipponi et al., in preparation (a), Beauchamp et al. 2007) and ventral intraparietal area VIP (Guipponi et al., in preparation (a-b), Avillac et al. 2007).

This finding opens the way to new investigations in the field of multisensory integration, incorporating the temporal prediction dimension. In particular, the Bayesian

framework has proven extremely successful in accounting for the behavioral (*e.g.* Fetsch et al. 2010) and single cell recording (*e.g.* Gu et al. 2008) manifestations of multi-sensory integration. It will be particularly interesting to extend this theoretical framework to our own observations.

Impact prediction and peri-personal space

Anticipating an impact to the body is of vital importance. In this respect, the observations reported here raise several crucial questions and predictions. In particular, no tactile enhancement should be observed when the trajectory of a visual stimulus does not predict an impact to the body. Is this the case? Or can we expect a security margin in which, even though the stimulus trajectory does not cross the body, it yet comes too close to it, thus enhancing tactile sensitivity? In any case, our results suggest a strong overlap between the coding of a defense peripersonal space and the predictive coding of approaching visual objects. Indirect elements of response can be extracted from the literature. For example, the ventral intraparietal area VIP is a multisensory visuo-auditory-tactile area (Duhamel et al. 1997; Bremmer et al. 2000; Avillac et al. 2005, 2007; Schlack et al. 2005, Guipponi et al. 2013, in preparation (a-b)) that is activated by both large field visual stimuli and stimuli approaching the face (Bremmer et al. 1999, 2000; Bremmer, Duhamel, et al. 2002; Bremmer, Klam, et al. 2002). At the same time, stimulations to this region induce a behavioral defense repertoire of whole body movements, suggesting that this region might also be involved in the coding of a defense peripersonal space. Interestingly, a recent report by Bremmer et al. (Bremmer et al. 2013) describes the neural bases of the encoding of movement in near extrapersonal space in area VIP. Guipponi et al. (in preparation, (c)) also describe, in a non-human primate fMRI study, the selective contribution of this cortical area to near space processing as compared to far space processing.

Bibliography

Avillac M, Ben Hamed S, Duhamel J-R. 2007. Multisensory integration in the ventral intraparietal area of the macaque monkey. J Neurosci Off J Soc Neurosci. 27:1922–1932.

Avillac M, Denève S, Olivier E, Pouget A, Duhamel J-R. 2005. Reference frames for representing visual and tactile locations in parietal cortex. Nat Neurosci. 8:941–949.

Ball W, Tronick E. 1971. Infant responses to impending collision: optical and real. Science. 171:818–820.

Beauchamp MS, Yasar NE, Kishan N, Ro T. 2007. Human MST but not MT responds to tactile stimulation. J Neurosci Off J Soc Neurosci. 27:8261–8267.

Bremmer F, Duhamel JR, Ben Hamed S, Graf W. 2000. Stages of self-motion processing in primate posterior parietal cortex. Int Rev Neurobiol. 44:173–198.

Bremmer F, Duhamel J-R, Ben Hamed S, Graf W. 2002. Heading encoding in the macaque ventral intraparietal area (VIP). Eur J Neurosci. 16:1554–1568.

Bremmer F, Graf W, Ben Hamed S, Duhamel JR. 1999. Eye position encoding in the macaque ventral intraparietal area (VIP). Neuroreport. 10:873–878.

Bremmer F, Klam F, Duhamel J-R, Ben Hamed S, Graf W. 2002. Visual-vestibular interactive responses in the macaque ventral intraparietal area (VIP). Eur J Neurosci. 16:1569–1586.

Bremmer F, Schlack A, Kaminiarz A, Hoffmann K-P. 2013. Encoding of movement in near extrapersonal space in primate area VIP. Front Behav Neurosci. 7:8.

Brozzoli C, Makin TR, Cardinali L, Holmes NP, Farnè A. 2012. Peripersonal Space: A Multisensory Interface for Body–Object Interactions. In: Murray MM, Wallace MT, editors.

The Neural Bases of Multisensory Processes. Frontiers in Neuroscience. Boca Raton (FL): CRC Press.

Cappe C, Thelen A, Romei V, Thut G, Murray MM. 2012. Looming signals reveal synergistic principles of multisensory integration. J Neurosci Off J Soc Neurosci. 32:1171–1182.

Cappe C, Thut G, Romei V, Murray MM. 2009. Selective integration of auditory-visual looming cues by humans. Neuropsychologia. 47:1045–1052.

Duhamel JR, Bremmer F, Ben Hamed S, Graf W. 1997. Spatial invariance of visual receptive fields in parietal cortex neurons. Nature. 389:845–848.

Fetsch CR, Deangelis GC, Angelaki DE. 2010. Visual-vestibular cue integration for heading perception: applications of optimal cue integration theory. Eur J Neurosci. 31:1721–1729.

Gu Y, Angelaki DE, Deangelis GC. 2008. Neural correlates of multisensory cue integration in macaque MSTd. Nat Neurosci. 11:1201–1210.

Guipponi O, Wardak C, Ibarrola D, Comte J-C, Sappey-Marinier D, Pinède S, Ben Hamed S. 2013. Multimodal convergence within the intraparietal sulcus of the macaque monkey. J Neurosci. 33:4128–4139.

Guipponi O, Odouard S, Wardak C, Ben Hamed S. (a). Evidence for a widespread stimulus-dependent visuo-tactile convergence network in the macaque monkey (Chapter 2).

Guipponi O, Clery J, Odouard S, Wardak C, Ben Hamed S. (b). Neural bases of impact prediction in the non-human primate (Chapter 4).

Guipponi O, Clery J, Odouard S, Wardak C, Ben Hamed S. (c). Distinct cortical networks for encoding near and far space in the non-human primate (Chapter 5).

Hyvärinen J, Poranen A. 1974. Function of the parietal associative area 7 as revealed from cellular discharges in alert monkeys. Brain J Neurol. 97:673–692.

Körding KP, Beierholm U, Ma WJ, Quartz S, Tenenbaum JB, Shams L. 2007. Causal inference in multisensory perception. PloS One. 2:e943.

Leo F, Romei V, Freeman E, Ladavas E, Driver J. 2011. Looming sounds enhance orientation sensitivity for visual stimuli on the same side as such sounds. Exp Brain Res Exp Hirnforsch Expérimentation Cérébrale. 213:193–201.

Maier JX, Chandrasekaran C, Ghazanfar AA. 2008. Integration of bimodal looming signals through neuronal coherence in the temporal lobe. Curr Biol CB. 18:963–968.

Maier JX, Ghazanfar AA. 2007. Looming biases in monkey auditory cortex. J Neurosci Off J Soc Neurosci. 27:4093–4100.

Maier JX, Neuhoff JG, Logothetis NK, Ghazanfar AA. 2004. Multisensory integration of looming signals by rhesus monkeys. Neuron. 43:177–181.

McDonald JJ, Teder-Sälejärvi WA, Hillyard SA. 2000. Involuntary orienting to sound improves visual perception. Nature. 407:906–908.

Parise CV, Spence C, Ernst MO. 2012. When correlation implies causation in multisensory integration. Curr Biol CB. 22:46–49.

Schiff W, Caviness JA, Gibson JJ. 1962. Persistent fear responses in rhesus monkeys to the optical stimulus of “looming”. Science. 136:982–983.

Schlack A, Sterbing-D’Angelo SJ, Hartung K, Hoffmann K-P, Bremmer F. 2005. Multisensory space representations in the macaque ventral intraparietal area. J Neurosci Off J Soc Neurosci. 25:4616–4625.

Shams L, Beierholm UR. 2010. Causal inference in perception. Trends Cogn Sci. 14:425–432.

Stein, B. E., & Meredith, M. A. (1993). The merging of the senses. Cambridge, MA: MIT Press.

Sugita Y, Suzuki Y. 2003. Audiovisual perception: Implicit estimation of sound-arrival time. Nature. 421:911.

Tyll S, Bonath B, Schoenfeld MA, Heinze H-J, Ohl FW, Noesselt T. 2013. Neural basis of multisensory looming signals. Neuroimage. 65:13–22.

Vagnoni E, Lourenco SF, Longo MR. 2012. Threat modulates perception of looming visual stimuli. Curr Biol CB. 22:R826–827.

Walker-Andrews AS, Lennon EM. 1985. Auditory-visual perception of changing distance by human infants. Child Dev. 56:544–548.

Figures

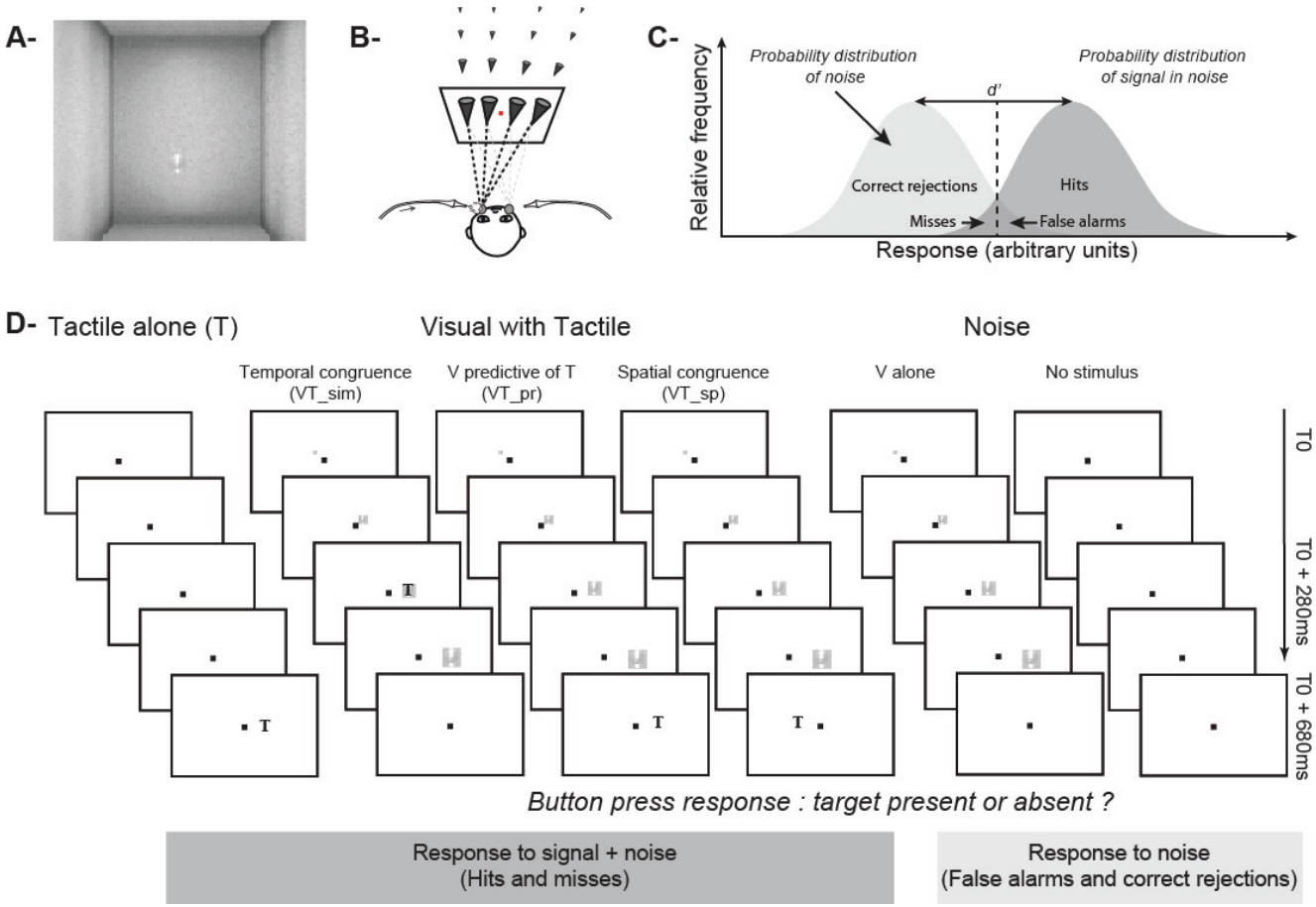

Figure 1: Experimental protocol. (A) Visual stimulus: video sequence of a cone in a 3D environment, looming towards the subject's face. (B) Experimental set up, air puff delivery and possible apparent looming cone trajectories. (C) Signal detection theory and d' measure estimation. (D) Possible variants of signal trials (tactile alone or visual with tactile) and noise trials (visual alone trials or no stimulus trials).

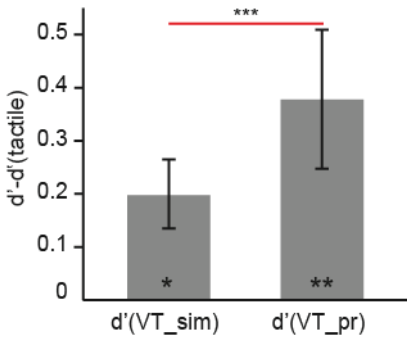

Figure 2: Temporal prediction versus temporal simultaneity. Bar plots represent the mean (+/- std) of the difference between the tactile d'(tactile) and the d' obtained when the tactile stimulus is applied during the visual video sequence (d'(VT_sim)) or following its offset at the predicted time of impact of the looming cone onto the subject's face (d'(VT_pr)). Statistical differences are indicated as follows: *, $p<0.05$; **, $p<0.01$; *** $p<0.005$. Stars in the bars represent the statistical difference with the d' (tactile). Statistical differences between d' (VT_sim) and d'(VT_pr) are indicated above the line joining the two conditions.

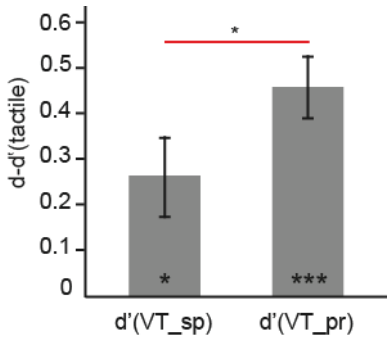

Figure 3: Spatial prediction. Bar plots represent the mean (+/- std) of the difference between the tactile d'(tactile) and the d' obtained when the tactile stimulus is applied following the offset of the looming cone onto the subject's face, at its predicted impact time, at the location predicted by the cone trajectory (d'(VT_pr)) or opposite (d'(VT_sp)). All else as in figure 2.

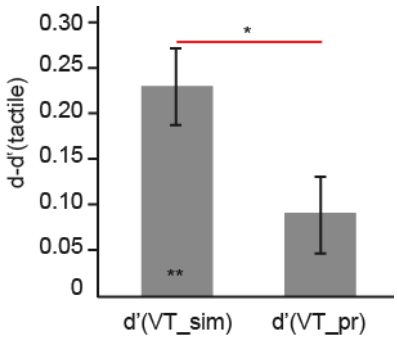

Figure 4: Trajectory cues, receding cone. Bar plots represent the mean (+/- std) of the difference between the tactile d'(tactile) and the d' obtained when the tactile stimulus is applied during the visual video sequence of a cone receding away from the subject's face (d'(VT_sim)) or following its offset (d'(VT_pr)). All else as in figure 2.

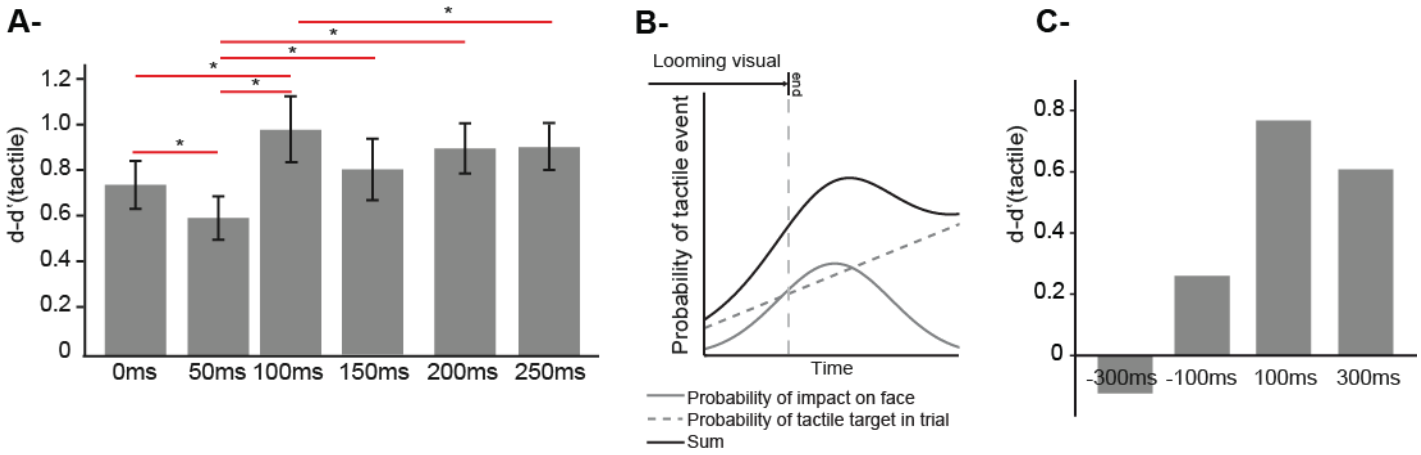

Figure 5: Temporal prediction window. (A) Bar plots represent the mean (+/- std) of the difference between the tactile d'(tactile) and the d' obtained when the tactile stimulus is applied at different temporal asynchronies from visual video sequence offset. All else as in figure 2. (B) Probabilistic model of the experimental observations in (A). (C) Same experiment as in (A) but with noise trials now including visual stimulus only trials. Less asynchronies are tested to keep the task manageable for the subjects.

Chapter 4

Neural Bases of Impact Prediction in the Non-Human Primate

Neural bases of impact prediction in the non-human primate

Abbreviated title: Multisensory integration for looming visual stimuli

Authors: Olivier Guipponi[1], Justine Cléry[1], Soline Odouard[1], Claire Wardak[1], Suliann Ben Hamed[1]

1. Centre de Neuroscience Cognitive, CNRS UMR 5229, 67 Bd Pinel, 69675 Bron cedex, Université Claude Bernard Lyon I

Corresponding author: Suliann Ben Hamed, Centre de Neuroscience Cognitive, CNRS UMR 5229, Université Claude Bernard Lyon I, 67 Bd Pinel, 69675 Bron cedex, France, benhamed@isc.cnrs.fr

Abstract

In the jungle, survival is highly correlated with the ability to detect and distinguish between a predator and a putative prey. From an ecological perspective, the predator becomes potentially harmful once it decides to attack its prey. Experimentally, such a situation can be modeled as a looming stimulus moving towards the subject of the experiment. In the present study, we investigate the multisensory visuo-tactile interactions in the context of the prediction of an impact to the body of such a looming stimulus. In particular, airpuffs (modeling the impact to the body) could be delivered either after the looming visual stimuli (temporal predictive condition), or during the visual sequence (simultaneous visuo-tactile presentation). Airpuffs could also be delivered either at the predicted side of impact to the face (spatially congruent condition), or to the opposite side (spatially incongruent condition). Interestingly, we report that the largest cortical network is obtained when the looming stimulus is temporal and spatial predicting the airpuff. This result challenges our current understanding of the neural bases of multisensory integrationand call for reconsidering the temporal coincidence rule according to which, multisensory integration, the phenomenon by which the sum of neuronal responses, in spikes per second, to unisensory stimulations is different from the neuronal activity in bimodal stimulation conditions (Avillac et al. 2007), is maximal when the stimuli from different sensory modalities are delivered at the same location and at the same time (Stein and Meredith, 1993).

Key words: visual, tactile, looming stimuli, fMRI, macaque monkey, multisensory integration.

Introduction

In the jungle, survival is highly correlated with the ability to detect and distinguish between a predator and a putative prey. From an ecological perspective, the predator becomes potentially harmful once it decides to attack its prey. Experimentally, such a situation can be modeled as a looming stimulus moving towards the subject of the experiment. In such a context, looming stimuli have been described to elicit stereotyped defensive behavior both in monkeys (Schiff et al. 1962) and in human infants (Ball and Tronick 1971). Interestingly, multisensory integration, the phenomenon by which the sum of neuronal responses, in spikes per second, to unisensory stimulations is different from the neuronal activity in bimodal stimulation conditions (Avillac et al. 2007), has been described as maximal when the stimuli from different sensory modalities are delivered at the same location and at the same time (Stein and Meredith 1993).

The underlying mechanism explaining maximal integration processes is explained by the causal inference model: cues from different sensory modalities are bound and represent a unique event if they match spatially and temporally (Körding et al. 2007; Shams and Beierholm 2010; Parise et al. 2012).

Here, functional magnetic resonance imaging (fMRI) in the non-human primate allows us to investigate the multisensory visuo-tactile interactions in the context of the prediction of an impact to the body. We thus presented a visual looming stimulus coming towards the face and a tactile stimulation (airpuff) either in isolation or played in the same blocks. When played together, we manipulate the spatial and temporal relationships between the visual and tactile stimulations so as to test either temporal prediction or spatial prediction aspects. To test for temporal prediction, airpuffs were either delivered during the presentation of the visual looming stimulus, or after its end, at the precise time at which the looming stimulus was

expected to impact the face. To test for spatial prediction, airpuffs were delivered at the predicted time of impact of the looming stimulus on the face, either at the expected location of impact or far away from it. We identify a large cortical network activated by predictive temporal visuo-tactile stimulations. Specifically, we demonstrate that the activity of this network is significantly enhanced both by temporal and spatial prediction. Overall, these results challenge our current understanding of the neural bases of multisensory integration and call for reconsidering the temporal coincidence rule (Stein and Meredith, 1993). We propose that, in the context of dynamic stimuli, multisensory integration might follow different spatiotemporal rules, depending on whether the sensory source is assumed as bimodal (*e.g.* the looming mosquito is buzzing) or whether one sensory modality is at the origin of the heteromodal sensory stimulation (*e.g.* the looming mosquito lands onto my skin).

Material and methods

Subjects and materials

Two rhesus monkeys (female Monkey Z, male Monkey E, 5-7 years old, 5-7 kg) participated to the study. The animals were implanted with a plastic MRI compatible headset covered by dental acrylic. The anesthesia during surgery was induced by Zoletil (Tiletamine-Zolazepam, Virbac, 15 mg/kg) and followed by Isoflurane (Belamont, 1-2%). Post-surgery analgesia was ensured thanks to Temgesic (buprenorphine, 0.3 mg/ml, 0.01 mg/kg). During recovery, proper analgesic and antibiotic coverage were provided. The surgical procedures conformed to European and National Institutes of Health guidelines for the care and use of laboratory animals.

During the scanning sessions, monkeys sat in a sphinx position in a plastic monkey chair positioned within a horizontal magnet (1.5-T MR scanner Sonata; Siemens, Erlangen, Germany) facing a translucent screen placed 90 cm from the eyes. Their head was restrained and equipped with MRI-compatible headphones customized for monkeys (MR Confon GmbH, Magdeburg, Germany). A radial receive-only surface coil (10-cm diameter) was positioned above the head. Eye position was monitored at 120 Hz during scanning using a pupil-corneal reflection tracking system (Iscan®, Cambridge, MA). Monkeys were rewarded with liquid dispensed by a computer-controlled reward delivery system (Crist®) thanks to a plastic tube coming to their mouth. The task, all the behavioral parameters as well as the sensory stimulations were controlled by two computers running with Matlab® and Presentation®. The fixation point the monkeys were instructed to fixate, as well as the visual stimuli, were projected onto a screen with a Canon XEED SX60 projector. Tactile stimulations were delivered through Teflon tubing and 2 articulated plastic arms connected to

distant air pressure electro-valves. Monkeys were trained in a mock scan environment approaching to the best the actual MRI scanner setup.

Task and stimuli

The animals were trained to maintain fixation on a red central spot (0.24°x0.24°) while stimulations (visual and/or tactile) were delivered. The monkeys were rewarded for staying within a 2°x2° tolerance window centered on the fixation spot. The reward delivery was scheduled to encourage long fixation without breaks (*i.e.* the interval between successive deliveries was decreased and their amount was increased, up to a fixed limit, as long as the eyes did not leave the window). The fixation spot was placed in the center of a background representing a 3D environment generated with the Blender software (http://www.blender.org/), at eye level. Both this 3D background and fixation point were present all throughout the runs (figure 1A). Visual and/or tactile stimuli were presented to the monkeys as follows.

Visual stimuli consisted in a low contrast dynamic 3D cone-shaped stimulus, moving from the back of the visual scene towards the face of the monkey (Figure 1A-B). The trajectory of this looming stimulus was adjusted so as to induce the percept of a potential impact on the monkey's face at two possible locations, on the left or right cheeks, close to the snout. The cone trajectory could originate from eight possible origins, four in the left hemifield and four in the right hemifield at +/- 0.32°, +/- 1.27°, +/- 3.16° and +/- 4.11° (figure 1B, showing only four trajectory origins). As a result, half of the cone trajectories crossed the mid-sagittal plane and induced a predicted impact to the face on the contralateral cheek with respect to the spatial origin of the cone (Figure 1B).

Tactile stimuli consisted in air puffs delivered at two possible locations on the monkey's face, on the left or right cheeks, close to the snout, at the impact location predicted

by the cone trajectory, close to the nose and the mouth (Figure 1B) with a pressure intensity set at 0.3bar. This barely perceivable airpuff intensity was chosen so as to maximize the multisensory integration processes expected to take place when combined with a visual stimulus. Airpuff duration was set to 50ms and successive airpuffs were separated by a random time interval ranging from 1500 to 2800ms.

The visual and tactile sensory modalities were tested in the same runs, either in separate blocks (unimodal stimulations) or in same blocks (bimodal stimulations). In the *visual unimodal blocks,* the movement of the visual cone had a duration of 550 ms and two looming stimuli were separated by a random timing ranging from 220 to 700. In the *tactile unimodal blocks,* airpuff duration was set to 50ms (as measured with a silicon pressure on-chip signal conditioned sensor, MPX5700 Series, Freescale™) and successive airpuffs were separated by a random time interval ranging from 1500 to 2800ms. For the bimodal conditions, we defined three different types of stimulation blocks: 1) *Simultaneous bimodal blocks (VT_sim),* in which the tactile stimulus was presented while the visual stimulus was approaching the face of the monkey (mid-course of the visual stimulus, airpuff latency as measured with the pressure sensor being account for), at the location at which the visual stimulus was expected to impact the face; 2) *Predictive bimodal blocks (VT_pr),* in which the tactile stimulus was presented at the moment when the visual stimulus was expected to impact the face (airpuff latency as measured with the pressure sensor being account for), at the spatial location of the expect impact; 3) *Spatially uncongruent bimodal blocks (VT_sp),* in which the tactile stimulus was presented at the moment when the visual stimulus was expected to impact the face, but at a location symmetrical to where the visual stimulus was expected to impact the face. In all these bimodal blocks, visual stimuli were presented with the same temporal dynamics as in the unimodal visual blocks. It is crucial to note that the visual and tactile stimuli were designed to have a low salience to maximize the multisensory integration.

Functional time series (runs) were organized as follows: 15-volume blocks of unimodal and bimodal stimulation blocks were followed by a 15-volume block of pure fixation baseline (Figure 1C); this sequence was played twice, resulting in a 180-volume run. The 6 types of blocks were presented in 10 counterbalanced possible orders.

Scanning

Before each scanning session, a contrast agent, monocrystalline iron oxide nanoparticle (Sinerem, Guerbet or Feraheme, AMAG, Vanduffel et al., 2001), was injected into the animal's femoral/saphenous vein (4-10 mg/kg). For the sake of clarity, the polarity of the contrast agent MR signal changes, which are negative for increased blood volumes, was inverted. We acquired gradient-echo echoplanar (EPI) images covering the whole brain (1.5 T; repetition time (TR) 2.08 s; echo time (TE) 27 ms; 32 sagittal slices; 2x2x2-mm voxels). A total of 61 (66) runs was acquired for M1 (/M2).

Analysis

A total of 59 runs for monkey Z and 61 runs for monkey E was selected based on the quality of the monkeys' fixation throughout each run (>85% within the tolerance window). Time series were analyzed using SPM8 (Wellcome Department of Cognitive Neurology, London, United Kingdom). For spatial preprocessing, functional volumes were first realigned and rigidly coregistered with the anatomy of each individual monkey (T1-weighted MPRAGE 3D 0.6x0.6x0.6 mm or 0.5x0.5x0.5 mm voxel acquired at 1.5T) in stereotactic space. The JIP program (Mandeville et al. 2011) was used to perform a non-rigid coregistration (warping) of a mean functional image onto the individual anatomies.

Fixed effect individual analyses were performed for each monkey, with a level of significance set at $p<0.05$ corrected for multiple comparisons (FWE, $t>4.89$, unless stated

otherwise). In all analyses, realignment parameters, as well as eye movement traces, were included as covariates of no interest to remove eye movement and brain motion artifacts. When coordinates are provided, they are expressed with respect to the anterior commissure. Results are displayed on coronal sections or on flattened maps obtained with Caret (Van Essen et al., 2001; http://www.nitrc.org/projects/caret/).

Regions of Interest. We performed regions of interest (ROI) analyses using MarsBar toolbox (Brett et al., 2002), based on the fixed effects individual analyses results. The ROIs were defined using the activations obtained at uncorrected level (t-scores>3.1).

Potential covariates. In all analyses, realignment parameters, as well as eye movement traces, were included as covariates of no interest to remove eye movement and brain motion artifacts. However, some of the stimulations might have induced a specific behavioral pattern biasing our analysis, not fully accounted for by the above regressors. For example, air-puffs to the face might have evoked facial mimics (as well as some imprecision in the point of impact of the air puff). While we cannot completely rule out this possibility, our experimental set-up allows to minimize its impact. First, monkeys worked head-restrained (to maintain the brain at the optimal position within the scanner, to minimize movement artifacts on the fMRI signal and to allow for a precise monitoring of their eye movements). As a result, the tactile stimulations to the face were stable in a given session. Airpuff intensity was very low and did not evoke overt behavioral responses such as eye blinks (Guipponi et al., in preparation) or facial mimics. When drinking the liquid reward, small lip movements occurred. These movements thus correlated with reward timing and were on average equally distributed over the different sensory runs and the different conditions within each run (we checked that the monkeys had equal performance amongst the different conditions within a given run). The center of the face air puffs were placed on the cheeks on each side of the monkey's nose at a location that was not affected by the lip movements. Second, monkeys were required to

maintain their gaze on a small fixation point, within a tolerance window of 2°x2°. This was controlled online and was used to motivate the animal to maximize fixation rates (as fixation disruptions, such as saccades or drifts, affected the reward schedule). Eye traces were also analyzed offline for the selection of the runs to include in the analysis (good fixation for 85% of the run duration, with no major fixation interruptions).

Results

Monkeys were exposed, in the same time series, to looming visual stimuli evolving in a virtual 3D environment (Figure 1A), to tactile stimulations (Figure 1B), or to bimodal visuo-tactile stimulations, while fixating a central point. Three distinct bimodal blocks were presented. The tactile stimulus could be presented simultaneously with the visual stimulus, at the precise location where the visual cue is predicted to impact the monkey's face (VT_sim). The tactile stimulus could be presented after the visual stimulus, at the predicted location and time of impact on the monkey's face (VT_pr). Last, the tactile stimulus could be presented simultaneously with the visual stimulus, but at the opposite location from where the visual cue is predicted to impact the monkey's face (VT_sp). In the following, we describe the general effect of bimodal as compared to unimodal presentations as well as the specific contribution of temporal prediction and spatial congruence onto multisensory integration. For the sake of clarity, the functional activation maps are presented only for monkey Z, while the specific spatial and temporal effects are described independently for each of monkeys Z and E.

Weak unimodal activations

The visual and tactile stimulations were specifically designed to have a low contrast (low contrast looming cone onto the 3D visual background, low intensity tactile stimuli) so as to maximize multisensory integration. This is confirmed by the weak overall activations that can be observed following the unimodal visual (Figure 2, upper panel, red activations) or tactile (Figure 2, upper panel, green activations) stimulation blocks.

Visual activations. Visual looming stimuli did not activate any striate or extrastriate cortical region, except for the medial temporal area (MT), bilaterally. Bilateral premotor activations were observed in the posterior convexity of the arcuate sulcus, in a cortical region possibly coinciding with premotor zone PMZ. Surprisingly, several cortical regions involved

in somatosensory processing were also activated by the looming visual stimulus, namely, the primary somatosensory cortex bilaterally (within the central sulcus, at a location coinciding with the representation of the center of the face, Krubitzer et al. 2004), the insular cortex bilaterally (Ig-Id granular and disgranular parts of the insula, within the lateral sulcus), and in the mid-cingulate sulcus unilaterally (in a region coinciding with areas 23d and 24d).

Tactile activations. Center of the face tactile stimulations expectedly activated the primary somatosensory cortex (central sulcus), at a location closely matching that of the central sulcus activations observed during visual unimodal stimulations. Bilateral tactile activations could also be observed bilaterally, a unilateral activation at the right anterior tip of the intraparietal sulcus (at a position possibly coinciding with the face region of area 2, Krubitzer et al. 2004, and the tip of the ventral intraparietal area VIP, Guipponi et al. 2013) as well as a unilateral activation at the right posterior convexity of the arcuate sulcus, closely matching the premotor zone activation observed during visual unimodal stimulations.

Bimodal stimuli produce a general

The flat maps for the activations obtained for the bimodal condition in which the visual looming stimulus is predictive of a spatially congruent tactile stimulation at the expected time of impact to the face are presented for monkey Z in Figure 2 (lower panel, magenta scale).These activations are strikingly more widespread than those observed during unimodal visual or tactile stimulations. Specifically, these include large portions of the striate and extrastriate cortex (areas V1, V2, V3, V3A), right medial temporal area MT (within the superior temporal sulcus), primary (within the central sulcus in a regions corresponding to area 3b) and secondary somatosensory cortices (SII/PV, within the upper bank if the lateral sulcus), the left insular cortex (Ig-Id granular and disgranular parts of the insula, within the lateral sulcus), parietal area PGm bilaterally, and right posterior cingulate area PECi.

A region of interest (ROIs) analysis allows us to confirm this observation (Figure 3A). In this analysis, we calculated the percentage of signal change (PSC) in the regions of interest defined by the functional contrast presented in Figure 2, for both monkey Z (presented in Figure 2, 22 ROIs in all) and monkey E (22 ROIs in all), for all of the different stimulation conditions (Visual unimodal, Tactile unimodal, predictive bimodal, simultaneous bimodal and spatially incongruent bimodal). The PSCs measured in these ROIs during each of the bimodal conditions is significantly higher than those measured during the unimodal conditions, describing a general enhancement of hemodynamic activity during bimodal stimulations as compared to unimodal stimulations. At closer inspection, the different bimodal conditions do not appear to evoke the same PSC changes across the different ROIs. This is further explored below.

Temporal prediction against temporal simultaneity

In the predictive bimodal condition (VT_pr), the tactile stimulus is presented at the expected impact location of the looming visual stimulus on the face, at the expected time of impact. In contrast, in the simultaneous bimodal condition (VT_sim), the tactile stimulus is presented at the expected impact location of the looming visual stimulus on the face, but while the visual stimulus is still halfway through its trajectory. Figure 3B represents the PSC change measured in the ROI defined in the left secondary somatosensory cortex of monkey Z during the unimodal tactile condition, the predictive bimodal condition and the simultaneous bimodal condition. All three PSCs are significantly different from the visual baseline condition across the different runs (t-test, $p<0.05$). Interestingly, the PSCs measured for the predictive bimodal condition are also significantly higher than those measured during the simultaneous bimodal condition (t-test, $p<0.05$, no statistical different between the tactile unimodal and simultaneous bimodal PSCs). This major trend is confirmed on the majority of

the ROIs identified by the predictive bimodal versus fixation contrast, both in monkey Z (Figure 3C, left panel, t-test, $p<0.0001$) and monkey E (Figure 3C, right panel, t-test, $p<0.0001$). A finer analysis will allow to specifically identify the cortical network distinctively encoding the predictive bimodal condition as compared to the simultaneous bimodal condition.

Spatial prediction

In the predictive bimodal condition (VT_pr), the tactile stimulus is presented at the expected impact location of the looming visual stimulus on the face, at the expected time of impact. In contrast, in the spatially incongruent bimodal condition (VT_sp), the tactile stimulus is presented at the expected impact time of the looming visual stimulus, but at the opposite location on the face. Figure 3D represents the PSC change measured in the ROI defined in the left secondary somatosensory cortex of monkey Z (same as in figure 3B) during the unimodal tactile condition, the predictive bimodal condition and the spatially incongruent bimodal condition. All three PSCs are significantly different from the visual baseline condition across the different runs (t-test, $p<0.05$). As observed above for the temporal prediction dimension, the PSCs measured for the predictive bimodal condition are significantly higher than those measured during the spatially incongruent bimodal condition (t-test, $p<0.05$, no statistical different between the tactile unimodal and spatially incongruent bimodal PSCs). This major trend is confirmed on the majority of the ROIs identified by the predictive bimodal versus fixation contrast, both in monkey Z (Figure 3C, left panel, t-test, $p<0.0001$) and monkey E (Figure 3C, right panel, t-test, $p<0.0001$). Here again, a finer analysis will allow to specifically identify the cortical network distinctively encoding the predictive bimodal condition as compared to the spatially incongruent bimodal condition.

N.B. This analysis is still ongoing. In particular, we have concentrated on the analysis of the cortical regions which contribute to the predictive coding of the tactile consequences of the looming stimulus. It needs to be noted that we also identify cortical regions which are more activated by simultaneous bimodal stimulations than predictive bimodal stimulations. Though this observation together with what is described in the present report has important functional implications, we decided not to include them for now (ongoing analysis).

Discussion

This on-going study confirms the fact that bimodal visuo-tactile stimulations elicit a more pronounced neuronal response than unimodal sensory stimulations, in a context of weak visual and tactile stimulations (Avillac et al. 2007; Stein and Stanford 2008; Stein et al. 2009). Additionally, our observations suggest that, in the context of looming visual stimuli, both temporal and predictive cues maximize the bimodal response in a well-identified cortical network. In the following, we discuss these observations in the context of multisensory integration.

Prediction of impact and multisensory integration

The main experimental condition considered in the present work is the condition in which the tactile stimulation is presented 100ms following the end of the looming stimulus, at the time at which this stimulus was expected to impact the monkey's face, and at the location predicted by it. Our work demonstrates that in the cortical regions which are significantly active by this condition in contrast with the fixation baseline, the hemodynamic response is maximized both by temporal prediction (predictive versus simultaneous bimodal contrast) and spatial prediction (predictive versus spatial incongruent bimodal contrast). This study thus provides the neural substrates underlying the enhancement of tactile detection by temporal and spatial visual cues, as described in the twin psychophysical study (Chapter 3). Interestingly, the network we observe in the predictive bimodal visuo-tactile condition is mainly composed of low-level visual areas (primary visual cortex, MST) and somatosensory sensory areas (primary and secondary somatosensory cortices) but no higher order associative cortical regions to the exception of posterior cingulate cortex and medial parietal cortex.

These observations will need to be contrasted with the network activated by the simultaneous bimodal condition in contrast with the fixation baseline.

Spatial prediction of impact. The trend we describe is a greater hemodynamic response when tactile stimulations are delivered at the location of the predicted impact of visual looming stimuli. Because visual stimuli could originate from 8 different locations in the far visual field (4 locations ipsilateral to the impact point and 4 contralateral) but predict only two possible impact locations to the face (left or right cheek), the spatial effects reported here cannot be accounted for by other aspects of the stimulus. Spatial congruence between different sensory cues has already been described to maximize multisensory integration in a context of static stimuli (Stein and Meredith 1993). The important point we emphasize here is that the spatial meaningful information is the impact location rather than the visual stimulus origin. This impact location is most probably inferred by the nervous system based on the looming stimulus spatial trajectory.

Temporal prediction of impact. Based on the notion of causal inference which proposes that two sensory events (a visual and an auditory signals) can be attributed to a unique underlying cause if they take place at the same time and spatial location (Körding et al. 2007; Shams and Beierholm 2010; Parise et al. 2012), we propose to extend this view to delayed sensory events which can be attributed to a unique underlying cause. Specifically, in our task, the looming visual stimuli, due to their dynamical properties, predict tactile impact on the face a short delay after their disappearance from the experimental screen. This view is corroborated by the observation of 1) an increased hemodynamical response in somatosensory regions (area 3b and insular cortex) during the visual unimodal condition, possibly corresponding to the expectation of a tactile stimulations following the looming stimulus and 2) an significant activation of somatosensory regions (areas 3b and SII/PV) during the

predictive bimodal condition. Interestingly, the anterior cingulate cortex activation is only observed during the unimodal visual stimulation, possibly reflecting prediction violation (Matsumoto et al. 2003; Rushworth et al. 2004; Walton et al. 2004; Quilodran et al. 2008): the looming stimulus is predicting an impact that does not take place.

Overall, our results suggest that the integration of visual looming stimuli and tactile impact stimulation is maximally represented in the brain with a temporal asynchrony between the sensory modality presentations. This indicates that the brain might be able to differentially process a situation in which multisensory sources are best interpreted as simultaneous sources (in which case, the laws of spatial and temporal synchrony are ecologically relevant, Stein and Meredith 1993), from a situation in which one multisensory source is at the origin of the heteromodal stimulus (in which case, the laws of spatial and temporal synchrony are violated for a more ecologically relevant causal inference framework).

The study of the neural bases of multisensory integration using fMRI

Single cell studies have a straight forward definition of cells performing multisensory integration. Their response in the bimodal stimulation should at the same time be significantly different from the cell's response to each unimodal stimulation and significantly different from the sum of the cell's response to these unimodal stimulations (Avillac et al. 2007; Stein and Stanford 2008; Stein et al. 2009). The study of the neural bases of multisensory integration using fMRI poses very specific analysis issues, most probably due to the non-linear relationship that exists between spike generation and the corresponding change in the hemodynamic response (Boynton et al. 1996; Dale and Buckner 1997; Heeger and Ress 2002). In particular, the choice of the baseline is a critical factor (Binder et al. 1999; Stark and Squire 2001; for review see James and Stevenson 2012) as well as the criteria for deciding that multisensory integration is indeed taking place (Calvert 2001; Beauchamp et al. 2004;

Beauchamp 2005; Laurienti et al. 2005). In the present study, the strictest fMRI criteria (same as those used in single cell recordings) do not allow us to highlight any ongoing multisensory integration, most probably due to the extremely low intensity stimuli used. Other criteria (*e.g.* statistical difference with either unimodal conditions) appear to be more appropriate. Though we are still working on refining these criteria, a key observation needs to be highlighted. Indeed, most of the regions activated by predictive bimodal stimuli fall in either visual or somatosensory cortices. Though our work and that of others (see Chapters 1 and 2) demonstrate that these regions are modulated by heteromodal projections, it is rather unexpected that their degree of response to predictive bimodal stimuli should be higher than that of higher order multimodal associative areas. We believe that this in itself is an indication that the integrative processes that are taking place can indeed be inferred from the changes in the hemodynamic responses.

Bibliography

Avillac M, Ben Hamed S, Duhamel J-R. 2007. Multisensory integration in the ventral intraparietal area of the macaque monkey. J Neurosci. 27:1922–1932.

Ball W, Tronick E. 1971. Infant responses to impending collision: optical and real. Science. 171:818–820.

Beauchamp MS. 2005. Statistical Criteria in fMRI Studies of Multisensory Integration. Neuroinformatics. 3:093–114.

Beauchamp MS, Lee KE, Argall BD, Martin A. 2004. Integration of auditory and visual information about objects in superior temporal sulcus. Neuron. 41:809–823.

Binder JR, Frost JA, Hammeke TA, Bellgowan PS, Rao SM, Cox RW. 1999. Conceptual processing during the conscious resting state. A functional MRI study. J Cogn Neurosci. 11:80–95.

Boynton GM, Engel SA, Glover GH, Heeger DJ. 1996. Linear systems analysis of functional magnetic resonance imaging in human V1. J Neurosci. 16:4207–4221.

Calvert GA. 2001. Crossmodal processing in the human brain: insights from functional neuroimaging studies. Cereb Cortex. 11:1110–1123.

Dale AM, Buckner RL. 1997. Selective averaging of rapidly presented individual trials using fMRI. Hum Brain Mapp. 5:329–340.

Guipponi O, Wardak C, Ibarrola D, Comte J-C, Sappey-Marinier D, Pinède S, Ben Hamed S. 2013. Multimodal convergence within the intraparietal sulcus of the macaque monkey. J Neurosci. 33:4128–4139.

Heeger DJ, Ress D. 2002. What does fMRI tell us about neuronal activity? Nat Rev Neurosci. 3:142–151.

James TW, Stevenson RA. 2012. The Use of fMRI to Assess Multisensory Integration. In: Murray MM, Wallace MT, editors. The Neural Bases of Multisensory Processes. Frontiers in Neuroscience. Boca Raton (FL): CRC Press.

Körding KP, Beierholm U, Ma WJ, Quartz S, Tenenbaum JB, Shams L. 2007. Causal inference in multisensory perception. PloS One. 2:e943.

Krubitzer L, Huffman KJ, Disbrow E, Recanzone G. 2004. Organization of area 3a in macaque monkeys: contributions to the cortical phenotype. J Comp Neurol. 471:97–111.

Laurienti PJ, Perrault TJ, Stanford TR, Wallace MT, Stein BE. 2005. On the use of superadditivity as a metric for characterizing multisensory integration in functional neuroimaging studies. Exp Brain Res. 166:289–297.

Mandeville JB, Choi J-K, Jarraya B, Rosen BR, Jenkins BG, Vanduffel W. 2011. fMRI of cocaine self-administration in macaques reveals functional inhibition of basal ganglia. Neuropsychopharmacol. 36:1187–1198.

Matsumoto K, Suzuki W, Tanaka K. 2003. Neuronal correlates of goal-based motor selection in the prefrontal cortex. Science. 301:229–232.

Parise CV, Spence C, Ernst MO. 2012. When correlation implies causation in multisensory integration. Curr Biol. 22:46–49.

Quilodran R, Rothé M, Procyk E. 2008. Behavioral shifts and action valuation in the anterior cingulate cortex. Neuron. 57:314–325.

Rushworth MFS, Walton ME, Kennerley SW, Bannerman DM. 2004. Action sets and decisions in the medial frontal cortex. Trends Cogn Sci. 8:410–417.

Schiff W, Caviness JA, Gibson JJ. 1962. Persistent fear responses in rhesus monkeys to the optical stimulus of "looming". Science. 136:982–983.

Shams L, Beierholm UR. 2010. Causal inference in perception. Trends Cogn Sci. 14:425–432.

Stark CE, Squire LR. 2001. When zero is not zero: the problem of ambiguous baseline conditions in fMRI. Proc Natl Acad Sci. 98:12760–12766.

Stein BE, Meredith MA. 1993. The merging of the senses. Cambridge, Mass.: MIT Press.

Stein BE, Stanford TR. 2008. Multisensory integration: current issues from the perspective of the single neuron. Nat Rev Neurosci. 9:255–266.

Stein BE, Stanford TR, Ramachandran R, Perrault TJ Jr, Rowland BA. 2009. Challenges in quantifying multisensory integration: alternative criteria, models, and inverse effectiveness. Exp Brain Res. 198:113–126.

Van Essen DC, Drury HA, Dickson J, Harwell J, Hanlon D, Anderson CH. 2001. An integrated software suite for surface-based analyses of cerebral cortex. J Am Med Informatics. 8:443–459.

Walton ME, Devlin JT, Rushworth MFS. 2004. Interactions between decision making and performance monitoring within prefrontal cortex. Nat Neurosci. 7:1259–1265.

Figures

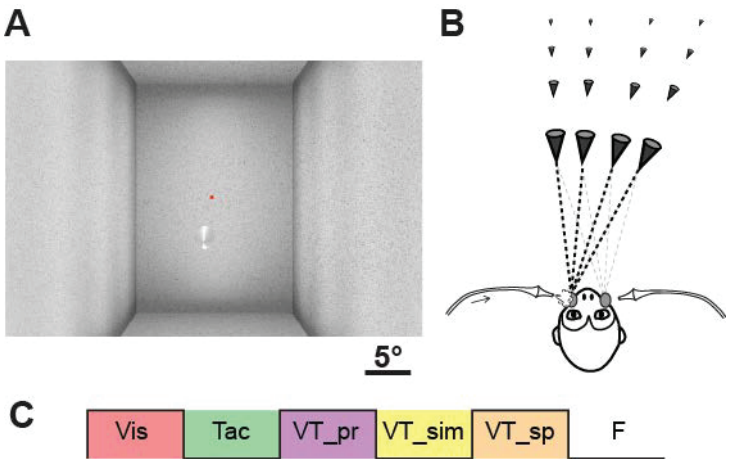

Figure 1: Experimental protocol. (A) Visual stimuli consisted in a video sequence of a cone placed in a 3D environment and looming towards the animal's face. The red dot corresponds to the spatial location the monkey is required to fixate in order to be rewarded. (B) Air puffs could be delivered either to the left or right cheek, coinciding with predicted impact of the looming cone on the monkey's face. The cone could originate from eight possible locations in the back of the visual scene, four to the right of the body midline and four to its left (only four cone origins are shown here, for the sake of clarity). (C) Block design (15 pulses per condition): visual unimodal (Vis), tactile unimodal (Tac), predictive bimodal (VT_pr), simultaneous bimodal (VT_sim), spatially incongruent bimodal (VT_sp) and fixation baseline (F). See text for details on each block stimulation parameters.

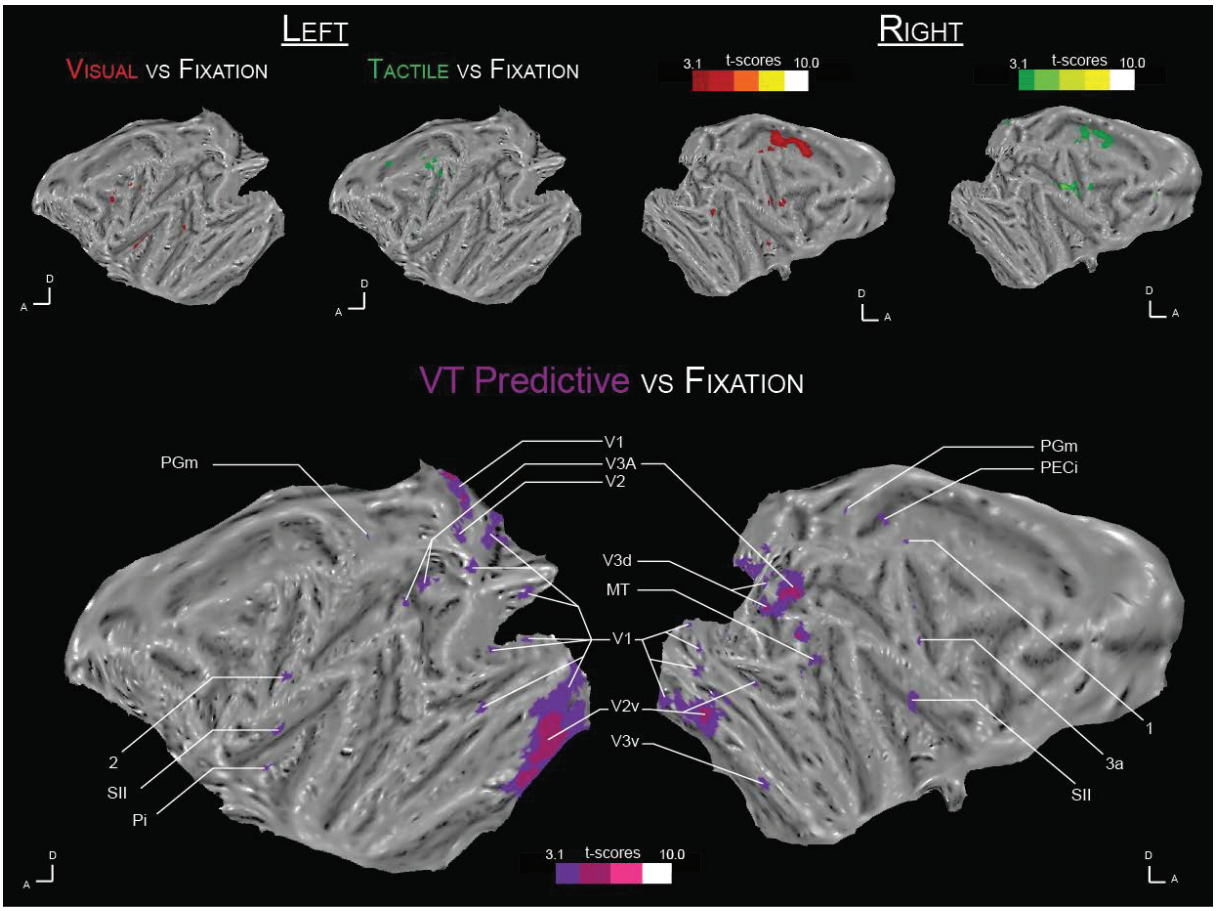

Figure 2: Visual, tactile and VisuoTactile predictive cortical activations. Activations are referred to Monkey Z and are presented its flattened cortex obtained with Caret. The upper part of the figure shows the left hemisphere (left-most flat maps) and right hemisphere (right most flat maps) activations: unimodal visual stimulation versus fixation contrast (red scale, the t scores = 3.1, at $p<0.001$, uncorrected level) and tactile unimodal stimulation versus fixation contrast (green scale, the t scores = 3.1, at $p<0.001$, uncorrected level). The lower part of the figure shows the VisuoTactile activation maps for tactile stimulations delivered at the time of impact predicted by the visual looming stimuli (magenta t-score scale). A, Anterior; D, Dorsal; MT: medial superior temporal area; Pi: parainsular cortex; PIP: posterior intraparietal area; PMZ: paramotor zone; PV, parietoventral cortex; SII: secondary somatosensory cortex; VIP: ventral intraparietal area; V1v: visual area V1, ventral part; V1c: visual area V1, central part; V1d: visual area V1, dorsal part; V2v: visual area V2, ventral

part; V2d: visual area V2, dorsal part; V3: visual area V3; V3A: visual area V3A; 2: somatosensory area 2; 6Vam: area 6Va, medial part; 7b: somatosensory area 7b; 7op: opercular area 7; 8as: area 8as; 11: orbitofrontal area 11; 13: orbitofrontal area 13; 24d: cingulate area 24d; 46p: area 46, posterior part. Cortical sulci: AS, arcuate sulcus; CgS, cingulate sulcus; CeS, central sulcus; IOS, inferior occipital sulcus; IPS, intraparietal sulcus; LaS, lateral (Sylvian) sulcus; LuS, lunate sulcus; OTS, occipital temporal sulcus; POS, parieto-occipital sulcus; PS, principal sulcus; STS, superior temporal sulcus.

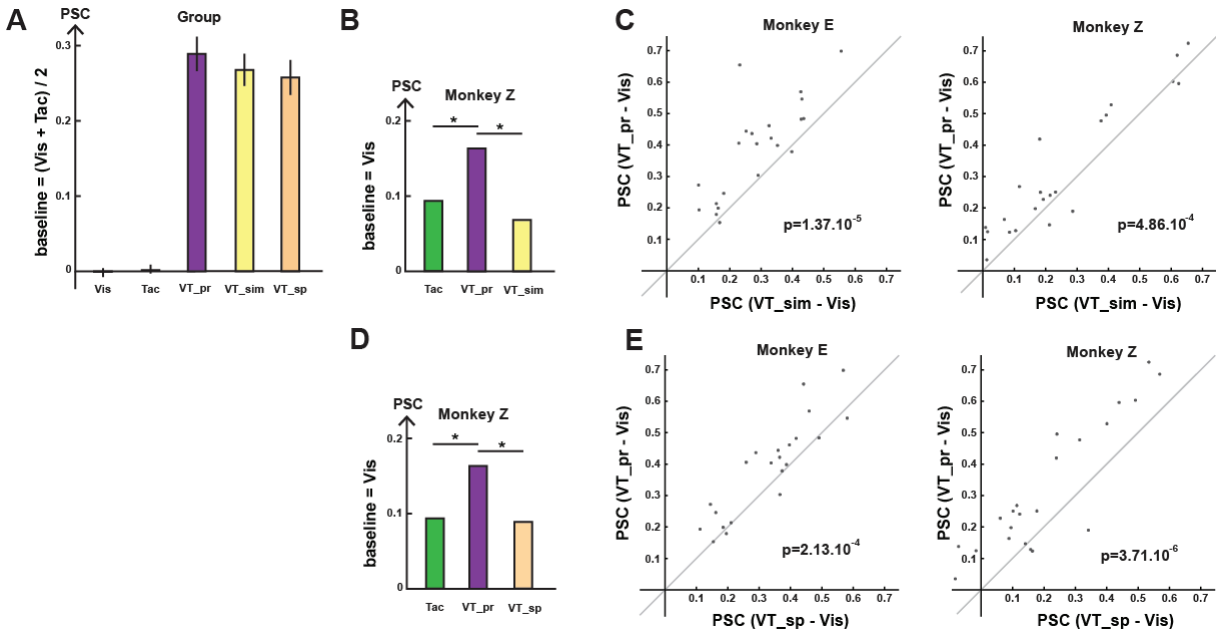

Figure 3: Effects of temporal prediction and spatial enhancement onto bimodal enhancement. (A) General bimodal enhancement. Percentage of signal change (PSC) relative to unimodal visual, unimodal tactile, and bimodal visuo-tactile stimulations: predictive bimodal (VT_pr), simultaneous bimodal (VT_sim) and spatial incongruence bimodal (VT_sp) conditions. Histograms represent the average of PSC extracted from the regions of interest (ROIs) defined by the VT_pr versus fixation contrast in both monkeys. The baseline is set by the average of unimodal visual and tactile scores of each ROI. Bimodal enhancement is maximized by spatial congruence: (B) PSC of unimodal tactile, bimodal VT_pr and VT_sim stimulation conditions extracted from a ROI defined in left SII (monkey Z, *: $p<0.05$). The baseline is set by the unimodal visual score in this ROI. (C) PSC of (VT_pr versus Vis) against (VT_sim versus Vis) for all the ROIs defined from (VT_pr vs fixation) contrast in monkey E (left panel) and monkey Z (right panel). Bimodal enhancement is maximized by temporal prediction: (D) PSC of unimodal tactile, bimodal VT_pr and VT_sp stimulation conditions extracted from a ROI defined in SII (monkey Z, *: $p<0.05$). The baseline is set by the unimodal visual score in this ROI. (E) PSC of (VT_pr versus Vis) against (VT_sp versus Vis)

for all the ROIs defined from (VT_pr vs fixation) contrast in monkey E (left panel) and monkey Z (right panel). (C, E) p values for paired t-tests are indicated for each monkey.

Chapter 5

Distinct Cortical Networks for Encoding Near and Far Space Processing in the Non-Human Primate

Distinct cortical networks for encoding near and far space

in the non-human primate

Abbreviated title: Near and far space processing in the non-human primate.

Authors: Olivier Guipponi[1], Justine Cléry[1], Soline Odouard[1], Claire Wardak[1], Suliann Ben Hamed[1]

1. Centre de Neuroscience Cognitive, CNRS UMR 5229, 67 Bd Pinel, 69675 Bron cedex, Université Claude Bernard Lyon I

Corresponding author: Suliann Ben Hamed, Centre de Neuroscience Cognitive, CNRS UMR 5229, Université Claude Bernard Lyon I, 67 Bd Pinel, 69675 Bron cedex, France, benhamed@isc.cnrs.fr

Abstract

While extra-personal space is often erroneously considered as a unique entity, early neuropsychological studies report a dissociation between near and far space processing both in humans and in monkeys. In the present study, we use functional magnetic resonance imaging (fMRI) in a naturalistic 3D environment to describe the non-human primate near space and far space cortical networks. Overall, we describe the co-occurrence of two extended functional networks respectively dedicated to near space and far space processing. Specifically, far space processing involves occipital, temporal, parietal, posterior cingulated as well as orbitofrontal regions, possibly subserving the processing of the shape and identity of the object. This network is only minimally affected by object size. In contrast, near space processing involves temporal, parietal and prefrontal regions, possibly subserving the preparation of an arm/hand mediated action towards the object used for the near space stimulation. Interestingly, this network also involves somatosensory regions, such as areas 2, 3 in the posterior central sulcus and SII/PV in the upper bank of the lateral sulcus, suggesting a cross-modal anticipation of touch by a nearby object. In addition, we also describe cortical regions that process both far and near space with a preference for one or the other.

This suggests a continuous encoding of relative distance to the body, in the form of a far-to-near or near-to-far gradient. The existence of such cortical gradients in space representation does not preclude the existence of a physically delineable peripersonal space, as described in numerous psychology and psychophysics studies.

Key words: naturalistic environment, near space, far space, macaque monkey, fMRI.

Introduction

While extra-personal space is often erroneously considered as a unique entity, early neuropsychological reports demonstrate that the unilateral ablation of the frontal eye fields produces, in the non-human primate, an inattention to contralateral objects, more pronounced for far objects than for near objects (Rizzolatti et al. 1983). In contrast, the unilateral ablation of frontal area 6 produces an inattention to contralateral objects, more pronounced for near objects than for far objects (Rizzolatti et al. 1983). In 1991, a single case study by Halligan and Marshall, present the first neuropsychological evidence for a left neglect in near space but not in far space after a unilateral right hemisphere stroke (Halligan and Marshall 1991). The finding of the opposite dissociation confirmed that, also for humans, far and near space are separately coded by the brain (Cowey et al. 1994, 1999; Vuilleumier et al. 1998), though a task dependence of far and near space processing deficits is observed (Keller et al. 2005; Aimola et al. 2012). Overall, these studies are in favor of the existence of two distinct networks, respectively involved in the processing of near and far space.

The neural bases of near space coding in humans involve a dorsal stream including the left dorsal occipital cortex, the left intraparietal and the left ventral premotor, while the coding of far space involves a ventral stream including the ventral occipital cortex bilaterally and the right medial temporal cortex (Weiss et al. 2000; Aimola et al. 2012). However, no specific influence on the neural mechanisms responsible for either perceptual or motor processes can be identified as a function of whether the task is being performed in the near or the far space (Weiss et al. 2003). Surprisingly, human ventral intraparietal area VIP shows no preference for any particular spatial range while the dorsal parieto-occipital sulcus (dPOS) demonstrates a near-space preference, with activation highest for near viewing (Quinlan and Culham 2007). This contrasts with a recent report near extrapersonal space movement encoding in the non-human primate VIP. Overall,

these observations are confirmed by transcranial magnetic stimulation (TMS). Indeed, the reversible perturbation of the right angular gyrus (ANG) alters near space perception while that of the right supramarginal gyrus (SMG) induces a higher perception deficit in far than in near space (Bjoertomt et al. 2002, 2009).

At the neuronal level, potential "peripersonal" neurons firing both when a tactile stimulus is delivered to the animal's skin and when a visual stimulus is presented in the space near the part of the body where the tactile field is located have been described in the prefrontal cortex (Gentilucci et al. 1988; Graziano et al. 1994; Gross and Graziano 1995; Fogassi et al. 1996). This corroborates the near space neglect observed following prefrontal area 6 lesions (Rizzolatti et al. 1983). The parietal far-near dissociation is less evident. Our own ventral intraparietal neuronal (Avillac et al. 2007) and fMRI (Guipponi et al. 2013) recordings in the non-human primates were performed in far space. On the other hand, Bremmer et al. (Bremmer et al. 2013) find a preferential encoding of movement in near space in this parietal cortical area, although no sensitivity to the 3D structure of static stimuli could be found in VIP (Durand et al. 2007).

Here, functional magnetic resonance imaging (fMRI) in the non-human primate allows us to describe near space and far space network in a naturalistic 3D environment. We confirm the existence of two distinct networks processing either near space or far space.

Material and Methods

Subjects and experimental setup

Two rhesus monkeys (female M1, male M2, 5-7 years old, 5-7 kg) participated to the study. The animals were implanted with a plastic MRI compatible headset covered by dental acrylic. The anesthesia during surgery was induced by Zoletil (Tiletamine-Zolazepam, Virbac, 15 mg/kg) and followed by Isoflurane (Belamont, 1-2%). Post-surgery analgesia was ensured thanks to Temgesic (buprenorphine, 0.3 mg/ml, 0.01 mg/kg). During recovery, proper analgesic and antibiotic coverage were provided. The surgical procedures conformed to European and National Health guidelines for the care and use of laboratory animals.

During the scanning sessions, monkeys sat in a sphinx position in a plastic monkey chair positioned within a horizontal magnet (1.5-T MR scanner Sonata; Siemens, Erlangen, Germany). Their head was restrained and they were equipped with MRI-compatible headphones customized for monkeys (MR Confon GmbH, Magdeburg, Germany). A radial receive-only surface coil (10-cm diameter) was positioned above the head. Monkeys were required to fixate a LED placed at 83cm away from their face, at eye level, aligned with their sagittal axis. Eye position was monitored at 120 Hz during scanning using a pupil-corneal reflection tracking system (Iscan®, Cambridge, MA), following a calibration procedure during which the fixation LED and 4 additional LEDs were sequentially switched on and off. These additional LEDs were subsequently removed during the main task during which only the central LED was present. Monkeys were rewarded with liquid dispensed by a computer-controlled reward delivery system (Crist®) thanks to a plastic tube coming to their mouth. The reward probability and quantity increased as fixation duration increased according to a subject-specific schedule, thus positively reinforcing fixation behavior. Fixation was considered as successful when the eyes remained in a window of 1° around the fixation LED.

The reward schedule was uncorrelated with the scanning schedule. The task and all the behavioral parameters were controlled by two computers running Matlab® and Presentation®. Monkeys were trained in a mock scan environment approaching to the best the actual MRI scanner setup. Actual scanning was performed once their fixation performance was maximized.

Task and stimuli

The animals were trained to maintain fixation on the red LED while facing a stable visual scene enriched so as to maximize depth cues. Once this behavior was stabilized, they were further trained to maintain fixation while 3D objects were presented at either 15 cm in front of their eyes (*i.e.* in the space between their head and the fixation LED) or 150 cm (*i.e.* in the space beyond the fixation LED), thus allowing to stimulated the space situated respectively near and far from the animals. Stimulations were achieved with either a small cube (3x3x3 cm) or a large cube (30x30x30 cm), attached to a rigid holding stick. These cubes had the same apparent size when the small cube was placed at 15cm from the subject and the larger cube was placed at 150cm, thus allowing to control for size effects. In order to maximize depth cues, the edges of the cubes were highlighted with red stripes and their transparent faces were ornamented with fractal pictures. During the stimulation duration, the cube was continuously agitated so as to prevent neuronal habituation. Three conditions were tested in blocks of 13 pulses: 1) the small cube presented in the near space; 2) the small cube presented in the far space and 3) the big cube presented in the far space. Both during training and testing, the cubes were approached, agitated and withdrawn from the target location (near or far space) by two experimenters out of the field of view, one controlling the small cube and the other the large cube. The stimulation instructions were delivered to them on a computer screen coupled to the experimental control system.

Functional time series (runs) were organized as follows (figure 1b): a 13-volume block of stimulation category 1 was followed by a 13-volume block of stimulation category 2, a 13-volume block of stimulation category 3, and a 13-volume block of pure fixation (baseline). Before the beginning (resp. after the end) of each block of stimulation, 1 pulse was dedicated to the approach (resp. withdrawal) of the appropriate cube towards (resp. away from) the target space. A given sequence was played three times, resulting in a 174-volume run. The blocks for the 3 categories were presented in 6 counterbalanced possible orders.

Scanning

Before each scanning session, a contrast agent, monocrystalline iron oxide nanoparticle (Sinerem, Guerbet or Feraheme, AMAG, Vanduffel et al., 2001), was injected into the animal's femoral/saphenous vein (4-10 mg/kg). For the sake of clarity, the polarity of the contrast agent MR signal changes, which are negative for increased blood volumes, was inverted. We acquired gradient-echo echoplanar (EPI) images covering the whole brain (1.5 T; repetition time (TR) 2.08 s; echo time (TE) 27 ms; 32 sagittal slices; 2x2x2-mm voxels). A total of 34 (22) runs was acquired for M1 (/M2).

Analysis

A total of 20 (15) runs were selected based on the quality of the monkeys' fixation throughout each run (>80% within the tolerance window). Time series were analyzed using SPM8 (Wellcome Department of Cognitive Neurology, London, United Kingdom). For spatial preprocessing, functional volumes were first realigned and rigidly coregistered with the anatomy of each individual monkey (T1-weighted MPRAGE 3D 0.6x0.6x0.6 mm or 0.5x0.5x0.5 mm voxel acquired at 1.5T) in stereotactic space. The JIP program (Mandeville et

al. 2011) was used to perform a non-rigid coregistration (warping) of a mean functional image onto the individual anatomies.

Fixed effect individual analyses were performed for each sensory modality in each monkey, with a level of significance set at $p<0.05$ corrected for multiple comparisons (FWE, $t>4.89$, unless stated otherwise). In all analyses, realignment parameters, as well as eye movement traces, were included as covariates of no interest to remove eye movement and brain motion artifacts. When coordinates are provided, they are expressed with respect to the anterior commissure. Results are displayed on flattened maps obtained with Caret (Van Essen et al. 2001; http://www.nitrc.org/projects/caret/).

Results

Monkeys were exposed, in the same time series, to naturalistic near or far space stimulations (see Figure 1 and method section for more details), while maintaining their gaze at an intermediate fixation location. This design allows us to describe the cortical networks involved in near and far space processing. All reported activations are identified using a group analysis, with a level of significance set at $p<0.05$ corrected for multiple comparisons (FWE, $t>4.89$). As a result, they reflect the activations that are common to both monkeys.

Naturalistic near and far space stimulations

Naturalistic near space stimulations with a small cube (figure 2, upper panel, small near vs. fixation contrast) activated occipital striate and extrastriate areas, the temporal cortex (superior temporal sulcus), the parietal cortex, the prefrontal cortex (arcuate sulcus and posterior and anterior parts of principal sulcus) as well as the orbitofrontal cortex. Far space stimulations with a far cube with the same apparent size as the near small cube (figure 2, middle panel, big far vs. fixation contrast) also activated a widespread cortical network including the striate and extrastriate cortex, the temporal cortex, the parietal cortex, the cingulate cortex, primary somatosensory cortex along the central sulcus, the prefrontal cortex along the arcuate sulcus and the principal sulcus as well as the orbitofrontal cortex. When far space was stimulated using a cube of the same real size as the small cube used for the near space stimulation (figure 2, lower panel, small far vs. fixation contrast), a similar though smaller cortical network was activated. In the following, we identify those cortical regions that are specifically involved in near space and far space processing respectively.

Near space cortical network

In a first step, we contrast the cortical activations obtained by the stimulation of near space by a small object to those obtained by the stimulation of far space by a large object of the same apparent size as the small object in the near space (Figure 3, upper panel, dark red shades). This contrast identifies bilateral cortical regions the contribution of which is higher for near space than for far space. These include occipital regions: in visual areas V1 and V2; parietal areas : the posterior intraparietal sulcus (IPS: ventral intraparietal area VIP, the posterior medial intraparietal area MIP, the anterior most part of the posterior intraparietal area PIP) as well as its anterior most tip (possibly anterior intraparietal area AIP), the medial parietal cortex and the parietal opercular region area 7op; temporal areas: medial superior temporal area MST, the temporoparietal associated area TPO in the medial mid-to-anterior bank of the superior temporal sulcus, the intraparietal sulcus associated area IPa, the tip of temporal area TAa, the dorsal portion of the subdivision TE1-3 and temporal area TF; insular regions: the granular and disgranular parts of the insular cortex and the parainsular cortex PI; somatosensory area SII within the medial bank of the lateral sulcus; the anterior cingulate sulcus (a sub-region of area 24d, possibly coinciding with the cingulate eye field CEFr, as well as a second regions at the extreme anterior tip of the cingulate sulcus); premotor cortex: dorsal premotor cortex, the frontal eye fields (area 8a as well as 8ac) and premotor area 4C including premotor zone PMZ; prefrontal area 46p; posterior orbitofrontal area 12.

When this contrast is additionally masked by the activations obtained by far space stimulations (exclusive 'far space stimulation vs. fixation' mask, uncorrected level, p=0.05), a network that is exclusively involved in near space processing can be identified (Figure 3, upper panel, hot colors with white outlines, *t* scores = 4.8 and above, FEW-corrected level). This analysis describes discrete bilateral regions within the majority of the cortical areas highlighted by the previous contrast.

Far space cortical network

Here, we perform the opposite contrasts as those defined above. We first contrast the cortical activations obtained by the stimulation of far space by a large object to those obtained by the stimulation of near space by a small object of the same apparent size as the large object in the far space (Figure 3, lower panel, dark blue shades). This contrast identifies bilateral cortical regions the contribution of which is higher for far space than for near space. These include larges sectors of the visual striate and extrastriate cortex: areas V1, V2, V3, V3A and V4; parietal cortical regions: the medial parietal convexity (area 5v), the lateral parietal convexity (area 7a, 7ab and 7b), the medial parietal cortex; temporal cortex: medial temporal area MT, inferior temporal areas Tea and Tem, temporal area TAa and the temporoparietal cortex Tpt; insular cortex: retroinsular cortex RI and a sub-region of the granular and disgranular parts of the insular cortex; the somatosensory areas 2 and 3; primary motor cortex; cingulate cortex: the posterior two thirds of the superior bank of the cingulate sulcus (possibly in areas 23c, 24/23c and 32); prefrontal area 46v; ventral premotor area 6Vam; rostral orbitofrontal area 14. Also some of the areas described above also appear to encode near space in preference to far space, they do so in distinct cortical regions, the contrasts presented in the upper and lower panels of figure 3 describing mutually exclusive cortical regions.

When this contrast is additionally masked by the activations obtained by near space stimulations (exclusive 'near space stimulation vs. fixation' mask, uncorrected level, p=0.05), a network that is specifically involved in far space processing can be identified (Figure 3, lower panel, blue colors with white outlines, *t* scores = 4.8 and above, FEW-corrected level). This analysis describes discrete bilateral regions within the majority of the cortical areas highlighted by the previous contrast.

Far space cortical network modulation by object size

While the small cube presented in near space had the same apparent size as the far cube presented in far space, these two objects had very different physical sizes ($3x3x3cm^3$ versus $30x30x30cm^3$). As a result, part of the far or near space network specificities described above could have been due to this size difference. In order to address this issue, we now compare the cortical activations obtained when stimulating far space with either a small cube or a large cube. No activations are observed with the *small object in far space* versus *large object in far space* contrast, suggesting that all the cortical regions that are involved in processing the small object in far space also contribute to the processing of the large object in far space. The inverse contrast reveals a large cortical network mostly identical to that revealed by the *large cube in far space* versus *fixation* contrast (Figure 4, dark blue shades).

When this contrast is additionally masked by the activations obtained by far space stimulations with the small cube (exclusive 'small cube in far space stimulation vs. fixation' mask, uncorrected level, p=0.05), a network that is specifically involved in the processing of the large cube in far space processing can be identified (Figure 4, blue colors with white outlines, *t* scores = 4.8 and above, FEW-corrected level). By construction, this network is distinct from the near space specific network highlighted in figure 3 (upper panel). It includes large sectors of the visual striate and extrastriate cortex, mostly coinciding with the peripheral visual field representation, the parieto-occipital cortex, the posterior parietal cortex, the medial parietal cortex, the anterior part of the superior temporal sulcus as well as a large extent of the orbitofrontal cortex and the frontal pole.

Discussion

In the present study, we identify the non-human primate networks associated with either the stimulation of near or far space with naturalistic dynamic objects, in the absence of any overt task. In the following, we discuss the functional dissociation between near and far space networks in the light of the related literature.

Near space specific cortical network

The near space specific cortical network we describe in the non-human primate is surprisingly large. It involves multisensory visuo-tactile cortical regions whose neurons have already been described to encode nearby objects relative to the body, namely, the ventral premotor cortex (F4: Rizzolatti et al. 1981and polysensory zone PZ: Graziano et al. 1994, 1997, 1999; Fogassi et al. 1996, in agreement with the description of a near space neglect following the ablation of the postarcuate cortex, as these lesions most probably included the polysensory zone PZ -Rizzolatti et al. 1983) and ventral intraparietal area VIP, within the fundus of the intraparietal sulcus (Duhamel et al. 1997, 1998; Avillac et al. 2005; Schlack et al. 2005; Bremmer et al. 2013; Guipponi et al. 2013). It additionally involves several other cortical areas whose contribution to near space processing has been overlooked up to now. These include dorsal premotor regions, just medial to the polysensory zone PZ. This observation is in agreement with the description, in human patients with a damage in the dorsolateral prefrontal cortex, of a near space specific neglect syndrome (Aimola et al. 2012). We also describe the involvement of posterior and medial parietal areas, which together with the observed activations in the fundus of the intraparietal cortex are in perfect agreement with the description of a near space neglect in patients with posterior parietal lesions including the fundus, medial and posterior parts of the intraparietal sulcus (Halligan and Marshall 1991).

Near space activations are also observed in the multisensory temporo-parietal area Tptwhich has direct projections to area VIP (Lewis and Van Essen 2000a, 2000b); anterior temporal regions within the fundus of the STS and on the inferior temporal convexity, suggesting a specific processing of the feature and identity of near objects within the ventral visual processing pathway.

Interestingly, near space specific activations can also be observed in area SII. This activation possibly reveals a general "attention-to-touch" process due to the anticipation of tactile stimulation to the body because of vicinity of the moving stimulus to the face. Alternatively, it could actuate the strong functional link between near space processing and the somatosensory representation of self. While previous studies have mostly assumed that this link is subserved by multisensory visuo-tactile brain areas (Makin et al. 2008; Blanke 2012), the present observations suggest that low level sensory areas might also be involved in the representation of space at the frontier of self. This observation might be due to the fact that, in contrast with previous studies, the stimulus is presented extremely close (15cm) to the face of the monkeys. At this distance, the $9cm^3$ moving cube can be viewed as a potentially dangerous object, all the more given that the monkeys cannot protect themselves from its presence (no escape, no goal-directed arm movements). This defensive attitude towards the near space stimulus could possibly also account for the observed bilateral orbitofrontal activation (area 12, Murray and Izquierdo 2007).

Overall, the non-human near space specific cortical network we describe here has major specificities as compared to the analog human cortical network. Indeed, we essentially describe bilateral cortical regions, while in humans, only the left dorsal occipital cortex, the left intraparietal and the left ventral premotor appear to be involved in near space processing (Weiss et al. 2000; Aimola et al. 2012). Additionally, this near space non-human primate cortical network involves many more areas than the human network. This could be due to the

fact that we stimulated near space at 15cm away from the subject's eyes while Weiss et al. (Weiss et al. 2000) for example, stimulated them at 70cm. Alternatively, this could be due to a genuine interspecies difference.

Far space specific cortical network

The far space specific cortical network we describe in the non-human primate is also very extended, involving large portions of the occipital cortex, as well as posterior temporal and superior temporal regions. This is similar to what is seen in humans as Weiss et al. (Weiss et al. 2000) describe a network involving the ventral visual stream including the ventral occipital cortex bilaterally and the right medial temporal cortex. These observations are in agreement with the description of a far space neglect following a temporal hematoma (Vuilleumier et al. 1998). However, we additionally describe the contribution of anterior superior parietal regions including areas 2, 3 and 5 and a small dorsal premotor region. This could correspond to the automatic activation of a reach-related network due to the presence of a neutral object in the far space. We are thus describing a functional near-to-far postero-anterior gradient both within the parietal cortex and within the dorsal premotor cortex. To our knowledge this is the first time that such a gradient is described and we propose that it might correspond to a differential reach-planning network within near and far space. The posterior cingulate cortex as well as anterior medial orbito-frontal regions also appear to specifically contribute to far space encoding. The functional significance of these activations needs to be further explored.

Rizzolatti et al. (Rizzolatti et al. 1983) describe a more pronounced hemineglect in the far space than in near space following prearcuate area 8 ablations. This contrasts with the fact that we identify no preferential coding of far space in this region, but rather a preferential

though not specific coding for near space. This discrepancy could reflect a task dependence of far and near space processing as described in humans (Keller et al. 2005; Aimola et al. 2012).

Relative encoding of near and far space

The description of a cortical network specific for near space processing and another complementary network specific for far space processing should not have as overlook the fact that large cortical regions contribute to the processing of both far and near objects, though favoring one over the other. This is for example the case of the lateral bank of the intraparietal sulcus and the adjacent convexity, including areas 7a, 7ab and 7b. Bimodal visuo-tactile neurons have been described in area 7b with very large receptive fields over the arm, leg, chest or even the skin of the whole body (Leinonen et al. 1979). Lesions of this region induce a neglect in peripersonal space (Matelli et al. 1984), leading to the idea that area 7b is involved in the perception of near space and in the organization of movements towards stimuli presented in peripersonal space. The fact that we describe a privileged coding of far space in this cortical regions calls for reassessment of its functional role in relation with space processing.

Overall, the description of large cortical regions having either a preference for near space processing or far space processing call for reappraising far space or near space specificity. Indeed, the alternative view that we would like to put forward in the light of our observations is that of a continuous encoding of relative distance to the body, in the form of a far-to-near or near-to-far gradient. In this context, far or near space specific regions represent the extreme points of this continuum. The idea of such a continuum is supported by the fact that no abrupt change in visuo-spatial neglect can be seen between near and far space (Cowey et al. 1999). Indirect evidence for such a continuum can also be found in a recent non-human fMRI study by Joly et al. (Joly et al. 2009), which describes disparity-related signals in far

space (monkeys are fixating at 57cm) in area F5a, at a location close to the bilateral inferior periarcuate far space activation in our figure 3. It is important to note that the existence of such a cortical far-to-near and a near-to-far gradient in space representation does not preclude the existence of a physically delineable peripersonal space, as described in numerous psychology and psychophysics study (Berti and Frassinetti 2000; Macaluso and Maravita 2010; Farnè et al. 2005; Ladavas and Serino 2008).

Overall we describe a clear dissociation for near and far space processing. These results open the way to the study of the how these two networks dynamically interact during action planning, tool use or as a function of the emotional or social contexts.

Bibliography

Aimola L, Schindler I, Venneri A. 2012. Task- and response related dissociations between neglect in near and far space: A morphometric case study. Behav Neurol.

Avillac M, Ben Hamed S, Duhamel J-R. 2007. Multisensory integration in the ventral intraparietal area of the macaque monkey. J Neurosci. 27:1922–1932.

Avillac M, Denève S, Olivier E, Pouget A, Duhamel J-R. 2005. Reference frames for representing visual and tactile locations in parietal cortex. Nat Neurosci. 8:941–949.

Berti A, Frassinetti F. 2000. When far becomes near: remapping of space by tool use. J Cogn Neurosci. 12:415–420.

Bjoertomt O, Cowey A, Walsh V. 2002. Spatial neglect in near and far space investigated by repetitive transcranial magnetic stimulation. Brain J Neurol. 125:2012–2022.

Bjoertomt O, Cowey A, Walsh V. 2009. Near space functioning of the human angular and supramarginal gyri. J Neuropsychol. 3:31–43.

Blanke O. 2012. Multisensory brain mechanisms of bodily self-consciousness. Nat Rev Neurosci. 13:556–571.

Bremmer F, Schlack A, Kaminiarz A, Hoffmann K-P. 2013. Encoding of movement in near extrapersonal space in primate area VIP. Front Behav Neurosci. 7:8.

Cowey A, Small M, Ellis S. 1994. Left visuo-spatial neglect can be worse in far than in near space. Neuropsychologia. 32:1059–1066.

Cowey A, Small M, Ellis S. 1999. No abrupt change in visual hemineglect from near to far space. Neuropsychologia. 37:1–6.

Duhamel JR, Bremmer F, Ben Hamed S, Graf W. 1997. Spatial invariance of visual receptive fields in parietal cortex neurons. Nature. 389:845–848.

Duhamel JR, Colby CL, Goldberg ME. 1998. Ventral intraparietal area of the macaque: congruent visual and somatic response properties. J Neurophysiol. 79:126–136.

Durand J-B, Nelissen K, Joly O, Wardak C, Todd JT, Norman JF, Janssen P, Vanduffel W, Orban GA. 2007. Anterior regions of monkey parietal cortex process visual 3D shape. Neuron. 55:493–505.

Farnè A, Demattè ML, Làdavas E. (2005) Neuropsychological evidence of modular organization of the near peripersonal space. Neurology. 65:1754–1758.

Fogassi L, Gallese V, Fadiga L, Luppino G, Matelli M, Rizzolatti G. 1996. Coding of peripersonal space in inferior premotor cortex (area F4). J Neurophysiol. 76:141–157.

Gentilucci M, Fogassi L, Luppino G, Matelli M, Camarda R, Rizzolatti G. 1988. Functional organization of inferior area 6 in the macaque monkey. I. Somatotopy and the control of proximal movements. Exp Brain Res. 71:475–490.

Graziano MS, Hu XT, Gross CG. 1997. Visuospatial properties of ventral premotor cortex. J Neurophysiol. 77:2268–2292.

Graziano MS, Yap GS, Gross CG. 1994. Coding of visual space by premotor neurons. Science. 266:1054–1057.

Graziano MSA, Reiss LAJ, Gross CG. 1999. A neuronal representation of the location of nearby sounds. Nature. 397:428–430.

Guipponi O, Wardak C, Ibarrola D, Comte J-C, Sappey-Marinier D, Pinède S, Ben Hamed S. 2013. Multimodal convergence within the intraparietal sulcus of the macaque monkey. J Neurosci. 33:4128–4139.

Halligan PW, Marshall JC. 1991. Left neglect for near but not far space in man. Nature. 350:498–500.

Joly O, Vanduffel W, Orban GA. 2009. The monkey ventral premotor cortex processes 3D shape from disparity. Neuroimage. 47:262–272.

Keller I, Schindler I, Kerkhoff G, von Rosen F, Golz D. 2005. Visuospatial neglect in near and far space: dissociation between line bisection and letter cancellation. Neuropsychologia. 43:724–731.

Ladavas E, Serino A. (2008) Action-dependent plasticity in peripersonal space representations. Cogn Neuropsychol. 25:1099–1113.

Leinonen L, Hyvärinen J, Nyman G, Linnankoski I. 1979. I. Functional properties of neurons in lateral part of associative area 7 in awake monkeys. Exp Brain Res. 34:299–320.

Lewis JW, Van Essen DC. 2000a. Mapping of architectonic subdivisions in the macaque monkey, with emphasis on parieto-occipital cortex. J Comp Neurol. 428:79–111.

Lewis JW, Van Essen DC. 2000b. Corticocortical connections of visual, sensorimotor, and multimodal processing areas in the parietal lobe of the macaque monkey. J Comp Neurol. 428:112–137.

Macaluso E, Maravita A. 2010. The representation of space near the body through touch and vision. Neuropsychologia. 48:782–795.

Makin TR, Holmes NP, Ehrsson HH. 2008. On the other hand: dummy hands and peripersonal space. Behav Brain Res. 191:1–10.

Mandeville JB, Choi J-K, Jarraya B, Rosen BR, Jenkins BG, Vanduffel W. 2011. FMRI of cocaine self-administration in macaques reveals functional inhibition of basal ganglia. Neuropsychopharmacol. 36:1187–1198.

Matelli M, Gallese V, Rizzolatti G. 1984. [Neurological deficit following a lesion in the parietal area 7b in the monkey]. Boll Della Soc Ital Biol Sper. 60:839–844.

Murray EA, Izquierdo A. 2007. Orbitofrontal cortex and amygdala contributions to affect and action in primates. Ann N Y Acad Sci. 1121:273–296.

Quinlan DJ, Culham JC. 2007. fMRI reveals a preference for near viewing in the human parieto-occipital cortex. Neuroimage. 36:167–187.

Rizzolatti G, Matelli M, Pavesi G. 1983. Deficits in attention and movement following the removal of postarcuate (area 6) and prearcuate (area 8) cortex in macaque monkeys. Brain J Neurol. 106 (Pt 3):655–673.

Rizzolatti G, Scandolara C, Matelli M, Gentilucci M. 1981. Afferent properties of periarcuate neurons in macaque monkeys. II. Visual responses. Behav Brain Res. 2:147–163.

Schlack A, Sterbing-D'Angelo SJ, Hartung K, Hoffmann K-P, Bremmer F. 2005. Multisensory space representations in the macaque ventral intraparietal area. J Neurosci. 25:4616–4625.

Van Essen DC, Drury HA, Dickson J, Harwell J, Hanlon D, Anderson CH. 2001. An integrated software suite for surface-based analyses of cerebral cortex. J Am Med Informatics Assoc JAMIA. 8:443–459.

Vuilleumier P, Valenza N, Mayer E, Reverdin A, Landis T. 1998. Near and far visual space in unilateral neglect. Ann Neurol. 43:406–410.

Weiss PH, Marshall JC, Wunderlich G, Tellmann L, Halligan PW, Freund HJ, Zilles K, Fink GR. 2000. Neural consequences of acting in near versus far space: a physiological basis for clinical dissociations. Brain J Neurol. 123 Pt 12:2531–2541.

Weiss PH, Marshall JC, Zilles K, Fink GR. 2003. Are action and perception in near and far space additive or interactive factors? Neuroimage. 18:837–846.

Figures

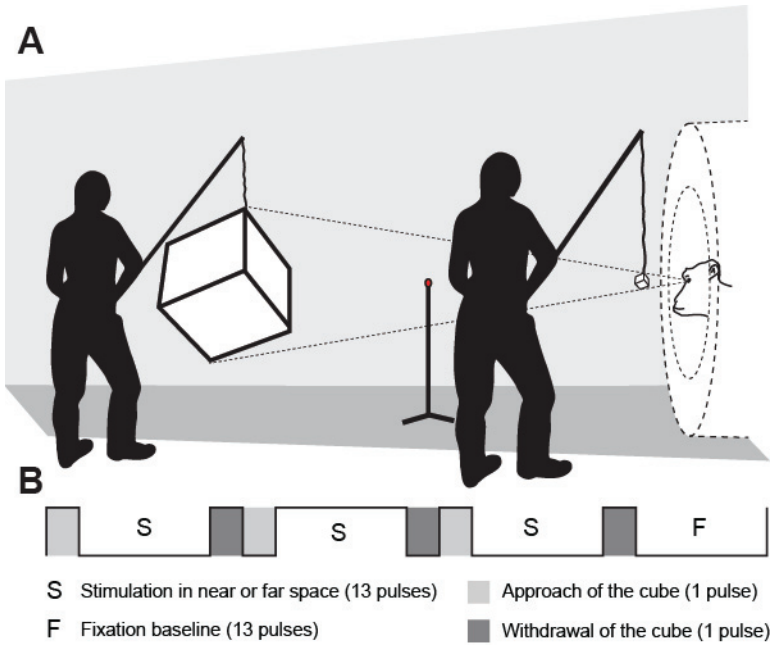

Figure 1: Experimental fMRI protocol. A) 3D naturalistic stimulations in near or far space (same apparent sizes). Fixation is achieved at an intermediate position (red fixation LED). B) Block design.

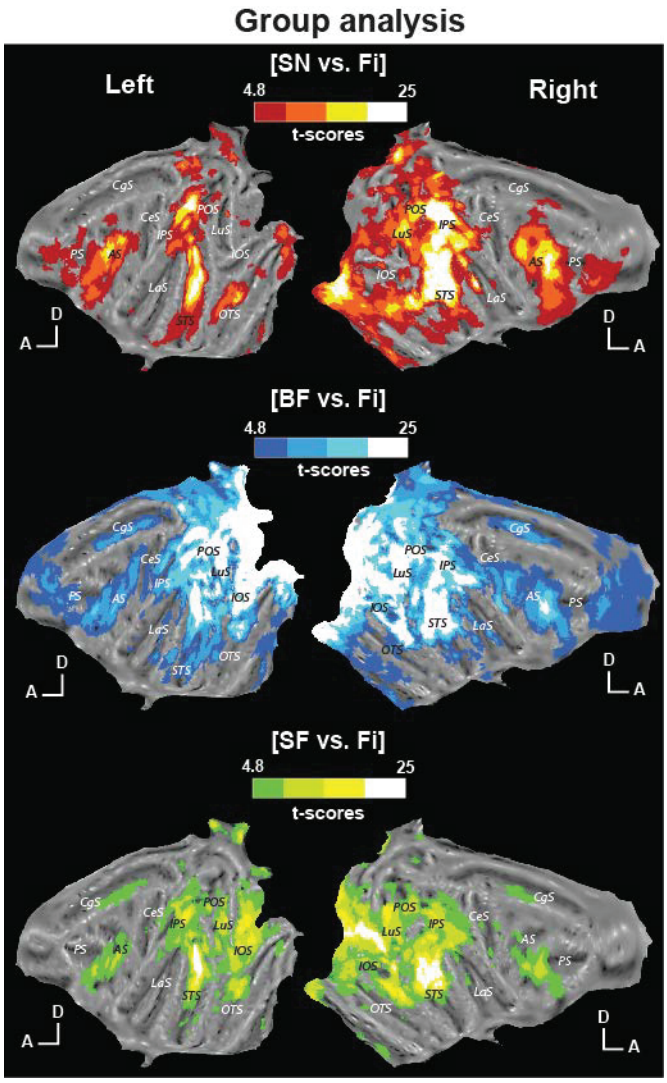

Figure 2: Near space and far space modality group analyses. Activations presented on the flattened representation of the reference monkey cortex obtained with Caret. The upper part of the figure shows the near space stimulated with the small cube (SN) versus fixation contrast (t scores = 4.8 at $p<0.05$, FWE-corrected level in the red scale). Middle and lower pannels present the far space respectively stimulated with the big (BF) and the small cubes (SF; t scores = 4.8 at $p<0.05$, FWE-corrected level respectively in the blue and green scales). A, Anterior; D, Dorsal; SN: small near; BF: big far; SF: small far. Cortical sulci: AS, arcuate sulcus; CgS, cingulate sulcus; CeS, central sulcus; IOS, inferior occipital sulcus; IPS, intraparietal sulcus; LaS, lateral (Sylvian) sulcus; LuS, lunate sulcus; OTS, occipital temporal sulcus; POS, parieto-occipital sulcus; PS, principal sulcus; STS, superior temporal sulcus.

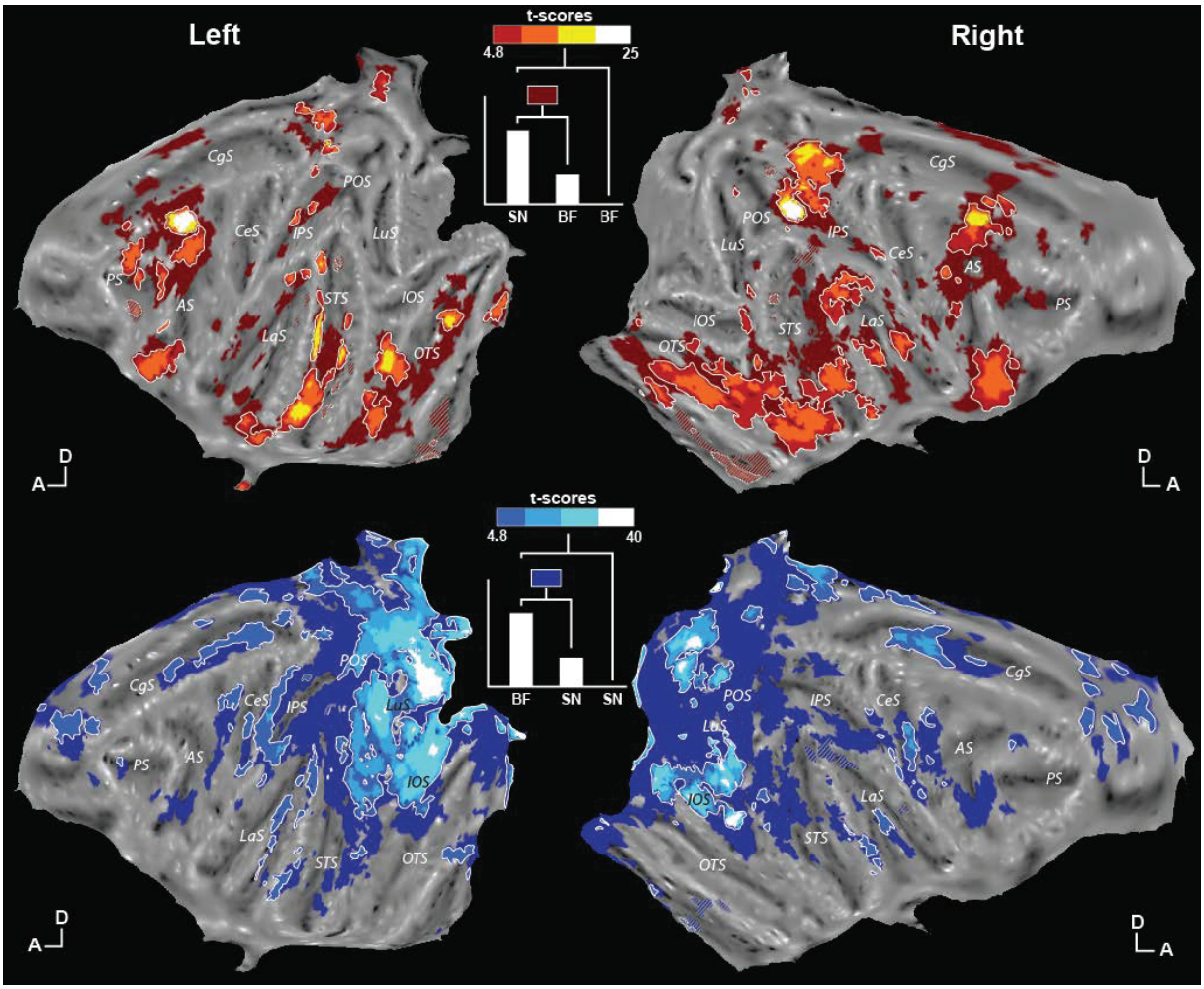

Figure 3: Specific near and far space networks. Activations presented on flattened maps of the reference monkey cortex. The upper panel presents the near space (stimulated with the small cube) versus the far space (stimulated with the big cube; t scores = 4.8 at $p<0.05$, FWE-corrected level in the red dark color). Lighter red color scale shows the specific near space network (exclusive mask for far space versus fixation baseline applied at uncorrected level $p<0.05$). The lower panel presents the far space (stimulated with the big cube) versus the near space (stimulated with the small cube; t scores = 4.8 at $p<0.05$, FWE-corrected level in the blue dark color). Lighter blue color scale shows the specific far space network (exclusive mask for near space versus fixation baseline applied at uncorrected level $p<0.05$). For other conventions, see Figure 2.

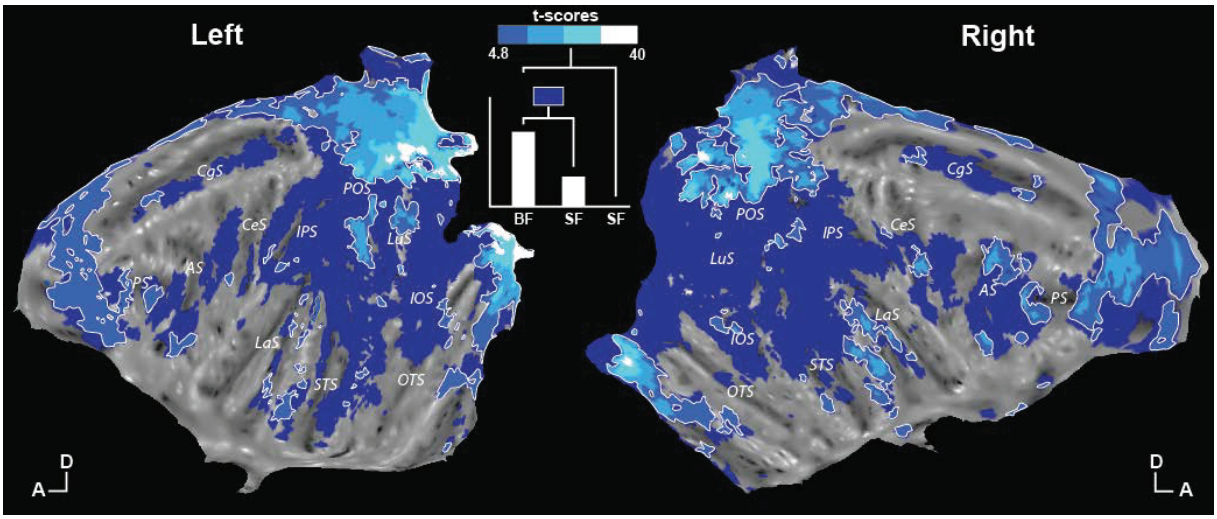

Figure 4: Object size specificity in far space. Activations presented on flattened maps of the reference monkey cortex. The maps present the far space (stimulated with the big cube) versus the far space (stimulated with the small cube; t scores = 4.8 at $p<0.05$, FWE-corrected level in the blue dark color). Lighter blue color scale shows the specific far space network dedicated to the big cube (exclusive mask for far space stimulated with the small cube versus fixation baseline applied at uncorrected level $p<0.05$). For other conventions, see Figure 2.

Chapter 6

Spontaneous Blink-Related Neural Correlates Reveal an Ensemble of Cortical Somatosensory Eye Fields

Submitted in Cerebral Cortex, June 11, 2013, CerCor-2013-00561
In revision

Spontaneous blink-related neural correlates reveal an ensemble of cortical somatosensory eye fields

Abbreviated title: Spontaneous blinks in the monkey

Authors: Olivier Guipponi[1], Soline Odouard[1], Serge Pinède[1], Claire Wardak[1], Suliann Ben Hamed[1]

1. Centre de Neuroscience Cognitive, CNRS UMR 5229, 67 Bd Pinel, 69675 Bron cedex, Université Claude Bernard Lyon I

Corresponding author: Suliann Ben Hamed, Centre de Neuroscience Cognitive, CNRS UMR 5229, Université Claude Bernard Lyon I, 67 Bd Pinel, 69675 Bron cedex, France, benhamed@isc.cnrs.fr

Abstract

Eyeblinks are defined as a rapid closing and opening of the eyelid. Three types of blinks are defined: spontaneous, reflexive and voluntary. These involve different neuronal substrates. In particular the parieto-frontal regions involved in oculomotor behavior are reliably activated during voluntary eye blinks and not during spontaneous eye blinks. Apart from this core consensus, the reported blink-related regions vary from one study to another, most probably due to experimental and analysis specificities. Here, we focus on spontaneous blink production. We describe its cortical correlates, using functional magnetic resonance imaging (fMRI) in the non-human primate. Our observations reveal an ensemble of cortical eye fields involved in the representation of the somatosensory, proprioceptive and visual correlates of blinks as well as of their homeostatic triggers. Specifically, we describe a core somatosensory network involving the area 2, area 3a/3b and area SII/PV eye fields, a larger network involving parietal (median intraparietal area MIP), cingulate (caudal cingulate eye field, CEFc), insular (parainsula) and prefrontal (ventral premotor area 6Vb) areas, as well as striate and extrastriate regions (V1, V3, V3A, and MST). These observations provide a unified description of the cortical spontaneous blink correlates, as compared to the human imaging studies available on the subject.

Key words: blink, fMRI, macaque, eye fields, spontaneous.

Introduction

Eyeblinks are defined as a rapid closing and opening of the eyelid. Three types of blinks are classically defined. *Spontaneous blinks* play an important role in the protection of the eye conjunctiva and the underlying cornea from dehydration, by regenerating the tear film over successive eyelid closures (Korb et al. 1994). *Reflexive blinks* are a defensive behavior to a situation of threat involving the head (Miwa et al. 1996; Valls-Solé et al. 1997; León et al. 2011). These blinks achieve the protection of the eyes by the eyelids and are often associated with other protective behaviors such as head and trunk withdrawal movements. *Voluntaryblinks*are under the control of volition (Bristow, Frith, et al. 2005; Hanakawa et al. 2008). Such blinks can be used during non-verbal communication. They can also be generated to protect the eyes voluntarily (*e.g.* protect the eyes from the sun, increase the tear film in order to get rid of a foreign body such as an insect or sand dust).

These different types of blinks appear to involve different neuronal substrates. For example, at the peripheral level, voluntary blinks activate a specific class of eyelid motor units that are not activated by any of the other types of eyeblinks (Gordon 1951). Likewise, bilateral voluntary blinks involve a specific rotation of the eye globe, known as the Bell's phenomenon (Collewijn et al. 1985). Differences can also be observed at the central level. Indeed, patients suffering from apraxia retain the ability to produce spontaneous blinks while they are profoundly impaired in the generation of voluntary eyeblinks (Colombo et al. 1982; van Koningsbruggen et al. 2012).

A majority of the studies on the neurophysiological substrates of blinks has focused on voluntary eyeblinks (Bodis-Wollner et al. 1999; Kato and Miyauchi 2003a, 2003b; Bristow, Frith, et al. 2005; Hanakawa et al. 2008; van Koningsbruggen et al. 2012). The few reports that have sought a direct comparison of the physiological tenants of the different types of

eyeblinks highlight interesting differences. In particular the parieto-frontal regions involved in oculomotor behavior, namely the frontal eye fields FEF and the lateral intraparietal area LIP, are reliably activated during voluntary eye blinks and not during spontaneous eye blinks (Gordon 1951; Colombo et al. 1982; Collewijn et al. 1985; van Koningsbruggen et al. 2012). Apart from this consensus, the reported blink-related regions vary from one study to another, most probably due to experimental and analysis specificities.

Here, we describe, using functional magnetic resonance imaging (fMRI) in the non-human primate, the cortical regions that are activated by spontaneous blink production. Our observations, discussed in the light of the numerous anatomical and connectivity studies available for this species, reveal an ensemble of cortical eye fields involved in the representation of the somatosensory, proprioceptive and visual correlates of blinks as well as of their homeostatic triggers. Specifically, we describe a core somatosensory network involving the area 2, area 3a/3b and area SII/PV eye fields, a larger network involving parietal (median intraparietal area MIP), cingulate (caudal cingulate eye field, CEFc), insular (parainsula) and prefrontal (ventral premotor area 6Vb) areas, as well as striate and extrastriate regions (V1, V3, V3A and MST). Importantly, we describe, in a unique study, the several spontaneous blink-related regions reported disparately in several human imaging studies, thus providing a unified description of the cortical spontaneous blink correlates.

Material and Methods

Subjects and materials

Two rhesus monkeys (female M1, male M2, 5-7 years old, 5-7 kg) participated in the study. The animals were implanted with a plastic MRI compatible headset covered by dental acrylic. The anesthesia during surgery was induced by Zoletil (Tiletamine-Zolazepam, Virbac, 5 mg/kg) and followed by Isoflurane (Belamont, 1-2%). Post-surgery analgesia was ensured thanks to Temgesic (buprenorphine, 0.3 mg/ml, 0.01 mg/kg). During recovery, proper analgesic and antibiotic coverage were provided. The surgical procedures conformed to European, and National Institutes of Health guidelines for the care and use of laboratory animals.

During the scanning sessions, monkeys sat in a sphinx position in a plastic monkey chair positioned within a horizontal magnet (1.5-T MR scanner Sonata; Siemens, Erlangen, Germany) facing a translucent screen placed 90 cm from the eyes. Their head was restrained and equipped with MRI-compatible headphones customized for monkeys (MR Confon GmbH, Magdeburg, Germany). A radial receive-only surface coil (10-cm diameter) was positioned above the head. Eye position was monitored at 120 Hz during scanning using a pupil-corneal reflection tracking system (Iscan®, Cambridge, MA). Monkeys were rewarded with liquid dispensed by a computer-controlled reward delivery system (Crist®) thanks to a plastic tube close to their mouth. The task, all the behavioral parameters as well as the sensory stimulations were controlled by two computers running with Matlab® and Presentation®. The fixation point the monkeys were instructed to fixate was projected onto a screen with a Canon XEED SX60 projector. Auditory stimulations were dispensed with a MR Confon GmbH system (Magdeburg, Germany). Tactile stimulations were delivered through Teflon tubing

and 6 articulated plastic arms connected to distant air pressure electro-valves. Monkeys were trained in a mock scan environment approaching to the best the actual MRI scanner setup.

Task and stimuli

The animals were trained to maintain fixation on a red central spot (0.24°x0.24°) while stimulations (auditory, or tactile) were delivered. The monkeys were rewarded for staying within a 2°x2° tolerance window centered on the fixation spot. The reward delivery was scheduled to encourage long fixation without breaks (*i.e.* the interval between successive deliveries was decreased and their amount was increased, up to a fixed limit, as long as the eyes did not leave the window). The two sensory modalities were tested in independent interleaved runs (see below for the organization of the runs).

Auditory stimulations. In both monkeys, we used ***coherent movement***, scrambled and static auditory stimuli. ***Scrambled stimulations*** were obtained by cutting the movement sounds in 100ms or 300ms segments and randomly mixing them. ***Static stimulations*** consisted of auditory stimuli evoking a stable stimulus in space (details are provided in Guipponi et al. 2013).

Tactile stimulations. They consisted in air puffs delivered to three different locations on the left and the right of the animals' body: 1) ***center*** of the face, close to the nose and the mouth; 2) ***periphery*** of the face, above the eyebrows; 3) ***shoulders*** (*cf.* Guipponi et al. 2013).

Functional time series (runs) were organized as follows: a 10-volume block of pure fixation (baseline) was followed by a 10-volume block of category 1 stimulus type, a 10-volume block of category 2 stimulus type, and a 10-volume block of category 3 stimulus type; this sequence was played four times, resulting in a 160-volume run. The blocks for the 3 categories were presented in 6 counterbalanced possible orders. A retinotopy localizer was run independently in the two monkeys using exactly the stimulations of Fize and colleagues

(Fize et al. 2003). This localizer is used to localize the central and peripheral representations of visual areas within each hemisphere, in both animals.

Scanning

Before each scanning session, a contrast agent, monocrystalline iron oxide nanoparticle (Sinerem, Guerbet or Feraheme, AMAG, (Vanduffel et al. 2001)), was injected into the animal's femoral/saphenous vein (4-10 mg/kg). For the sake of clarity, the polarity of the contrast agent MR signal changes, which are negative for increased blood volumes, was inverted. We acquired gradient-echo echoplanar (EPI) images covering the whole brain (1.5 T; repetition time (TR) 2.08 s; echo time (TE) 27 ms; 32 sagittal slices; 2x2x2-mm voxels). During each scanning session, the runs of different modalities and different orders were pseudorandomly intermixed. A total of 37 (42) runs was acquired for auditory stimulations in M1 (/M2) and36 (40) runs for tactile stimulations.

Analysis

A total of 25 (31) runs were selected for the auditory stimulation condition in M1 (M2), 18 (20) for the tactile stimulation condition and 20 (24) for the retinotopy localizer based on the quality of the monkeys' fixation throughout each run (>85% within the tolerance window). Time series were analyzed using SPM8 (Wellcome Department of Cognitive Neurology, London, United Kingdom). For spatial preprocessing, functional volumes were first realigned and rigidly coregistered with the anatomy of each individual monkey (T1-weighted MPRAGE 3D 0.6x0.6x0.6 mm or 0.5x0.5x0.5 mm voxel acquired at 1.5T) in stereotactic space. The JIP program (Mandeville et al. 2011) was used to perform a non-rigid coregistration (warping) of a mean functional image onto the individual anatomies. For each run and each animal, we extracted the timings of the blink events as follows. Blinks

correspond to a stereotyped closure of the eye lids. During this interval, the tracking of the pupil by the video eye-tracker is disrupted, resulting in a saturation of the eye signal (Figure 1A and 1C). The duration of the eye blinks varies from one subject to another (VanderWerf et al. 2003). Here, we defined eyeblink events as the onset of an eye signal saturation of less than 100ms for Monkey 1 and less than 200ms for Monkey 2. This allowed us to exclude other saturation events (*e.g.* saccades larger than 25° of eccentricity, eyes closed resting monkey etc). These blink events were then convolved with the appropriate hemodynamic response function (*i.e.* evoked by dextran-coated iron oxide agents, MION; Figure 1B) and the output of this operation was used as a regressor. Results are displayed on individual flattened maps obtained with Caret (Van Essen et al. 2001; http://www.nitrc.org/projects/caret/). The results are shown both at $p<0.05$ corrected for multiple comparisons (FEW, $t>4.89$) and $p<0.001$ uncorrected level. We also extracted the Inter-Blink Intervals (IBI) for each monkey and each run.

When coordinates are provided, they are expressed with respect to the anterior commissure.

Kruskal-Wallis test. A one-way Kruskal-Wallis test was performed in order to investigate whether the different conditions within a given run evoked statistically significant, different number of blinks. This analysis was also used to test whether 1) the auditory and the tactile conditions result in a different number of blinks and 2) the blink events were statistically different across animals. Whenever the Kruskal-Wallis null hypothesis was rejected, a Mann-Whitney post-hoc test was further used to specify the conditions in which blink generation was most affected.

Results

The results specifically identify spontaneous (as opposed to reflexive or voluntary) blink-related cortical activations. In a first section, we analyze the monkeys' blinking behavior. We then report the cortical sites which are reliably activated by eye blinks, both during auditory and tactile stimulation runs.

Behavioral analysis

For each monkey and each run, we extracted the timestamps at which eye blinks were produced. These blink events can easily be identified from the eye traces as short duration signal saturation periods due to the occlusion of the pupil as can be seen in figure 1A and the corresponding close-up in figure 1C. Signal saturation periods appear as sharp transient drops in the eye trace. The duration of the eye blinks varies from one subject to another (VanderWerf et al. 2003). The eye blinks of monkey M1 lasted less than 100ms while monkey M2 had longer blinks (upper duration threshold of 200ms). These blink events are clearly distinct from saccades which result in smaller amplitude changes in the eye traces compared to the blinks. They are also clearly distinct from eye closed resting or sleeping periods which last significantly longer. In the following, we consider only the runs during which the monkey achieved fixation for more than 85% of the entire duration of the run. This allows to minimize the potential noise induced by eye movement and resting periods.

Monkey M1 produced an average of 17.5 (median: 16.6) blinks per minute, while monkey M2 had a mean blink rate of 7.3 (median: 6.5) blinks per minute (Kruskal-Wallis test, $p<0.0001$, Table 1). The corresponding inter-blink intervals are represented in figure 2 for each of monkey M1 (2A, mean=3.4, median=2.1) and monkey M2 (2B, mean=8.2, median=7.2). These inter-blink interval distributions are not Gaussian (Kolmogorov-Smirnov

test, monkeys M1 and M2, $p<10^{-14}$), indicating that blink generation is produced by a non-gaussian process.

Monkey M1 produced significantly more eye blinks during the auditory runs (mean: 18.7 blinks.min^{-1}, median: 18.4) than during the tactile runs (mean: 15.9 blinks.min^{-1}, median: 14.4, $p<0.05$). In monkey M2 this difference was not significant (tactile runs, 8.0 blinks.min^{-1}, median: 6.5, auditory runs, 6.8 blinks.min^{-1}, median: 6.5, Kruskal-Wallis test, $p=0.09$).

Within a given sensory stimulation run, stimulations varied in block. Auditory stimulations could be present or absent (*fixation baseline* condition). When present, they could thus either elicit the percept of static auditory source (*static* condition), the percept of a moving source around the head (*movement* condition) or the percept of a random spatial non-localized auditory source (*scrambled* condition, see (Guipponi et al. 2013) for details). Similarly, tactile stimulations could be present or absent (*fixation baseline* condition). When present, they could be directed either to the *center of the face*, to the *periphery of the face* or else to the *shoulders* (Guipponi et al. 2013). Auditory stimulation conditions did not affect blink rate in either monkeys (Kruskal-Wallis test, auditory stimulation condition main factor, monkey M1, $p<0.50$, monkey M2, $p<0.77$, Table 1). These different conditions could thus be considered as evoking only spontaneous blinks in both monkeys. Tactile stimulation conditions did not affect blink rate in monkey M1 (Kruskal-Wallis test, tactile stimulation condition main factor, monkey M1, $p<0.12$). In contrast, the blink rate of monkey M2 was strongly dependent upon the tactile stimulation condition ($p<0.0001$). Post-hoc Mann-Whitney tests reveal that the *Center of the face* condition evoked a higher number of blinks compared to the three other tactile conditions (*Periphery of the face* condition, $p<0.002$; *Shoulder* condition, $p<0.001$; *fixation baseline* condition, $p<0.0003$, Table 1). In this *Center of the face* condition, both spontaneous and reflexive blinks thus seemed to be evoked, at least in monkey M2 (see also Discussion).

Functional analysis

In order to identify the cortical correlates of spontaneous eye blinks, we performed a conjunction analysis for both the auditory and the tactile blink regression analyses. This conjunction analysis allows to identify blink-related activations that are independent from the sensory conditions and that correlate with the blink pattern common to both conditions, *i.e.* spontaneous eye blinks. The blink events were convoluted with the appropriate hemodynamic response function (evoked by dextran-coated iron oxide agents, MION, Vanduffel et al. 2001). The resulting signal (Figure 1B and 1C, lower part) was used as a regressor for the whole brain analysis. The outcome of this analysis is presented for each individual monkey (uncorrected level, $p<0.001$, figure 3). Table 2 provides a detailed description of the localization (coordinates with respect to the anterior commissure) and size (in voxels) of the obtained activations. Activations are considered as robust when identified in both monkeys and in at least 3 out of the 4 hemispheres.

Eye blinks activated somatosensory area 2, at the anterior tip of the intraparietal sulcus (3 hemispheres out of four); somatosensory areas 3a and 3b, on the anterior and posterior banks as well as in the fundus of the central sulcus (all four hemispheres); the somatosensory complex SII/PV (3 hemispheres out of four). The bilateral somatosensory areas 3a/3b and SII/PV activations are represented on the corresponding coronal section of both monkeys, in figure 4. Blink-related activations were found in somatosensory area 1 in only one hemisphere out of four (in the right hemisphere of monkey M1) and are thus considered as less reliable. Activations were also found in somatosensory parainsular area Pi (also known as the disgranular insular cortex, Id). Anterior to Pi, the activity of ProM, a subdivision of the frontal opercular region PrCo highly correlated with spontaneous eye blink production in three hemispheres out of four while prefrontal area 6Vb was found to be responsive to blinks only in monkey M1 (both hemispheres). Parietal activations were found in medial parietal area

MIP in all hemispheres. Medially, blinks activated a posterior region close to V1, identified as area PGm (three hemispheres out of four), and an anterior region above the anterior cingulate sulcus, identified as area 24d (in all hemispheres). In addition, monkey M1 presented a blink-related activation in two symmetrical locations on the convexity above the ascending posterior branch of the central sulcus of each hemisphere, as well as a bilateral activation on the upper bank at the anterior tip of the cingulate cortex. An orbitofrontal blink-related response was also observed in the left hemisphere of monkey M2, in a region corresponding to areas 11 and 13.

Reliable blink-related activations were finally observed in early striate and extrastriate areas: in V1 (three hemispheres out of four), in the ventral portion of V2 (three hemispheres out of four), in areas V3-V3A (three hemispheres out of four), and in V2d specifically, in monkey M1, bilaterally. In monkey M1, this V3-V3A activation at the junction of the lunate and the intraparietal sulci, potentially extends, in both hemispheres into posterior intraparietal area PIP. Remarkably, all these striate and extra-striate activations fell exclusively within the peripheral visual field representation (figure 5, blue regions), as defined by standard retinotopic localizers (Fize et al. 2003).

Discussion

In the present study, we describe the whole brain cortical activations correlating with non-voluntary eyeblinks as measured in a fixation task during which the monkeys received either auditory stimulations or tactile stimulations to the face.

Blink-related behavior in the active monkey

Inter-individual variability in blink rate is well documented in both humans and non-human primates and appears to be under the dependence of dopaminergic regulation (Karson 1983; Taylor et al. 1999). A gender difference has also been described, females producing more blinks than males (Pult et al. 2013). This matches our observations on the two monkeys involved in the present study, the female producing up to 2.5 more blinks than the male.

As described in the introduction, blinks can be *voluntary, reflexive* or *spontaneous.* The blinks produced by the two monkeys during the fixation task they are required to perform are clearly non-voluntary. Our results mainly describe spontaneous blinks neural correlates. However, this requires further consideration. The blinks produced during the auditory stimulation context (auditory runs) can be considered as essentially spontaneous. Indeed, the auditory stimuli were designed to elicit a non-threatening percept of a dynamic sound moving in the peri-personal space around the head, and the monkeys didn't show any difficulty at maintaining fixation in such a context. In contrast, the blinks produced during the tactile stimulation context (tactile runs) consist in a mixture of spontaneous and reflexive eye blinks. This was particularly clear when the air-puff tactile stimulations were initially introduced during the training phase. This correlated with a drastic drop in the fixation performance and a high correlation between blinking events and tactile stimulation events. Monkeys progressively habituated to the air-puffs and fixation performance increased back to our run

selection criteria (fixation maintained during 85% of the run duration or more, see methods). This habituation also correlated with a decrease in blink rates back to the spontaneous blinking rate for periphery of the face and shoulder stimulation conditions, as described in the results. Air-puffs to the center of the face, directed to the sensitive skin on each side of the snout, still induced more eye blinks than all other conditions. This sensory condition can thus be considered to elicit both spontaneous and reflexive eye blinks. As a result, though the majority of the blinks produced by the monkeys are spontaneous blinks, a small proportion corresponds to reflexive blinks.

Analysis and potential confounds

The functional description presented here is based on a conjunction analysis describing the blink-related cortical activations that are obtained both during the auditory and the tactile stimulation contexts. As a result, we can state that we are actually describing the neural bases of spontaneous blinks, *i.e.* those areas that are activated both during the spontaneous blinks generated during the auditory stimulation task and the spontaneous plus reflexive blinks generated during the tactile stimulation task.

This conjunction analysis also allows us to control for non-random blinking behavior induced by a specific experimental context (see Hupé et al. 2012 for a discussion on the consequences of fMRI methodology on blink studies). It is indeed unlikely that both sensory stimulation contexts used here induce, for example, shared attentional or decisional modulations, or shared eye movement strategies. Confirming this fact, none of the identified cortical blink-related areas can be associated with any of these potential confounds.

The only parameter that is shared between the two types of experimental contexts, apart from the fixation requirements is the random reward schedule. This reward event is

much more frequent than the blink event, across all runs, including in monkey M1 in spite of its high blinking rate. As a result, reward-related signals contribute both to the signal of interest (blink-related) and to the remaining signal of non-interest. Confirming that this is the case and that our observations are not contaminated by reward-related information, the activations obtained in the central sulcus remarkably spare its anterior tip, which has been described as related to somato-sensation around and within the mouth, including the teeth, the tongue, the palate and the throat (Padberg et al. 2005).

Neural bases of spontaneous eye blinks.

A core somatosensory network. Spontaneous blink-related activations are obtained in a core somatosensory network composed of the upper face fields of three key somatosensory areas. ***Area 2*** activations are reliably observed on the medial bank of the anterior most tip of the intraparietal sulcus. This location corresponds to a subsector of area 2 face field (figure 4A, Pons and Kaas 1986; Padberg et al. 2005), situated posterior to the perioral and intraoral area 2 subsector described by Schwarz and Fredrickson (1971) and Iwamura (2000), and medial to vestibular area 7t, which is located on the lateral bank of the anterior most tip of the intraparietal sulcus (Schwarz and Fredrickson 1971; Lewis and Van Essen 2000). Note that this 2 face field is partially overlapping with the PF cytoarchitectonic region described by (Gregoriou et al. 2006) and characterized by oro-facial somatosensory responses (Rozzi et al. 2008), though none of these studies mention a potential extension of this face region within the medial tip of the intraparietal sulcus, nor specific peri-orbital responses. ***Areas 3a/3b*** activations are situated on the anterior and posterior banks as well as in the fundus of the central sulcus, in the upper portion of its lower half extent, at a location described to represent the upper face (figure 4A, nose, cheeks, orbital region, including brows and forehead, Nelson et al. 1980; Krubitzer et al. 2004; Zhang and Britten 2004; Padberg et al. 2005; Wang et al.

2007; Seelke et al. 2012), consistent with the projection field of the ophthalmic branch of the trigeminal nerve (Nelson et al. 1980). The areas 3a/3b activations appear to spare the perioral and intraoral (Martin et al. 1999) as well as the arm-hand somatosensory representation, confirming the fact that our analysis is not confounded by potential variables of non-interest such as reward taking or uncontrolled for arm-movements. Reliable activations are also observed in the ***somatosensory SII complex***. The extent of this activation varied between the two monkeys and across hemispheres. In three hemispheres out of four, two distinct activation peaks can be identified, possibly corresponding to SII and PV respectively. As seen for the previous somatosensory areas, these activations are located within the face region of these somatosensory areas (figure 4B, Krubitzer et al. 1995).

Blinks, including spontaneous blinks, are expected to induce self-periorbital tactile stimulations, hence the observed tactile activation in the periorbital face region of different areas discussed above. However, self-generated tactile stimulations are known to induce weaker activations than tactile stimulations generated by another agent (Jiang et al. 1991; Chapman 1994). For example, tickling one-self is far less efficient than being tickled by someone else (Weiskrantz et al. 1971; Blakemore et al. 1998, 2000), because a feedforward efferent copy of the expected outcome of the action gates the sensory input within the somatosensory areas (Chapin and Woodward 1981; Blakemore et al. 1998). To our knowledge, previous fMRI studies on the neural substrates of spontaneous blinks did not highlight any specific activation in any of these early somatosensory processing areas (Hanakawa et al. 2008), to the exception of a single case study describing blink-related activations in the eye representation of the sensory cortex in a patient suffering from chronic corneal pain, both in the presence and absence of a noxious corneal stimulation (Moulton et al. 2012). As a result, the somatosensory activations we describe in our monkeys could be due to eye fatigue and corneal dryness induced by the fixation requirements they are submitted to.

This would be in line with the cingulate and insular blink-related activations we describe below.

A larger cortical network. Blink-related activations are also found in the medial bank of the intraparietal sulcus, in both hemispheres of both monkeys. These activations are located anteriorly to the medial intraparietal area MIP, cytoarchitectonically identified by (Lewis and Van Essen 2000), possibly overlapping their medial ventral intraparietal area VIP_m and their ventral area 5, 5v. It is clearly situated medially to the multisensory visuo-tactile and auditory-visuo-tactile site that we describe in the fundus of the intraparietal sulcus and which we attribute to the ventral intraparietal area VIP (Guipponi et al. 2013), and lies within the electrophysiologically defined area MIP (Colby and Duhamel 1991). Interestingly, this region coincides with a portion of the medial intraparietal sulcus in which low threshold microstimulations elicit non-voluntary blinks in awake monkeys (Thier and Andersen 1998). We also describe another parietal blink-related activation on the medial wall, in a region corresponding to the posterior most portion of area PGm (nomenclature of Pandya and Seltzer 1982) or 7m (nomenclature of Cavada and Goldman-Rakic 1989a). This region is considered as a higher-order supplementary somatosensory association area (Pandya and Barnes 1987) connected with area 3a/3b, area 2, SII/PV and MIP (Leichnetz 2001). It has also been involved in oculomotor behavior (Thier and Andersen 1998), and indeed, it has recurrently been described as projecting to the frontal eye field FEF and supplementary eye field SEF oculomotor structures (Pandya and Barnes 1982; Cavada and Goldman-Rakic 1989b; Leichnetz 2001). Last but not least, it is recurrently identified in monkey fMRI studies describing the neural bases of saccadic behavior (precuneus in Kagan et al. 2010; Wilke et al. 2012) with a privileged functional connectivity with the FEF (Hutchison et al. 2012). All this taken together is compatible with the presence of a peri-orbital representation and a blink-related activation in this region as reported here. Overall we propose that the blink-related

activations reported in these two posterior associative regions (MIP and PGm) reflect the sensory consequences of eyelid closure, similarly to what has been described in the somatosensory core regions, rather than their active motor correlate, as no specific blink-related activation can be described in key cortical oculomotor regions such as the frontal eye field FEF or the supplementary eye field SEF.

A second medial blink-related region is also reliably identified in both hemispheres of both monkeys on the upper bank of the middle sector of the cingulate sulcus, matching the cytoarchitectonic definition of area 24d (Vogt et al. 2005) at a location compatible with the posterior cingulate face area (caudal portion of the M3 region, Morecraft et al. 1996, 2001) and the most caudal cingulate eye field (CEFc, Wang et al. 2004; Amiez and Petrides 2009). Early single cell recording studies (Olson et al. 1996) as well as more recent monkey fMRI studies describe oculomotor neuronal responses in this region (Ford et al. 2009; Kagan et al. 2010; Hutchison et al. 2012; Wilke et al. 2012). Corroborating this observation, this region is connected with the frontal eye fields (Huerta et al. 1987; Bates and Goldman-Rakic 1993; Morecraft et al. 1993). Retrograde transneuronal rabies virus tracing highlights strong polysynaptic projections from a region compatible with CEFc to the orbicularis oculi muscles responsible for eyelid closure (day 5,Gong et al. 2005). In monkey M1, an additional medial activation is identified in both hemispheres anterior to CEFc, possibly corresponding to CEFr. Indeed, microstimulations to CEFr evoke eye movements (Gentilucci et al. 1988; Godschalk et al. 1995) and this region, oligosynaptically connected to the extraocular motoneurons (Moschovakis et al. 2004) as well as to cortical oculomotor structures such as the FEF and SEF (Huerta et al. 1987; Bates and Goldman-Rakic 1993; Morecraft et al. 1993; Luppino et al. 2003), is activated during oculomotor behavior. Still in monkey M1, in both hemispheres, a last cingulate region in the caudal most upper bank of the cingulate sulcus is possibly matching medial PE and PEci. Little direct anatomical and electrophysiological evidence is

available regarding the contribution of this region to oculomotor behavior, though it appears to be activated by saccade execution in several monkey fMRI studies (Koyama et al. 2004; Baker et al. 2006) and microstimulations produce blinks (Thier and Andersen 1998).

Reliable blink-related activation can also be seen around the anterior pole of the lateral sulcus, in two distinct regions identified as the parainsular cortex Pi and the ProM proisocortical subdivision of the frontal opercular cortex PrCo. In addition, a bilateral ventral premotor 6Vb blink-related activation can also be seen in monkey M1. Interestingly, retrograde transneuronal rabies virus tracing highlight strong polysynaptic projection from both Pi and ProM to the orbicularis oculi muscles responsible for eyelid closure (day 5,Gong et al. 2005). Pi, ProM and 6Vb are densely interconnected and reciprocally connected to the cingulate cortex, and specifically to CEFr (Barbas and Pandya 1987; Preuss and Goldman-Rakic 1989; Tokuno et al. 1997; Cipolloni and Pandya 1999; Morecraft et al. 2012). Complementing this indirect evidence for a contribution of these cortical regions in periorbital somatosensory processing, facial receptive fields have been described in Pi (Augustine 1996; Zhang et al. 1999) in particular during nociceptive stimulations (Zhang et al. 1999).

Cingulate and insular cortex activations are alsoreported in human blink studies (Bristow, Frith, et al. 2005; Hanakawa et al. 2008; Lerner et al. 2009; Hupé et al. 2012). The insula is highly interconnected with both the cingulate cortex, the frontal opercular cortex and the ventral most part of the premotor cortex, defining a limbic cortical network of sensory processing and integration (Barbas and Pandya, 1987; Preuss and Goldman-Rakic, 1996; Morecraft et al., 2007, 2012). In particular, the insula is considered as an integration center of visceral sensory and motor functions (Craig 2002), subserving the processing and the perception of internal stimuli and activating higher order representations of sympathetic homeostasis in response to stress (Craig 2005). It is also proposed to be involved in the proprioceptive awareness of blinks (Bristow, Frith, et al. 2005; Hupé et al. 2012). And indeed,

the suppression of the urge to blink produces reliable insular and anterior cingulate functional activations in humans (Lerner et al. 2009). In this present study, the monkeys are required to maintain fixation over 85% of the total length of the runs, and blinks are processed so as not to interrupt the reward schedule and are thus not considered as fixation breaks. This fixation requirement is very demanding and puts a lot of stress on the eyes (all subjects of visual psychophysics experiments report on this). All this taken together indicates that these spontaneous blink-related activations can be viewed as cortical correlates of homeostatic signals of corneal dryness and possibly to pain eye-related signal.

Overall, the somatosensory blink-related network and the larger cortical network described above allow to identify an ensemble of cortical fields that are involved in the somatosensory and/or proprioceptive representation of the eyes and their homeostasis. To our knowledge, this is the first time that such a network is reported, providing a precise whole-brain localization of these cortical eye fields and their potential intra-individual variability.

*Striate and extra-striate cortical areas.*The blink-related activations observed in the striate and extrastriate visual areas deserve a specific discussion. Blinks induce changes in visual illumination, due to the rapid closure of the eyelids and the occlusion of the pupil. We remain unaware of these changes most probably due to blink suppression mechanisms. As a result, part of the cortical activations that correlates with spontaneous blinks are actually due to the visual consequences of eyelid closure onto the retinal input. This retinal sweep is expected to produce large field visual motion stimulations, mostly at the periphery of the retina. Corroborating this interpretation, the blink-related activations we report in V1, V2 and V3 are located within the peripheral visual field representation. In addition, we identify blink-related responses in medial superior temporal area MST which is known to process large field stimulations (Saito et al. 1986; Duffy and Wurtz 1991), but not in the medial temporal area MT which is described to favor local motion processing (Albright and Desimone 1987). In

line with these observations, several studies report similar striate and extrastriate blink-related BOLD activations that are independent of the visual context of the task (Hupé et al., 2012, Tse et al., 2010; Berma et al., 2012). Indeed, these activations are observed both when subjects are required to maintain fixation while presented with a large range of visual stimuli (size, color, speed), and in the absence of these visual stimuli (Hupé et al., 2012).

Functional differences between spontaneous and voluntary blinks

It is worth noting that several key oculomotor regions described in human voluntary blink production studies such as the frontal eye field FEF, the supplementary eye field SEF and the lateral intraparietal area LIP (Bodis-Wollner et al. 1999; Kato and Miyauchi 2003b; Bristow, Frith, et al. 2005; Hanakawa et al. 2008; van Koningsbruggen et al. 2012) are not activated in the present study nor in human studies describing the neural correlated of spontaneous blinking (Yoon et al. 2005; Tse et al. 2010; Hupé et al. 2012). These regions, which are largely described as being at the origin of eye movement production and control (Wardak et al. 2011), are also thought to be at the origin of the blink-generation command (Bristow, Haynes, et al. 2005). In addition, the fronto-parietal network, including FEF and LIP, plays a key role in visuo-spatial attention (Corbetta and Shulman 2002). This network is anti-correlated with the default-mode network (DMN, Vincent et al. 2007) and its level of activity is proposed to be dependent on the overall degree of attentional engagement of subjects in a given behavior (Anticevic et al. 2012; Wen et al. 2013). Corroborating this fact, Nakano et al. (2013) describe a blink-related activation in the DMN when subjects are viewing videos as compared to blank screens. This DMN activation correlates with a significant functional deactivation of the fronto-parietal network. The authors interpret this observation in terms of an attentional modulation of blink-related DMN activation by the cognitive context.

All this taken together indicates that while voluntary blinks engage cortical oculomotor regions, spontaneous blink studies reveal the sensory correlated of blinks, both in terms of homeostatic triggers (eye dryness, eye strain, pain) and in terms of sensory consequences.

Abbreviations

Cortical areas

MIP medial intraparietal area

MST medial superior temporal area

PEci area PE, cingulate part

PGm area PG, medial area

Pi parainsular cortex

PIP posterior intraparietal area

ProM promotor area

PV parietoventral cortex

SII secondary somatosensory cortex

V1 visual area V1

V2v visual area V2, ventral part

V2d visual area V2, dorsal part

V3 visual area V3

V3A visual area V3A

1, 2 somatosensory areas 1 and 2

3a, 3b somatosensory areas 3a and 3b

6Vb ventral premotor area 6Vb

11 orbitofrontal area 11

13 orbitofrontal area 13

24d cingulate area 24d

Cortical sulci

AS arcuate sulcus

CgS cingulate sulcus

CeS central sulcus

IOS inferior occipital sulcus

IPS intraparietal sulcus

LaS lateral (Sylvian) sulcus

LuS lunate sulcus

OTS occipital temporal sulcus

POS parieto-occipital sulcus

PS principal sulcus

STS superior temporal sulcus

Acknowledgments: We thank S. Maurin for technical support and J.L. Charieau and F. Hérant for animal care. This work was supported by Agence Nationale de la Recherche (ANR-05-JCJC-0230-01).

Bibliography

Albright TD, Desimone R. 1987. Local precision of visuotopic organization in the middle temporal area (MT) of the macaque. Exp Brain Res. 65:582–592.

Amiez C, Petrides M. 2009. Anatomical organization of the eye fields in the human and non-human primate frontal cortex. Prog Neurobiol. 89:220–230.

Anticevic A, Cole MW, Murray JD, Corlett PR, Wang X-J, Krystal JH. 2012. The role of default network deactivation in cognition and disease. Trends Cogn Sci. 16:584–592.

Augustine JR. 1996. Circuitry and functional aspects of the insular lobe in primates including humans. Brain Res Brain Res Rev. 22:229–244.

Baker JT, Patel GH, Corbetta M, Snyder LH. 2006. Distribution of activity across the monkey cerebral cortical surface, thalamus and midbrain during rapid, visually guided saccades. Cereb Cortex. 1991. 16:447–459.

Barbas H, Pandya DN. 1987. Architecture and frontal cortical connections of the premotor cortex (area 6) in the rhesus monkey. J Comp Neurol. 256:211–228.

Bates JF, Goldman-Rakic PS. 1993. Prefrontal connections of medial motor areas in the rhesus monkey. J Comp Neurol. 336:211–228.

Blakemore SJ, Wolpert D, Frith C. 2000. Why can't you tickle yourself? Neuroreport. 11:R11–16.

Blakemore SJ, Wolpert DM, Frith CD. 1998. Central cancellation of self-produced tickle sensation. Nat Neurosci. 1:635–640.

Bodis-Wollner I, Bucher SF, Seelos KC. 1999. Cortical activation patterns during voluntary blinks and voluntary saccades. Neurology. 53:1800–1805.

Bristow D, Frith C, Rees G. 2005. Two distinct neural effects of blinking on human visual processing. Neuroimage. 27:136–145.

Bristow D, Haynes J-D, Sylvester R, Frith CD, Rees G. 2005. Blinking suppresses the neural response to unchanging retinal stimulation. Curr Biol. 15:1296–1300.

Cavada C, Goldman-Rakic PS. 1989a. Posterior parietal cortex in rhesus monkey: I. Parcellation of areas based on distinctive limbic and sensory corticocortical connections. J Comp Neurol. 287:393–421.

Cavada C, Goldman-Rakic PS. 1989b. Posterior parietal cortex in rhesus monkey: II. Evidence for segregated corticocortical networks linking sensory and limbic areas with the frontal lobe. J Comp Neurol. 287:422–445.

Chapin JK, Woodward DJ. 1981. Modulation of sensory responsiveness of single somatosensory cortical cells during movement and arousal behaviors. Exp Neurol. 72:164–178.

Chapman CE. 1994. Active versus passive touch: factors influencing the transmission of somatosensory signals to primary somatosensory cortex. Can J Physiol Pharmacol. 72:558–570.

Cipolloni PB, Pandya DN. 1999. Cortical connections of the frontoparietal opercular areas in the rhesus monkey. J Comp Neurol. 403:431–458.

Colby CL, Duhamel JR. 1991. Heterogeneity of extrastriate visual areas and multiple parietal areas in the macaque monkey. Neuropsychologia. 29:517–537.

Collewijn H, van der Steen J, Steinman RM. 1985. Human eye movements associated with blinks and prolonged eyelid closure. J Neurophysiol. 54:11–27.

Colombo A, De Renzi E, Gibertoni M. 1982. Eyelid movement disorders following unilateral hemispheric stroke. Ital J Neurol Sci. 3:25–30.

Corbetta M, Shulman GL. 2002. Control of goal-directed and stimulus-driven attention in the brain. Nat Rev Neurosci. 3:201–215.

Craig AD. 2002. How do you feel? Interoception: the sense of the physiological condition of the body. Nat Rev Neurosci. 3:655–666.

Craig ADB. 2005. Forebrain emotional asymmetry: a neuroanatomical basis? Trends Cogn Sci. 9:566–571.

Duffy CJ, Wurtz RH. 1991. Sensitivity of MST neurons to optic flow stimuli. I. A continuum of response selectivity to large-field stimuli. J Neurophysiol. 65:1329–1345.

Fize D, Vanduffel W, Nelissen K, Denys K, Chef d'Hotel C, Faugeras O, Orban GA. 2003. The retinotopic organization of primate dorsal V4 and surrounding areas: A functional magnetic resonance imaging study in awake monkeys. J Neurosci. 23:7395–7406.

Ford KA, Gati JS, Menon RS, Everling S. 2009. BOLD fMRI activation for anti-saccades in nonhuman primates. Neuroimage. 45:470–476.

Gentilucci M, Fogassi L, Luppino G, Matelli M, Camarda R, Rizzolatti G. 1988. Functional organization of inferior area 6 in the macaque monkey. I. Somatotopy and the control of proximal movements. Exp Brain Res. 71:475–490.

Godschalk M, Mitz AR, van Duin B, van der Burg H. 1995. Somatotopy of monkey premotor cortex examined with microstimulation. Neurosci Res. 23:269–279.

Gong S, DeCuypere M, Zhao Y, LeDoux MS. 2005. Cerebral cortical control of orbicularis oculi motoneurons. Brain Res. 1047:177–193.

Gordon G. 1951. Observations upon the movements of the eyelids. Br J Ophthalmol. 35:339–351.

Gregoriou GG, Borra E, Matelli M, Luppino G. 2006. Architectonic organization of the inferior parietal convexity of the macaque monkey. J Comp Neurol. 496:422–451.

Guipponi O, Wardak C, Ibarrola D, Comte J-C, Sappey-Marinier D, Pinède S, Ben Hamed S. 2013. Multimodal convergence within the intraparietal sulcus of the macaque monkey. J Neurosci. 33:4128–4139.

Hanakawa T, Dimyan MA, Hallett M. 2008. The representation of blinking movement in cingulate motor areas: a functional magnetic resonance imaging study. Cereb Cortex. 1991. 18:930–937.

Huerta MF, Krubitzer LA, Kaas JH. 1987. Frontal eye field as defined by intracortical microstimulation in squirrel monkeys, owl monkeys, and macaque monkeys. II. Cortical connections. J Comp Neurol. 265:332–361.

Hupé J-M, Bordier C, Dojat M. 2012. A BOLD signature of eyeblinks in the visual cortex. Neuroimage. 61:149–161.

Hutchison RM, Gallivan JP, Culham JC, Gati JS, Menon RS, Everling S. 2012. Functional connectivity of the frontal eye fields in humans and macaque monkeys investigated with resting-state fMRI. J Neurophysiol. 107:2463–2474.

Iwamura Y. 2000. Bilateral receptive field neurons and callosal connections in the somatosensory cortex. Philos Trans R Soc Lond B Biol Sci. 355:267–273.

Jiang W, Chapman CE, Lamarre Y. 1991. Modulation of the cutaneous responsiveness of neurones in the primary somatosensory cortex during conditioned arm movements in the monkey. Exp Brain Res. 84:342–354.

Kagan I, Iyer A, Lindner A, Andersen RA. 2010. Space representation for eye movements is more contralateral in monkeys than in humans. Proc Natl Acad Sci. 107:7933–7938.

Karson CN. 1983. Spontaneous eye-blink rates and dopaminergic systems. Brain J Neurol. 106 (Pt 3):643–653.

Kato M, Miyauchi S. 2003a. Functional MRI of brain activation evoked by intentional eye blinking. Neuroimage. 18:749–759.

Kato M, Miyauchi S. 2003b. Human precentral cortical activation patterns during saccade tasks: an fMRI comparison with activation during intentional eyeblink tasks. Neuroimage. 19:1260–1272.

Korb DR, Baron DF, Herman JP, Finnemore VM, Exford JM, Hermosa JL, Leahy CD, Glonek T, Greiner JV. 1994. Tear film lipid layer thickness as a function of blinking. Cornea. 13:354–359.

Koyama M, Hasegawa I, Osada T, Adachi Y, Nakahara K, Miyashita Y. 2004. Functional magnetic resonance imaging of macaque monkeys performing visually guided saccade tasks: comparison of cortical eye fields with humans. Neuron. 41:795–807.

Krubitzer L, Clarey J, Tweedale R, Elston G, Calford M. 1995. A redefinition of somatosensory areas in the lateral sulcus of macaque monkeys. J Neurosci. 15:3821–3839.

Krubitzer L, Huffman KJ, Disbrow E, Recanzone G. 2004. Organization of area 3a in macaque monkeys: contributions to the cortical phenotype. J Comp Neurol. 471:97–111.

Leichnetz GR. 2001. Connections of the medial posterior parietal cortex (area 7m) in the monkey. Anat Rec. 263:215–236.

León L, Casanova-Molla J, Lauria G, Valls-Solé J. 2011. The somatosensory blink reflex in upper and lower brainstem lesions. Muscle Nerve. 43:196–202.

Lerner A, Bagic A, Hanakawa T, Boudreau EA, Pagan F, Mari Z, Bara-Jimenez W, Aksu M, Sato S, Murphy DL, Hallett M. 2009. Involvement of insula and cingulate cortices in control and suppression of natural urges. Cereb Cortex. 1991. 19:218–223.

Lewis JW, Van Essen DC. 2000. Corticocortical connections of visual, sensorimotor, and multimodal processing areas in the parietal lobe of the macaque monkey. J Comp Neurol. 428:112–137.

Luppino G, Rozzi S, Calzavara R, Matelli M. 2003. Prefrontal and agranular cingulate projections to the dorsal premotor areas F2 and F7 in the macaque monkey. Eur J Neurosci. 17:559–578.

Mandeville JB, Choi J-K, Jarraya B, Rosen BR, Jenkins BG, Vanduffel W. 2011. FMRI of cocaine self-administration in macaques reveals functional inhibition of basal ganglia. Neuropsychopharmacol. 36:1187–1198.

Martin RE, Kemppainen P, Masuda Y, Yao D, Murray GM, Sessle BJ. 1999. Features of cortically evoked swallowing in the awake primate (Macaca fascicularis). J Neurophysiol. 82:1529–1541.

Miwa H, Yamaji Y, Abe H, Mizuno Y. 1996. Evaluation of the somatosensory evoked blink response in patients with neurological disorders. J Neurol Neurosurg Psychiatry. 60:539–543.

Morecraft RJ, Geula C, Mesulam MM. 1993. Architecture of connectivity within a cingulo-fronto-parietal neurocognitive network for directed attention. Arch Neurol. 50:279–284.

Morecraft RJ, Louie JL, Herrick JL, Stilwell-Morecraft KS. 2001. Cortical innervation of the facial nucleus in the non-human primate: a new interpretation of the effects of stroke and related subtotal brain trauma on the muscles of facial expression. Brain J Neurol. 124:176–208.

Morecraft RJ, Schroeder CM, Keifer J. 1996. Organization of face representation in the cingulate cortex of the rhesus monkey. Neuroreport. 7:1343–1348.

Morecraft RJ, Stilwell-Morecraft KS, Cipolloni PB, Ge J, McNeal DW, Pandya DN. 2012. Cytoarchitecture and cortical connections of the anterior cingulate and adjacent somatomotor fields in the rhesus monkey. Brain Res Bull. 87:457–497.

Moschovakis AK, Gregoriou GG, Ugolini G, Doldan M, Graf W, Guldin W, Hadjidimitrakis K, Savaki HE. 2004. Oculomotor areas of the primate frontal lobes: a transneuronal transfer of rabies virus and [14C]-2-deoxyglucose functional imaging study. J Neurosci. 24:5726–5740.

Moulton EA, Becerra L, Rosenthal P, Borsook D. 2012. An approach to localizing corneal pain representation in human primary somatosensory cortex. Plos One. 7:e44643.

Nakano T, Kato M, Morito Y, Itoi S, Kitazawa S. 2013. Blink-related momentary activation of the default mode network while viewing videos. Proc Natl Acad Sci. 110:702–706.

Nelson RJ, Sur M, Felleman DJ, Kaas JH. 1980. Representations of the body surface in postcentral parietal cortex of Macaca fascicularis. J Comp Neurol. 192:611–643.

Olson CR, Musil SY, Goldberg ME. 1996. Single neurons in posterior cingulate cortex of behaving macaque: eye movement signals. J Neurophysiol. 76:3285–3300.

Padberg J, Disbrow E, Krubitzer L. 2005. The organization and connections of anterior and posterior parietal cortex in titi monkeys: do New World monkeys have an area 2? Cereb Cortex. 1991. 15:1938–1963.

Pandya D.N., Barnes C.L. Architecture and connections of the frontal lobe. In: Perecman E., editor. The frontal lobes revisited. IRBN; New York: 1987. pp. 41–72.

Pandya DN, Seltzer B. 1982. Intrinsic connections and architectonics of posterior parietal cortex in the rhesus monkey. J Comp Neurol. 204:196–210.

Pons TP, Kaas JH. 1986. Corticocortical connections of area 2 of somatosensory cortex in macaque monkeys: a correlative anatomical and electrophysiological study. J Comp Neurol. 248:313–335.

Preuss TM, Goldman-Rakic PS. 1989. Connections of the ventral granular frontal cortex of macaques with perisylvian premotor and somatosensory areas: anatomical evidence for somatic representation in primate frontal association cortex. J Comp Neurol. 282:293–316.

Pult H, Riede-Pult BH, Murphy PJ. 2013. A new perspective on spontaneous blinks. Ophthalmology. 120:1086–1091.

Rozzi S, Ferrari PF, Bonini L, Rizzolatti G, Fogassi L. 2008. Functional organization of inferior parietal lobule convexity in the macaque monkey: electrophysiological characterization of motor, sensory and mirror responses and their correlation with cytoarchitectonic areas. Eur J Neurosci. 28:1569–1588.

Saito H, Yukie M, Tanaka K, Hikosaka K, Fukada Y, Iwai E. 1986. Integration of direction signals of image motion in the superior temporal sulcus of the macaque monkey. J Neurosci. 6:145–157.

Schwarz DW, Fredrickson JM. 1971. Rhesus monkey vestibular cortex: a bimodal primary projection field. Science. 172:280–281.

Seelke AMH, Padberg JJ, Disbrow E, Purnell SM, Recanzone G, Krubitzer L. 2012. Topographic Maps within Brodmann's Area 5 of macaque monkeys. Cereb Cortex. 1991. 22:1834–1850.

Taylor JR, Elsworth JD, Lawrence MS, Sladek JR Jr, Roth RH, Redmond DE Jr. 1999. Spontaneous blink rates correlate with dopamine levels in the caudate nucleus of MPTP-treated monkeys. Exp Neurol. 158:214–220.

Thier P, Andersen RA. 1998. Electrical microstimulation distinguishes distinct saccade-related areas in the posterior parietal cortex. J Neurophysiol. 80:1713–1735.

Tokuno H, Takada M, Nambu A, Inase M. 1997. Reevaluation of ipsilateral corticocortical inputs to the orofacial region of the primary motor cortex in the macaque monkey. J Comp Neurol. 389:34–48.

Tse PU, Baumgartner FJ, Greenlee MW. 2010. Event-related functional MRI of cortical activity evoked by microsaccades, small visually-guided saccades, and eyeblinks in human visual cortex. Neuroimage. 49:805–816.

Valls-Solé J, Valldeoriola F, Tolosa E, Marti MJ. 1997. Distinctive abnormalities of facial reflexes in patients with progressive supranuclear palsy. Brain J Neurol. 120 (Pt 10):1877–1883.

Van Essen DC, Drury HA, Dickson J, Harwell J, Hanlon D, Anderson CH. 2001. An integrated software suite for surface-based analyses of cerebral cortex. J Am Med Informatics Assoc Jamia. 8:443–459.

Van Koningsbruggen MG, Peelen MV, Davies E, Rafal RD. 2012. Neural control of voluntary eye closure: a case study and an fMRI investigation of blinking and winking. Behav Neurol. 25:103–109.

VanderWerf F, Brassinga P, Reits D, Aramideh M, Ongerboer de Visser B. 2003. Eyelid movements: behavioral studies of blinking in humans under different stimulus conditions. J Neurophysiol. 89:2784–2796.

Vanduffel W, Fize D, Mandeville JB, Nelissen K, Van Hecke P, Rosen BR, Tootell RB, Orban GA. 2001. Visual motion processing investigated using contrast agent-enhanced fMRI in awake behaving monkeys. Neuron. 32:565–577.

Vincent JL, Patel GH, Fox MD, Snyder AZ, Baker JT, Van Essen DC, Zempel JM, Snyder LH, Corbetta M, Raichle ME. 2007. Intrinsic functional architecture in the anaesthetized monkey brain. Nature. 447:83–86.

Vogt BA, Vogt L, Farber NB, Bush G. 2005. Architecture and neurocytology of monkey cingulate gyrus. J Comp Neurol. 485:218–239.

Wang X, Zhang M, Cohen IS, Goldberg ME. 2007. The proprioceptive representation of eye position in monkey primary somatosensory cortex. Nat Neurosci. 10:640–646.

Wang Y, Matsuzaka Y, Shima K, Tanji J. 2004. Cingulate cortical cells projecting to monkey frontal eye field and primary motor cortex. Neuroreport. 15:1559–1563.

Wardak C, Olivier E, Duhamel J-R. 2011. The relationship between spatial attention and saccades in the frontoparietal network of the monkey. Eur J Neurosci. 33:1973–1981.

Weiskrantz L, Elliott J, Darlington C. 1971. Preliminary observations on tickling oneself. Nature. 230:598–599.

Wen X, Liu Y, Yao L, Ding M. 2013. Top-down regulation of default mode activity in spatial visual attention. J Neurosci. 33:6444–6453.

Wilke M, Kagan I, Andersen RA. 2012. Functional imaging reveals rapid reorganization of cortical activity after parietal inactivation in monkeys. Proc Natl Acad Sci. 109:8274–8279.

Yoon HW, Chung J-Y, Song M-S, Park H. 2005. Neural correlates of eye blinking; improved by simultaneous fMRI and EOG measurement. Neurosci Lett. 381:26–30.

Zhang T, Britten KH. 2004. Clustering of selectivity for optic flow in the ventral intraparietal area. Neuroreport. 15:1941–1945.

Zhang ZH, Dougherty PM, Oppenheimer SM. 1999. Monkey insular cortex neurons respond to baroreceptive and somatosensory convergent inputs. Neuroscience. 94:351–360.

Tables

Table 1

	All		***Auditory***				***Tactile***				
		All	Mvt	Scramb	Static	Fix	***All***	Center	Periph	Shld	Fix
M1	***17.5/16.6***	***18.7/18.4***	18.0/18.0	19.5/17.3	17.5/16.6	19.9/20.9	***15.9/14.4***	20.6/15.1	14.6/12.6	15.4/16.6	12.9/12.3
M2	***7.3/6.5***	***6.8/6.5***	6.7/6.5	7.5/6.5	6.3/6.5	6.7/6.5	***8.0/6.5***	11.4/11.5	7.2/5.8	6.9/5.8	6.6/5.8

Table1. Blink rates (in blinks per min, mean/median) for monkeys M1 and M2, as a function of sensory stimulation modality and specific sensory stimulation condition.Mvt (Moving auditory stimuli), Scramb (Scrambled auditory stimuli), Static (Static auditory stimuli), Center (Center of the face tactile stimuli), Periph (Periphery of the face tactile stimuli), Shld (Shoulder tactile stimuli), Fix (Fixation condition with no sensory stimulation).

Table 2

	M1 / Lefthemisphere		*M1 / Right hemisphere*		*M2 / Lefthemisphere*		*M2 / Right hemisphere*	
Visual areas								
V1	-	-	[8; -26; 0]	6.5	[-10; -24; -1]	4.6	[8; -39; 7]	3.2
					[-9; -36; -1]	3.7	[14; -31; -2]	3.6
					[-8; -35; -2]	4.2		
V2v	[-5; -34; -7]	3.5	[4; -33; -4]	5.7	[-17; -27; -9]	3.3	-	-
					[-15; -25; -7]	3.3		
V2d	*[-8; -28; -5]*	*4.3*	*[4; -34; -2]*	*5.5*	-	-	-	-
V3/V3A	[-6; -32; 0]	6.5	[8; -31; 1]	6.4	[-13; -28; 6]	3.2	-	-
MST	[-11; -23; 0]	6.2	[13; -24; 4]	6.1	[-12; -24; 10]	3.2	-	-
Parietal area								
MIP	[-8; -23; 13]	3.5	[9; 19; 11]	3.3	[-11; -17; 13]	3.9	[12; -19; 14]	3.5
			[9; -23; 10]	4.0				
Medial areas								
PGm	[-4; -28; 0]	7.4	[4; -31; 1]	7.2	-	-	[4; -21; 3]	5.2
PEci	*[-2; -18; 17]*	*4.2*	*[0; -15; 18]*	*3.8*	-	-	-	-
	[-6; -24; 18]	*3.2*	*[5; -22; 17]*	*4.3*				
area 24d	[-5; 9; 16]	3.5	[1; 7; 18]	4.4	[-5; -2; 14]	3.8	[1; 2; 17]	3.6
	[1; 7; 18]	4.4	[4; 0; 18]	3.2				
	[-4; 6; 17]	3.9	[5; -3; 16]	3.6				
	[-5; -3; 17]	3.1						
	[-1; -6; 16]	3.1						
Somatosensory cortex								
Area 1/2	-	-	*[26; -2; 2]*	*4.9*	-	-	-	-
Area 2	[-17; -15; 10]	4.2	[17; 15; 13]	4.6	-	-	[15; -15; 14]	4.4

Area 3a/3b	[-20; -5; 9]	3.6	[18; -8; 13]	4.6	[-14; -8; 12]	5.1	[13; -8; 12]	6.6
SII/PV	[-18; 0; 5]	4.5	[20; -8; 4]	5.0	[-16; -9; 6]	4.0	-	-
	[-24; -17; 8]	*3.3*	*[20; -18; 7]*	*5.6*	-	-	-	-
Insular and precentral cortex								
Pi	[-18; 1; -2]	3.7	[18; 0; 23]	6.6	-	-	[15; -3; 2]	3.2
ProM	[-22; 10; -1]	3.7	[22; 8; -1]	4.4	[-22; 6; -1]	4.3	[23; 5; 0]	5.6
Prefrontal areas								
6Vb	*[-24; 9; 5]*	*4.4*	*[22; 9; 7]*	*3.4*	-	-	-	-
Orbitofrontal areas								
Area 11	-	-	-	-	*[-12; 14; 6]*	*4.0*	-	-
Area 13	-	-	-	-	*[-8; 13; 5]*	*3.5*	-	-

Table 2. Summary of the blink-related cortical activations, per monkey (M1/M2), per hemisphere (Left/Right). For each area, peak location (x,y,z coordinates with respect to the anterior commissure) and ROI size (uncorrected level, 0.01) are indicated. Black prints code for the areas identified in three or more hemispheres. Gray italic prints code for the areas identified in two or less hemispheres. The areas are identified and labeled in reference to the nomenclature used in the Lewis and Van Essen atlas as available in Caret and in the Scalable brain atlas http://scalablebrainatlas.incf.org.

Figures

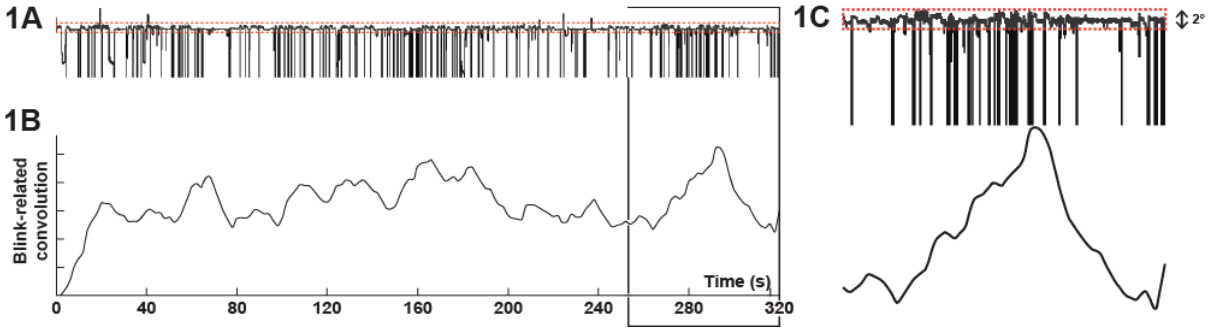

Figure 1: Extraction of eyeblink events and resulting theoretical convolved signal. A. Vertical eye position recorded over time. The trace presented has been extracted from a single run. Sharp transient drops of the signal characterize blink events. The red dashed-line box represents the 2° fixation window the monkeys are rewarded to stay in. Signal outside this window is identified as fixation breakdown and referred to either saccades or blinks depending on the amplitudes and durations of these events. B. Blink-related convoluted signal. The temporal occurrence of the blink events are convoluted with the appropriate hemodynamic response function (see Material and Methods for more details). In this figure the resulting signal has been temporally aligned with the vertical eye trace. C. Close-up of vertical eye position and the resulting convoluted signal extracted from Fig. 1A and 1B (black rectangle). A high blink event frequency is associated with an increase in the convoluted response function.

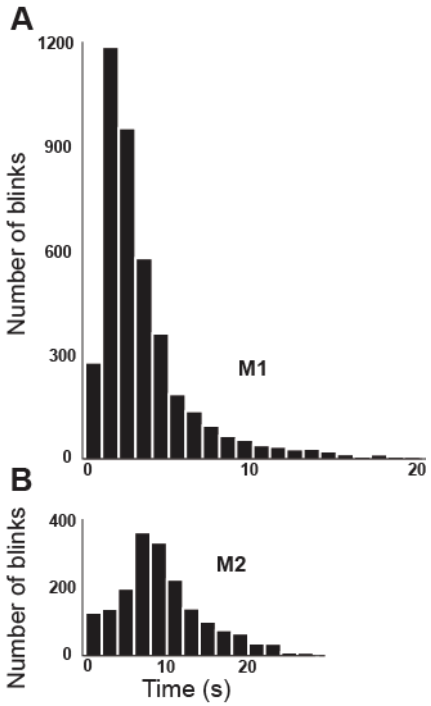

Figure 2: Inter-blink interval distributions. The temporal extraction of blink events gives access to the temporal intervals between two consecutive blinks. These inter-blink intervals are represented for monkey M1 (upper part) and monkey M2 (lower part). Because of the significant blink rate differences between both monkeys, time bins are adjusted to the behavior of each monkey (100ms for M1, 200ms for M2).

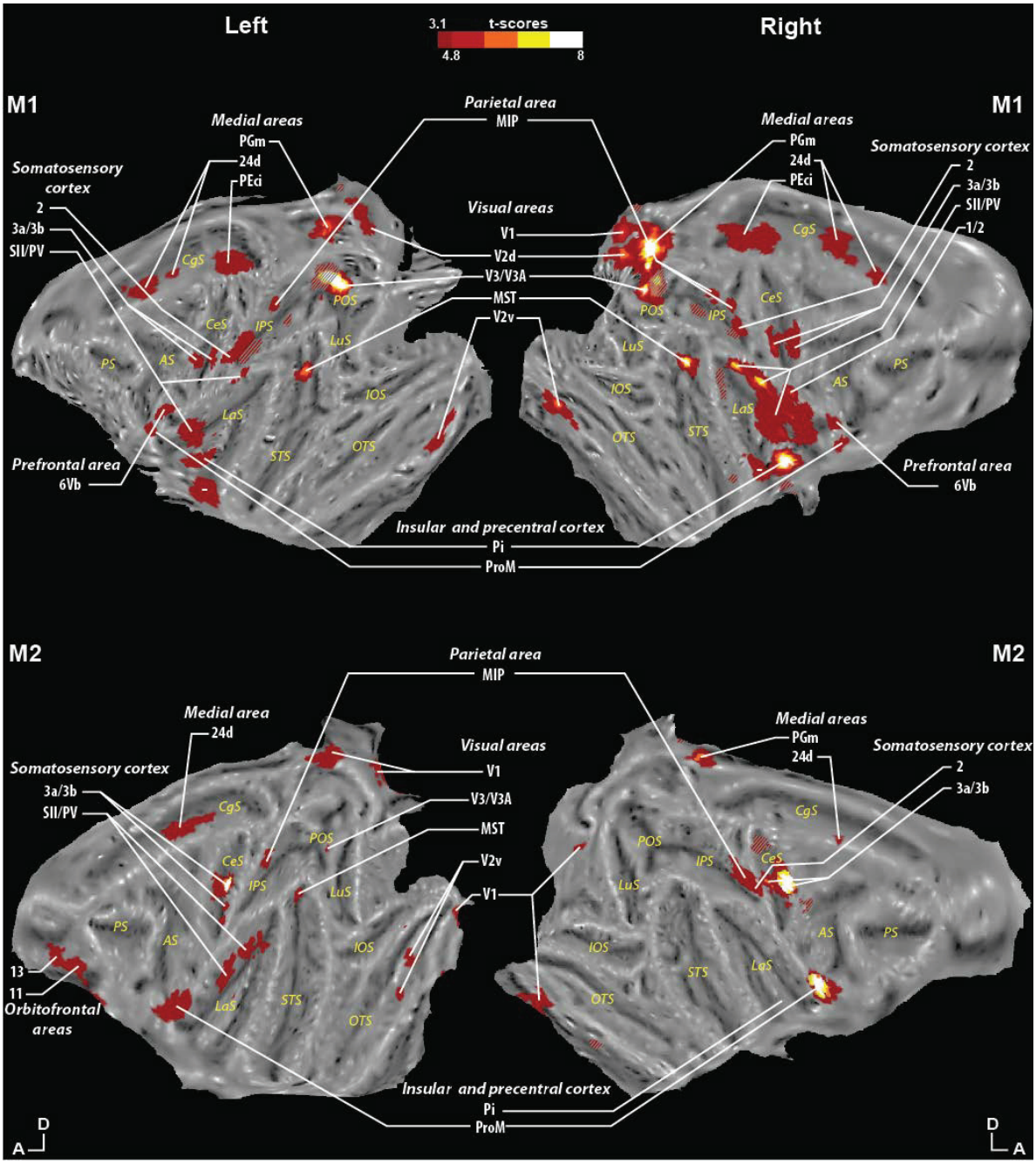

Figure 3: Representation of the blink-related activations on whole brain flat maps. The activations (monkey M1: upper part and monkey M2: lower part) result from the correlation of the blink-related response function and the hemodynamic functional signal (red color t-score scale, color transition being adjusted to t-scores=4.8 FWE corrected level). Orientation: A, anterior; D, dorsal. Cortical areas: MIP, medial intraparietal area; MST, medial superior temporal area; PEci, cingulate part of area PE; PGm, medial part of area PG; Pi, parainsular

cortex; ProM, promotor area; PV, parietoventral cortex; SII, secondary somatosensory cortex; V1, visual area V1; V2,ventral part of visual area V2; V2d, dorsal part of visual area V2; V3, visual area V3; V3A, visual area V3A; 1, somatosensory area 1; 2,somatosensory area 2; 3a, somatosensory area 3a; 3b, somatosensory area 3b; 6Vb, ventral premotor area 6Vb; 11, orbitofrontal area 11; 13, orbitofrontal area 13; 24d, cingulate area 24d. Cortical sulci: AS, arcuate sulcus; CgS, cingulate sulcus; CeS, central sulcus; IOS, inferior occipital sulcus; IPS, intraparietal sulcus; LaS, lateral (Sylvian) sulcus; LuS, lunate sulcus; OTS, occipital temporal sulcus; POS, parieto-occipital sulcus; PS, principal sulcus; STS, superior temporal sulcus.

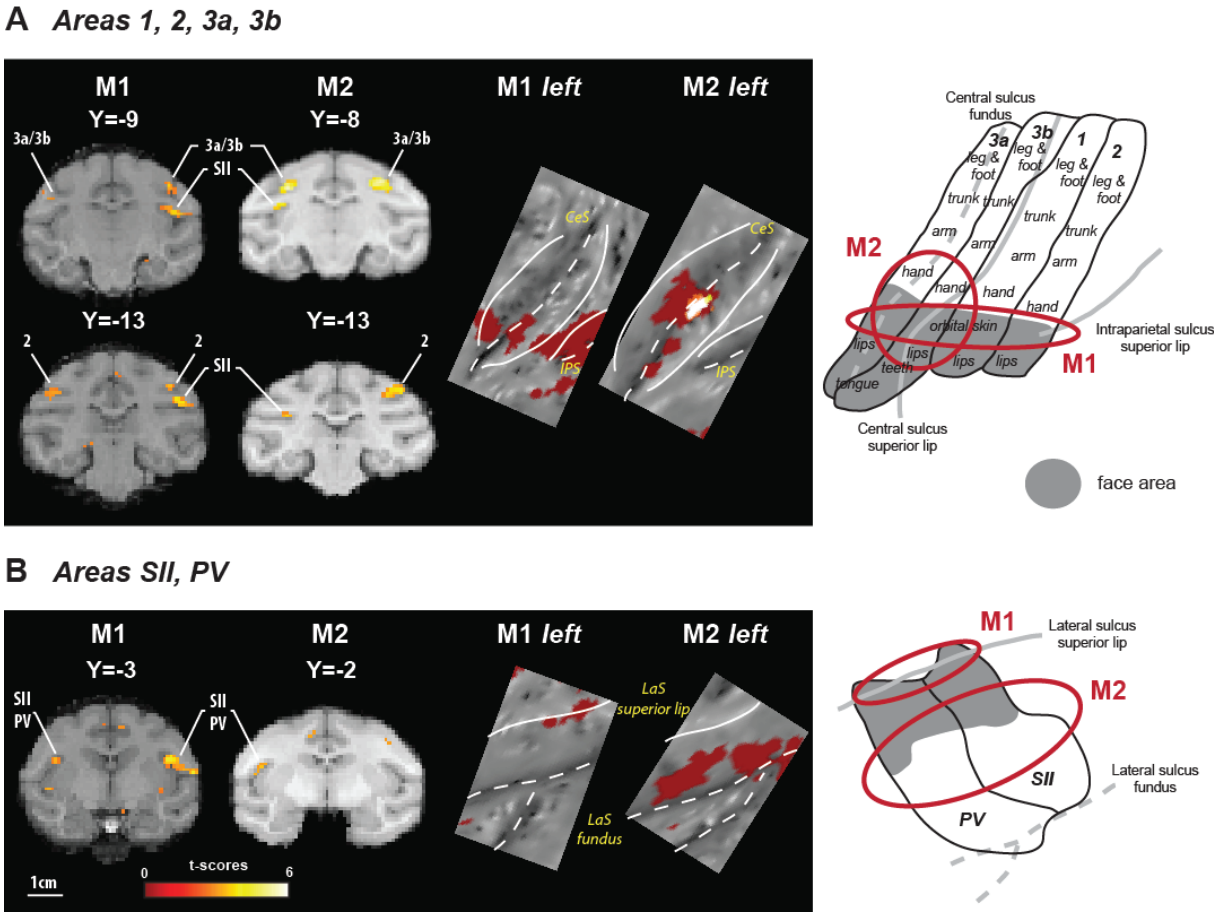

Figure 4: Topographic somatosensory activations in areas 1, 2, 3a and 3b (A) and in the complex SII-PV (B). On the left are displayed statistical parametric maps (SPMs) showing the bilateral activations relative to the blink events in both monkeys (yellow scale, $p<0.001$, uncorrected level). In the middle, the same activations are shown on a portion of the flattened map for the left hemisphere in both monkeys. The topographic organization for the corresponding regions is presented on the right part (A: adapted from Krubitzer et al. 2004, Padberg et al. 2005, Seelke et al. 2012; B: adapted from Krubitzer et al. 1995). The grey areas correspond to the face representations. The solid lines correspond to the lips of the sulci, the dashed lines to the fundus of the sulci. In red are represented the approximative locations of our blink-related activations (as presented in the middle part of the figure) on these topographic maps. Abbreviations are given in Fig. 3.

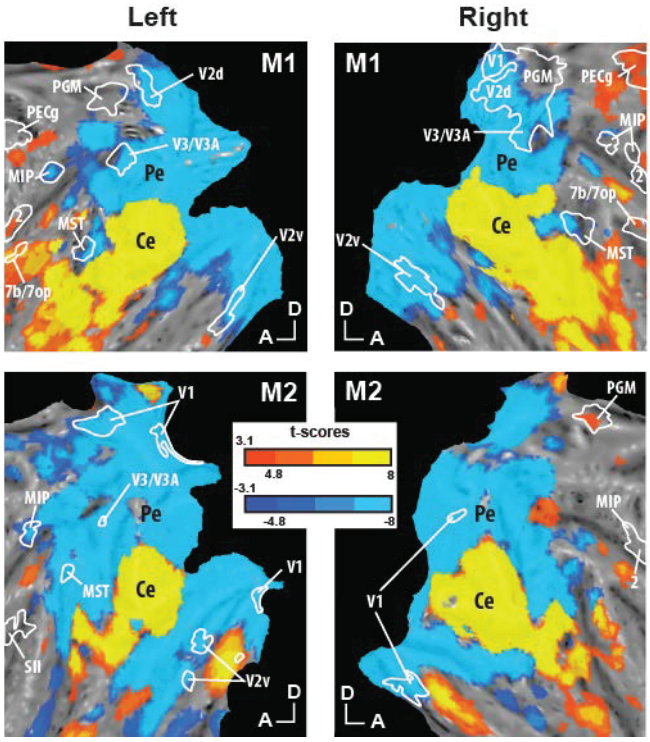

Figure 5: Close-up of the occipital representations of the blink-related activations (boundaries in white solid lines) superimposed on retinotopic central (yellow scale, color transition being adjusted to t-scores=4.8 FWE corrected level) and peripheral (blue scale) visual fields. Ce: central visual field; Pe: peripheral visual field. Other abbreviations as in Fig. 3.

CONCLUSIONS & PERSPECTIVES

The aim of the present thesis was to investigate the neural basis of self-representation using functional magnetic resonance imaging (fMRI) in the awakenon-human primate. The macaque monkey is strikingly comparable to humans in terms of both brain organization and cognitive capacities. This animal model has been studied for more than a century and remains today the most powerful animal model of human brain functions. However, since most of the data acquired in the macaque monkey come from electrophysiology and data collected in humans come from non-invasive neuroimaging techniques, it is often difficult to directly compare the outcomes of human and macaque monkey studies. Applying fMRI to the non-human primate is the obvious next step to bridge the gap between these two major sources of knowledge.

The construction and representation of self as an independent individual, autonomously acting on its environment, deeply relies on somatosensation (*i.e.* the primary processing of somatosensory cortical inputs) and somatoperception (*i.e.* the process of perceiving the body itself, and particularly of ensuring somatic perceptual constancy – Longo et al. 2010). It also deeply relies on the continuous interaction of the body with its environment, including the remapping of information from the body surface into an egocentric reference frame (Duhamel et al. 1997) as well the remapping of information from the external world through their contact with the body (Azañón et al. 2010; Longo et al. 2010). These processes recruit multisensory cortical regions which are thought to be at the core of body ownership, *i.e.* the feeling that our body is indeed our own (Petkova et al. 2011). Interestingly, multisensory cortical areas are also involved in the coding of peripersonal space, that is the portion of space that surrounds the body somatosensory limits and is closest to it (Macaluso and Maravita 2010; for review, Brozzoli et al. 2012 in The neural bases of multisensory processes).

In the present thesis, the first study allowed us to describe the mapping of the intraparietal sulcus of the macaque monkey in response to visual, tactile and auditory

stimulations. In particular, we describe a parietal cortical region coding stimulus movement irrespectively of the sensory modality describing it, located in the fundus of the intraparietal sulcus, in area VIP. It would be particularly relevant to complement this mapping of the intraparietal sulcus by describing the spatial extent of the vestibular projections onto these regions. Indeed, previous electrophysiological work has demonstrated the existence of vestibular responsive neurons in the intraparietal sulcus of the macaque monkey (Bremmer et al. 2002; Schlack et al. 2002; Chen et al. 2011). A crucial prediction derived from our work is that vestibular inputs will overlap with the amodal movement-related region (Guipponi et al. 2013). We propose that this amodal representation of relative self-movement is a key component in the construction of peripersonal space. Interestingly, our observations highlight strong homologies between macaque and human VIP organization.

In a second study, we describe the spatial cortical pattern of visuo-tactile cortical convergence and we show that, in addition to higher-order temporal, parietal, prefrontal, cingulate and orbito-frontal areas, we identify visuo-tactile convergence in low-level visual and somatosensory areas, in accordance with the heteromodal connections previously described in early sensory processing areas (Falchier et al. 2002; Rockland and Ojima 2003; Wallace et al. 2004; Cappe and Barone 2005; Budinger et al. 2006; de la Mothe et al. 2006; Smiley et al. 2007). The extent of this heteromodal influences is striking when compared with the sparse inter-areal anatomical projections between these cortical regions. We also show that the profile of this visuo-tactile convergence is functionally shaped by the physical properties of the stimuli used for the mapping, suggesting that visuo-tactile convergence could actually be even more prevailing than what we describe. Last, functional connectivity within this large visuo-tactile convergence network appears to change between the tactile and the visual stimulation context, suggesting that this network could be dynamically tuned by the sensory context as well as possibly by the behavioral context. Manipulating the nature of the

stimuli (static/in movement, large-field/local, intensity of the tactile stimulations) could be interesting to describe the spatial modulation of the network we reported.

The next step of our investigation was to question 1) how the visuo-tactile network we described is modulated by an experimental design in which stimuli intrude into the animal peripersonal space, and 2) how multisensory presentation of stimuli impacts cortical activations, *i.e.* this study allow us to compare the convergence cortical sites identified in the second study with the putative multisensory integrative cortical sites. The experiment we designed was composed of visual looming stimuli coming towards the monkey face and tactile stimulations (airpuffs) to mimic the impact of the looming stimuli on the monkey face.

The general multisensory integration framework, includingresults obtained in the team (Avillac et al. 2007), states that multisensory integration is maximized by spatial and temporal congruence (same spatio-temporal origin of both sensory modalities, *e.g.* the dog is barking). Here, we reasoned that visuo-tactile integration, in particular around the face, should not follow this rule. Indeed, we rarely experience seeing the mosquito that is drawing blood from our cheek. However, we often experience a feeling of anticipated touch to the skin when we see the very same mosquito approaching our cheek. As a result, we decided to probe the hypothesis that in the context of visuo-tactile integration around the face, maximal multisensory integration should take place when the tactile stimulus follows the visual stimulus and is predicted by it. We confirmed in chapters 3 and 4 that, in the context of visual objects approaching the face, multisensory integration is maximized not by temporal simultaneity but rather by the predictive nature of the visual stimulus upon the tactile stimulation. Data collected in humans in a tactile detection task showed that lowest tactile detection thresholds (maximal Dprime) were obtained when the visual stimulus was temporally predictive of the tactile stimulus rather than when both stimuli were presented simultaneously. The fMRI twin experiment led in the macaque monkey suggests that a sub-portion of the multisensory integrationcortical network is more widespread and strongly

activated in the specific condition of delayed presentation of tactile stimulation with respect to the approaching visual stimulus, in agreement with our working hypothesis. This on-going study shows that most of the cortical sites are located in the primary visual (striate and extrastriate areas) and in the primary and secondary somatosensory areas.

This finding opens the way to new investigations in the field of multisensory integration, incorporating the temporal prediction dimension. In particular, the Bayesian framework has proven extremely successful in accounting for the behavioral (*e.g.* Fetsch et al. 2010) and single cell recording manifestations of multi-sensory integration (*e.g.* Gu et al. 2008). It will be particularly interesting to extend this theoretical framework to our own observations.

Early neuropsychological studies demonstrate a dissociation between near and far space processing both in monkeys (Rizzolatti et al. 1983) and in humans (Halligan and Marshall 1991) after specific ablations or strokes. Our observations, describing the cortical networks involved in near and far space processing in a real naturalistic environment presented in Chapter 5, confirm the existence of two distinct networks for near and far space representation. Our neuroimaging results could drive single cell recording experiments to unveil the precise neuronal computations underlying our description of near and far space. In particular, we could investigate peripersonal defense space representation and its dynamical adjustment to the social and non-social environment. This could be done by manipulating the emotional or social contents of the stimuli presented.

Conclusion

Overall our results show that part of multisensory convergence sites we identified are further involved in the multisensory integration of visuo-tactile processing. We have additionally probed the cortical representation of near and far space and interestingly described overlapping regions with multisensory integrative regions. As a result, we propose

that the multisensory convergence and integration are involved in the cortical representation of near space. This hypothesis, based on neuroimaging data, needs to be further investigated in the same animals thanks to single-cell recording techniques to precisely probe the specific pattern of activations.

Bibliography

Avillac M, Ben Hamed S, Duhamel J-R. 2007. Multisensory integration in the ventral intraparietal area of the macaque monkey. J Neurosci. 27:1922–1932.

Azañón E, Longo MR, Soto-Faraco S, Haggard P. 2010. The posterior parietal cortex remaps touch into external space. Curr Biol. 20:1304–1309.

Bremmer F, Klam F, Duhamel J-R, Ben Hamed S, Graf W. 2002. Visual-vestibular interactive responses in the macaque ventral intraparietal area (VIP). Eur J Neurosci. 16:1569–1586.

Brozzoli C, Makin TR, Cardinali L, Holmes NP, Farnè A. 2012. Peripersonal Space: A Multisensory Interface for Body–Object Interactions. In: Murray MM, Wallace MT, editors. The Neural Bases of Multisensory Processes. Frontiers in Neuroscience. Boca Raton (FL): CRC Press.

Budinger E, Heil P, Hess A, Scheich H. 2006. Multisensory processing via early cortical stages: Connections of the primary auditory cortical field with other sensory systems. Neuroscience. 143:1065–1083.

Cappe C, Barone P. 2005. Heteromodal connections supporting multisensory integration at low levels of cortical processing in the monkey. Eur J Neurosci. 22:2886–2902.

Chen A, DeAngelis GC, Angelaki DE. 2011. Representation of vestibular and visual cues to self-motion in ventral intraparietal cortex. J Neurosci Off J Soc Neurosci. 31:12036–12052.

De la Mothe LA, Blumell S, Kajikawa Y, Hackett TA. 2006. Cortical connections of the auditory cortex in marmoset monkeys: core and medial belt regions. J Comp Neurol. 496:27–71.

Duhamel JR, Bremmer F, Ben Hamed S, Graf W. 1997. Spatial invariance of visual receptive fields in parietal cortex neurons. Nature. 389:845–848.

Falchier A, Clavagnier S, Barone P, Kennedy H. 2002. Anatomical evidence of multimodal integration in primate striate cortex. J Neurosci. 22:5749–5759.

Fetsch CR, Deangelis GC, Angelaki DE. 2010. Visual-vestibular cue integration for heading perception: applications of optimal cue integration theory. Eur J Neurosci. 31:1721–1729.

Gu Y, Angelaki DE, Deangelis GC. 2008. Neural correlates of multisensory cue integration in macaque MSTd. Nat Neurosci. 11:1201–1210.

Guipponi O, Wardak C, Ibarrola D, Comte J-C, Sappey-Marinier D, Pinède S, Ben Hamed S. 2013. Multimodal convergence within the intraparietal sulcus of the macaque monkey. J Neurosci. 33:4128–4139.

Halligan PW, Marshall JC. 1991. Left neglect for near but not far space in man. Nature. 350:498–500.

Longo MR, Azañón E, Haggard P. 2010. More than skin deep: body representation beyond primary somatosensory cortex. Neuropsychologia. 48:655–668.

Macaluso E, Maravita A. 2010. The representation of space near the body through touch and vision. Neuropsychologia. 48:782–795.

Petkova VI, Khoshnevis M, Ehrsson HH. 2011. The perspective matters! Multisensory integration in ego-centric reference frames determines full-body ownership. Front Psychol. 2:35.

Rizzolatti G, Matelli M, Pavesi G. 1983. Deficits in attention and movement following the removal of postarcuate (area 6) and prearcuate (area 8) cortex in macaque monkeys. Brain J Neurol. 106 (Pt 3):655–673.

Rockland KS, Ojima H. 2003. Multisensory convergence in calcarine visual areas in macaque monkey. Int J Psychophysiol. 50:19–26.

Schlack A, Hoffmann K-P, Bremmer F. 2002. Interaction of linear vestibular and visual stimulation in the macaque ventral intraparietal area (VIP). Eur J Neurosci. 16:1877–1886.

Smiley JF, Hackett TA, Ulbert I, Karmas G, Lakatos P, Javitt DC, Schroeder CE. 2007. Multisensory convergence in auditory cortex, I. Cortical connections of the caudal superior temporal plane in macaque monkeys. J Comp Neurol. 502:894–923.

Wallace MT, Ramachandran R, Stein BE. 2004. A revised view of sensory cortical parcellation. Proc Natl Acad Sci. 101:2167–2172.

TITRE en français

Bases neurales de la représentation de soi chez le primate non-humain, par une approche d'imagerie par résonance magnétique fonctionnelle (IRMf).

RESUME en français

L'objectif de cette thèse est d'identifier les bases neurales de la représentation de soi chez le primate non-humain, par une approche d'imagerie par résonnance magnétique fonctionnelle. Nous avons pour cela étudié la convergence multimodale 1) à l'échelle de l'aire par la description de la cartographie du sillon intraparietal dans un contexte de stimulations auditives, tactiles et visuelles et 2) à l'échelle du cerveau entier où nous décrivons précisément les sites de convergence visuo-tactile au niveau cortical. Nous avons également étudié le phénomène d'intégration multisensorielle dans un contexte visuo-tactile dynamique, pour lequel nous montrons que les effets comportementaux (étude psychophysique menée chez l'homme) et le réseau d'activations cortical sont maximisés quand le stimulus visuel prédit le stimulus tactile plutôt que lors de leur présentation simultanée. Enfin, nous avons étudié la représentation de l'espace en caractérisant les bases neurales de l'espace proche et de l'espace lointain à partir d'un dispositif expérimental naturaliste et nous montrons l'existence de deux réseaux corticaux qui traitent séparément les informations appartenant à l'espace proche et à l'espace lointain.

TITRE en anglais

Neural Basis of Self-Representation in the Non-Human Primate thanks to Functional Magnetic Resonance Imaging (fMRI)

RESUME en anglais

The aim of this thesis is to investigate the neural basis of self-representation in the non-human primate. We studied the multimodal convergence both 1) at the area level precisely mapping auditory, tactile and visual convergence in the intraparietal sulcus and 2) at the whole brain level capturing the spatial pattern of visuo-tactile cortical convergence. We also investigated the neural network subserving multisensory integration in a dynamical visuo-tactile context, showing that the strongest behavioral and cortical are obtained when the visual stimuli is predictive of the tactile stimulus rather than during simultaneous presentations. Finally, we studied the representation of space by characterizing the neural bases of near space and far space in a real naturalistic environment, thus providing the neural grounds for the observed behavioral and neuropsychological dissociation between near and far space processing.

DISCIPLINE : Neurosciences

MOTS-CLES : Imagerie par Résonance Magnétique Nucléaire (IRMf), aire VIP, convergence multisensorielle, intégration multisensorielle, psychophysique, singe macaque, espace.

Centre de Neuroscience Cognitive, UMR 5229
CNRS- Université Claude Bernard Lyon 1
67 boulevard Pinel - 69675 Bron cedex